

https://dspace.org/

The WNT signalling pathway in systemic sclerosis

Frost, Jacqueline Michelle

2016-10-19
http://hdl.handle.net/10539/21243

Downloaded from a DSpace repository. https://dspace.org/



UNIVERSITY OF THE
WITWATERSRAND,
JOHANNESBURG

The Wnt signalling pathway in systemic sclerosis

Jacqueline Michelle Frost

A thesis submitted to the Faculty of Health Sciences, University of the Witwatersrand, Johannesburg, in fulfilment for the degree of Doctor of Philosophy

2016

Declaration

I declare that this work is my own work, unless otherwise stated. It is being submitted for the degree of Doctor of Philosophy, at the University of the Witwatersrand. It has not been submitted for any other degree at any other University.

Jacqueline M. Frost
10 June 2016

Dedication

To my parents, Margaret and Peter Frost, without whose constant support and love, none of what I have achieved would have been possible, and to my husband Carl, for his endless support throughout my studies.

I love you all.

Acknowledgements

My supervisors and mentors: Professors Mohammed Tikly and Michèle Ramsay and to Dr Xavier Estivill, my host at the Centre for Genomic Regulation (CRG, Barcelona), thank you for all your advice, help and encouragement.

Dr Luchen Pillay (Dermatology, Chris Hani Baragwanath Academic Hospital), for always making yourself available to perform the skin biopsy procedure on the patients.

Dr Ridwan Mia, for assisting me with the collection of the control samples.

Colleagues at the CRG in Barcelona, who helped me with many aspects of my project from the study design (Kelly Rabionet and Eulalia Marti) to the technical (Anna Houben and Anna Puig) to the bioinformatics and data analysis (Marc Friedlander, Georgia Escaramis, Sarah Bonin and Kelly Rabionet). I appreciate all the help very much.

Ravi Govender, for your help with excel when I needed it most.

John-paul McCrone, for your continued interest in the progress of my thesis and for reviewing it when it was done.

CRG-Wits-Novartis Scientist Exchange program for allowing me the opportunity to spend six months in the beautiful city of Barcelona to complete my laboratory work. It was a fantastic experience both professionally and personally and I am very grateful.

The National Health Laboratory Service Research Trust Grant for funding.

The financial assistance of the National Research Foundation (NRF) towards this research is hereby acknowledged. Opinions expressed and conclusions arrived at, are those of the author and are not necessarily to be attributed to the NRF.

Abstract

Systemic sclerosis (SSc) is a complex autoimmune disease involving the immune system, vasculature and extracellular matrix. Dysregulation of the Wnt pathway has been implicated in the development of fibrosis in SSc and is proposed to contribute to a failure to maintain tissue homeostasis and appropriate immune response.

The objective of this research study was to explore the role of altered Wnt pathway gene regulation in the development of fibrosis in black South African SSc patients with early, diffuse disease (dcSSc). The first aim was to examine differential gene expression in the Wnt pathway and the second aim to examine differential expression of microRNAs that potentially target Wnt pathway genes.

Skin biopsies from eight black South African patients with dcSSc, samples from both the forearm (affected skin) and the back (unaffected skin), and eight ethnically matched healthy control skin samples were examined. The Wnt pathway RT^2 Profiler qPCR Array (84 Wnt pathway genes) was used to assess differential gene expression, single gene TaqMan assays for validation and small RNA-sequencing for microRNA analysis. Data analysis was done using HTqPCR, NormqPCR and DESeq2 software.

Gene expression patterns revealed five distinct differentially expressed gene clusters. Two clusters displayed genes that were upregulated in both affected and unaffected SSc skin compared to controls (one showing a more heterogeneous pattern than the other). Another showed consistently decreased gene expression and two revealed more complex patterns responsible for delineating the patients into two groups. The gene

expression was validated for five genes. The sRNA-seq data showed differential expression of 31 miRNAs that target the Wnt pathway genes, including miR-335 and miR204 that are important regulators of normal tissue development. Other dysregulated miRNAs have been linked to fibrotic and autoimmune diseases.

In this group of dcSSc patients, there is differential gene expression of several Wnt pathway genes that delineate the patients into two distinct groups. This could point to differences in disease aetiology leading to distinct clinical outcomes, such as inflammation. Together with the differentially expressed microRNAs, the findings indicate a substantial contribution of epigenetic changes to the pathogenesis, progression and diverse clinical features of dcSSc.

Abbreviations

A	Arginine
ac	Acetylation
ACA	Anti-centromere antibody
ACR	American College of Rheumatology
ACTB	Actin B
AML	Acute Myeloid Leukemia
ANA	Anti-nuclear antibody
ATA	Anti-topoisomerase antibody
BANK1	B-cell scaffold protein with ankyrin repeats 1
bp	Base pair
C	Cytosine
CALM1	Calmodulin 1
CAV	Caveolin
CCND2	Cyclin D2
cDNA	Complementary DNA
COL1A1	Collagen type 1 alpha 1
CRP	C-reactive protein
CSNK1A1	Casein kinase 1 alpha 1
Ct	Threshold cycle
CTGF	Connective tissue growth factor
CTLA	Cytotoxin T-lymphocyte associated protein 4
CTNNBIP1	Catenin beta interacting protein 1
dcSSc	Diffuse cutaneous systemic sclerosis
DKK	Dickkopf
DLCO	Diffusing capacity of the lung for carbon monoxide
DNA	Deoxyribose nucleic acid
DNMT	DNA Methyltransferases
Dr	Doctor
DZ	Dizygotic
ECM	Extracellular matrix
ESR	Erythrocyte sedimentation rate
EULAR	European League Against Rheumatism
F	Female
FBXW11	F-box and WD repeat domain containing 11
FEV1	Forced expiratory volume
FLI1	Friend leukemia integration 1 transcription factor
FOXC1	Forkheadbox C1
FRAT1	Frequently rearranged in advanced T-cell lymphomas
FRZB	Frizzled-related protein
FVC	Forced vital capacity
FZD	Frizzled
G	Guanine
H	Histone

HATs	Histone acetyltransferases
HCM	Hypertrophic cardiomyopathy
HCC	Hepatocellular carcinoma
HDACs	Histone deacetylases
His	Histidine
HLA	Human leukocyte antigen
hMSCs	Human mesenchymal stem cells
HSPA12A	Heat shock 70kDa protein 12A
HT	High throughput
IBD	Inflammatory Bowel Disease
IL	Interleukin
IPF	Idiopathic pulmonary fibrosis
IRF	Interferon regulatory factor
JNK	c-Jun N-terminal kinase
JUN	Jun-proto oncogene
K	Lysine
L	Liter
lcSSc	Limited cutaneous systemic sclerosis
LEF1	Lymphoid enhancer-binding factor 1
LRP	Low-density lipoprotein receptor-related protein
M	Male
me	Methylation
MEST	Mesoderm specific transcript
mg	Milligram
miRNA	Micro-RNA
ml	Milliliter
mm	Millimeter
MMC	Mouse mesangial cells
mmHg	Millimeter of mercury
mmol	Millimol
MMP	Matrix metalloproteinase
mRNA-seq	Messenger RNA sequencing
MRSS	Modified Rodnan skin score
MS	Multiple sclerosis
MT1A1	Metallothionein 1A
MYC	Myc proto oncogene
MZ	Monozygotic
NAV2	Neuron navigator 2
NCBI	National Center for Biotechnology Information
ncRNA	Non-coding RNA
ng	Nanogram
NGS	Next generation sequencing
PCA	Principal component analysis
PCR	Polymerase chain reaction
PITX2	Paired-like homeodomain 2
PORCN	Porcupine homolog

PRICKLE1	Prickle homolog 1
Pro	Proline
PTPN	Protein tyrosine phosphatase, non-receptor
QC	Quality control
qPCR	Quantitative PCR
RA	Rheumatoid arthritis
RHOA	Ras homolog gene family, member A
RIN	RNA Integrity number
RNA	Ribose nucleic acid
RNA-i	RNA-interference
RNA-seq	RNA-sequencing
rs	Reference SNP
RUVBL1	RuvB-like AAA ATPase 1
SFRP	Secreted frizzled-related protein
SLE	Systemic lupus erythematosus
SNP	Single nucleotide polymorphism
SOX17	SRY (sex determining region Y)-box 17
sRNA-seq	Small RNA sequencing
SSc	Systemic Sclerosis
STAT	Signal transducer and activator of transcription
T	Thymine
T1D	Type 1 diabetes
TGF	Transforming growth factor
TLR	Toll-like receptor
Tsk	Tight skin mouse
USA	United States of America
vs	Versus
WIF1	Wnt inhibitory factor 1
Wnt	Wingless-related integration
µl	Microliter

Table of Contents

Declaration ii

Dedication iii

Acknowledgements iv

Abstract v

Abbreviations vii

Table of Contents x

List of Figures xiii

List of Tables xiv

Chapter 1

Introduction and Literature Review 1

1.1. Historical background of systemic sclerosis 1
1.2. Classification criteria 2
1.3. Epidemiology 4
1.3.1. Prevalence 4
1.3.2. Environmental risk factors 6
1.3.2.1. Silica 6
1.3.2.2. Organic solvents 7
1.3.2.3. Toxins 8
1.3.2.4. The microbiome 9
1.3.3. Systemic sclerosis and malignancies 9
1.3.4. Genetic risk factors 10
1.4. Epigenetic modifications 13
1.4.1. DNA Methylation 13
1.4.2. Histone Modifications 14
1.5. Pathogenesis 15
1.6. The clinicopathological triad 16
1.7. Understanding fibrosis 19
1.7.1. Endothelial cells 19
1.7.2. T-cells 20
1.7.3. Fibroblasts 20
1.8. Animal models 23
1.9. Gene expression in SSc 26
1.10. Prognosis and treatment 26
1.11. Study objective and aims 28

Chapter 2

Wnt pathway gene expression in SSc 30

2.1. Introduction 30
2.1.1. The Notch and Hedgehog pathways 31
2.1.2. The canonical Wnt pathway 32

2.1.3. The non-canonical Wnt pathways 34
2.1.4. The role of the Wnt pathway in fibrotic disease 34
2.1.5. The morphogen pathways in systemic sclerosis 37
2.1.6. The Wnt pathway in systemic sclerosis 38
2.1.7. Previous gene expression studies in SSc 39
2.2. Materials and Methodology 42
2.2.1. Participants 42
2.2.1.1. Systemic sclerosis patients 42
2.2.1.2. Control subjects 44
2.2.2. Laboratory Methods 45
2.2.2.1. Collection and transportation of samples 45
2.2.2.2. RNA Extraction 46
2.2.2.3. Wnt pathway RT^2 Profiler PCR Array 46
2.2.2.4. Validation of RT^2 Profiler PCR Array data 49
2.3. Results 52
2.3.1. Demographic and clinical features of patients with SSc 52
2.3.2. Demographic data for control individuals 53
2.3.3. RNA Quality 53
2.3.4. qPCR array normalization 53
2.3.5. Wnt pathway gene expression 57
2.3.6. Differentially expressed genes in both affected and unaffected skin samples compared to controls 60
2.3.7. Differential gene expression differentiating the two clusters (A and B) and their relationship to patient groups 1 and 2 65
2.3.8. Gene expression patterns and specific clinical features 68
2.3.9. Validation of RT^2 Profiler PCR Array using single gene TaqMan assays 70

2.4. Discussion 76
2.4.1. Genes upregulated in affected and unaffected SSc skin compared to controls (Red and Blue clusters) 78
2.4.2. Genes downregulated in affected and unaffected SSc skin compared to controls (Green cluster) 84
2.4.3. Genes whose differential expression differentiates the two clusters A and B (Orange and Purple) 87
2.4.4. Summary 93
2.4.5. Limitations 96
2.4.6 Strenghs of the study 97
2.4.7. Future studies 98

Chapter 3

Expression of microRNAs that target Wnt pathway genes 100
3.1. Introduction 100
3.1.1. Epigenetics in autoimmune diseases 100
3.1.2. DNA Methylation and histone modification in SSc 103
3.1.3. Micro-RNA 104
3.1.4. Micro-RNA modulation of the Wnt pathway 105
3.1.5. miRNAs in fibrosis 106
3.1.6. The role of micro-RNAs in SSc 110
3.2. Materials and Methodology 112
3.2.1. Subjects 112
3.2.2. sRNA-sequencing library preparation 112

3.2.3. Data analysis 114
3.2.3.1. sRNA-sequencing data analysis 114
3.2.3.2. Quality Control 114
3.2.3.3. Target prediction 115
3.3. Results 116
3.3.1. Significantly differentially expressed miRNA 116
3.3.2. Wnt pathway predicted targets 117
3.3.3. miRNA expression in SSc skin 119
3.3.4. miRNA expression in affected SSc skin 119
3.3.5. miRNA expression in unaffected SSc skin 119
3.4. Discussion 124
3.4.1. miRNAs in autoimmunity, inflammation and fibrosis 124
3.4.2. miRNAs differentially expressed in affected skin 126
3.4.3. miRNAs differntially expressed in unaffected skin 130
3.4.4. Summary 130
3.4.5. Limitations 136
3.4.6. Future studies 137

Chapter 4

Conclusion **140**

References **144**

Appendices **163**
Appendix A – Ethics Certificate *163*
Appendix A2 – Amendment to ethics certificate *164*
Appendix B – Patient and Control Information and Consent forms *165*
Appendix C - miRNeasy mini Kit (Qiagen) *170*
Appendix D – RNA Quality and Quantity *171*
Appendix E – List of genes on the Wnt pathway qPCR array *172*
Appendix F - RT^2 Profiler PCR Array Protocol *173*
Appendix G – TaqMan Gene Expression Assays *177*
Appendix H – Clinical data *179*
Appendix I– Dates samples were extracted and processed for qPCR *180*
Appendix J - Summary Table of the gene cluster colours and patient groups *181*
Appendix K - Normalised expression to ACTB *182*
Appendix K - Normalised expression to ACTB and HPRT1 *187*
Appendix L – Graphs of Ct values across samples (validation experiments) *192*
Appendix M – Gene expression ratios (GOI vs Houskeeping genes: ΔCt) *195*
Appendix N – Fold change gene expression for affected and unaffected skin *194*
Appendix O - NEBNext small RNA Library Prep for Illumina *196*
Appendix P – miRNA QC graphs *202*

List of Figures

Figure 1.1. Mechanism of Fibrogenesis 16
Figure 1.2. Schematic diagram of the clinicopathological triad of systemic sclerosis 17
Figure 1.3. Tissue damage resulting in fibrosis 19
Figure 1.4. Histopathologic features of affected tissues 23
Figure 2.1. The Wnt signaling pathways 33
Figure 2.2. Summary of the qPCR RT^2 Profiler Array workflow 47
Figure 2.3. Schematic diagram of methodology used in this study 51
Figure 2.4. Housekeeping gene selection 54
Figure 2.5. Principal component analysis plot containing all samples analysed 55
Figure 2.6. PCA plots for forearm samples and back samples, each with controls 56
Figure 2.7. Gene expression results normalized in three different ways 58
Figure 2.8. Clustering of samples from the gene expression heatplots 60
Figure 2.9. Section of heatplot containing the red cluster of genes 61
Figure 2.10. Section of heatplot containing the blue cluster of genes 63
Figure 2.11. Section of heatplot containing the green cluster of genes 64
Figure 2.12. Genes in the orange and the purple gene clusters that are differentiating the two patient groups, 1 and 2 65
Figure 2.13. The gene clusters marked in orange and purple show genes, showing those genes with differential expression between cluster A and cluster B 69
Figure 2.14. The ΔCt gene expression ratio values, obtained for the qPCR array experiments, for each of the six chosen genes for validation; A) AXIN1, B) LEF1, C) FZD2, D) WNT5B, E) WNT7A and F) FGF4 72
Figure 2.15. Box and Whisker plots of gene expression ratios (ΔCt) calculated for each sample group 75
Figure 2.16. Level of gene expression for controls, cluster A genes and cluster B genes across the 84 genes of the Wnt pathway qPCR array 77
Figure 2.17. Genes observed as being up and downregulated in this study and their role in the canonical or non-canonical Wnt pathways 94
Figure 3.1. Potential consequences of abnormal miRNA regulation in immune responses and functions (Pauley et al., 2009) 103
Figure 3.2. Flowchart summary of methodology 113
Figure 3.3. Principal component analysis of the sRNA-seq results 117
Figure 3.4. Graph representing the number of significantly differentially expressed miRNAs found to target the 29 Wnt pathway genes in involved and uninvolved skin of SSc patients 118
Figure 3.5. Graph representing the number of Wnt pathway genes that the miRNAs are predicted to target in both involved and uninvolved skin 123
Figure 3.6. Schematic representation of the canonical and non-canonical Wnt pathways with the genes observed as differentially expressed in Chapter 2 and the miRNAs in Chapter 3 135

List of Tables

Table 1.1. Preliminary criteria for the classification of systemic sclerosis 3
Table 1.2. The 2013 ACR/EULAR criteria for classification of systemic sclerosis 3
Table 1.3. Population differences in the manifestation of SSc 6
Table 1.4. Novel SSc associated SNPs in non-HLA genes 12
Table 1.5. Table of targeted, antifibrotic therapies for systemic sclerosis 28
Table 2.1. Control sample demographic data including age and sex 45
Table 2.2. Summary of demographic, clinical and laboratory data for the patients 52
Table 2.3. Genes significantly upregulated in SSc cases both affected and unaffected skin, compared to controls (red gene cluster) 61
Table 2.4. Genes upregulated in SSc cases, both affected and unaffected skin compared to controls (blue cluster) 63
Table 2.5. Genes significantly downregulated in both affected and unaffected SSc skin compared to controls 65
Table 2.6. Differential gene expression observed in Patient Group 1 for the orange and purple gene clusters 66
Table 2.7. Differential gene expression observed in Patient Group 2 for the orange and purple gene clusters 67
Table 2.8. Summary of the qPCR array expression values and rationale for choosing these six specific genes for validation 71
Table 2.9. Summary of the differential expression values for the five genes chosen for validation observed in both the qPCR array experiment and the TaqMan validation experiments 74
Table 3.1. miRNAs that have been associated with the development of fibrosis 108
Table 3.2. Significantly differentially expressed miRNAs in involved and uninvolved skin compared to controls that were predicted to target Wnt pathway genes 120
Table 3.3. Most significantly differentially expressed miRNAs observed in this study 132

Chapter 1

Introduction and Literature Review

1.1. Historical background of systemic sclerosis

Scleroderma, or systemic sclerosis (SSc), is a multisystem autoimmune disease characterized by a constellation of vascular injury, immune abnormalities and fibrosis. The clinical manifestations of this disease are heterogeneous and depend on the presence and varying degrees of internal organ involvement (LeRoy et al., 1988).

Cases of skin diseases with similar descriptions to SSc can be found in ancient writings, such as those of Hippocrates around 460 - 370 B.C. (Armando Laborde and Young, 2012). However, it is uncertain whether these ancient writings are true examples of the disease, as these descriptions were often vague and inexact. The first modern account of SSc is attributed to the Italian physician, Carlo Curzio, in 1753 (Roberts-Thomson and Walker, 2006), who described a female patient with variable thickening and hardness of the skin across the body, skin tightness around the mouth and hardness around the neck area. One of his students, Giovambattista Fantonetti, is credited with being the first to recognise the condition as a disease entity, calling it “sclermia circumscripia” (Benedek and Rodnan, 1982a).

It was almost a century later when descriptions of the disease reappeared in the medical literature, when a physician in Paris rediscovered the disease and opened areas of

discussion for French and English clinicians who at this time called the disease “sclerema neonatorum” (Benedek and Rodnan, 1982b).

By 1900, more than 500 cases of SSc had been reported and discussed in the medical literature, reflecting the interest in this disease in the clinical setting (Benedek and Rodnan, 1982b). The modern “father” of SSc is Carwille LeRoy, who was one of the first rheumatologists to apply modern scientific methods to study fibroblasts from SSc patients. He showed SSc fibroblasts had the ability to synthesise and secrete excess collagen *in vitro*. He was also among the first to show that vascular endothelium is a primary target in SSc (Silver, 2002).

1.2. Classification criteria

Classification criteria for diseases are pragmatic as they establish, with reasonable certainty, that a particular patient or group of patients has a particular disease (Fries et al., 1994). In rheumatic diseases, classification criteria are used principally for research purposes. In this regard, SSc is particularly challenging as it includes a broad spectrum of clinical features. As such, preliminary criteria were developed and proposed during a meeting of the American Rheumatism Association’s Scleroderma Criteria Cooperative Study (Masi et al., 1980). The major criterion for a definite diagnosis of SSc is skin thickening that extends from the fingers proximal to the metacarpophalangeal joints, with minor critera also being proposed as shown in Table 1.1. Together, these criteria are the official American College of Rheumatology (ACR)/European League Agaianst Rheumatism (EULAR) classification criteria of systemic sclerosis. However, a limitation of

the criteria is that they do not perform well in patients with limited cutaneous involvement (Lonzetti et al., 2001).

Table 1.1. Preliminary criteria for the classification of systemic sclerosis

Presence of either:

The major criterion: proximal scleroderma

Or

Two of the three minor criteria:

a) *Sclerodactyly*
b) *Digital pitting of fingertips or loss of substance of the digital finger pad*
c) *Bilateral basal pulmonary fibrosis*

These criteria were revised more recently to improve the sensitivity to detect early and milder forms of the disease (van den Hoogen et al., 2013) Table 1.2.

Table 1.2. The 2013 ACR/EULAR criteria for classification of systemic sclerosis. *Patients with a total score of >9 are classified as having definite SSc (van den Hoogen et al., 2013)*

Item	Sub-items	Score
1. Skin thickening of the fingers of both hands extending proximal to the metacarpophalangeal joints		9
2. Skin thickening of the fingers	• Puffy fingers	2
	• Sclerodactyly of the fingers	4
3. Fingertip lesions	• Digital tip ulcers	2
	• Fingertip pitting scars	3
4. Telangiesctasia		2
5. Abnormal nailfold capillaries		2
6. Pulmonary arterial hypertentsion and/or intestitial lung disease	• Pulmonary arterial hypertension	2
	• Interstitial lung disease	2

7. Raynauds phenomenon		3
8. SSc-related autoantibodies	• Anticentromere • Anti-topoisomerase I • RNA Polymerase II	3

There are, broadly speaking, two subsets of SSc (LeRoy et al., 1988). Patients with diffuse cutaneous SSc (dcSSc) typically have skin thickening of the proximal and distal extremities, the trunk and face, and commonly involves internal organs. Patients with limited cutaneous SSc (lcSSc) have skin thickening which is limited to the face and neck, and distal to the elbows and knees, have less internal organ fibrosis but are more prone to vascular changes such as digital gangrene and pulmonary arterial hypertention in the latter stages of disease (Smith and Chan, 2010).

1.3. Epidemiology

1.3.1. Prevalence

Systemic sclerosis has a worldwide distribution and is more frequent in females, with a female to male ratio varying between 3-8:1 (Selmi et al., 2006). Age of onset is usually middle-aged between 35-50 years (Hinchcliff and Varga, 2008). There are various hypotheses for the striking female predominance of SSc. There are a limited number of published reports that have investigated the relationship of pregnancy with development of SSc in females. A study by Cockrill et al. (2010) compared pregnancy histories of 172 SSc patients with that of their healthy sisters (n=256). What this study found was a positive association between parity and the risk of SSc (OR= 2.8). Another hypothesis is that of microchimerism, the persistence of fetal cells in maternal tissues, which has long been proposed as a trigger for scleroderma or other autoimmune

diseases (Adams Waldorf and Nelson, 2008). Fetal microchimerism has also been suggested as an explanation for the increased female to male ratio in these diseases.

The prevalence of SSc differs between populations, suggesting a partly genetic etiology. The prevalence of the disease in the United States is approximately 18/100 000 (Furst, 2011) and is observed more frequently in African Americans than in Caucasians (Bogatkevich et al., 2007). The prevalence of SSc in the Choctaw Indians from Oklahoma was reported to be 469/100 000, the highest recorded prevalence in the world (Arnett et al., 1996). In general, dcSSc is more common in non-Caucasian populations and lcSSc is more common in Caucasians. For example, Thai patients have a higher incidence of anti-topoisomerase antibody (ATA) and are more likely to have diffuse disease compared with Australian Caucasians (Chen et al., 2003). African Americans and Hispanics are more likely to have diffuse skin involvement and pigment changes compared to Caucasians, who tend to have more facial telangiectasia (visibility of small, dilated blood vessels near the surface of the skin) (Chen et al., 2003).

The disease has historically been considered rare in sub-Saharan Africans (Silman and Newman, 1996) although has been recognised in various parts of the subcontinent. In the early 1980s, only two cases of SSc were reported in a teaching hospital in Nigeria (Somorin and Mordi, 1980) whereas the disease is widely reported in South Africa, with an incidence among goldminers being approximately 2.5 fold more than the general population (7.3-8.1/100 000 vs. 0.33/100 000) (Cowie and Dansey, 1990, Tager and Tikly, 1999). More recent studies from Nigeria have reported more cases, the majority of which are female all with dcSSc (Adelowo and Oguntona, 2009). Table 1.3 highlights

some of the population specific differences observed in patients with SSc.

Table 1.3. Population differences in the manifestation of SSc. *As seen in the Caucasian, Asian, African-American and South African populations*

	Caucasian[1,2,3] n = 1808[1] n = 199[2] n = 2945[3]	**Asian[4]** n = 68	**African-American[1,2,3,5]** n = 409[1] n = 64[2] n = 203[3] n=39[5]	**South African[6,7]** n = 63[9] n = 17[7]
Percent female	82%	85%	82%	87%
Average age of onset	54 years	46 years	45 years	35 years
Diffuse disease	43%	38%	69%	68%
ANA positive	84%	79%	97%	98%
ATA positive	19%	35%	31%	25%
Pulmonary involvement	33%	52%	54%	56%
Renal disease	10%	2%	13%	13%

[1] (Gelber et al., 2013), [2] (Nietert et al., 2006), [3] (Steen et al., 2012), [4] (Low, 2013), [5] (McNearney et al., 2007), [6] (Tager and Tikly, 1999), [7] (Frost et al., 2012)
ANA = Anti-nuclear antibody; ATA = Anti-topoisomerase antibody

1.3.2. Environmental risk factors

There is evidence to support the impact of environmental factors on the occurrence and severity of SSc.

1.3.2.1. Silica

Cases have been documented with the co-existence of silicosis and progressive SSc in Europe, Japan the USA and in Africa (Sluis-Cremer et al., 1985). Particulate silica is

released in gold-mining, rock-drilling, cement work and brick laying (Marie and Gehanno, 2015). SSc was uncommon in early studies from Africa, with only one case documented in Nigeria and six in Zimbabwe over a 10-year period (Greenwood, 1968, Lutalo, 1985). Erasmus, a pathologist in Pretoria was the first to observe an association between gold mining and SSc in South Africa in the late 1950s (Erasmus, 1957). He noted the increased prevelance of progressive SSc in the Johannesburg area in white gold miners who were exposed to dust containing a high perecentage of (>30%) free silica (Erasmus, 1957). Subsequent studies documented cases of SSc in both white and black gold miners (Cowie, 1987). A 2012 meta-analysis of 16 studies, with a total of 1101 cases demonstarted that SSc patients were more often exposed to silica and the risk appeared to be higher in males (Miller et al., 2012). Occupational exposure to silica has also been noted as a predictive parameter for SSc severity (Diot et al., 2002), with those patients who have been exposed developing more frequently diffuse disease, higher skin scores and interstitial lung disease (Marie et al., 2015). The pathogenic mechanisms by which silica contribute to the development of SSc remains unclear, though it is thought to be a strong T-cell adjuvant. Thus exposure to silica in a genetically predisposed individual will trigger a dysregulated immune reponse resulting in tissue damage and a systemic inflammatory response (Maeda et al., 2010).

1.3.2.2. Organic solvents

Organic solvents are those compounds that can be separated into aliphatic-chain compounds (hexane), aromatic compounds (benzene and xylene) and chlorinated compounds (Marie and Gehanno, 2015). A few common uses for organic solvents are for dry-cleaning, paint thinners, nail polish removers and stain removers (Marie et al., 2014).

The association between SSc and exposure to organic solvents was first described by in 1957 by Reinl (Reinl, 1957). In 2009 a study observed a correlation between solvent exposure and SSc (52) and a 2012 meta-analysis confirmed this, with the risk of developing SSc associated with solvent exposure being higher in males than females (Miller et al., 2012). Additionally, a large case-control study showed marked association between SSc and organic solvents for white spirit, aromatic and chlorinated solvents, ketones and trichloroethylene (Marie et al., 2014). As with silica exposure, occupational exposure to organic solvents has been found to be a predictive parameter for SSc severity, with those patients who were exposed versus non-exposed patients exhibiting more frequently, diffuse disease, digital ulcers and severe microangiopathy (Marie et al., 2015). The pathogenic mechanisms of organic solvents and SSc remain unclear but there is speculation that the organic solvents may link with nucleic acids and proteins resulting in immune disruptors and thus leading to increased risk of SSc (Miller et al., 2012).

1.3.2.3. Toxins

Toxic oil syndrome occured in Spain in 1981, affecting approximately 20 000 people, and was linked to the consumption of contaminated rapeseed oil (Hill et al., 1995). These patients presented clinically with; oedema, contractures, Raynauds phenomenon and fibrosis of the dermis, suggesting a scleroderma-like syndrome (Alonso-Ruiz et al., 1986). In the United States an association was made between ingesting tryptophan to treat insomnia and a syndrome characterized by scleroderma-like skin abnormalities that developed 1 to 18 months after the start of therapy. All patients had histopathological changes in the dermis and subcutaneous tissue typical of scleroderma (Silver et al., 1990).

1.3.2.4. The microbiome

Research into the role that the microbiome, specifically gut microbiota, might play in the immune system started in the late 1990's (Penders et al., 2007). The microbiome has been suggested to play a role in the development of autoimmune diseases such as RA, MS and fibromyalgia (Wu et al., 2009). Numerous studies demonstrate that altered microbiota can induce or intensify inflammation in inflammatory bowel disease (IBD). The etiology of SSc-related lower gastro-intestinal tract dysfunction is unknown and there are no effective treatment options for these patients. Alterations in microbial composition may potentially be a pathogenic factor in gastro-intestinal tract dysfunction in SSc. A recent study by (Volkmann et al., 2016) revealed that the intestinal microbiome of SSc patients is enriched with inflammatory bacteria. This study investigated the microbiome of the gut in 17 SSc patients and 17 healthy controls and found that inflammatory bacteria enrich the microbiomes of SSc patients while protective bacteria were reduced. Additionally, SSc patients exhibiting a microbiota flora similar to patients with Crohn's disease. There was an enrichment of bacteria species *Erwinia* and *Trabulsiella* in the SSc patients with the most severe disease symptoms systemic sclerosis patients with the most severe symptoms. This is an interesting finding as it suggests that the microbiomes not only differ between the SSc patients and controls, but also differ between patients and these differences may contribute to the clinical symptoms observed in these patients.

1.3.3. Systemic sclerosis and malignancies

There is a substantial amount of evidence to suggest an increased incidence of malignancies in autoimmune rheumatic diseases such as Sjögren's syndrome, RA and SSc

(Szekanecz et al., 2012). Malignant tumors are reported in 3–11 % of SSc patients (Siau et al., 2011, Wooten, 2008). The risk for cancer has been found to be 1.5-fold higher in SSc patients when compared to the general population (Olesen et al., 2010), with the majority of malignancies being solid tumors, lung and breast cancers (Onishi et al., 2013). Malignancy in SSc may be due cytotoxic agents, primarily cyclophosphamide used in the treatment of SSc, as well as exposure to chemicals or smoking that may further increase the risk of developing cancer (Szekanecz et al., 2012). Adequate treatment and follow-up of SSc patients may help to lower the risk of malignancies secondary to SSc (Kasifoglu et al., 2016).

1.3.4. Genetics risk factors

The genetics of the disease is complex with several lines of evidence supporting a genetic component to susceptibility to SSc. Studies have shown that the incidence of the disease is 1.5% in families with a history of the disease compared to 0.026% in the general population (Luo et al., 2013). An increased relative risk of 3.07 of developing the disease in first-degree relatives of affected individuals has been reported (Frech et al., 2010). Twins studies, though few in the case of SSc, indicate low disease concordance rates of 4.2% in monozygotic twins (MZ) and 5.6% in dyzogotic twins (DZ) (Arnett et al., 2001, Feghali-Bostwick et al., 2003, Selmi et al., 2012). Although the concordance rate amongst twins is low for clinical disease, there have been reports of high concordance in terms of immunological and molecular features of the disease. A large twin study suggested that concordance for ANA reactivity was 90% in MZ twins and 40% in DZ twins (Feghali-Bostwick et al., 2003). Thus, although concordance rate amongst MZ twins is

low, the high concordance with molecular and immunological features of the disease suggests a genetic predisposition for development of SSc.

Genetic association studies are a useful tool to study the molecular aetiology of complex diseases. Complex diseases are caused by genetic variation in several genes, each with a minor contribution to the overall relative risk, as well as exposure to environmental risk factors. Combinations of genetic variants, particularly single nucleotide polymorphisms (SNPs), not only influence susceptibility to complex diseases but are also associated with specific aspects of the disease phenotype. The literature reports many studies on associations between various genes and SSc susceptibility or severity (Bossini-Castillo et al., 2012, Bossini-Castillo et al., 2013, Sharif et al., 2012, Mayes et al., 2014).

The human leukocyte antigen (HLA) region contains genes that encode products that are known to play an important role in the adaptive immune response. In addition several HLA genotypes have been associated with autoimmune diseases, since the first report of an association with systemic lupus erythematosus in 1971 (Grumet et al., 1971). A study conducted in South Africa showed associations of various HLA genotypes with different SSc subtypes. Increased frequencies of DR2, DRB1*0301 and DRB1*11 were observed in SSc patients with the limited cutaneous subtype, while patients with diffuse cutaneous disease had increased frequencies of DRB1*1101, DRB1*15, DQB1*0301/4 and DPB1*1301. It was also noted that within a subgroup of patients with pulmonary fibrosis, there was an increase in DRB1*15 and DPB1*1301 (Tikly et al., 2004).

In recent years, several non-HLA genes have been reported as having an association with susceptibility to SSc (Broen et al., 2012b), particularly tumour necrosis factor-α (Sato et al., 2004), endothelin (Fonseca et al., 2006) and fibrillin (Tan et al., 2001). Table 1.4 lists the newly described non-HLA genes associated with SSc. All of these studies are able to provide potential insight into the pathogenesis and aetiology of the disease. Many studies have shown strong association between polymorphisms and the presence of antibodies, which are hallmarks of SSc, such as ATA or anti-centromere (ACA) reactivity (Fanning et al., 1998).

Table 1.4. Non-HLA SNPS associated with SSc

Gene	SNP	Association	Population	Study design	Reference
IRF8	rs11642873	lcSSc	European/ Spanish	Candidate gene	(Gorlova et al., 2011)
TN1P1	rs2233287	SSc	European	Immunochip	(Bossini-Castillo et al., 2013)
TLR2	Pro631His	dcSSc	European	Candidate gene	(Broen et al., 2012a)
MIF-173	-173*C	dcSSc	European	Candidate gene	(Bossini-Castillo et al., 2011)
IL12RB2	rs3790567	SSc	European	Candidate gene	(Bossini-Castillo et al., 2012)
CAV1	rs959173	lcSSc	European/ Italian	Candidate gene	(Manetti et al., 2012)
STAT 4	rs7574861 rs10168266	dSSc	Asian/ Chinese	Candidate gene	(Yi et al., 2013)
IRF5	rs20046040	dSSc	European/French	GWAS	(Dieude et al., 2010)
BANK1	rs10516487 rs3733197	dSSc dSSc	European/French European/German	Candidate gene	(Dieude et al., 2009)

The information generated by genetic association studies could prove to be valuable in diagnosis or therapy, though the results have to be interpreted with caution, as the risk alleles are not strongly predicted and these studies have limitations with respect to sample size, whether it is a candidate gene study or a genome wide association study.

Due to the variability of the disease phenotypes, epigenetic modifications that alter gene expression have been suggested as additional factors that could modify the SSc phenotype (Jungel et al., 2011).

1.4. Epigenetic modifications

Epigenetics refers to the heritable changes in gene expression that do not involve changes to the DNA sequence (Bird, 2007). The epigenetic regulation of gene expression is a dynamic process that plays a pivotal role in normal cell growth and differentiation (Strietholt et al., 2008). There are three main epigenetic mechanisms, DNA methylation, histone modification and RNA interference (RNAi), the latter of which will be discussed in further detail in Chapter 3 (Cheng et al., 2008).

1.4.1. DNA Methylation

DNA methylation involves the addition of a methyl group to the fifth carbon in cytosine residues, thus converting these to 5 methylcytosines (Ehrlich et al., 1982). DNA methyltransferases (DNMTs) are responsible for catalysing the methylation process by donating a methyl group to the 5-cytosine residue. DNMT1 is the most abundant, and is responsible for maintenance of hemimethylated sites generated during DNA replication. DNMT2 acts on transfer RNA, while DNMT3a is responsible for methylation during embryogenesis. DNA Methyltransferases are susceptible to inhibition by chemicals and

are sensitive to environmental influences which both have an effect on gene expression patterns (Richardson, 2008).

Importantly, to note that DNA methylation varies between cell and tissue types as it is a dynamic process that involves both methylation and demethyaltion (Liang et al., 2011). When the DNA is methylated, transcription is usually repressed, reciprocally when the DNA is unmethylated, transcription is activated. There are four possible DNA methlylation patterns. The first is the methylation of CpG islands in the promoter regions of genes (Fan and Zhang, 2009). These CpG island regions exceed more than 500 base pairs with GC contents higher than 55% (Illingworth and Bird, 2009). Approximately 60% of human gene promoters are associated with CpG islands, which in their inherent state must be unmethylated to allow transcription to occur (Bird, 2002). The second pattern of DNA methlyation is that of CpG island shores, regions of lower CpG density but still in close proximity to CpG islands. Most tissue specific methylation occurs in these shore regions (Fan and Zhang, 2009). The third pattern occurs in gene bodies, methylated to ensure correct transcription, preventing spurious transcritption initiation (Ball et al., 2009). Finally, hypermethylation of repetitive sequences protecting chromosomal integrity by preventing chromosome instability and translocations (Portela and Esteller, 2010).

1.4.2. Histone Modification

DNA is tightly organised within the chromatin. Euchromatin is uncondensed and transcriptionally active whereas heterochromatin is condensed and transcriptionally inactive rendering the genes in that area silenced. In order to achieve these states of transcriptional activity, the chromatin is dynamically modified by either histone

acetyltransferases (HATs) or histone deacetylases (HDACs). HATs catalyse histone acetylation and this hyperacetylation of the N-terminus of the histones is associated with the opening of the chromatin. This enhances the rate of gene transcription and therefore expression (de Ruijter et al., 2003). Alternatively, HDACs remove the acetyl group from the histones resulting in hypoacetylation, reducing the space between the chromatin and the DNA. This hinders transcription factors from binding to the DNA, leading to the silencing of genes in the region (Briggs et al., 2002).

1.5. Pathogenesis

There has been considerable research toward investigating and elucidating the pathogenic processes involved in the development of SSc. Factors affecting susceptibility and the initiating event remain unknown, however as SSc is a multifactorial disease, there are genetic as well as an environmental components. The complex interaction of fibrogenesis, inflammation and vascular dysfunction that contribute to the development of SSc can be seen in Figure 1.1. In SSc, repeated vascular injury combined with the failure to correctly resolve the inflammatory response and repair the endothelium evokes both adaptive and innate immunologic mechanisms, including accumulation of macrophages and neutrophils in affected tissues. This inflammation phase is characterized by T-cell activation. Vascular remodelling appears to be preceded by endothelial dysfunction. There is consistent evidence that microvascular endothelial cell activation leading to cell damage occurs early in SSc. The cctivated endothelial cells ubiquitously express adhesion molecules, which promote inflammatory infiltrates by enabling the migration of inflammatory cells through the endothelium. However, the initial trigger of endothelial cell activation remains elusive. It is proposed that primary

activation of endothelial cells in SSc includes autoantibodies showing cross-reactivity between epitopes and specific surface molecules of endothelial cells leading to apoptosis (Abraham et al., 2009). Profibrotic factors secreted by activated T-cells promote fibroblast activation and the synthesis and secretion of the extracellular matrix. Persistent production and deposition of extracellular matrix components within connective tissues leads to replacement fibrosis, tissue contraction and permanent scarring (Denton et al., 2006).

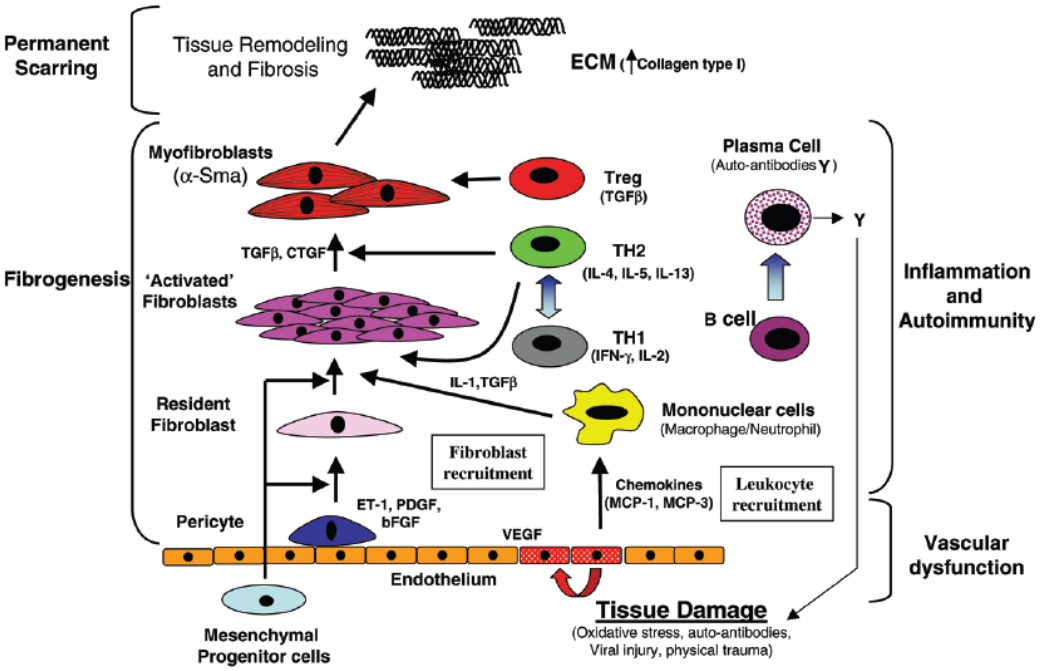


Figure 1.1. The mechanism of fibrogenesis. *Fibrogenesis or tissue damage is critical to the activation, recruitment and expansion of mesenchymal cells, which promotes the secretion of various chemokines and growth factors (Denton et al., 2006).*

1.6. The clinicopathological triad

The disease is a multi-system disease, which is heterogeneous and has an unknown etiology (Varga and Abraham, 2007). Progression of the disease is known to involve

three main systems including the immune system, the vasculature system and the extracellular matrix (ECM) (Whitfield et al., 2003), see Figure 1.2.

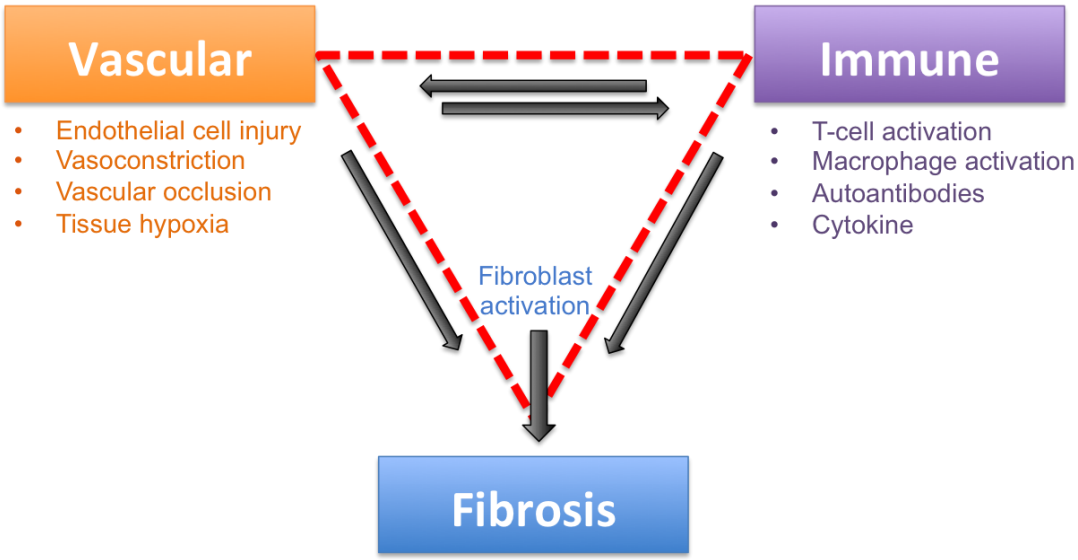


Figure 1.2. Schematic diagram of clinicopathologial triad of systemic sclerosis. *Consisting of vascular damage, immune activation and development of fibrosis.*

Clinically the disease can be separated into diffuse cutaneous systemic sclerosis (dcSSc) and limited cutaneous systemic sclerosis (lcSSc). The clinical manifestation of each of these sub-groups is widespread skin thickening in dcSSc and skin thickening that is limited to the face and distal extremities in lcSSc (Steen, 1998). The most common manifestations of SSc are the presence of specific autoantibodies with more than 90% of patients having antinuclear antibodies in their serum. Anti-topoisomerase 1 antibodies are almost exclusively present in sera from patients with the diffuse form of SSc, with a higher prevalence of these autoantibodies seen in African American patients (Maul et al., 1989). Anti-centromere antibodies are present most often in the sera of patients with the limited form of the disease. These two autoantibodies are mutually exclusive, coexisting in the same patient only in rare instances. Although autoantibodies are very

common in SSc, they are not directly involved in the clinical manifestations of the disease and it is generally accepted that their titres do not correlate with disease activity or clinical severity (Derk and Jimenez, 2003). Anti-RNA-polymerase III (anti-RNAP III) is now included in 2013 American College of Rheumatology (ACR) classification criteria for SSc. This autoantibody is used to predict disease severity. The prevalence of anti-RNAP III among SSc patients has been estimated from 4-22% worldwide with distinct population differences. A higher frequency has been noted in Caucasian populations as seen in England (11.7%) and Sweden (22%), while a lower frequency is noted in Japan (5%). Similar to other autoantibodies present in SSc, anti-RNAP III has low sensitivity (10-10%), but is highly specific for SSc (98.8%) (Satoh et al., 2009). Furthermore, anti-RNAP III is highly associated with the diffuse subtype of the disease as well as associated with scleroderma renal crisis and skin changes. Recently, this autoantibody has been associated with malignancy in patients with SSc. In a study by Moinzadeh et al. (2014) it was observed that there is a significantly increased frequency of cancers among patients with anti-RNAP III compared to ACA and anti-Scl-70.

The majority of SSc patients suffer from Raynaud's phenomenon, which is an episodic event, characterised by pallor and pain in the peripheries in response to cold stress (Young-Min et al., 2001). This symptom is caused by micro-vascular abnormality leading to reduced blood flow resulting in digital ulcers and, in some cases, gangrene (Kuwana, 2006). Other symptoms of SSc include muscle weakness (myositis), problems of the digestive system and pulmonary arterial hypertension (Clements, 2000).

Fibrosis is particularly significant in the diffuse form of the disease (Varga and Abraham, 2007). Basic remodelling of the ECM occurs causing the architecture of the skin to become disrupted and this leads to fibrosis of not only the skin but also many internal organs. The lungs, gastrointestinal tract and heart are the worst affected by the fibrotic process. Most patient morbidity is due to fibrosis of the internal organs (Yazawa et al., 2000). Once fibrosis is initiated, there is escalation of the synthesis of fibrosis through multiple amplification loops that are generated as a consequence of tissue damage, hypoxia and oxidative stress as well as an increase in matrix stiffness, as demonstrated in Figure 1.3. (Bhattacharyya et al., 2012).

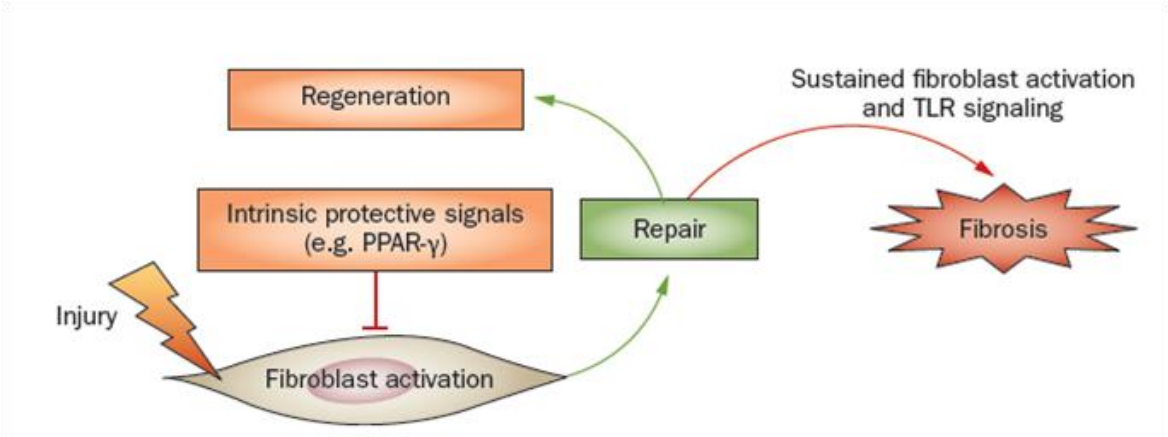


Figure 1.3. Tissue damage resulting in fibrosis. *Following normal injury, fibroblasts are activated initiating repair and thus tissue regeneration is complete. If the injury comes from a recurrent source, TLR ligands activate innate immune signalling, which enhances fibrogenic responses and establishes a self-amplifying vicious cycle of fibrogenesis (Wei et al., 2011b).*

1.7. Understanding fibrosis

1.7.1. Endothelial cells

The endothelium is a highly specialised and complex organ involved in many important functions. It enables a compatible interface facilitating blood circulation, inhibits excessive platelet aggregation and coordinates vascular tone, which serves to inhibit ECM deposition. The endothelium has many prominent endocrine functions, the most

important of which is the control of inflammation (Abraham and Distler, 2007). Healthy functioning of the endothelium is crucial for remodelling of blood vessels during times of tissue growth and repair. Dysfunction of the endothelium is an important component of many human diseases, including those characterized by inflammation and fibrosis (Figure 1.3). Endothelial dysfunction contributes to inflammatory and fibrotic connective tissue diseases, particularly SSc and the dysfunction that is observed results from endothelial cell injury leading to the generation of an inflammatory process and endothelial cell activation (Ross, 1999).

1.7.2. T-cells

T-cells play a crucial role in SSc although their precise role has not been fully clarified. It is likely that T cell-derived cytokines contribute to the development of fibrosis. A study by Fuschiotti et al. (2009) focused on the ability of CD4+ and CD8+ T cells to produce cytokines following *in vitro* activation. They concluded that dysregulation of IL-13 production by CD8+ T cells is important in the pathogenesis of SSc and appears to be critical in the predisposition to more severe forms of cutaneous disease. Abnormalities in the cellular immunity of SSc patients consist of chronic mononuclear cell infiltration of tissues and the dysregulation of lymphocytes, growth factor and the production of autoantibodies, together with an activation and expansion of CD4+T cells which is considered to be important in the development and maintenance of SSc (Besliu et al., 2009).

1.7.3. Fibroblasts

The most common cell type found in connective tissue are the spindle-shaped fibroblasts. These are found in the majority of organs and are essential for connective

tissue homeostatis (Hinz et al., 2007). An imbalance in the deposition of extracellular matrix (ECM) leads to the fibrotic phenotype observed in SSc skin (Varga and Abraham, 2007). Fibroblasts regulate the metabolism of ECM through the expression of matrix metalloproteinases (MMPs) which degrade collagen and the expression of their inhibitors, the tissue inhibitors of metalloproteinases (TIMPs) (Young-Min et al., 2001). The fibroblast cell type is the primary contributor to the fibrosis observed in SSc patients. In connective tissue diseases, fibroblasts migrate towards injured tissue and, due to growth factors secreted by immune cells, differentiate into myofibroblasts (Gilbane et al., 2013). Myofibroblasts accumulate at the site of the injured tissue and deposit and remodel ECM. In normal wound healing, the myofibroblasts are lost from the injury site, whereas in the cases of fibrosis, they remain (Tomasek et al., 2002). The persistent accumulation of the myofibroblasts in connective tissue is responsible for the uncontrolled prodcution of ECM during the develpoment of fibrotic patholgies such as SSc (Shi-wen et al., 2012). Histological analysis of SSc skin has shown an abundance of myofibroblasts involved in lesional skin and fibrotic areas of organs from SSc patients (Chen et al., 2005).

The master regulator of both wound healing and pathological fibrosis is the pleiotropic cytokine, transforming growth factor beta (TGFß) (Leask, 2006, Ihn, 2008, Bhattacharyya et al., 2011). TGFß is secreted by platelets, macrophaghes, T-cells and fibroblasts and promotes fibroblast migration, differentiation, proliferation and survival as well as upregulating the synthesis of ECM components such as collagen (Blobe et al., 2000). An increase in the number of TGFß receptors has been linked to the development of fibrosis. Increased expression of TGFß in SSc fibroblasts suggests that TGFß stimulation is

responsible for the maintenance of the activated SSc fibroblast phenotype, even in the absence of any exogenous stimulus (Yamane et al., 2002, Pannu et al., 2006, Varga and Pasche, 2009).

The main control of TGFß signaling is exercised by the SMAD system, including the SMAD2 and SMAD3 activators and the SMAD7 inhibitor (Varga, 2002). The SMAD (a family of proteins similar to the gene products of the Drosophila gene 'mothers against decapentaplegic' (*Mad*) and the C. elegans gene *Sma*) pathway specifically related to the TGFß pathway and is upregulated in SSc (Mori et al., 2003). SMAD binding elements are found in most of the promoters of TGFß-inducible genes, including pro-collagens and connective tissue growth factor (CTGF). Dysregulation and function of SMAD2 and SMAD3 as well as SMAD7 has been documented in SSc fibroblasts and possibly contribute to the initiation or the perpetuation of the abnormal fibrotic response (Dong et al., 2002, Ishida et al., 2006).

In addition to TGFß, there are other growth factors that are important in the pathogenesis of SSc, such as CTGF and platelet derived growth factor (PDGF) (Zimmermann and Pizzichini, 2013). Levels of CTGF have been observed to be higher in lesional SSc skin compared to normal skin (Wei et al., 2011a). PDGF releases profibrotic mediators such as IL-6 and MCP-1 and is produced by fibroblasts and macrophages. Higher levels of PDGF have been reported in lungs of SSc patients (Ludwicka et al., 1995). Thus, stimulation of TGFß contributes to the SSc fibrotic phenotype via the activation of various pathways including the non-SMAD pathway (Bhattacharyya et al., 2008) and the canonical Wnt signaling pathway (Sato, 2006, Wei et al., 2012).

Histopathology of affected skin biopsies from SSc patients demonstrates a noticeable thickening of the entire dermis and sub dermal tissues, accumulation of thick collagen bundles and thick fibrous tissue extending across adipose tissue (Gilbane et al., 2013). When observing histopathological sections from SSc skin, usually elongated, spindle-shaped fibroblasts can be seen throughout the upper dermis and appear diffusely arranged among thickened collagen bundles. The presence of myofibroblasts is also often observed in affected fibrotic skin (Kissin et al., 2006). Figure 1.4 shows histopathology results for a skin biopsy taken from an SSc patient in the rheumatology clinic at Chris Hani Baragwanath Hospital. These two images show the appearance of increased dermal collagen as well as loss of adipose tissue in this patient.

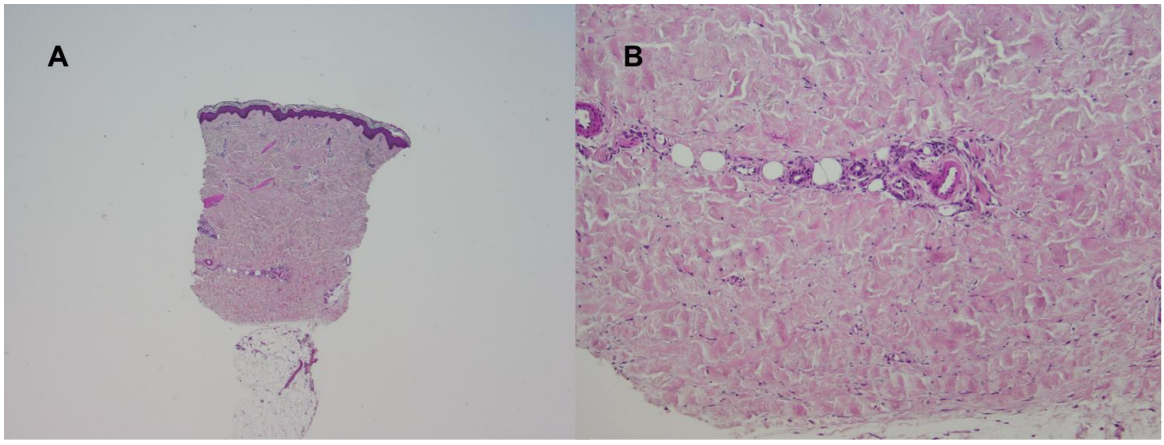


Figure 1.4. Histopathologic features of affected tissue from an SSc patient at Chris Hani Baragwanath Academic Hospital*. A) A biopsy with a squared off appearance and increase in dermal collagen. B) Loss of adipose tissue around skin adnexal structures.*

1.8. Animal models

Animal models help to inform about mechanism of disease and there are models that are able to replicate the different aspects of the human disease phenotype, including fibrosis, vascular and inflammation (De Langhe and Lories, 2015). Fibrosis is the hallmark

feature of the disease and is the major cause of morbidity and mortality in SSc patients. It is therefore not surprising that animal models reflecting this specific phenotype are most commonly used for research (Morin et al., 2015).

The best characterised and most widely used genetic mouse model for SSc is the type 1 tight-skin (Tsk1) mouse. This strain was originally identified by a spontaneous mutation and shows skin with diffuse tethering shortly after birth with more evident tightening as the mice age (Green et al., 1976). A series of elegant genetic mapping studies identified an in-frame tandem partial duplication in the fibrillin 1 gene, as the mutation responsible for the phenotype (Siracusa et al., 1996). The phenotypic effects of this mutation in these mice relate to the central structural role of fibrillin in microfibrils and elastic fibers (Kielty et al., 1998). Mutant fibrillin alters expression of developmental regulators, which suggests that pathogenesis is mediated by the TGFβ and Wnt pathways (Bayle et al., 2008, Lemaire et al., 2010). A limitation of the Tsk1 model is the absence of inflammatory and immune independent pathogenesis.

Bleomycin is a drug used in cancer treatment and has been used as a potent initiator of tissue injury and fibrosis in mice and other animal species (Jimenez and Christner, 1994). The mechanisms for bleomycin-induced tissue injury and fibrosis are complex, including profibrotic mediators such as TGFβ and also innate immune and inflammatory mediators such as IL-1 and IL-6 (Gasse et al., 2007, Saito et al., 2008). A strength of this model is that it is likely to replicate some of the complexity of fibrotic initiation in human disease. In wild-type mice the fibrosis can be lethal, but if mice survive, there is generally slow resolution of the fibrotic pathology (Jimenez and Christner, 1994). This is in contrast to

most human lung pathology but is an important reminder that fibrosis may be reversible under some circumstances. As well as being a well-established model for lung fibrosis, there has been considerable use of bleomycin as an inducer of skin changes that reflect the skin fibrosis in SSc (Yamamoto et al., 1999). The model of bleomycin-induced skin fibrosis is the most widely used model for pathogenic studies of SSc. It has been used to explore candidate therapies for the fibrotic phase of the disease. A limitation of the model is that the process is more appropriate for a prevention paradigm rather than the treatment of established fibrosis. This suggests that the model lends itself better as a model for early stage SSc in the skin (Christner and Jimenez, 2004).

A new model of fibrosis has been described that results from the induced overexpression of Wnt10b (Wei et al., 2011b). These mice show replacement of subcutaneous fat by collagen. Consistent with these *in vivo* effects, Wnt overexpression *in vitro* in fibroblasts and pre-adipocytes show a blockade of adipogenesis and upregulated profibrotic gene expression. These effects are similar to changes seen in SSc skin, suggesting that Wnts might contribute to fibrosis in SSc through altered developmental programming of pre-adipocytes.

A recent study on the most appropriate mouse model to use to study human SSc, skin gene expression was compared in 3 mouse models of sclerodermatous graft-versus-host disease (sclGVHD), bleomycin-induced fibrosis and Tsk1/+ or Tsk2/+ mice. The results were then mapped to human orthologs and compared to SSc skin biopsy-derived gene expression. Gene expression in the sclGVHD and bleomycin-induced fibrosis mouse models corresponded to gene expression patterns observed in the inflammatory

molecular subset of SSc. By contrast, the Tsk2/+ mice showed gene expression corresponding to the fibroproliferative SSc subset. This study reveals similarities in gene expression between different mouse models of SSc and specific molecular subsets of SSc, this will have an impact on the design of future animal model studies as well as help understanding the mechanism of disease (Sargent et al., 2016).

1.9. Gene Expression in SSc

Genome-wide technologies such as microarray and next generation sequencing platforms allow investigators to assess the expression of large numbers of mRNAs simultaneously in cultured cells or a specific tissue. Often the differences detected in gene expression between SSc patients and healthy controls provide insight into the mediators, intracellular pathways and regulators of transcription and how they affect the diseased tissue or cell. The use of these technologies to identify differential gene expression in SSc patients has the potential to advance our understanding of the molecular pathogenesis in end-target tissues and cells in this disease. This topic will be discussed in more detail in Chapter 2, Section 2.1.7.

1.10. Prognosis and treatment

Clinical outcomes in SSc patients have improved in the last decade. The disease is, however, still incurable and the diffuse cutaneous form of the disease carries the highest risk of fatality within the connective tissue diseases, carrying a 55% survival rate at 10 years (Varga and Abraham, 2007).

To date, no single therapeutic intervention has been fully effective in retarding or reversing skin or major organ fibrosis. Several agents have shown variable efficacy, including cyclophosphamide, methotrexate, D-penicillamine and more recently mycophenolate mofetil. Glucocorticoids, either as monotherapy or in combination with other drugs, have been widely used to treat SSc (Kallenberg et al., 1984). The tyrosine kinase inhibitor, Imatinib, was shown to reduce dermal fibrosis in the bleomycin induced fibrosis mouse model (Akhmetshina et al., 2009). However, pilot studies in human SSc patients have shown that the drug has little effect and is associated with a range of side effects (Distler and Distler, 2009). Table 1.5. lists the novel and fibrosis-targeted therapies that are currently available for the treatment of SSc.

The routine use of biologic therapies in other rheumatic diseases has lead clinicians to consider how trageted therapy could be applied in the treatment of SSc. Using targeted therapeutics could generate substantial progress in the understanding of disease progress and pathogenesis. It would be necessary to consider that targeted therapies for SSc may be specific to a particular subset of patients, or a specific stage of disease (Denton and Ong, 2013).

Several drugs have been trialed in SSc, none with convincing or definite evidence of having antifibrotic properties. Some of the drugs are currently on the market for other clinical indications such as Rituximab and Tocilizumab, both RA drugs, as well as Imatinib, a drug for Chronic Myeloid Leukaemia. Other drugs have been specifically designed for

SSc such as CAT-192, which is a biologic targeting TGFβ. All of these drugs have thus far failed to show any benefit.

Table 1.5. Table of targeted, antifibrotic therapies for systemic sclerosis (Beyer et al., 2012b)

Mechanism of Action	**Drugs and compounds**
B cell depletion	Rituximab
Interleukin-6 (receptor) blockade	Tocilizumab
TGFβ-1 neutralising antibodies	CAT-192, Fresolimumab
Tyrosine kinase inhibitors	Imatinib, Dasatinib, Nilotinib
Peroxisome proliferator-activated receptor ϒ antagonists	Thiozolidinediones
Histone deacetylase inhibitors	Trichostatin A, selective HDAC inhibitors
DNA methyltransferase inhibitors	5-Aza-2-deoxycytidine
Inhibition of canonical Wnt pathway	None
Inhibition of the Hedgehog pathway	Smo antagonists
Inhibition of the Notch pathway	ϒ-secretase inhibitors

1.11. Study objectives and aims

The broad objective of the study was to explore the role of altered Wnt pathway gene regulation in the development of skin fibrosis in black South Africans with dcSSc. This was to be achieved through two specific aims:

Specific Aims:

1. Examine differential gene expression, in the skin tissue, of a set of 84 genes in the Wnt signaling pathway using a qPCR assay, and validate a selection of these results by single gene TaqMan gene expression assays. This aim is hypothesis driven

2. Examine the differential expression of microRNAs that could potentially target Wnt pathway genes by small RNA profiling using sRNA-sequencing. This aim is exploratory.

These two aims will be expanded upon in the following two chapters. These chapters will each include a more specific introduction, materials and methods, results and discussion in the context of our current knowledge. Chapter 4 will bring the different aspects of the overall study together in a brief conclusion.

Chapter 2

Wnt pathway gene expression in SSc patients

In recent years, several groups have used microarray technology to analyse the gene expression profile of SSc skin (Whitfield et al., 2003, Gardner et al., 2006). Among the findings, downregulation of the Wnt inhibitory factor (*WIF1*) and upregulation of secreted frizzled related protein 4 (*SFRP4*) have been detected in SSc skin. As the Wnt/ß-catenin signalling pathway plays a critical role in the development of adult tissue homeostasis, it is not surprising that several groups have implicated the dysregulation of this canonical Wnt pathway in the development of fibrosis in SSc (Bayle et al., 2008). The capability of Wnt proteins in the canonical pathway to induce fibroblast activation, together with evidence of chronic Wnt/ß-catenin signalling in tissue samples from patients, supports an important role for this developmental pathway in SSc (Bhattacharyya et al., 2012). This has highlighted the need to better understand the role of the Wnt pathway in the pathogenesis of the disease and to explore the potential of manipulating Wnt/ß-catenin signalling as a proposed novel antifibrotic therapeutic approach.

2.1. Introduction

In 1982 a gene that was activated in virally induced breast tumours in mice was discovered and called *Wnt1* (Wingless-Type MMTV integration site family member 1) (Nusse and Varmus, 1982). A few years later, the *Drosophila Wingless* (*wg*) gene, in *Drosophila melanogaster,* which controls segment polarity during larval development was found to be a

homolog of *Wnt1* (Rijsewijk et al., 1987). In 1989, the first assay to study the Wnt pathway in vertebrates was developed, when mouse *Wnt1* mRNA was injected into early *Xenopus* embryos causing the body axis of the frog to duplicate (McMahon and Moon, 1989). The subsequent combined observations in *Drosophila* and *Xenopus* unveiled a highly conserved signalling pathway, the canonical Wnt cascade.

The Wnt signaling pathway, together with the Notch and Hedgehog pathways comprise the morphogen pathways of development. These signaling cascades are central to regulating embryonic organ development and adult tissue homeostasis. Morphogen pathways are tightly controlled due to their effect on cell proliferation. Under certain physiological conditions, the coordinated activation of these pathways aids in tissue regeneration and cell renewal (Beyer et al., 2012a).

2.1.1. The Notch and Hedgehog pathways

Notch proteins are highly conserved transmembrane receptors, with a principal function in the regulation of developmental processes, such as differentiation and proliferation (He and Dai, 2015). Activation of this pathway requires ligands to interact with Notch receptors to trigger a cascade of proteolytic cleavages by a metalloprotease enzyme (Sharma et al., 2011). Recently, activated Notch signaling has also been observed to have profibrotic activity (Dees et al., 2011a). Activation of Notch signaling induces the expression of alpha smooth muscle actin (α-SMA) and collagen 1 in alveolar epithelial cells in rats with lung fibrosis, suggesting that this pathway is involved in epithelial-mesenchymal transition (EMT) processes (Matsuno et al., 2012). Elevated levels of Notch ligands and receptors have also been reported in several glomerular diseases and tubulointerstitial fibrosis (Niranjan et al.,

2008, Murea et al., 2010). Overexpression of Notch in renal tubular cells is observed and upregulation of Notch1 increases ECM production (Bielesz et al., 2010).

The Hedgehog signaling pathway is a highly conserved pathway that orchestrates the processes of embryogenesis, development and tissue remodeling in many organ systems (Briscoe, 2009). There are three hedgehog genes that control development in vertebrates, of which sonic hedgehog (*SHH*) is the most well studied and understood (Jenkins, 2009). SSH signaling has been implicated in the regulation of tissue repair in injury and in wound healing after tissue damage (Choi et al., 2011). In lung diseases specifically, *SHH* expression is upregulated and it is thought that the pathway is involved in the remodeling of damaged pulmonary epithelium (Stewart et al., 2003). The SHH pathway elicits its effects by activating target genes, of which the best characterized for SHH are *Gli-1* and *Snail1*. The latter is a key transcription factor mediating the EMT and fibroblast migration (He and Dai, 2015). As well as eliciting an activating effect on target genes, SHH is thought to directly control the expression of a number of fibrogenic genes including fibronectin (*FN*) and collagen 1 (*COL1*), genes that are involved in myofibroblast activation and ECM production (Ding et al., 2012).

2.1.2. The canonical Wnt pathway

Signalling by the Wnt family of secreted glycoproteins is a fundamental mechanism that directs cell proliferation, cell polarity and cell fate determination during development and tissue homeostasis (Logan and Nusse, 2004, Pfaff et al., 2011, Akhmetshina et al., 2012). Mutations within genes in the Wnt pathway have been linked to diseases such as cancers (Clevers, 2006). The most critical and well-studied Wnt pathway is the canonical Wnt pathway, which functions by regulating the level of the transcriptional co-activator, ß-

catenin (Figure 2.1). In the absence of Wnt activation, cytoplasmic ß-catenin protein is constantly degraded, preventing ß-catenin from reaching the nucleus and thereby repressing Wnt target genes. Alternatively, when a Wnt ligand binds to the transmembrane Frizzled receptor (FZD) and its co-receptor LRP6 (low density lipoprotein receptor-related protein 6), ß-catenin is phosphorylated making it more stable and also able to migrate into the nucleus, activating Wnt target genes (MacDonald et al., 2009). The canonical Wnt pathway, either directly or indirectly, regulates organ system formation during embryogenesis (Komiya and Habas, 2008).

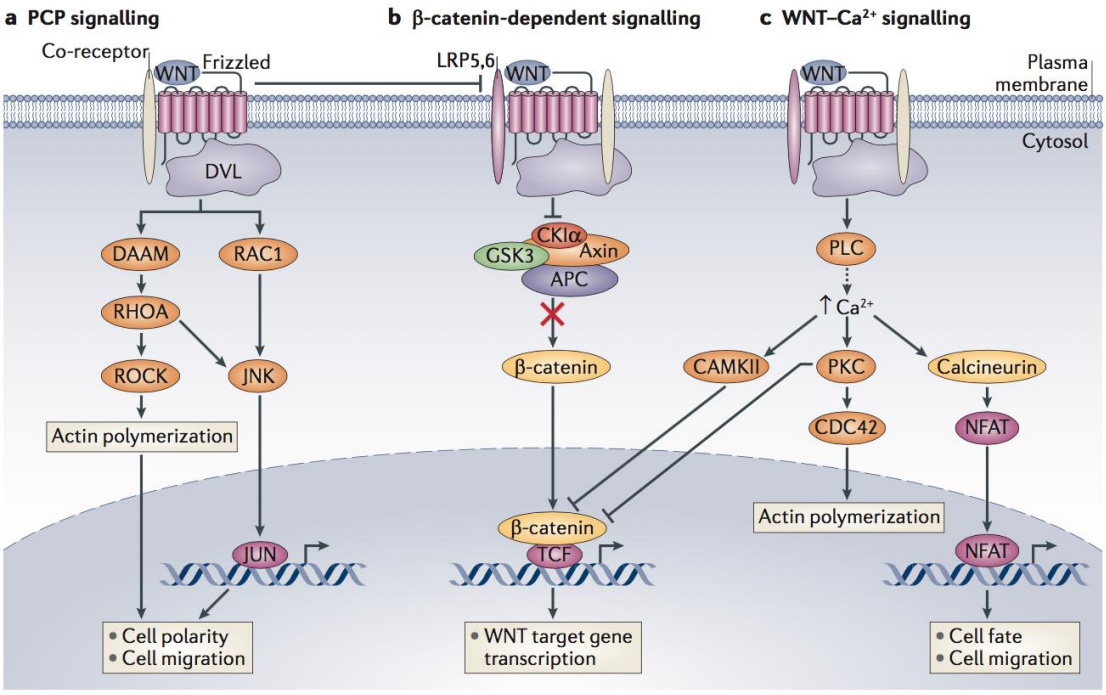


Figure 2.1. The Wnt signalling pathways. *(a) Planar cell polarity (PCP) signalling activates RHO kinase (ROCK) and JUN-N-terminal kinase (JNK). This non-canonical Wnt pathway regulates cell motility, polarity and the morphogenic movements of cells. (b) In the canonical Wnt pathway, Wnt signals via frizzled receptors activate the dishevelled protein, stabilising ß-catenin, which is transported into the nucleus activating transcription of Wnt target genes. (c) The WNT–Ca^{2+} pathway activates Ca^{2+} and calcineurin, leading to stimulation of nuclear factor activated T cells (NFAT). This regulates the downstream transcription of genes that control cell fate and migration (Niehrs, 2012).*

2.1.3. The non-canonical Wnt pathways

Referred to as the β-catenin independent pathways, the non-canonical pathways consist of the planar cell polarity (PCP) and the Wnt/Ca^{2+} pathways (Komiya and Habas, 2008). The defining features of the PCP pathway is its regulation of the actin cytoskeleton for directed migration and that the pathway appears to function independently of transcription (Komiya and Habas, 2008). The Wnt4, Wnt5a and Wnt11 ligands signal via the non-canonical pathway. Wnt11 also plays a crucial role in early axis formation via the canonical pathway (Tao et al., 2005). In the non-canonical pathway, the Wnt signal is mediated through frizzled receptors (FZD) independent of the LRP5/6 co-receptor (He et al., 2004).

The Wnt/Ca^{2+} pathway was discovered when some Wnt ligands and FZD receptors were found to stimulate intracellular Ca^{2+} release from the endoplasmic reticulum via G-proteins (Kohn and Moon, 2005). Wnt5a, Wnt11 and Fzd2 are capable of intracellular Ca^{2+} release, without affecting the stabilization of β-catenin (Slusarski et al., 1997). The role of the Wnt/Ca^{2+} pathway during embryogenesis includes the negative regulation of dorsal axis formation and regulation of tissue separation (Slusarski et al., 1997). It is clear that Wnt signaling is complex and may exert effects on a number of developing cellular systems.

2.1.4. The role of the Wnt pathway in fibrotic disease

ß-catenin plays a cell-type specific role in normal wound healing (Bielefeld et al., 2011). Levels of ß-catenin are elevated in mesenchymal cells during the proliferation phase, thus believed to regulate proliferation rate and invasiveness of dermal fibroblasts. When a response to wound healing is dysregulated a number of epithelial and mesenchymal disorders can occur, such as aggressive fibromatosis and Dupuytren's contracture.

Fibroproliferative disorders range in severity but all display biochemical and cellular similarities to those observed in dysregulated wound healing (Bowley et al., 2007).

In aggressive fibromatosis, for example, a locally invasive soft tissue lesion composed of a clonal proliferation of spindle (fibroblast-like) cells, somatic mutations in the ß-catenin gene result in ß-catenin protein stabilization and thus activation of Wnt target genes. It is also thought that, as ß-catenin is located in the nucleus in aggressive fibromatosis, this could suggest a role in nuclear transcription (Tejpar et al., 2001).

Dupuytren's contracture is another example of a localised fibrotic disease where benign fibrosis of the palmar surface of the hands and fingers occurs. A recent a case-control study showed that 11 SNPs in nine different genes were associated with the disease in over 2000 patients. Of note, six of the nine genes were found to act in the Wnt pathway, namely *WNT4, SFRP4, WNT2, SULF1, RSPO2* and *WNT7B* (Dolmans et al., 2011).

Renal interstitial fibrosis and glomerular sclerosis are hallmark features of diabetic neuropathy and the canonical Wnt pathway has been implicated in the development of this fibrosis (He et al., 2009). In a study using normal mouse kidney and a model of interstitial kidney fibrosis, induced by unilateral urethral obstruction the expression of Wnt ligands, Frizzled receptors and the DKK family of inhibitors was studied. There were various patterns of gene expression observed between the fibrotic and normal kidney, but the genes that were upregulated in the fibrotic kidney specifically were *Wnt2b*, *Wnt3*, *Wnt9a*, *Fzd3*, *Fzd10*, *Dkk3* and *Dkk4* (He et al., 2009). Ultimately this study demonstrated that there is an upregulation in Wnt signalling following tissue injury.

In a study of Hepatitis C induced fibrosis, eight Wnt pathway genes were significantly associated with fibrosis risk, including *SFRP2*, *SFRP1*, *FZD1* and *FZD4* (Liu et al., 2013). The Wnt pathway has also been implicated in the pathogenesis of pulmonary fibrosis (Pfaff et al., 2011) and in the development of asthma (Sharma et al., 2010, Wang et al., 2013a). Idiopathic pulmonary fibrosis (IPF) is a lung disease of unknown etiology and is characterised by alterations of the alveolar epithelium, myofibroblast activation, and increased ECM deposition. Recently, reactivation of the developmental WNT/β-catenin pathway has been linked with pulmonary fibrosis. In the bleomycin murine model of pulmonary fibrosis, Aumiller et al. (2013) observed the proinflammatory cytokine IL-1β to be significantly dysregulated, in alveolar epithelial Type II cells, following treatment with WNT3a. They also reported significant up-regulation of IL-1β and IL-6 in bronchoalveolar lavage fluid in bleomycin-induced lung fibrosis *in vivo*. Taken together these findings reveal that the alveolar epithelium is a relevant source of proinflammatory cytokines induced by active WNT/β-catenin in pulmonary fibrosis. Another study by Lam et al. (2014) indicated that the Wnt coreceptor, Lrp5, is a driver of lung fibrosis in mice and a marker of disease progression and severity in humans with IPF. Altered gene expression of Wnt signalling pathway genes was found in a study profiling patients with osteoarthritis, suggesting that both the Wnt pathway and *TGFß* may in part explain the pathogenesis of this disease (Hopwood et al., 2007). There is mounting evidence that the Wnt pathway is dysregulated in many different disorders that have an element of fibrosis, albeit in different organs and tissues.

2.1.5. The morphogen pathways in systemic sclerosis

Morphogen signaling pathways are not only crucial to normal development but are also implicated in the pathogenesis of fibrotic disorders. There is growing evidence that indicates enhanced activation of Wnt, Notch, or Hedgehog signaling is a driving force in a variety of fibrotic diseases, including SSc (Beyer and Distler, 2013).

There are three ligands that stimulate the hedgehog signaling pathway; desert hedgehog (DHH), Indian hedgehog (IHH), and sonic hedgehog (SHH). SHH is the predominant ligand in skin. The hedgehog ligands undergo lipid modifications, which affect the properties of these ligands, enhancing membrane association and potentiating secretion. Gli-proteins in hedgehog signaling are protected from phosphorylation and thus degradation (Gallet, 2011). In fibrotic SSc tissue, overexpression of Shh leads to accumulation of Gli-proteins, which results in increased target gene transcription. Experimental evidence demonstrates that Shh induces fibroblast activation and collagen release, thus the pro-fibrotic effects of hedgehog signaling can be used to target the development of fibrosis (Horn et al., 2012).

Activation of the Notch signaling occurs upon binding of membrane-bound Notch ligands to notch receptors on a target cell. Notch signaling is essential for cell differentiation and tissue homeostasis in both normal development and during adulthood (Dees et al., 2011a). Dysregulated Notch signaling is linked to many pathological conditions, including the development of fibrosis, where Notch signaling is activated in SSc skin samples (Dees et al., 2011b). Notch signaling is also activated in mouse models of SSc, where it has been shown that inhibition of the Notch pathway can inhibit experimental dermal fibrosis (Kavian et al., 2010). Apart from SSc, enhanced Notch signaling seems to be crucially involved in renal

fibrosis (Sirin and Susztak, 2012).

2.1.6. The Wnt pathway in systemic sclerosis

Several animal model studies of SSc suggest that there is dysregulation of the Wnt pathway. In the tight skinned (Tsk) mouse model has been used to understand the phenotypic skin changes of SSc even though it lacks pathologic features such as an early inflammation (Smith and Chan, 2010). In this model, perturbations in Wnt/ß-catenin signalling aggravate markers of injury and fibrosis in a variety of different tissues (Lam and Gottardi, 2011). The expression of Wnt-10b is increased in mice with bleomycin-induced fibrosis. Furthermore, transgenic mice expressing Wnt-10b showed dermal fibrosis, fibroblast activation and increased collagen deposition. Explanted fibroblasts from these mice demonstrated persistent Wnt/β-catenin signalling and elevated collagen and α-smooth muscle actin gene expression. The authors concluded that these Wnt-10b–transgenic mice represent a novel animal model for investigating Wnt signalling in the setting of fibrosis (Wei et al., 2011b).

As the Wnt/ß-catenin signalling pathway plays a critical role in the development of adult tissue homeostasis, it is not surprising that several groups have implicated the dysregulation of this canonical Wnt pathway in development of fibrosis in SSc (Bayle et al., 2008). These groups used microarray technology to analyse the gene expression profile of SSc skin (Whitfield et al., 2003, Gardner et al., 2006). Among the findings, downregulation of the Wnt inhibitory factor (*WIF1*) and the upregulation of secreted frizzled related protein 4 (*SFRP4*) were found in SSc skin. Skin samples from SSc patients have also shown increased levels of ß-catenin and of the target genes such as *AXIN2* (Wei et al., 2011a, Akhmetshina et al., 2012, Nusse, 2012). The role of this developmental pathway in SSc is suggested by the

potential of Wnt proteins in the canonical pathway to induce fibroblast activation alongside evidence of chronic Wnt/ß-catenin signalling in tissue samples (Bhattacharyya et al., 2012).

The activation of the Wnt signalling pathway in various fibrotic diseases, as well as its potent profibrotic effects in various model systems, highlights the canonical Wnt pathway as an interesting candidate for anti-fibrotic therapies (Akhmetshina et al., 2012, Beyer et al., 2012c). The potential ability to block Wnt/ß-catenin signalling would represent a novel antifibrotic therapeutic approach, thus the role of the pathway in the development of fibrosis deserves further investigation.

2.1.7. Previous gene expression studies in SSc

Gene expression focused studies have found that analyzing gene expression in end-target tissues displays more robust and consistent differences than those found in cultured cells. This is not only true in SSc, but also in other diseases such as cancer (Perou et al., 2000, Ross et al., 2000).

Early studies of differential gene expression in dcSSc skin showed obvious and consistent changes in gene expression when comparing the SSc skin samples to healthy control samples. One study used microarray technology to analyse and compare gene expression changes in SSc skin from affected tissue obtained from the forearm and unaffected tissue obtained from the back, from four SSc patients and four healthy controls. The results indicated more than 2700 differentially expressed genes when comparing either affected and/or unaffected skin samples with unaffected controls (Whitfield et al., 2003). Two

important findings resulted from this study. Firstly, that the affected and unaffected tissue samples often showed very similar, and in some cases nearly identical, disease-specific patterns of gene expression. This finding was similar to our own study looking at the differential expression of *MMP1*, *TIMP1* and *HGF* in scleroderma skin (Frost et al., 2012). Secondly, differences in gene expression could be mapped not only to fibroblasts but also to a variety of other cell types, including epithelial cells, smooth muscle cells and T-cells (Milano et al., 2008). Another study, that also used microarray technology, analysed the affected skin from eight dcSSc patients compared to seven controls. In this study, 1800 differentially expressed genes were identified including those of the TGFβ and Wnt pathways, suggesting that these growth factors may play important roles in disease pathogenesis (Gardner et al., 2006).

The heterogeneity of SSc with respect to the clinical phenotype is well recognized, but less well understood at the molecular level. To address this, a genome wide study using skin biopsy samples from dcSSc, lcSSc and localised (morphea) scleroderma and healthy control individuals were performed. The study design assessed affected (forearm) and unaffected (back) skin biopsies from the same patients (Milano et al., 2008). Seventeen of 22 patients showed nearly identical, disease-specific gene expression between affected and unaffected skin tissue pairs. A set of 995 “intrinsic” genes were selected because they showed the most consistent expression differences between forearm-back sample pairs for individuals, but the most variability across patients. This selection emphasised consistent, patient-specific gene expression signatures rather than the differences between affected and unaffected skin biopsies from the same patient. The results of the study indicated that the patients could be grouped into four categories based on the differential expression signatures

identified. One subset of patients showed a gene expression signature suggesting cell proliferation, which included two distinct diffuse subsets. A second subset included dcSSc, lcSSc and morphea patients and showed a gene expression signature suggesting inflammation. A third subset that included mostly lcSSc patients and two healthy controls showed a heterogeneous gene signature, termed the "limited" subset. Finally, a subset consisting mainly of healthy controls as well as several lcSSc and dcSSc patients showed gene expression most comparable to healthy controls and were thus termed the "normal-like" subset (Milano et al., 2008). These results have been replicated in a second independent sample of dcSSc patients compared to healthy controls where the results indicated that the patients can be grouped according to the proliferation, inflammatory and normal-like groups (Pendergrass et al., 2012). Although it is interesting that the gene expression signatures in the SSc skin biopsies did not divide into the two major clinical disease subtypes of diffuse and limited cutaneous disease, these results demonstrate that the heterogeneity of the disease can be captured objectively using gene expression profiling (Milano et al., 2008). The most important outcome of these studies is that like breast cancer, SSc can be divided into multiple subsets of patients all of whom display different patterns of gene expression (Perou et al., 2000, Sorlie et al., 2001). These differential gene expression profiles or signatures are probably driven by different molecular mechanisms and thus may potentially require different therapies (Julka et al., 2008). The altered *in vitro* behavior of SSc fibroblasts has been studied and has been considered a useful correlate for *in vivo* changes of fibroblast function. More recently, however, gene expression studies performed on isolated fibroblasts from SSc skin have provided insights and brought to light some controversies related to the utility of cultured fibroblasts in such studies (Zhou et al., 2001, Tan et al., 2005, Zhou et al., 2005). Using microarray technology, Zhou et al. identified

only 32 differentially expressed genes using an uncorrected t-test ($p < 0.05$) when analysing the cultured fibroblast cells from dermal tissue of eight dcSSc and three lcSSc patients compared to cultured fibroblast cells from seven healthy controls (Zhou et al., 2001).

There are no published studies focusing specifically on Wnt signalling in Africans, where dcSSc is the predominant disease subtype. The specific aim for the study in this chapter was to examine differential gene expression for a set of 84 genes in the Wnt signaling pathway. Using a qPCR assay (Qiagen) in skin biopsies from SSc patients and controls. Ethics approval for the study was obtained through the Human Research Ethics Committee (Medical) of the University of the Witwatersrand, with certificate number M120512 (Appendix A).

2.2. Materials and Methodology

2.2.1. Participants

2.2.1.1. Systemic sclerosis patients

Consenting black South African SSc patients from the Chris Hani Baragwanath Academic Hospital (Appendix B) who fulfilled the 1980 ACR criteria for classification of scleroderma (Masi et al., 1980), had diffuse cutaneous disease (dcSSc) (LeRoy et al., 1988) and with less than 5 years of disease duration, defined as the start of non-Raynauds phenomenon features of SSc, were included in the study. Patients with a history of scleroderma related renal crisis were excluded. Nine patients were recruited from each of whom two skin biopsies were taken, one from the forearm (clinically affected skin) and one from the back (clinically unaffected skin). Clinical and laboratory features that were documented by the same clinician at the time of taking the biopsy samples were:

1. Modified Rodnan skin score (MRSS):

Clinical assessment of the extent and severity of subcutaneous skin thickening was done using the MRSS, where on a scale from 0 (normal) to 3 (severe) at 17 anatomic areas were evaluated, yielding a maximum score of 51 (Furst et al., 1998). The assessment was done by a single trained medical professional to avoid inter-observer variability and on the day when the skin biopsies were done.

2. Interstitial lung disease:

Interstitial lung fibrosis was defined on the basis of bibasal lung fibrosis evident on either plain radiographs of the chest or high resolution computed tomography of the lungs with a predominantly restrictive pattern on pulmonary function testing.

3. Pulmonary hypertension:

Defined as a resting right ventricular systolic pressure of >40mmHg on echocardiography (Gaine and Rubin, 1998).

4. Myositis:

Symmetrical muscle weakness with at least 2 of the following three features; typical electromyelographic changes, raised serum creatine kinase, muscle degeneration or inflammation (Bohan and Peter, 1975a, Bohan and Peter, 1975b).

5. Acute phase response tests:

C-reactive protein (CRP) was done using nephelometry (normal range between 1.0 and 3.0mg/L, high >10mg/L). The Erythrocyte sedimentation rate (ESR) was done using an automated analyser (normal <30mm/hour).

6. Serum complement C3 and C4:

Serum levels of C3 and C4 are determined antigenically by a turbidimetric procedure. Turbidity testing determines the cloudiness of a solution and measuring the loss of intensity

of a light beam that passes through that solution. Levels of between 0.2 and 1.0 are considered low (Palarasah et al., 2011).

7. Valentini global disease activity score:

The Valentini disease activity score was used to assess overall disease activity. It scores for a high MRSS, presence of scleredema, presence of digital necrosis, severity of RP, presence of arthritis, change in cardio respiratory symptoms, abnormal lung diffusion capacity (DLCO), raised ESR >30mm/hour and hypocomplementemia with maximum score of individual parameters ranging 0.5 to 2 giving a maximum total of 10. The disease is considered active if the score is equal to or greater than 3 according to the Valentini disease activity score (Valentini et al., 2001).

2.2.1.2. Control subjects

Control skin samples were obtained from eight consenting (Appendix B), otherwise healthy individuals undergoing reconstructive plastic surgery at Helen Joseph Academic Hospital. The skin samples were mainly either from the breast (n=4) or from the forearm (n=4). Table 2.1 is a summary of the control samples.

Table 2.1. Control sample demographic data including age and sex

Control	Age (years)	Biopsy site	Sex
1	29	Forearm	F
2	33	Forearm	M
3	40	Breast	F
4*	35	Breast	F
5	38	Breast	F
6	31	Forearm	M
7	34	Forearm	M
8	30	Breast	F

*This sample was unusable for laboratory assays due to an inability to amplify the cDNA during qPCR, and was therefore discarded

2.2.2. Laboratory Methods

2.2.2.1. Collection and Transportation of samples

Two 4mm punch skin biopsies were taken from each patient, one from clinically affected skin taken 4cm proximal to the ulna styloid (Whitfield et al., 2003) on the dorsum of the left forearm and one from clinically unaffected skin taken from the upper back. Skin samples from control individuals were collected from either the forearm (n=4) or breast (n=4). The skin samples for both patients and controls were immediately placed in a 15ml tube filled with RNAlater (Qiagen) and stored at -20°C until RNA preparation, which occurred within 6 months of the biopsy being taken. The laboratory work for this project was undertaken and completed at the Center for Genomic Regulation (CRG) in Barcelona, Spain.

2.2.2.2. RNA Extraction

The tissue was weighed and then transferred into 1000µl Qiazol (Qiagen), in which the cells were disrupted using a Polytron homogenizer (Fischer Scientific). RNA was purified using the RNeasy miRNA kit, according to the manufacturer's protocol (Qiagen) (Appendix C).

RNA quality and quantity

Two methods were used to assess the quality and quantity of RNA. Firstly 1µl of each sample was loaded onto a Nanodrop 1000 (Thermo Scientific) to assess the absorbance at two different wavelengths. The ratio of absorbance at 260 nm and 280 nm is used to assess the purity of the RNA. A ratio of ~2.0 (260/280) is generally accepted as an indication of RNA uncontaminated by protein. If the ratio is appreciably lower, it may indicate the presence of protein. Secondly, the RNA quality was assessed using the Bioanalyser (Agilent Technologies). An RNA Integrity Number (RIN) score is generated for each sample on a scale of 1-10 (1=lowest; 10=highest) as an indication of RNA quality. A RIN number of greater than seven is considered suitable to proceed with library preparation. The RNA concentration and RIN numbers for the samples used in this project can be found in Appendix D.

2.2.2.3. Wnt pathway RT^2 Profiler PCR Array

cDNA synthesis

RNA extraction from tissue produces small amounts of RNA. These small yields are not always sufficient for reliable gene expression analysis, even when using sensitive techniques such as qPCR. For this reason the RT^2 PreAMP cDNA Synthesis Kit and RT^2 PreAMP Pathway Primer Mix specific for the Wnt pathway (Qiagen) was used for this experiment. The protocol consists of two steps, cDNA synthesis followed by preamplification. During the

amplification step, the RT^2 PreAMP Pathway Primer Mix enables amplification of cDNA specific for the genes targeted by the RT^2 Profiler PCR Array. These kits allow for cDNA synthesis from as little as 1–100 ng total RNA from fresh/frozen tissue samples. The workflow for the qPCR array is shown in Figure 2.2.

Gene expression qPCR array

The Human Wnt Signalling Pathway RT^2 Profiler PCR Array (Qiagen) uses qPCR to profile the expression of 84 genes that are involved in Wnt-mediated signal transduction. This array contains Wnt signalling ligands and receptors as well as other downstream signalling molecules of the Canonical, PCP and Wnt/CA^{2+} pathways. In addition, regulators of Wnt signalling are included as well as downstream target genes (Appendix E). The array also contains five housekeeping genes in order to perform relative expression analysis. The 384-well qPCR array was run on the ABI 7900HT Real-time PCR machine (Applied Biosystems). A complete protocol can be found in Appendix F.

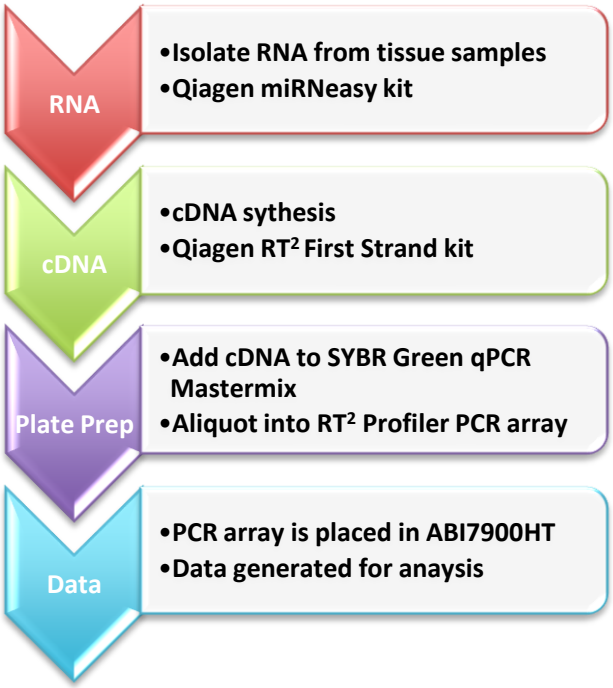


Figure 2.2 Summary of the qPCR RT^2 Profiler Array workflow

qPCR data analysis

Qiagen provides a web-based qPCR array analysis programme for the gene expression arrays (http://www.sabiosciences.com/pcrarraydataanalysis.php). In order to verify the results obtained from this web-based programme, data were also analysed using an R/Bioconductor package called HTqPCR. Gene expression was normalised to the expression of at least one housekeeping gene, and then fold change expression for each gene was calculated using the $2^{-\Delta\Delta Ct}$ method as previously described (Livak and Schmittgen, 2001). Differential expression between sample groups was considered significant with a fold change >2 and an adjusted p-value equal to or less than 0.05 (Benjamini–Hochberg rule).

qPCR data normalisation

Selecting the correct housekeeping gene for normalisation is extremely important in a qPCR experiment. mRNA transcription comparisons across different samples can only be deciphered with normalization relative to an appropriate housekeeping gene prior to assessment of differential expression. The transcription of the housekeeping gene should be constant across all samples and should not be regulated or influenced by the experimental parameter under investigation (i.e. case vs. controls). The pre-designed RT^2 Profiler qPCR array used in the present study contains five housekeeping genes with which to normalise the data. During quality control of the data, manual selection of the appropriate housekeeping gene is allowed by using the raw C_t threshold data from these genes. It is possible to normalise the data to either one or all of the housekeeping genes present on the array. It is important to note that the best candidate housekeeping genes are the genes where the difference in C_t values is most constant across samples.

2.2.2.4. Validation of RT^2 Profiler PCR Array data

cDNA Synthesis

Reverse transcription was done using the High Capacity RNA-to-cDNA kit (Thermo-Fisher Scientific), with an input of 250ng of total RNA per sample. Reactions for each RNA sample as well as NRT (no reverse transcriptase) controls were set up as per the standard protocol in the kit. The cDNA was then quantified, normalised and stored at -20°C.

TaqMan Gene Expression Assays

To accurately measure gene expression across samples in a qPCR experiment, samples of equal concentration must be used. In the validation experiments, 25ng of total cDNA was added to each reaction. The TaqMan gene expression assays were ordered from off-the-shelf pre-designed assays available from Thermo-Fisher Scientific. As per qPCR requirements, three endogenous controls, or housekeeping genes were selected for the validation experiments; *ACTB*, *HPRT1* and *RPLP0*. Six other genes that showed significant differential gene expression were also selected for validation (see Section 2.3.8). Samples were run in triplicate for each assay, NRT as well as NAC (no amplification) controls were used as well as a calibrator sample on each qPCR plate. The TaqMan gene expression assays were run in 384-well plates in the ABI-7900HT Real-Time PCR machine. The protocol for the TaqMan qPCR is available in Appendix G.

Validation qPCR data analysis

After the qPCR run, the data were analysed using the RQ (relative quantification) software on the ABI 7900HT Real-Time PCR machine. Following the instruction manual for this purpose, specific parameters for the analysis of the data must be configured. This includes

selecting the endogenous control samples, adjusting baseline and threshold values and viewing the amplification plots. Once this has been done, the data can be exported for further analysis using a choice of software. For the purpose of this study, the R/Bioconductor packages ReadqPCR and NormqPCR were used (Perkins et al., 2012). An overview of the workflow used in this study is shown in Figure 2.3.

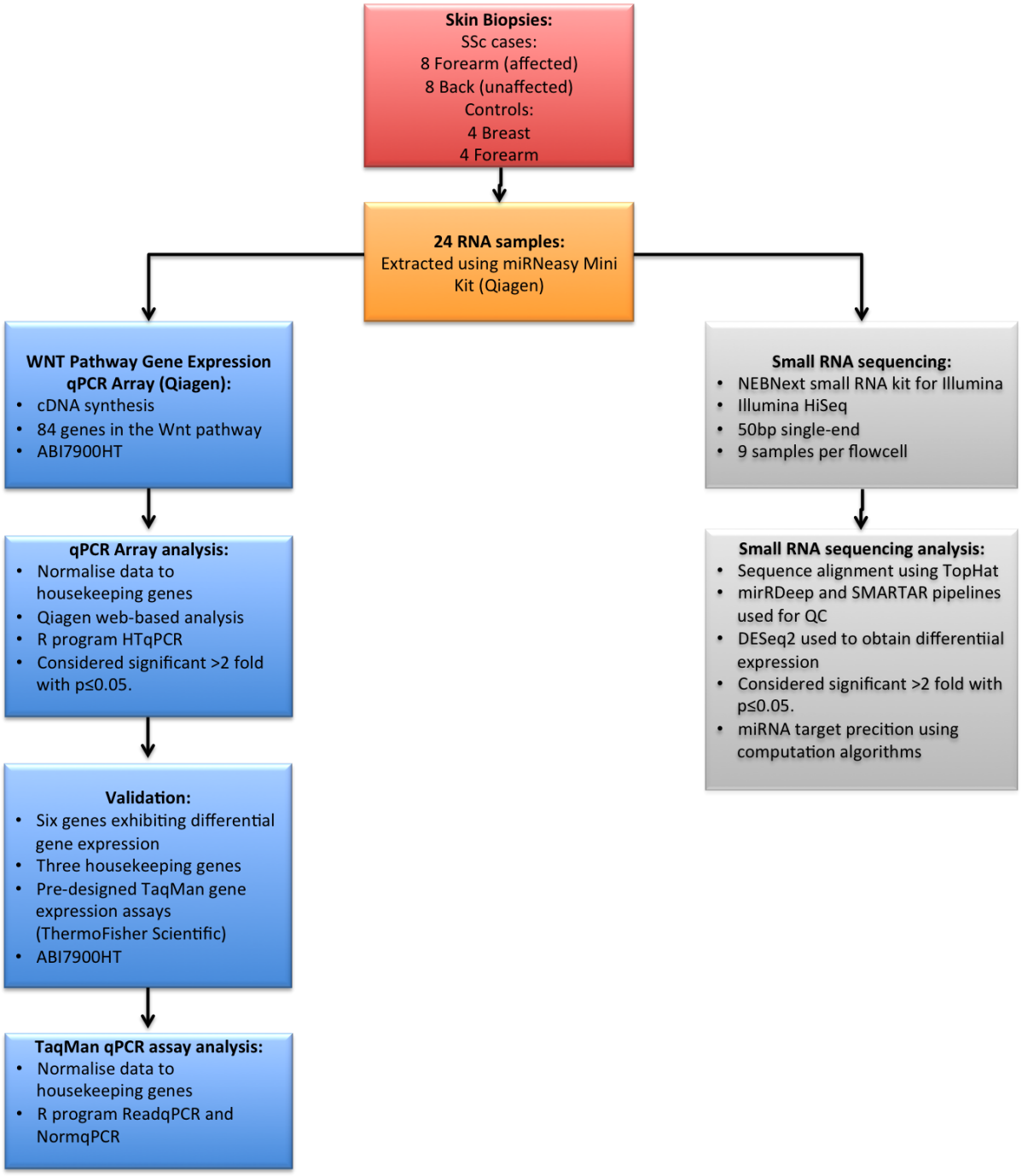


Figure 2.3. Schematic diagram of the methodology used in this study. *The qPCR techniques and analyses described in blue are relevant for Chapter 2.*

2.3. Results

2.3.1. Demographic and clinical features of patients with SSc

The demographic, clinical and laboratory data for the patient group are summarised in Table 2.2. The complete clinical data are presented in Appendix H. Notably, all patients recruited for the study were black, the majority was female (n=7), and the mean disease duration was just under 3 years. The group had extensive skin involvement, active disease as measured by the Valentini score, half had ILD and two thirds had muscle involvement.

Table 2.2. Summary of demographic, clinical and laboratory data for the 8 systemic sclerosis patients included in this study

Clinical feature	Patients (n=8)
Female: Male ratio	7:1
Age in years - *mean (SD*)	52.6 (5.8)
Disease duration in months - *mean (SD*)	31.5 (15.6)
Valentini Disease activity - *mean (SD*)	4.2 (1.7)
MRSS - *mean (SD*)	18.3 (11.7)
Involved skin score - *mean (SD*)	1.87 (0.83)
Interstitial lung disease	50% (n=4)
Myositis	37.5% (n=3)
CRP - *mean (SD*)	12.5 (7.06)
Elevated ESR	75% (n=6)
ANA positive	100% (n=8)
Low C4	100% (n=8)

MRSS - modified Rodnan skin score, CRP - C-reactive protein, ESR - erythrocyte sediment rate
ANA - anti-nuclear antibodies

The clinical characteristics of these patients reflects what has been observed in bigger cohorts (Tager and Tikly, 1999). In keeping with the results from that previous study, all patients were ANA positive and this is not surprising as all the patients had diffuse disease. The large proportion of patients who had an elevated ESR is again similar to previous findings in SSc patients of African descent (Tager and Tikly, 1999). Nine patient samples were collected for the study, but patient 1 (samples P1 and 1B) was excluded from subsequent analysis due to a technical artifact in the data.

2.3.2. Demographic data for control individuals

The mean age of the individuals in the control samples was 33 years and 5 out of the 8 of the individuals were female.

2.3.3. RNA Quality

The samples were all good quality with an average RIN of 8 (6.2 – 9.2). These data can be found in Appendix D. The validation experiments were done almost two years after the initial RNA extraction and experiments. It would have been optimal to check the quality of the RNA before the validation, especially as they had been transported from Barcelona to Johannesburg. Unfortunately the RNA quality could not be assessed for the validation experiments as there was very little RNA available, and therefore the RNA quality was unknown.

2.3.4. qPCR array normalization

For this study, three iterations for normalization were performed in order to determine the best option for the most appropriate differential expression comparison for the Wnt pathway genes. The RT^2 Profiler PCR Array includes five housekeeping genes, the most

stable of which should be chosen for normalisation. The Ct values across samples for the five housekeeping genes can be seen in Figure 2.4, where *ACTB* (*Actin-ß*) and *HPRT1* (*hypoxanthine phosphoribosyltransferase 1*) displayed consistent and reliable expression across samples with little variation in Ct values across cases and controls. In the first iteration of data normalization, all samples were normalised relative to the expression of *ACTB* before comparative analyses were performed. The second iteration was performed using two housekeeping genes, *ACTB* and *HPRT1*. Finally, data were normalised to three housekeeping, as literature suggests normalization should be done to multiple housekeeping genes (Silver et al., 2006) genes using *ACTB*, *HPRT1* and *RPLP0*.

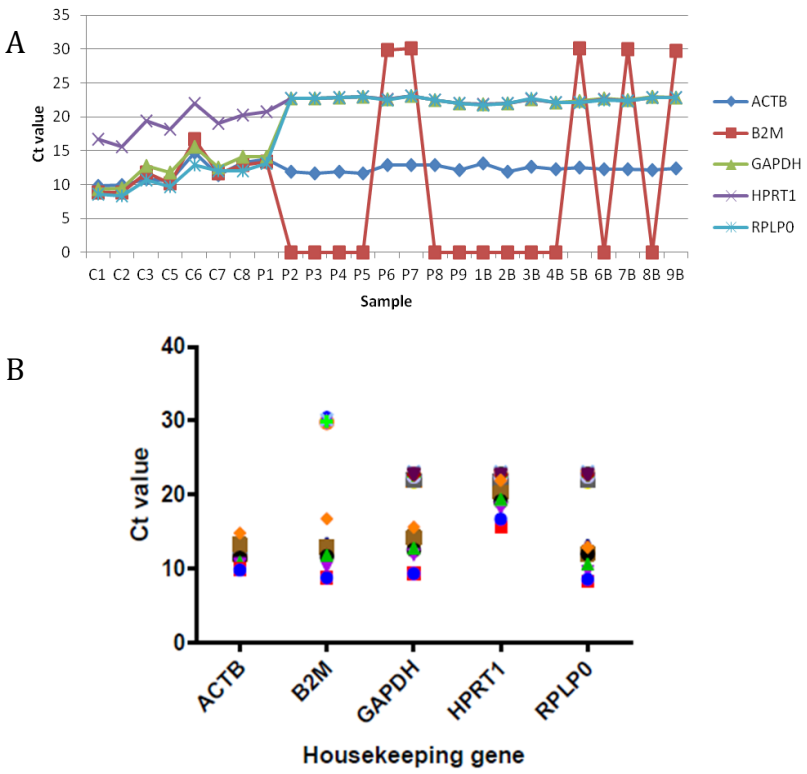


Figure 2.4. Housekeeping gene selection. *Graph A plots the Ct values across patients for the five housekeeping genes. Graph B plots of the Ct values for all samples according to the housekeeping genes. These graphs indicate that the most stable and consistent gene expression of housekeeping genes for normalisation are ACTB and HPRT1.*

The labeling system for the samples was P1 to P9 for the 9 forearm samples and 1B to 9B for the back samples from SSc patients, in later analyses only 8 patients were included (Patient 1 was excluded as explained below). To determine the clustering of the samples according to their gene expression profiles, a principal component analysis (PCA) was performed (Figure 2.5). When considering this plot, it is interesting to note that Patient 1 behaves differently to the other patients, as the forearm sample (P1) can be seen within the cluster of controls samples (C) and the back sample (1B) does not cluster with any group in the PCA. Samples from patient 1 were therefore excluded. Of interest is the segregation of the patient samples into two distinct clusters each containing both forearm and back samples.

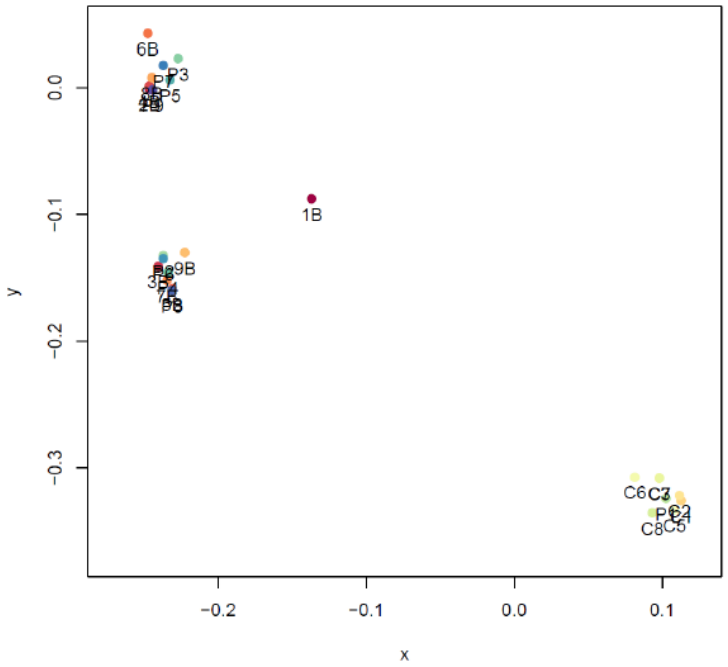


Figure 2.5. Principal component analysis plot containing all samples analysed. *This plot clearly shows the two sub-groups of patient samples clustering separately from each other and from the control samples. The two samples from Patient 1 do not cluster in the two patient clusters and was therefore excluded.*

As there are two distinct sub-groups into which samples from patients (forearm and back samples in both clusters) cluster in this study, it was decided to re-analyse the data separating by the forearm samples from the back samples before analysis.

Principal Component Analysis (PCA) was performed by separating the forearm samples and the back samples to understand the sub-grouping of the patient samples (Figure 2.6). Two distinct clusters form in each of the PCA plots for the patients (PCA plot A has the forearm samples only and PCA plot B has the back samples only). Forearm samples P2, P4, P6 and P8 cluster together (plot A), as do the back samples for these same patients in (plot B) (2B, 4B, 6B and 8B). In both plots the other cluster contains samples from the four remaining patients; P3, P5, P7, P9 and 3B, 5B, 7B, 9B.

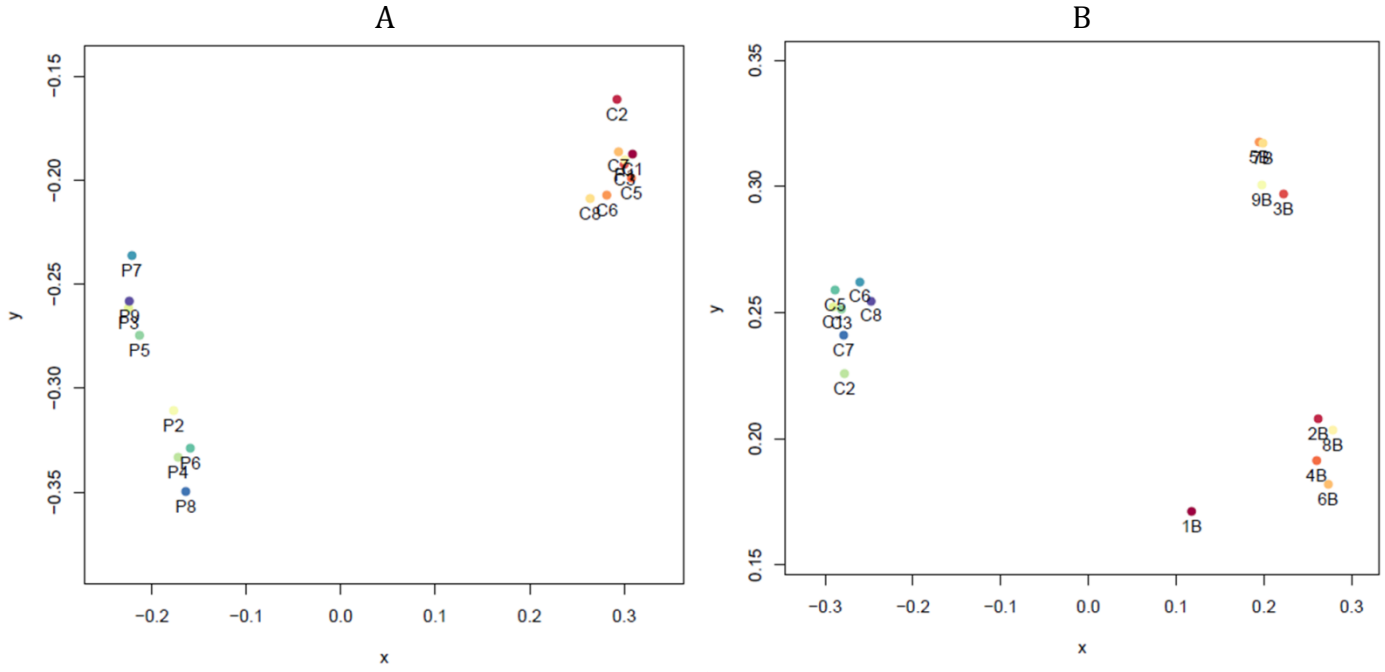


Figure 2.6. PCA plots for forearm samples and back samples, each with controls. *Plot A shows the forearm samples (P1-P9) and the controls, with two clear clusters forming for the patients. Plot B depicts the back samples (1B-9B) and the controls, once again with two distinct clusters forming for the patient samples.*

Due to the clustering of the samples in the PCA plots of Figure 2.6, the order in which the samples were processed in the data generation experiments was scrutinized to exclude a possible batch effect. Closer inspection of the dates on which the samples were processed indicates that there is unlikely to be a batch effect (Appendix I). Therefore the way in which the samples were handled and processed is not the cause of the clustering the samples in the PCA plots.

2.3.5. Wnt pathway gene expression

After each iteration of data normalization, mRNA expression and relative fold-changes were calculated for each of the 84 Wnt pathway genes on the array using the web-based analysis software (Qiagen) and the HTqPCR analysis program in R. Heatplots were generated in order to gain a better understanding of gene expression patterns. Figure 2.7 shows the three heatplots for the different analyses.

In Figure 2.7 there are several clusters of genes identified in the heatplot using the two housekeeping genes to normalize the data. These clusters are colour coded according to the observed differential expression of the genes within the clusters. The red cluster contains genes that are upregulated in all SSc skin samples, both affected and unaffected skin, compared to controls. The green cluster contains genes that are downregulated in all SSc samples, both affected and unaffected skin, compared to controls. The blue cluster contains genes that are generally upregulated in all SSc samples compared to controls, although this cluster of genes shows heterogeneous differential expression, some genes being upregulated in some but not all the samples.

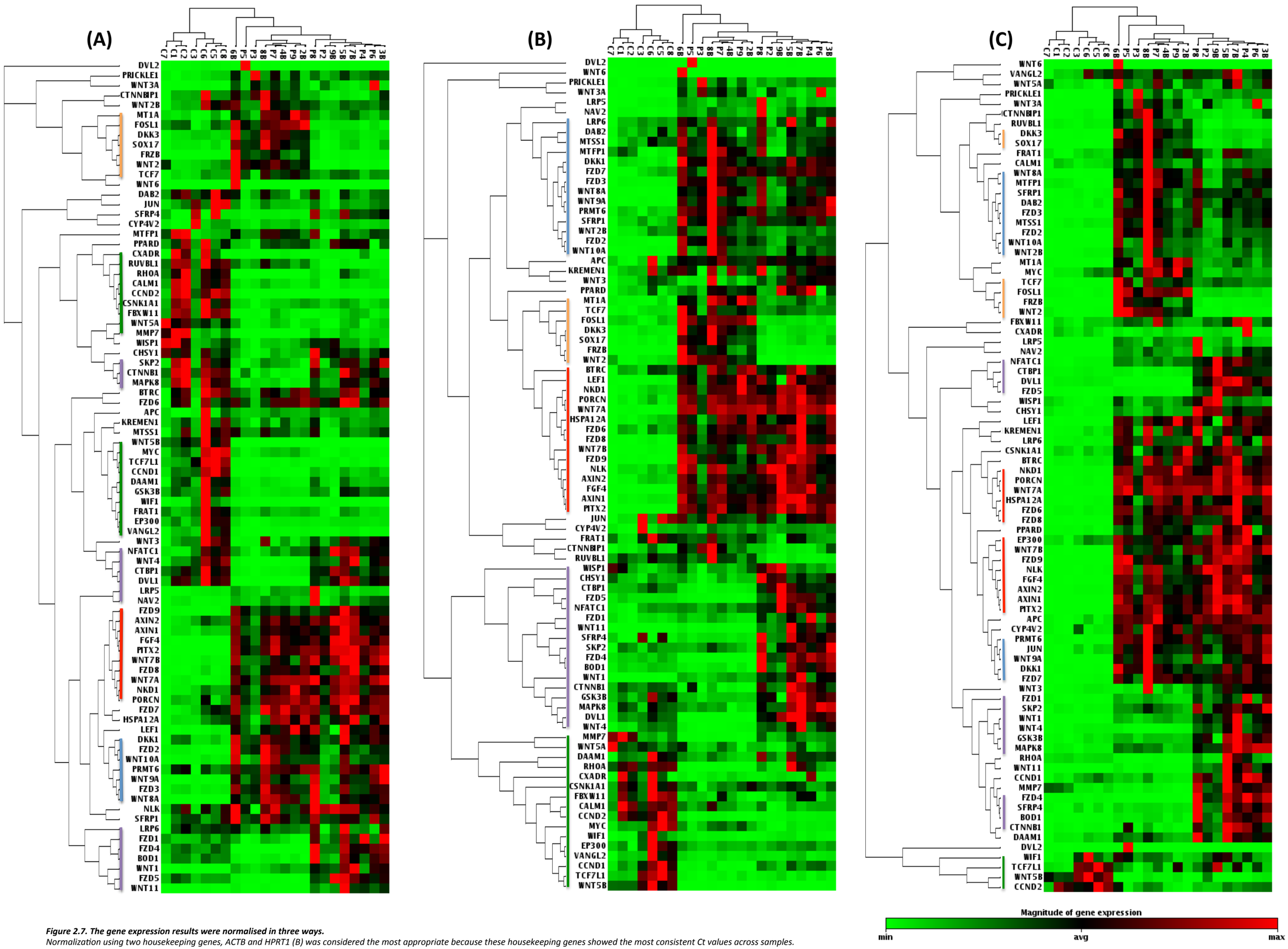


Figure 2.7. The gene expression results were normalised in three ways.
Normalization using two housekeeping genes, ACTB and HPRT1 (B) was considered the most appropriate because these housekeeping genes showed the most consistent Ct values across samples.
For each comparison the clusters of genes were colour-coded according to the gene expression pattern observed. Gene upregulated in all SSc skin samples, both affected and unaffected, compared to controls (Red).
Genes that are downregulated in all SSc samples, both affected and unaffected, compared to controls (Green). Genes generally upregulated in all SSc samples compared to controls, although differential expression is heterogeneous (Blue).
Finally genes, which, according to their differential expression, differentiate the patient samples into the two distinct group, as observed in the PCA plots (Orange and Purple). (A) Normalization using only ACTB and (C) Normalization using ACTB, HPRT1 and RPLP0

Finally the orange and the purple clusters contain genes that, according to their differential expression, differentiate the patient samples into the two distinct clusters (each containing forearm and back samples from all patients, though never a forearm and a back sample from the same patient), shown more clearly in the PCA plots in Figures 2.5 and 2.6. It is also worth noting that across all three iterations of normalization, the clustering of the samples for patients and controls is identical (Figure 2.8). A description of the colour coding and patient groups is summarized in a table in Appendix J.

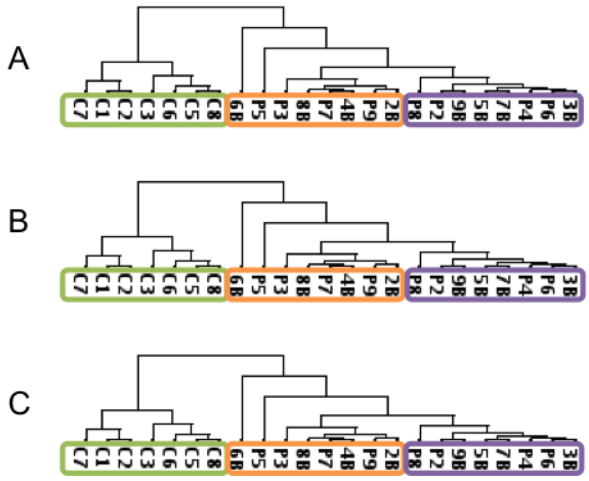


Figure 2.8. Clustering of samples from the gene expression heatplots. *(A) Normalisation performed using only ACTB, (B) normalization using ACTB and HPRT1 and (C) normalisation using three housekeeping genes, ACTB, HPRT1 and RPLP0. The green cluster of samples are the control samples, the orange group will be referred to as sample cluster A, and the purple group will be referred to as sample cluster B. Note that samples are paired, for example P2 (forearm) is paired with B2 (back) from patient 2.*

Only results for data normalised to two housekeeping genes will be presented and discussed. The results of the normalization against one and three housekeeping genes can be found in the appendices. Data normalised to *ACTB* (Appendix K) and then *ACTB*, *HPRT1* and *RPLP0* (Appendix L).

2.3.6. Differentially expressed genes in both affected and unaffected skin samples compared to controls

Relative gene expression in the patient samples (both affected and unaffected) as well as controls can be seen in the heatplot (Figure 2.7, (B)). For a large proportion of the genes, all the patient samples (affected and unaffected skin) display a different gene expression profile compared to controls. These differences are most prominently observed in the red, blue and green gene clusters in the heatplots.

Firstly, in the red gene cluster, 15 of the 84 genes present on the qPCR array, were upregulated in both the affected skin and the unaffected skin samples compared to controls, Figure 2.9.

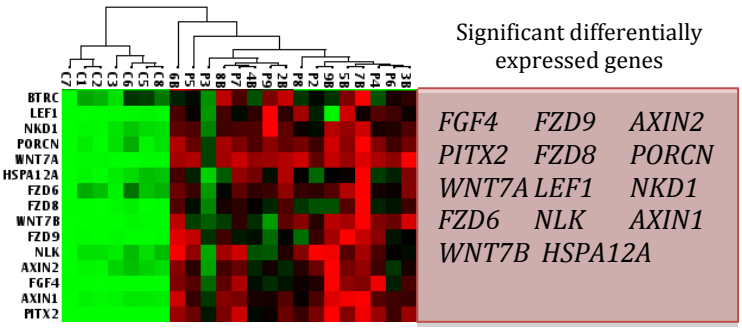


Figure 2.9. Section of heatplot containing the red cluster of genes. *15 are observed to be upregulated in affected and unaffected SSc skin compared to controls, 14 of these significantly differentially expressed.*

Only Fourteen of these 15 genes were significantly differentially expressed (Adj. $p<0.05$) in both affected and unaffected skin compared to controls (Table 2.3).

Table 2.3. Genes significantly upregulated in SSc cases both affected and unaffected skin, compared to controls (red gene cluster)

	Wnt signalling pathway qPCR Array					
Gene	**Affected skin v Controls Fold change**	**Adj p-value**	**Unaffected skin v Controls Fold change**	**Adj p-value**	**Affected skin v Unaffected skin Fold change**	**Adj p-value**
FGF4	19.99	*0.00957*	20.28	*0.00532*	-1.40	0.59
PITX2	10.54	*0.00426*	10.77	*0.00213*	-0.08	0.96
WNT7A	8.09	*0.00638*	8.30	*0.00426*	-0.25	0.95
WNT7B	7.23	*0.01596*	7.77	*0.01064*	-1.05	0.59
FZD9	7.11	*0.01915*	7.62	*0.01170*	-1.00	0.65
FZD8	6.45	*0.00319*	7.01	*0.00851*	-0.29	0.85
LEF1	6.09	*0.01809*	5.67	*0.01915*	-0.82	0.56
NKD1	4.35	*0.01277*	4.75	*0.00745*	-0.91	0.60
AXIN1	4.24	*0.00106*	4.67	*0.00106*	-1.88	0.59
AXIN2	3.92	*0.00851*	4.27	*0.01277*	-1.55	0.59
PORCN	3.20	*0.00532*	3.48	*0.00319*	-1.28	0.59
HSPA12A	2.96	*0.02766*	3.68	*0.01489*	-1.05	0.59
FZD6	2.18	*0.01489*	2.62	*0.00957*	-0.82	0.56
NLK	2.04	*0.02553*	2.23	*0.01596*	-0.71	0.65

Amongst the upregulated genes two are Wnt signaling molecules (*WNT7A* and *WNT7B*) and three are frizzled receptors (*FZD6, FZD8* and *FZD9*). Two of the upregulated genes, *AXIN1* and *AXIN2* are antagonists to the Wnt pathway. This mixture of Wnt ligands, frizzled receptors and pathway antagonists emphasizes the complexity of signaling and that dysregulation throughout the signaling cascade of the pathway could contribute to disease pathogenesis. Notably *LEF1* is upregulated in SSc skin. *LEF1* binds to B-catenin in the nucleus

to initiate transcription of downstream Wnt pathway target genes, such as *FGF4*, which is observed as the gene with the highest magnitude of differential expression.

Secondly, the blue gene cluster contains genes that are generally upregulated in both affected and unaffected SSc skin compared to controls, although the differential expression is relatively heterogeneous. Fourteen genes are observed in this cluster in the heatplot, while only 10 of these reach significance (Adj. p<0.05) (Figure 2.10).

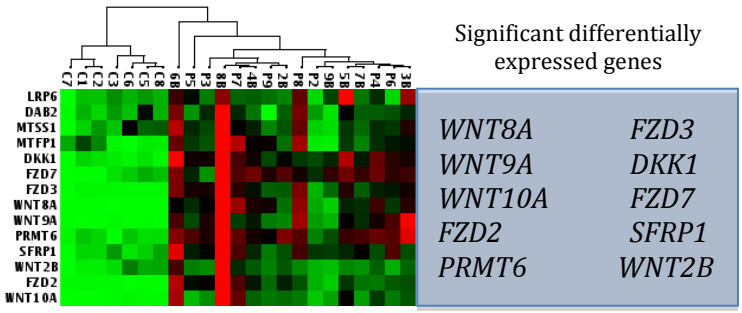


Figure 2.10. Section of heatplot containing the blue cluster of genes. *14 are observed to be upregulated in affected and unaffected SSc skin compared to controls, 10 of these significantly differentially expressed. The expression pattern in this cluster is heterogeneous, this could be due to the high expression observed in sample 8B, which could be due to a normalization artefact.*

The 10 significantly differentially expressed genes are shown in Table 2.4. Notably, there are four Wnt ligands upregulated in this group, *WNT8A*, *WNT9A*, *WNT10A* and *WNT2*. Three frizzled receptors are upregulated, *FZD2, FZD3* and *FZD7* as is one pathway antagonist, *DKK1.* Again there is dysregulation across the signaling cascade of the pathway, although this dysregulation is more heterogeneous across patient samples than is observed in the red gene cluster.

Table 2.4. Genes upregulated in SSc cases, both affected and unaffected skin compared to controls, although differential expression observed is relatively heterogeneous (blue cluster)

	Wnt signalling pathway qPCR Array					
Gene	**Affected skin v Controls Fold change**	**Adj p-value**	**Unaffected skin v Controls Fold change**	**Adj p-value**	**Affected skin v Unaffected skin Fold change**	**Adj p-value**
WNT8A	16.21	*0.01383*	15.97	*0.02340*	-1.50	0.60
WNT9A	7.03	*0.02340*	7.14	*0.02447*	0.33	0.96
WNT10A	6.22	*0.02872*	6.83	*0.03191*	-0.67	0.65
FZD2	6.00	*0.02021*	6.21	*0.02766*	-0.58	0.65
FZD3	5.49	*0.01170*	5.67	*0.02128*	-0.51	0.59
DKK1	3.66	*0.00213*	3.98	*0.01702*	-1.32	0.65
FZD7	3.47	*0.01064*	3.99	*0.00638*	-1.32	0.59
SFRP1	2.93	*0.01702*	3.05	*0.02660*	-1.00	0.65
PRMT6	2.59	*0.00745*	2.82	*0.01383*	-0.86	0.59
WNT2B	2.13	*0.03936*	2.59	*0.04255*	-0.81	0.59

Lastly, the green cluster of genes contains the genes that were observed to be mostly downregulated in affected and unaffected SSc skin compared to controls (Figure 2.11).

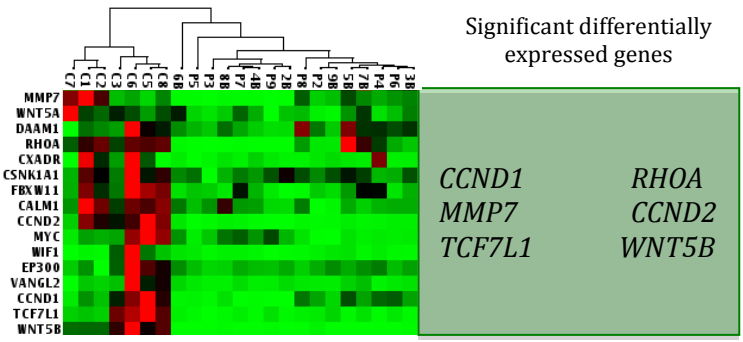


Figure 2.11. Section of heatplot containing the green cluster of genes. *16 are observed to be downregulated in affected and unaffected SSc skin compared to controls, 6 of these significantly differentially expressed.*

In the heatplot, 16 genes are observed in this cluster, although only 6 of these genes were observed as significantly underexpressed. The significantly differentially expressed genes are shown in Table 2.5.

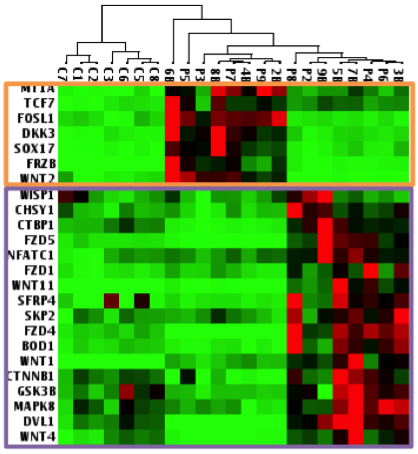
Table 2.5. Genes significantly downregulated in both affected and unaffected SSc skin compared to controls

	Wnt signalling pathway qPCR Array					
Gene	**Affected skin v Controls Fold change**	**Adj p-value**	**Unaffected skin v Controls Fold change**	**Adj p-value**	**Affected skin v Unaffected skin Fold change**	**Adj p-value**
CCND1	-1.93	*0.04681*	-2.02	*0.04149*	-0.39	0.95
MMP7	-3.23	*0.04468*	-2.85	*0.04894*	-0.28	0.94
TCF7L1	-3.58	*0.03298*	-3.67	*0.03617*	-0.06	0.96
RHOA	-4.28	*0.02128*	-3.80	*0.04681*	-0.05	0.96
CCND2	-5.20	*0.02234*	-4.82	*0.01809*	-0.28	0.85
WNT5B	-9.59	*0.02447*	-9.97	*0.02021*	-0.43	0.71

WNT5B is a known initiator of the non-canonical Wnt pathway. The other genes that are notably downregulated are *CCND1*, *CCND2* and *MMP7*, and are downstream target genes of the activated Wnt signaling pathway. An interesting finding in the heatplot, where for some of the genes, the controls display differential expression within the control sample group. Closer inspection of this reveals that controls 1, 2, 6 and 7 were those samples taken from forearm tissue and controls 3, 5 and 8 were those samples taken from breast tissue. Clearly for these specific genes; *MYC, WIF1, EP300, VANGL2*, *CCND1, TCF7L1* and *WNT5B* there is, to some degree, tissue specific differential gene expression observed in the control samples.

2.3.7. Differential gene expression differentiating the two clusters (A and B) and their relationship to patient groups 1 and 2

In the orange and purple gene clusters the differential gene expression patterns are opposite depending on which patient group (1 and 2) the SSc affected and unaffected skin samples cluster in according to the PCA plots shown in Figures 2.5 and 2.6. The affected skin samples of Patients 2, 4, 6 and 8 display upregulation of the genes in the purple gene cluster, while the unaffected skin samples are downregulated for these genes. For the second patient group, Patients 3, 5, 7, and 9, the genes in the orange cluster are upregulated in the affected skin samples and downregulated in the unaffected skin samples. This is shown graphically in Figure 2.12.



	Patient Group 1 (2, 4, 6, 8)	Patient Group 2 (3, 5, 7, 9)
Affected SSc skin	Upregulated genes	Upregulated genes
	Downregulated genes	Downregulated genes
Unaffected SSc skin	Upregulated genes	Upregulated genes
	Downregulated genes	Downregulated genes
Controls	Downregulated genes	Downregulated genes

Figure 2.12. Genes in the orange and the purple gene clusters that are differentiating the two patient groups, 1 and 2. *The two patient groups show opposite gene expression patterns for the subset of those genes in the orange and purple clusters. The affected skin of patients in Group 1 shows upregulation of genes in the purple cluster, while the unaffected skin show a "normal-like" expression profile. The affected skin of patients in Group 2 shows upregulation of genes in the orange cluster, while the unaffected skin show a "normal-like" expression profile.*

The pattern of gene expression observed for the orange and purple gene clusters in Figure 2.12 show distinct differences in the SSc patient affected and unaffected skin samples. The differential gene expression for Patient Group 1 (Patients 2, 4, 6 and 8) and Patient Group 2 (patients 3, 5, 7 and 9) is shown in Tables 2.6 and Table 2.7, respectively.

Table 2.6. Differential gene expression observed in Patient Group 1 for the orange and purple gene clusters. *The affected and unaffected skin for the patients in this group (Patients 2, 4, 6 and 8) exhibit opposite patterns of gene expression for the genes in these two clusters.*

Affected SSc skin vs Controls					
Gene	**Fold change**	**Adj p-value**	**Gene**	**Fold change**	**Adj p-value**
CHSY1	2.87	*0.0102*	***MT1A1***	-2.88	*0.003*
CTBP1	2.42	*0.0019*	***TCF7***	-10.46	*0.041*
FZD5	6.28	*0.0002*	***DKK3***	-2.78	*0.003*
NFATC1	4.92	*0.0007*	***SOX17***	-3.54	*0.003*
FZD1	5.67	*0.019*	***FRZB***	-9.4	*0.001*
WNT11	17.93	*0.019*			
SKP2	2.5	*0.0167*			
FZD4	7.72	*0.0012*			
BOD1	2.5	*0.0167*			
WNT1	21.51	*0.0012*			
CTNNB1	1.9	*0.0093*			
MAPK8	2.92	*0.0341*			
DVL1	2.5	*0.0024*			
WNT4	3.55	*0.0241*			
Unaffected SSc skin vs Controls					
Genes	**Fold change**	**Adj p-value**	**Gene**	**Fold change**	**Adj p-value**
MT1A1	7.47	*0.005*	***CHSY1***	-6.46	*0.006*
TCF7	11.87	*0.006*	***CTBP1***	-4.91	*0.001*
FOSL1	14.31	*0.001*	***FZD5***	-3.75	*0.001*
SOX17	2.31	*0.027*	***NFATC1***	-2.55	*0.019*
FRZB	10.09	*0.006*	***FZD1***	-2.28	*0.052*
WNT2	14.74	*0.003*	***WNT11***	-9.65	*0.042*
			SFRP4	-2.28	*0.052*
			SKP2	-5.63	*0.068*
			FZD4	-3.48	*0.031*
			BOD1	-2.55	*0.019*
			WNT1	-3.51	*0.001*
			CTNNB1	-4.91	*0.001*
			MAPK8	-2.78	*0.003*
			DVL1	-6.52	*0.003*
			WNT4	-9.09	*0.04*

In Patient group 1, affected skin, 14 of the 17 genes in the purple cluster are upregulated while 5 of the 7 orange cluster genes are downregulated compared to controls. In the unaffected skin, 6 of the 7 orange cluster genes are upregulated while 15 of the 17 purple cluster genes are downregulated compared to controls.

Table 2.7. Differential gene expression observed in Patient Group 2 for the orange and purple gene clusters. *The affected and unaffected skin for the patients in this group (Patients 3, 5, 7 and 9) exhibit opposite patterns of gene expression for the genes in these two clusters.*

Affected SSc skin vs Controls					
Gene	**Fold change**	**Adj p-value**	**Gene**	**Fold change**	**Adj p-value**
MT1A1	24.13	*0.002*	***CTBP1***	-10.67	*0.004*
TCF7	6.94	*0.001*	***FZD5***	-4.08	*0.005*
FOSL1	11.00	*0.003*	***NFATC1***	-2.57	*0.043*
DKK3	21.39	*0.002*	***FZD4***	-2.57	*0.043*
SOX17	34.78	*0.002*	***BOD1***	-1.92	*0.033*
FRZB	27.11	*0.002*	***MAPK8***	-13.72	*0.04*
WNT2	15.03	*0.069*	***WNT4***	-20.92	*0.032*
Unaffected SSc skin vs Controls					
Genes	**Fold change**	**Adj p-value**	**Gene**	**Fold change**	**Adj p-value**
CHSY1	2.79	*0.001*	***TCF7***	-8.85	*0.046*
CTBP1	3.15	*0.003*	***SOX17***	-5.68	*0.046*
FZD5	11.19	*0.012*	***FRZB***	-8.37	*0.001*
NFATC1	7.14	*0.001*			
FZD1	6.92	*0.003*			
WNT11	3.15	*0.009*			
SKP2	3.65	*0.005*			
FZD4	7.05	*0.003*			
BOD1	5.65	*0.001*			
WNT1	5.31	*0.004*			
MAPK8	2.26	*0.008*			
DVL1	4.07	*0.003*			
WNT4	5.74	*0.007*			

There are a smaller number of genes that reach a differential gene expression level of significance when analyzing the Patient Group 2 compared to the controls. In affected skin, all 7 of the orange cluster genes are upregulated while only 7 of 17 purple cluster genes are

downregulated. In unaffected skin, 13 of 17 purple cluster genes are downregulated while 3 of the 7 orange cluster genes are upregulated.

2.3.8. Gene expression patterns and specific clinical features

Subgroup analysis with respect to the presence of interstitial lung disease (ILD) and inflammatory myositis (present in 4 out of 8 and 3 out of 8 patients, respectively), showed three patients with ILD (Patients 2, 6 and 8) and the three patients with myositis (Patients 2, 4 and 6) all clustered into a single gene expression defined cluster, such that their affected skin samples fall into cluster B and the unaffected skin samples fall in cluster A. Thus, the majority of patients who exhibit either ILD or myositis and therefore, a more inflammatory response to disease cluster in patient group 1 according to differential gene expression (Figure 2.13.). The affected skin samples of Patient Group 1 fall into cluster B while the unaffected skin from these patients fall into cluster A. The opposite is true for Patient Group 2; their affected skin samples are in cluster A while their unaffected skin samples are in cluster B.

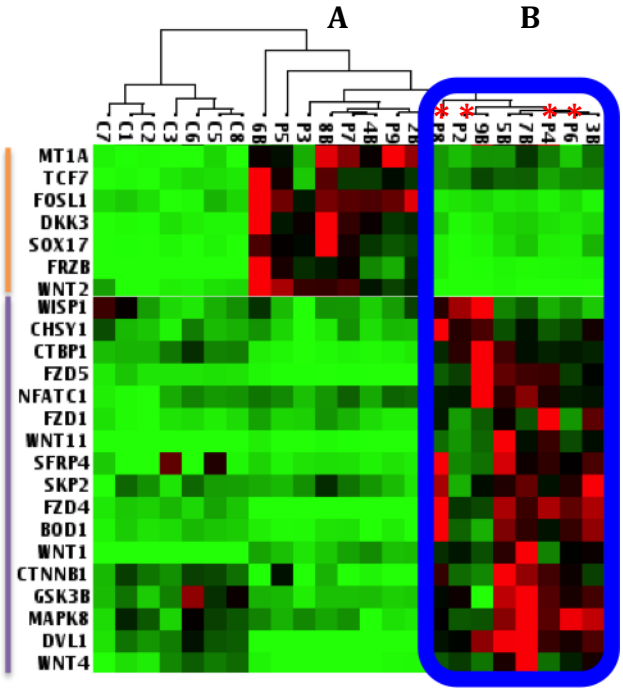


Figure 2.13. The gene clusters marked in orange and purple show genes, showing those genes with differential expression between cluster A and cluster B. *Patients with ILD and myositis are observed to have their affected skin samples segregate mostly in cluster B, highlighted in blue and their unaffected skin samples segregate mostly in cluster A. These patients affected skin samples are indicated in the figure with an asterisk (*).*

Patient numbers are too few to do a robust and convincing correlation between gene expression and the clinical symptoms of ILD and myositis. However, many of the genes that are upregulated in patient group 1 affected skin samples in cluster B such as *WNT1, WNT11* and *MAPK8* are mediators of an inflammatory response. Since the affected skin sample for these patients with either ILD or myositis fall into cluster B, and it is known that the extent of skin involvement can often be a proxy for the extent of organ involvement in the patient, it makes sense for them to cluster in this way.

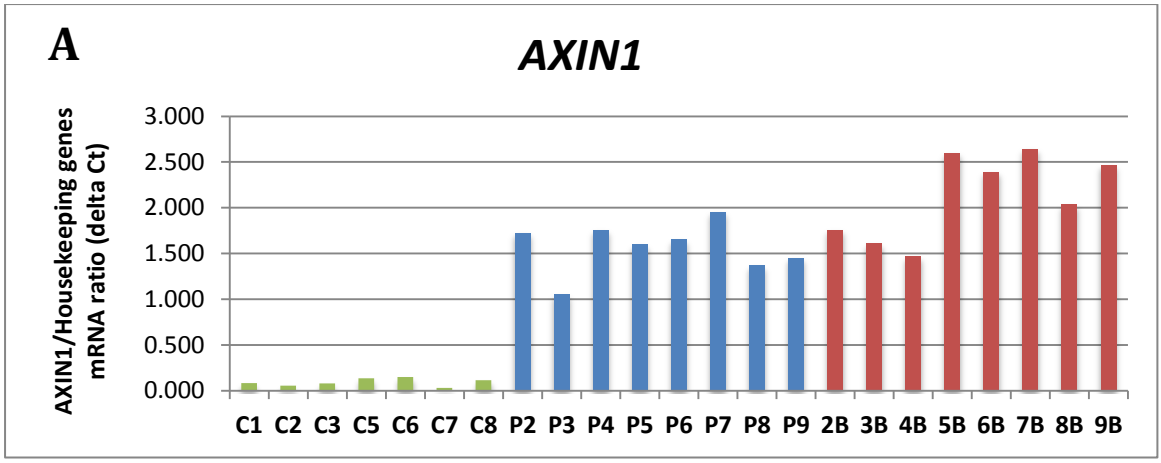
2.3.9. Validation of RT^2 Profiler qPCR Array using single gene TaqMan assays

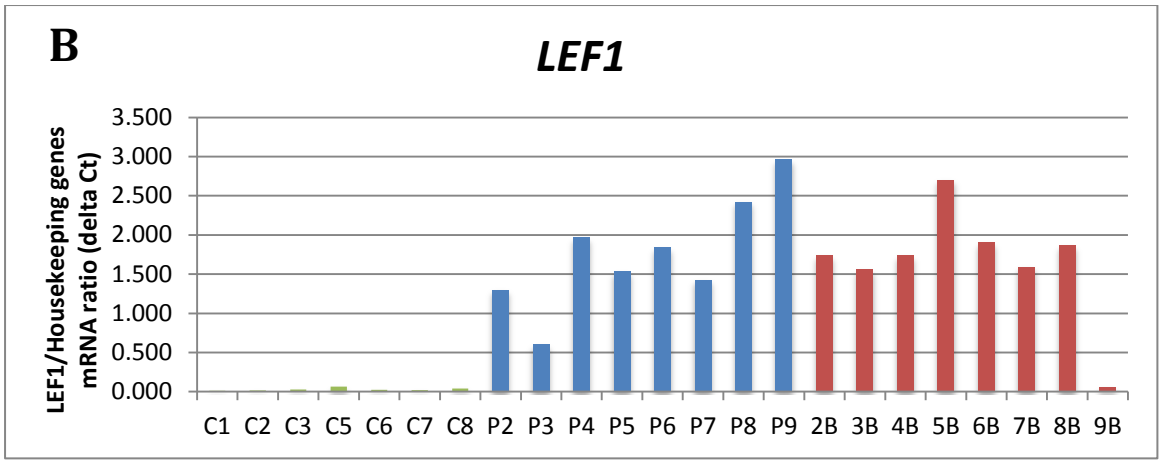
The validation of the qPCR array results was limited to only six genes due to costs constraints. With more than 30 of the 84 Wnt pathway genes exhibiting differential expression it was not possible to validate each of them using a secondary assay. The subset of six genes was chosen using specific criteria including the magnitude of differential gene expression (fold change), the significance levels observed (p-value) and also their role in the Wnt pathway. Two Wnt ligands were chosen; *WNT7A* as an initiator of the canonical wnt pathway and *WNT5B* as a potent activator of the non-canonical Wnt pathway. A frizzled receptor was chosen, *FZD2*, which plays the role of Wnt ligand receptor in both pathways. An antagonist of the Wnt pathway was also chosen for validation, *AXIN1. LEF1* was chosen as it binds to ß–catenin in the nucleus leading to downstream transcription of Wnt target genes, such as *FGF4*. All of the TaqMan assays apart from *FGF4* were successfully optimised and permitted data analysis for the purpose of validation. The TaqMan methodology is the gold-standard for validation of qPCR array gene expression experiments. A summary of the fold change expression values as well as the rationale for choosing these specific genes can be seen in Table 2.8.

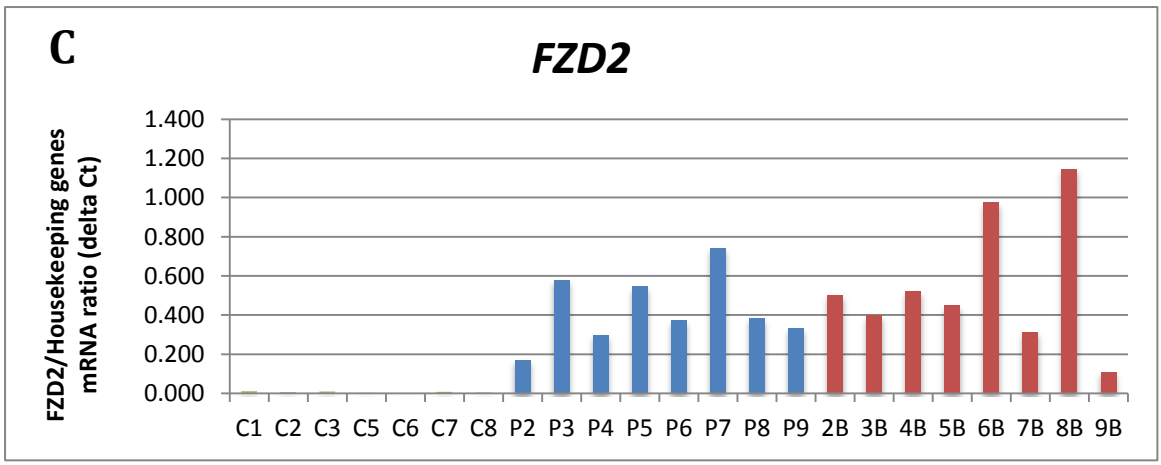
Table 2.8. Summary of the qPCR array expression values and rationale for choosing these six specific genes for validation

Gene	Affected skin v controls Fold change	p-value	Unaffected skin v controls Fold change	p-value	Rationale
AXIN1	4.24	*0.001*	4.67	*0.001*	Negative regulator of the Wnt pathway. Activated when the pathway is active to control persistent signalling. Profibrotic properties.
LEF1	6.09	*0.018*	5.67	*0.019*	Located in the nucleus. B-catenin in the nucleus binds to *LEF1* leading to transcription of Wnt target genes. Profibrotic properties.
FZD2	6.00	*0.020*	6.21	*0.027*	Frizzled receptor to which Wnt molecules bind. Plays a role in both the canonical and the non-canonical Wnt pathway.
WNT7A	8.09	*0.006*	8.30	*0.0042*	Potent stimulator of the canonical Wnt pathway. Profibrotic properties.
WNT5B	-9.56	*0.021*	-9.97	*0.020*	Stimulator of the non-canonical Wnt pathway. Profibrotic properties.
FGF4	19.99	*0.009*	20.28	*0.005*	Involved in cell growth and proliferation. Is a downstream target of Wnt signalling, activated through B-catenin binding to *LEF1*. Profibrotic properties.

The gene expression ratios (ΔCt) from the qPCR array experiment indicated that the genes chosen for validation had significant gene expression differences between the control samples and the patient samples (both from affected and unaffected skin derived RNA) (Figure 2.14).


A
AXIN1
AXIN1/Housekeeping genes mRNA ratio (delta Ct)
3.000
2.500
2.000
1.500
1.000
0.500
0.000
C1 C2 C3 C5 C6 C7 C8 P2 P3 P4 P5 P6 P7 P8 P9 2B 3B 4B 5B 6B 7B 8B 9B


B
LEF1
LEF1/Housekeeping genes mRNA ratio (delta Ct)
3.500
3.000
2.500
2.000
1.500
1.000
0.500
0.000
C1 C2 C3 C5 C6 C7 C8 P2 P3 P4 P5 P6 P7 P8 P9 2B 3B 4B 5B 6B 7B 8B 9B


C
FZD2
FZD2/Housekeeping genes mRNA ratio (delta Ct)
1.400
1.200
1.000
0.800
0.600
0.400
0.200
0.000
C1 C2 C3 C5 C6 C7 C8 P2 P3 P4 P5 P6 P7 P8 P9 2B 3B 4B 5B 6B 7B 8B 9B

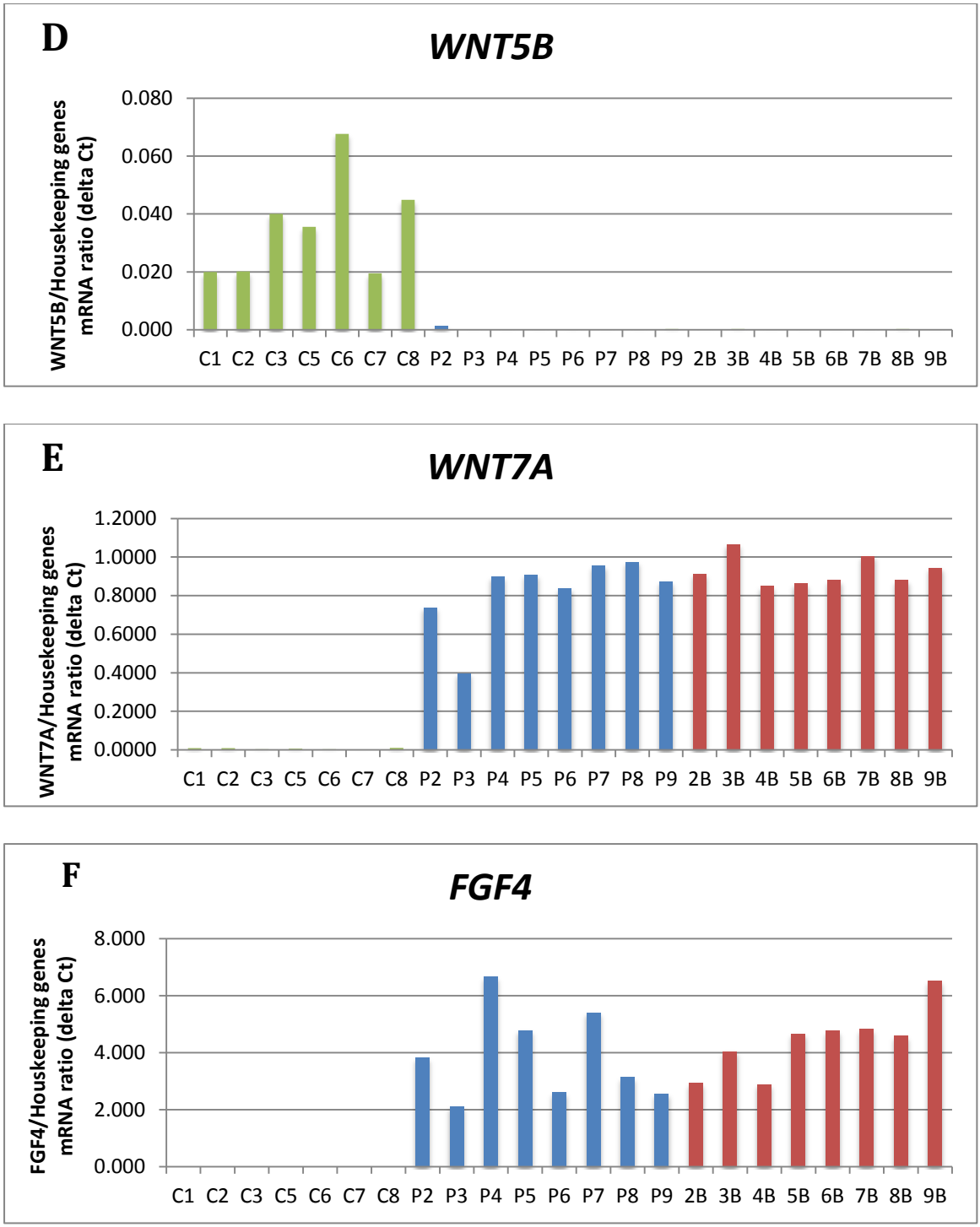


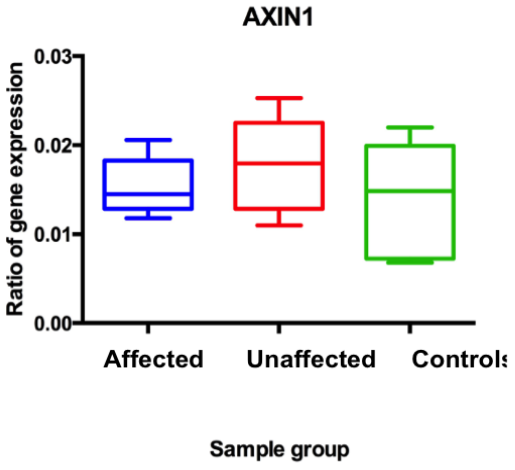
Figure 2.14. The ΔCt gene expression ratio values, obtained for the qPCR array experiments, for each of the six chosen genes for validation; A) AXIN1, B) LEF1, C) FZD2, D) WNT5B, E) WNT7A and F) FGF4. *The ΔCt values for control samples are shown in green, the affected SSc skin samples are shown in blue and the unaffected SSc skin samples are shown in red. These ratios are calculated from the Ct values obtained from the qPCR array experiment, normalised to two housekeeping genes, ACTB and HPRT1.*

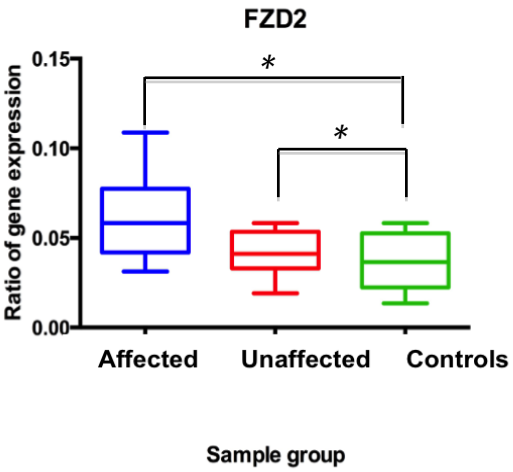
Analysis of the TaqMan qPCR data reveal that the direction of the differential expression is consistent with the original qPCR array data, although the magnitude of the differential expression is much lower in the TaqMan assay (Table 2.9). This is possibly due to sample degradation over a period of two years despite the fact the samples were stored at -80°C. The assay for *FGF4* unfortunately did not amplify for any of the samples, thus could not be included in the analysis of the data.

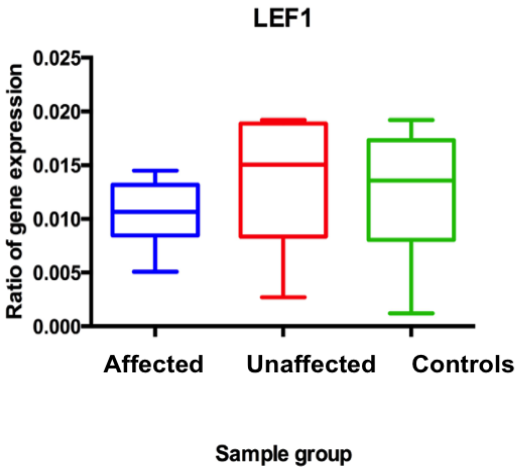
Table 2.9. Summary of the differential expression values for the five genes chosen for validation observed in both the qPCR array experiment and the TaqMan validation experiments

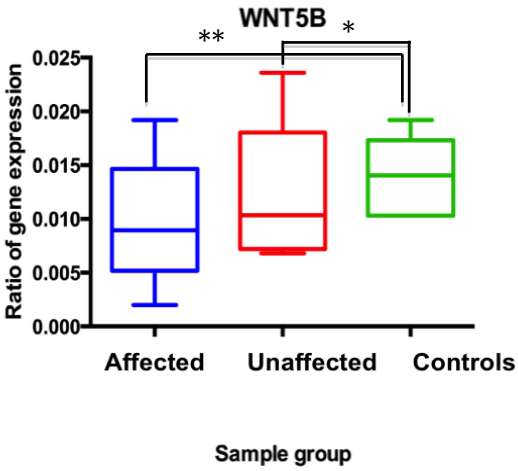
	Affected skin vs Controls		**Unaffected skin vs Controls**	
Gene	**Relative Fold change (qPCR array)**	**Relative Fold change (TaqMan)**	**Relative Fold change (qPCR array)**	**Relative Fold change (TaqMan)**
AXIN1	4.24	3.63	4.67	1.90
LEF1	6.09	2.80	5.67	1.19
FZD2	6.00	1.11	6.21	2.64
WNT7A	8.09	1.51	8.30	2.59
WNT5B	-9.59	-1.55	-9.97	-3.10

For the validation experiment, genes were normalised to three housekeeping genes; *ACTB*, *HPRT1* and *RPLP0*. This method of normalisation is justified, as the Ct values across all samples (cases and controls) for all three housekeeping genes were consistent. The Ct values across the triplicate runs for each sample can be found in Appendix M. The gene expression ratios (ΔCt) calculated for each sample are shown graphically in Appendix N. The gene expression ratio between the housekeeping genes and the genes of interest (ΔCt) for each sample group are shown in Figure 2.15.


AXIN1
Ratio of gene expression
0.03
0.02
0.01
0.00
Affected
Unaffected
Controls
Sample group


FZD2
Ratio of gene expression
0.15
0.10
0.05
0.00
*
*
Affected
Unaffected
Controls
Sample group


LEF1
Ratio of gene expression
0.025
0.020
0.015
0.010
0.005
0.000
Affected
Unaffected
Controls
Sample group


WNT5B
Ratio of gene expression
0.025
0.020
0.015
0.010
0.005
0.000
**
*
Affected
Unaffected
Controls
Sample group

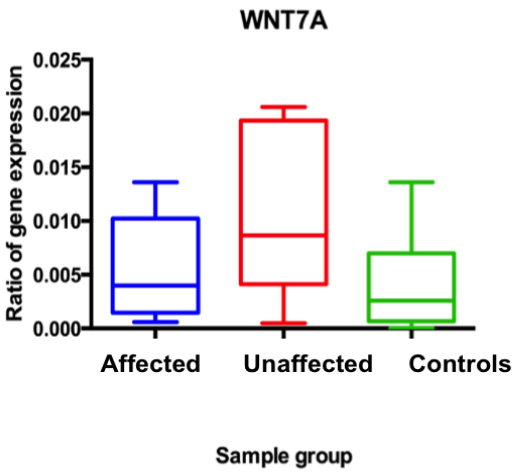

WNT7A
Ratio of gene expression
0.025
0.020
0.015
0.010
0.005
0.000
Affected
Unaffected
Controls
Sample group

Figure 2.15. Box and Whisker plots of gene expression ratios (ΔCt) calculated for each sample group. *SSc affected skin (Blue), unaffected (Red) and controls (Green). Significant differential expression was observed in FZD2 for affected skin (p=0.01) as well as unaffected skin (p= 0.05) compared to controls. Similarly, WNT5B showed a differential expression in affected skin (p=0.008) and unaffected skin (p=0.01) compared to controls.*

The differential gene expression within SSc patients, comparing the affected and unaffected skin in each patient, is shown in in Appendix N.

2.4. Discussion

The aim of our study was to determine if genes in the Wnt signaling pathway are dysregulated in black South African patients with early diffuse cutaneous SSc, and if this dysregulation contributes to the development of fibrosis in these patients. Early principal component analysis of the gene expression profiles seen in both affected SSc skin and unaffected SSc skin placed the patients into two distinct groups. This observation was unusual as the two groups each contained a mixture of samples, affected skin and unaffected skin from different patients. A closer look at the heatplot generated for the qPCR array revealed two distinct clusters of genes, those in a self-labeled orange cluster and those in a self-labeled purple cluster, which showed an interesting pattern of gene expression which explained the clustering of the samples into these distinct patient groups. The discussion that follows will focus on five genes that were chosen for validation, as well as highlight several other differentially expressed genes that may play a role in fibrosis, autoimmunity or inflammation. Figure 2.16 depicts the levels of differential gene expression across the 84 genes of the Wnt pathway array. The coloured blocks are consistent with the groups of gene clusters that showed internal consistency with regard to differential gene expression.

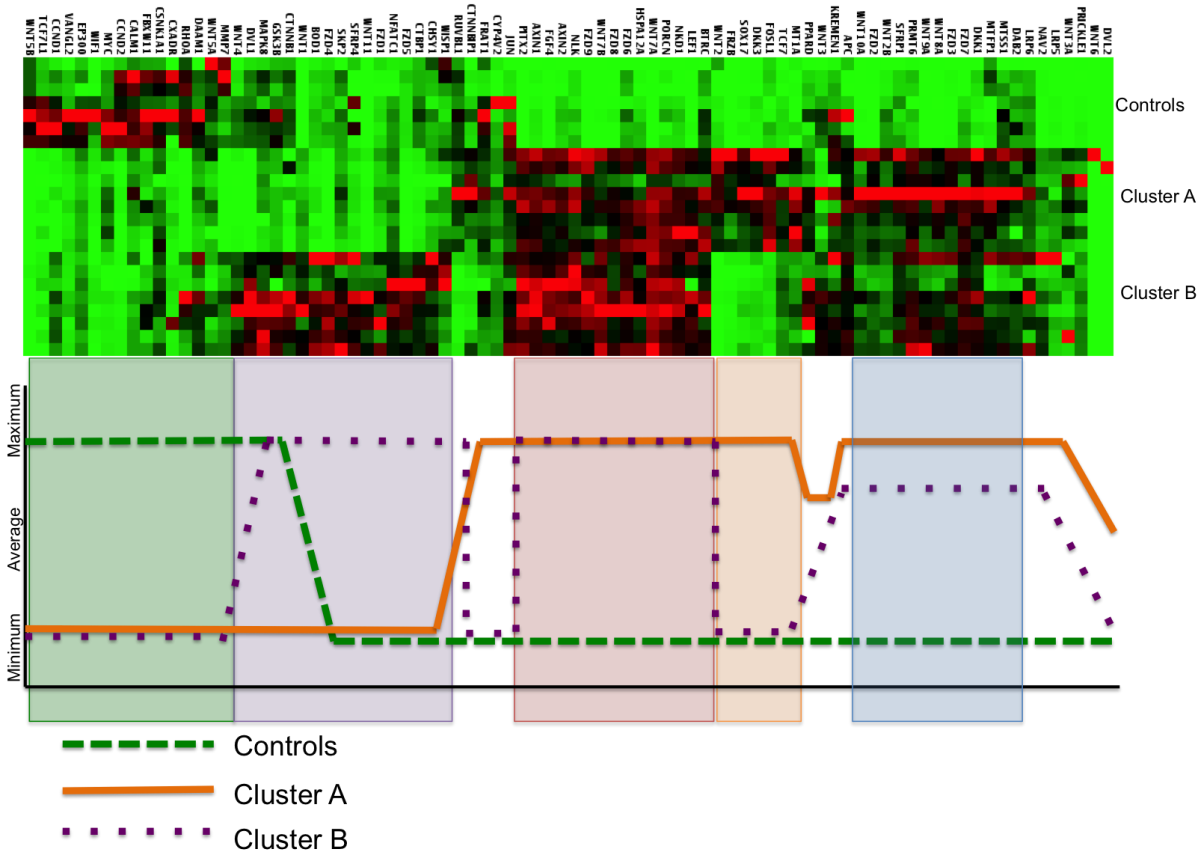


Figure 2.16. Level of gene expression for controls, cluster A genes and cluster B genes across the 84 genes of the Wnt pathway qPCR array. *Genes downregulated in SSc skin compared to controls (green), upregulated in SSc skin compared to controls (red and blue). Genes that differentiate the two patient groups 1 and 2 into expression categories cluster A and cluster B (orange and purple).*

In this group of early, diffuse cutaneous SSc patients, there is differential gene expression of several Wnt pathway genes in SSc compared to controls. The expression patterns observed were validated in five differentially expressed genes. As the results of the qPCR were validated in the direction of differential expression (though not in fold difference, as has been shown in other studies), it is justifiable to discuss the potential impact of the differentially expressed genes evaluated using the qPCR array data. The genes that will be discussed first fall into the red, blue or green gene clusters as seen on the heatplots in Figure 2.7.

2.4.1. Genes upregulated in both affected and unaffected SSc skin compared to control skin (Red and Blue gene clusters)

Both *FZD2* and *LEF1* were upregulated in affected and unaffected SSc skin compared to controls. *FZD2* clustered into the blue gene cluster while *LEF1* can be found in the red cluster of genes. In affected SSc skin both *FZD2* and *LEF1* are overexpressed by 6-fold ($p=0.02$ and $p=0.01$ respectively). Similar levels of differential gene expression were observed in the unaffected skin for these two genes. *FZD2* is upregulated by 6.2-fold ($p=0.02$) while *LEF1* is upregulated by 5.7-fold ($p=0.01$). These findings are consistent with other studies (Wei et al., 2012, Konigshoff et al., 2008). The binding of Wnt ligands to receptors, such as FZD2 and the co-receptors LRP5 and LRP6 inhibits the activation of glycogen synthetase kinase 3 β (GSK3β). This in turn blocks the phosphorylation and degradation of β-catenin. Thus active β-catenin is able to translocate into the nucleus of the cell where it binds to LEF1, thus mediating the transcription of downstream target genes (Wei et al., 2012). Similar to the findings by Wei et al. (2012), the present study also noted an increase in the expression of the Wnt ligand *WNT3A,* which has been described as a potent activator of the canonical Wnt pathway and is able to induce β-catenin activation, stimulate fibroblast proliferation and profibrotic gene expression. The combination of increased Wnt ligand expression (*WNT3A*) and increased Wnt receptor expression (*FZD2*) could be expected to give rise to the hyperactivation of the canonical Wnt pathway. Both *FZD2* and *LEF1* were chosen as candidates to validate using the pre-designed single gene TaqMan assays. The differential expression of these two genes in the skin of SSc patients was supported by the TaqMan qPCR results, although the fold change in expression was considerably less. Differences in fold change observed between qPCR arrays and TaqMan

validation are common (Gaj et al., 2008), but the results have validated in terms of the upregulation of gene expression.

The Wnt ligand, *WNT7A* was found to be upregulated in both affected and unaffected skin compared to controls and is clustered within the red gene cluster. In affected skin *WNT7A* was upregulated by 8-fold (p=0.006) and was upregulated in unaffected by 8.3-fold skin (p=0.004). Expression of fibronectin (FN) provides feedback stimulation of WNT7A signalling through an FZD7/SDC4 receptor complex. Initial proliferative response to injury commits myogenic cells to release FN, which once ligated to the receptor complex at this stage of muscle regeneration induces WNT7A to induce expansion of the satellite stem cell pool. As the master regulator of fibrosis, *TGFβ* triggers the production of FN*,* which is necessary to potentiate *WNT7A* signalling through the receptor complex in turn controlling stem cell numbers (Bentzinger et al., 2013). The eight-fold increase in *WNT7A* is therefore consistent with increased fibrosis due to the profibrotic properties of this ligand.

Both *AXIN1* and *AXIN2* are negative regulators of the Wnt signalling pathway. They function by suppressing the pathway in the absence of a Wnt ligand. In this study, both of these genes are significantly upregulated in both affected and unaffected SSc skin compared to controls and are thus found within the red cluster of genes. *AXIN1* shows an increase of 4.2-fold in gene expression in affected skin (p=0.008) and 4.6-fold increase in unaffected skin (p=0.001). *AXIN2* is increased by 3.9-fold (p=0.008) in affected skin and 4.2-fold in unaffected skin (p=0.01). *AXIN2* is believed to function by promoting phosphorylation and thus degradation of cytosolic ß-catenin. This gene has also been hypothesised to function as part of a negative-feedback mechanism for the Wnt signalling pathway, which could serve

to limit the duration and/or intensity of the Wnt-initiated signal (Jho et al., 2002). *AXIN2* expression was observed to overlap with the expression of members of the Wnt family, suggesting that the expression of *AXIN2* might be induced by Wnt signalling. Similar findings were reported by Akhmetshina et al. (2012), but only in cultured fibroblasts from affected and unaffected skin of SSc patients, bleomycin-challenged mice and tsk-1 mice. The increased expression of both *AXIN1* and *AXIN2* observed in the unaffected skin samples from SSc patients could suggest that these two genes, specifically *AXIN2,* are upregulated in response to the activation of the Wnt pathway in these tissues. This could be a possible compensatory mechanism. There are no phenotypic signs of fibrosis in the unaffected skin, which could be explained by increased *AXIN* expression in response to Wnt activity. This corresponds to observations that the expression of *AXIN2* is elevated in several tumours and tumour cell lines that are induced by Wnt/ß-catenin signalling (Jho et al., 2002).

Soluble frizzled-related proteins (SFRPs) function as modulators of Wnt signaling upon binding of Wnt ligands. SFRPs structurally resemble Wnt frizzled receptors and can inhibit β-catenin signaling by working as Wnt-decoy receptors (Jones and Jomary, 2002), thus SFRPs are Wnt antagonists that directly bind to Wnt ligands (Kawano and Kypta, 2003). *SFRP1* is differentially expressed in both the affected and the unaffected SSc skin in this study, and can be found in the blue cluster of genes. The affected skin fold change was 2.9 (p=0.01) according to qPCR array data. Results were similar for the unaffected skin with respect to this gene, a fold change of 3.0 (p=0.028) was observed using the qPCR array data.

In fibrosis related to SSc, recent studies show evidence of *SFRP* downregulation in fibroblasts from fibrotic lesions. This raises the possibility that fibroblasts from these lesions may be more sensitised to Wnt signals. Fibroblasts from both SSc fibrotic lungs and IPF lungs

express less *SFRP1* compared with controls (Hsu et al., 2011) and a reduction in the level of *SFRP1* was independently observed in fibroblasts derived from keloid lesions (Russell et al., 2010). The development of fibrosis is a complex mechanism, with the balance between pro-fibrotic and anti-fibrotic molecules hanging precariously in balance. Although there are studies to suggest that down-regulation of *SFRP1* is involved in the development of fibrosis, there are also others together with the present study which indicate that the opposite is also true. An increase in the expression of *SFRP1* can also lead to progression of fibrosis.

Increased expression of *sfrp1* was recently found in a mouse model of bleomycin-induced lung fibrosis. Assessing the role of two Wnt antagonists, *Sfrp1* and *Frzb,* expression of both was observed to be upregulated in lung tissue of the mouse model. It was also found that recombinant *SFRP1* counteracts the TGFβ-induced upregulation of type I collagen expression in both pulmonary epithelial cells and fibroblasts (De Langhe et al., 2014). Results from this study indicate that an upregulation of both *Sfrp1* and *Frzb* was able to induce fibrosis in the mouse model. In the present study we observe an increase in *SFRP1* and this could lead to an increase in the development of fibrosis in the SSc patients. There is experimental support to indicate *SFRP1* plays a role in the progression and onset of osteoarthritis. A recent study demonstrated that these proteins are able to differentially modulate joint homeostasis, highlighting that the fine-tuning of Wnt signaling in joint homeostasis plays a role in disease progression (Thysen et al., 2015).

FGF4, a gene that is a direct transcriptional target for LEF1, as it has a functionally important binding site for LEF1/TCF proteins and is stimulated by Wnt signaling (Kratochwil et al., 2002). It is part of the FGF family, which consists of 22 structurally related proteins (Zhang et

al., 2006). Mostly the FGFs are mitogens that stimulate various cellular functions including differentiation, migration and proliferation. Apart from playing a critical role in embryonic development (Arao et al., 2013), these activities are also important in a wide variety of physiological and pathological processes including vasculogenesis (Wesche et al., 2011) and wound healing (Ropiquet et al., 2000). Aberrant activation or amplification of the FGF/FGFR family genes underlie a wide number of cancer types (Parish et al., 2015). In the present study, the *FGF4* gene showed the highest differential expression in SSc skin. The affected skin showed a fold change of 19.9 (p=0.009) and unaffected skin showed a fold change of 20.2 (p=0.005).

As this gene displayed the highest differential expression between SSc skin and controls it was chosen as a candidate for the validation experiment. Unfortunately, the assay could not be optimized as the qPCR assay did not amplify the cDNA and thus no results were obtained for the validation study. *FGF4* is expressed from the early stage of embryonic development in foetal life and has essential roles in cell differentiation, morphogenesis and proliferation of a variety of cell types (Yamamoto et al., 2000, Yasuda et al., 2014). A study by Murakami et al. (2008), found that continuous FGF signaling in endothelial cells is required for the maintenance of endothelial homeostasis and vascular integrity. Expression of *FGF4* plays a role in wound healing and overexpression may trigger the development of fibrosis in the skin of the SSc patients. A study by Shams et al. (2015) showed that treatment of liver fibrosis in mice with fgf4 resolved the fibrotic phenotype.

DKK1 is a secreted protein that negatively regulates the Wnt signalling pathway. Similar to AXIN1 and AXIN2, DKK1 also participates in a negative feedback loop, but rather than acting

intracellularly, acts at the cell surface. DKK1 expression can be upregulated via ß–catenin, but it also has the capacity to inhibit Wnt signaling. The DDK1 feedback loop was confirmed in a study in which DKK1 was overexpressed in a fraction of human blastoma cells, which frequently exhibit active Wnt signaling (Niida et al., 2004). Not surprisingly then, *DKK1* expression was altered in the present study. It was upregulated by 3.5-4.0-fold in the affected and unaffected skin. These findings are at odds with the work of Dees and Distler (2013) and Akhmetshina et al. (2012). In the latter study cultured fibroblasts of SSc patients were found to have a decrease in *DKK1* expression. Some of the reasons for this discordance include the fact that whole tissue was studied in our study as opposed to cultured fibroblasts; the patient profile might be different with respect to disease duration, ethnicity and the site of the tissue biopsy. However, their study did show that *DDK1* in mice inhibited TGFβ stimulation of the Wnt pathway. Another possible explanation for the discrepancy is that the effects of DKK on Wnt signaling depends on the concentration of the respective Wnt or DKK ligands, as well as on the sensitivity of the effector cells due to receptor availability (Pfaff et al., 2011). Taken together the results suggest that increased *DDK1* expression is a compensatory phenomenon in some cases as in our SSc skin samples and that activation of the Wnt pathway in this instance stimulates *DKK1* expression. Clearly, further work needs to be done to better understand the role of *DKK1* in SSc.

Together these upregulated genes function throughout the Wnt signaling pathway; from ligands, *WNT7A* and *SFRP1* to a transmembrane frizzled receptor *FZD2,* intercellular molecules such as *LEF1,* which is responsible for the downstream initiation of transcription of *FGF4*. It is clear from these data that there is an upregulation of genes throughout the signaling cascade in these SSc patients. As most of these genes are in effect responsible for

the development of a profibrotic phenotype, whether they interact with TGFβ, the mediator of the fibrotic response like *WNT7A* or they are involved in wound healing and keloid development like *FGF4,* the dysregulation of these genes in these patients is further evidence of a mechanism for the development of fibrosis in these SSc patients.

2.4.2. Genes downregulated in affected and unaffected SSc skin compared to controls (Green cluster)

There are 16 genes observed as downregulated in this study in affected and unaffected skin compared to controls, but only six of these genes reached a level of significance in differential expression. This cluster of genes was interesting in that 7 of the genes, including *TCF7L1* and *MYC,* showed tissue specific differential expression in the control samples, correlating to whether the tissue sample was a forearm or a breast tissue sample.

In this study, *WNT5A* was shown to be moderately downregulated in affected SSc skin with a fold change of -1.8 (p=0.03) compared to controls. *WNT5A* is an inducer of the non-canonical signalling pathway when it binds to FZD, ROR1 or RYK and activates the ß-catenin-independent non-canonical Wnt/Ca^{2+} and Wnt/planar cell polarity pathways (Corbett et al., 2015). Several studies have suggested that *WNT5A* is not just an inhibitor of Wnt/ß-catenin signalling but rather enhances it. This is supported with evidence showing that *WNT5A* activates Wnt/ß-catenin signalling in the development of the skull and conversely that Wnt/ß-catenin signalling was reduced in skin. *WNT5A* thus is able to both inhibit and activate the Wnt/ß-catenin pathway in a tissue-specific and temporal-specific manner (Okamoto et al., 2014). A previous study by Frost et al. (2012) found that hepatocyte growth

factor (*HGF*), which induces mitogenic and cell motility responses, was upregulated in skin biopsy samples from patients with SSc. In line with this, a study showed that HGF has the ability to down-regulate the expression of *WNT5A*. This seems to indicate that *WNT5A* is downstream of *HGF* signalling and suggests a link in the mechanism of cell motility control by this growth factor (Huguet et al., 1995).

The gene that displayed the greatest down-regulation in SSc patients was *WNT5B* with a fold change of -9.5, p=0.02 in affected skin and -9.9, p=0.02 in unaffected skin compared to controls. This should be considered carefully however, as this gene displayed tissue specific expression in the control samples. WNT5B is a non-canonical Wnt ligand that has 80% homology with WNT5A, another non-canonical Wnt ligand (Saitoh and Katoh, 2001). Non-canonical Wnt signaling plays an important role in both development and in various diseases, including cancer. Most of our knowledge of non-canonical pathway signaling in the literature comes from studies on *WNT5A*, much less has been done on *WNT5B* and other non-canonical Wnt ligands (Sugimura and Li, 2010, Kikuchi et al., 2012). In triple negative breast cancer, aberrant activation of the Wnt/β-catenin pathway is effected by an increased expression of *WNT5B* (Yang et al., 2014b). A study on the role of the Wnt/β-catenin pathway in renal interstitial fibrosis found that most Wnt ligands were upregulated in fibrotic kidney samples, except for three, one of which is *WNT5B* (He et al., 2009). This gene is also overexpressed in patients with inflammatory bowel disease (You et al., 2008). It is clear that dysregulation of the *WNT5B* gene is essential in the role of cancer development as well as fibrosis and an autoimmune disease like inflammatory bowel disease. It is possible that downregulation of this gene in SSc patients plays a role in the pathogenesis of the disease.

This gene was validated using TaqMan qPCR. Differential expression observed in both affected and unaffected skin was decreased, consistent with the qPCR array results.

A Wnt target gene that was shown as differentially expressed in the SSc patients was *CCND2*. In affected skin gene expression showed a -5.2 fold change (p=0.022) and in unaffected skin a -4.82 fold change (p=0.01). The protein encoded by this gene belongs to the highly conserved cyclin family, whose members are characterized by a dramatic periodicity in protein abundance through the cell cycle. In respect of the Wnt pathway, GSK3β regulates the levels of CCND1 and CCND2 through phosphorylation and promoting degradation (Diehl et al., 1998). A study found that GSK3β plays an important role in modulating the expression of both CCND1 and CCND2 and in certain conditions CCND2 is more sensitive to GSK3β (Huang et al., 2007). A recent study by Boulter et al. (2015) showed that *CCND2* is consistently downregulated following Wnt pathway inhibition. However, a decrease in the expression of *CCND2* due to promoter hypermethylation is an early event in the development of breast cancer (Evron et al., 2001).

Together these data indicate that the dysregulation of these genes are correlated with the disease phenotype in our patients and that several of the patients have a fibrotic disease phenotype, which is consistent with the upregulation of genes associated with fibrosis in this and other disease traits. The data also indicate that, in addition to the canonical Wnt pathway, the non-canonical pathways are also dysregulated, as the two potent activators of the non-canonical pathways, *WNT5A* and *WNT5B* are differentially expressed in these SSc patients.

2.4.3. Genes whose differential expression differentiates the two clusters of samples, cluster A and cluster B (Orange and purple gene clusters)

The expression patterns of the genes in the orange and purple gene clusters were particularly interesting, as these gene expression patterns appeared to explain the patient clustering observed in the principal component analysis. The affected skin samples of Patients 2, 4, 6 and 8 display upregulation of the genes in the purple gene cluster, while the unaffected skin samples are downregulated for these genes. For the second patients group, Patients 3, 5, 7, and 9, the genes in the orange cluster are upregulated in the affected samples and down regulated in the unaffected samples. In our study, there was both increased and decreased expression of *TCF7.* The affected skin of Patient Group 1 was downregulated by 10-fold (p=0.04), while the unaffected skin of these patients displayed increased levels of *TCF*, being upregulated by 11.8-fold (p=0.006) compared to controls. In patient group 2, *TCF* was upregulated in the affected skin by 6-94-fold (p=0.001) and the unaffected skin was downregulated by -8.9-fold (p=0.04). The formation of the β-catenin-TCF/LEF complex stimulates the activation of several downstream target genes including CCND1, c-MYC and c-JUN (He et al., 1998). The TCF family of transcription factors, and specifically TCF7 are essential to the regulation of canonical Wnt pathway signaling (Hrdlickova et al., 2014). TCF7 coupled to LEF1 is a transcription factor that mediates Wnt/β-catenin responses. As both *TCF7* and *LEF1* are upregulated in this study, the formation of this complex could be an important transcriptional regulator of the Wnt pathway.

MT1A is a protein coding gene, that is localised primarily in the nucleus of a cell. There was both increased and decreased expression of *MT1A*, in our study. The affected skin of Patient

Group 1 was downregulated by 2.8-fold (p=0.003), while the unaffected skin of these patients displayed increased expression levels, being upregulated by 7.4-fold (p=0.005) compared to controls. In Patient Group 2, *MT1A* was dramatically upregulated in the affected skin by 21-fold (p=0.001), while it was not significantly differentially expressed in the unaffected skin of these patients. Several lines of evidence suggest that once metallothioneins become extracellular, they are intimately involved in the regulation of immune responses, they do this by interacting with cells of the immune system and are able to modify the functional activities of T and B-cells. Elevated levels of metallothionein has been found in several autoimmune diseases, including RA (Youn et al., 2002). MT1A has been implicated in the development of keloids. Studies have indicated that various metallothionein (MT) isoforms were up-regulated in keloid keratinocyte, and also implicated in the regulation of NF-kB activity, which is known to be involved in inflammatory and growth responses, including keloid formation (Messadi et al., 2004). There is however, conflicting evidence as to whether MT is a positive or a negative regulator of NF-kB activity. This could possibly be explained by the different functions of MT, whether it is active in the cytoplasm or nucleus of the cell, and could also be tissue or cell type dependant (Toh et al., 2010). There is also evidence in the literature which supports the role of MT in the development of fibrosis. Sato et al. (2000) suggested that MT might contribute to protection of parenchymal cells in the liver against progression of fibrosis, and observed that MT was absent in fibrotic areas but present in non-fibrotic parenchymal cells. Another study by Wang et al. (2005) observed that MT knockout mice were more susceptible to fibrosis.

The Dickkopf (Dkk) family of proteins was discussed with respect to DKK1 in the section above. This family of proteins includes DKKs 1-4, which is an antagonist of Wnt signaling

(Krupnik et al., 1999). The DKKs, particularly DKK3 are downregulated in a variety of cancer cells, such as hepatocellular carcinoma (HCC), prostate cancer and melanoma (Niehrs, 2006). The functional role of DKK3, specifically in Wnt signaling is not well understood.

There was both increased and decreased expression of *MT1A*, in our study. In our study, *DKK3* displayed significant differential expression in the affected skin of Patient Group 1, with a downregulation of -2.7-fold (p=0.003) compared to controls, and increased expression in the unaffected skin of Patient Group 2 (21.3-fold, p=0.002). *DKK3* is the only Dkk family member abundantly expressed in normal lung, but silenced by promoter hypermethylation in a large fraction of lung cancer cell lines and lung tumors. A study by Yue et al. (2008) suggested that epigenetic inactivation of DKK3 activates the Wnt/b-catenin pathway, thereby promoting the growth of lung cancer cells. In another cancer related study, *DKK3* was shown to be upregulated by more than 2-fold in 75.8% of the esophageal adenocarcinomas that were studied (Wang et al., 2015). Another study identified DKK3 as a novel regulator in determining B cell fate and function, therefore having a function in development of inflammation and possibly related to autoimmunity.

In this study, the *FZD5* gene clustered in the purple cluster together with *FZD4*. There was both increased and decreased expression of *FZD5* in our study. The affected skin of Patient Group 1 was upregulated by 6.2-fold (p=0.0002), while the unaffected skin of these patients displayed decreased expression levels, being downregulated by 3.7-fold (p=0.001) compared to controls. In Patient Group 2, *FZD5* was downregulated in the affected skin by 4-fold (p=0.005), while it was upregulated in the unaffected skin of these patients by 11-fold (p=0.01). Frizzled receptors are located at the surface of Wnt responsive cells and are found

exclusively in the plasma membrane. Some evidence suggests that these frizzled receptors can internalise and are part of a mechanism for regulating the extracellular levels of Wnt protein and the response to Wnt ligands (Huang and Klein, 2004). As mentioned previously, the binding of Wnt ligands to the various frizzled receptors play a pivotal role in regulating several developmental processes during embryonic development. Although there are several Wnt ligands and FZD receptors, the specificity of these interactions still remains unclear. A recent study systematically mapped several of the Wnt-FZD interactions and revealed that *WNT3A* activated the canonical Wnt signalling pathway through *FZD4* and *FZD5* (Dijksterhuis et al., 2015). Information related to FZD5 with respect to SSc is limited although a study in 2006 demonstrated that FZD5 together with WNT5A is able to regulate inflammatory responses in human mononuclear cells. Their experiments showed that both WNT5A and FZD5 are capable of regulating IL-12 and interferon production in an antigen-driven setting, such as would be induced by microbial stimulation. The findings of this study implicate that the Wnt pathway, specifically WNT5A and FZD5 in having the ability to bridge innate and adaptive immunity to infections (Blumenthal et al., 2006).

Soluble frizzled-related proteins, as mentioned earlier, function as modulators of Wnt signaling upon binding of Wnt ligands (Jones and Jomary, 2002), thus SFRPs are Wnt antagonists that directly bind to Wnt ligands. According to the gene expression patterns observed in our study, *SFRP4* was only moderately significantly differentially expressed in the unaffected skin from Patient Group 1. This gene was downregulated by 2.2-fold ($p=0.05$) compared to controls. In a study by Bayle et al. (2008), *Sfrp4* expression was increased in Tsk mouse skin, in addition to upregulated *Wnt2* expression. The expression of these two genes was also correlated with the expression of *Fbn-1* in these mice, with the data suggesting

that *Wnt2* and *Sfrp4* contribute to matrix remodeling. *SFRP4* mRNA expression is increased in the skin of SSc patients (Gardner et al., 2006). To confirm this, (Bayle et al., 2008) analyzed *SFRP4* mRNA in affected and unaffected skin from 12 SSc patients and they found that *SFRP4* was significantly increased in affected skin compared to controls (7.2-fold increase). The results of our study are contradictory to both the Gardner et al. (2006) and the Bayle et al. (2008) studies as we found the gene to be downregulated.

The orange and the purple gene clusters are those genes that appear to show opposite patterns of differential expression between the samples. The patients separate into two distinct groups, which was first noted in the heatplot and confirmed in the PCA plots. It remains uncertain why these two groups of patients should be so obviously separate and have different gene expression patterns in the affected and the unaffected skin with regard to a subset of genes in the Wnt pathway. There was no apparent batch effect with respect to sample collection, RNA extraction or qPCR array plate preparation. A closer look at the clinical features of the patients does not reveal anything that could potentially differentiate the two groups, however it is clear that Patient Group 1 are those patients with clinical symptoms associated with inflammation, such as ILD and myositis. There are a number of genes that are observed in the orange and purple gene clusters that have previously been associated with inflammation, the two Wnt ligands, *WNT1* and *WNT11* in particular. In the affected skin of patients from Patient Group 1, those patients with either ILD or myositis, there is a marked increase in expression of both of these ligands. *WNT1* is upregulated by 21-fold ($p=0.001$) and *WNT11* is upregulated by 17.9-fold ($p=0.01$) in the affected skin of these patients compared to controls. Interestingly, these genes are not significantly differentially expressed in the affected skin of the patients from Patient Group 2; the group

of patients we hypothesise have a more fibrotic disease phenotype. A recent study investigated the relationship between *WNT1*, NF-κβ and inflammatory responses. The investigators found that *WNT1* increased the expression levels of NF-κβ protein thus enhancing the secretion of inflammatory molecules such as IL-6 and TNF-α. They concluded that as these inflammatory molecules are released, *WNT1* participates in an inflammatory response (Zhao et al., 2015). Similarly, in a study related to the expression of Wnt pathway genes in inflammatory bowel disease (IBD), the expression of *WNT11*, as well as *SOX17* was significantly increased in the inflamed mucosa tissue samples from patients with IBD compared to controls (Hughes et al., 2011), suggesting that these genes play a role in the inflammatory response. In a study of patients with obesity, *WISP1* (Wnt1-inducible signalling pathway protein 1) was linked to the inflammatory response of the disease (Murahovschi et al., 2015). Finally, *MAPK8*, also known as *JNK1*, is hyperactivated in breast cancer and in a recent study was linked to both a fibrotic and an inflammatory component of the cancer (Lisanti et al., 2014). In our study, MAPK8 is upregulated in the affected skin of patients from Patient Group 1 by 2.92-fold (p=0.03) and downregulated in the affected skin from patients in Patient Group 2 (-13.7-fold, p=0.04). Perhaps at a molecular level, there are indeed two distinct subtypes of diffuse cutaneous SSc in the group of patients we studied. The genes that are upregulated in Cluster B appears to be those that if dysregulated modulate the inflammatory response through different mechanisms. This would need to be tested in a larger group of patients to increase the power of the correlation between clinical data and gene expression.

2.4.4. Summary

A number of genes with a profibrotic action are upregulated in the affected and unaffected skin samples from the SSc patients. From the results of this study *WNT1* and *WNT7A,* which are among the genes that are upregulated*,* are ligands responsible for activating the canonical Wnt pathway and their potent profibrotic effect appears to be involved in the progression of the clinical manifestation of SSc. *AXIN1* and *AXIN2* also exhibit profibrotic action and are upregulated in the SSc skin samples. Although the AXINs are antagonists of the Wnt pathway, they are initiated when the Wnt pathway is activated, confirming that the canonical Wnt pathway is indeed constitutively activated in these patients. LEF1 binds to ß-catenin in order to activate the transcription of downstream Wnt target genes. In this study*,* *LEF1* and *CTNNBB1* were upregulated in SSc skin. LEF1 is also a profibrotic mediator. *CCND2* and *CCND1*, both downstream target genes of the Wnt pathway were observed to be downregulated in the SSc skin samples. *WNT5A* and *WNT5B* are both initiators of the non-canonical Wnt pathway with profibrotic properties. *WNT5A* was found to be upregulated in SSc skin, while *WNT5B* was observed as the gene that showed the greatest magnitude of down regulation in the SSc skin samples. A number of antifibrotic mediators were found to be upregulated in the SSc skin samples compared to controls, these included *DKK1* and *SFRP1.* This upregulation of antifibrotic mediators as well as antagonists of the Wnt pathway could be a compensatory mechanism for the active Wnt pathway in these patients as well as a response to the profibrotic actions of the other genes. From this study it is clear that the homeostasis required for a normal, non-fibrotic phenotype is dependent on a very delicate balance between the expressions of genes with profibrotic versus antifibrotic functions.

Figure 2.17. is a graphic summary showing the genes observed as up or down regulated in this study and the role that they play in either the canonical or the non-canonical Wnt pathways. It is clear that there is dysregulation of genes not only in the canonical Wnt pathway, but also in the non-canonical pathway.

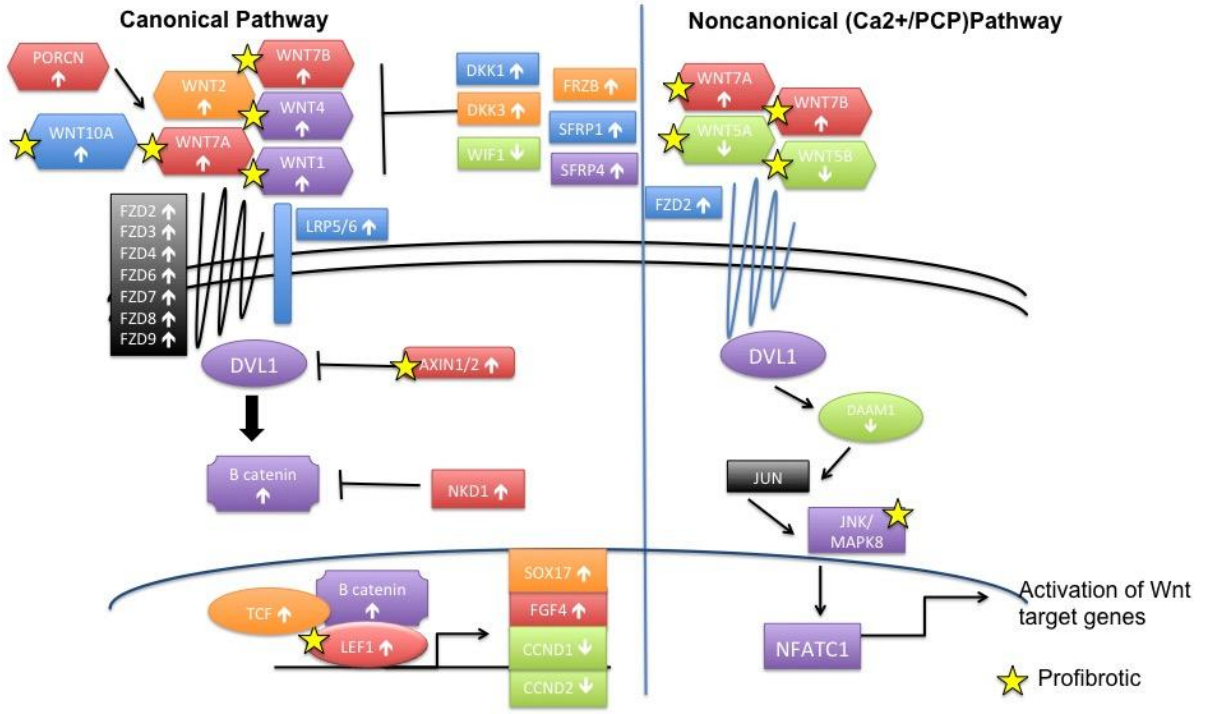


Figure 2.17. Genes observed as being up and downregulated in this study and their role in the canonical or non-canonical Wnt pathways. *Genes with profibrotic effects are marked with a yellow star. The colour of the genes is consistent with the gene cluster in which they are found in the heatplot. The dysregulation of the genes in this diagram result in a signalling cascade in both the canonical and non-canonical Wnt pathways that lead to a pro-fibrotic phenotype.*

This diversity of gene expression patterns within SSc patients has been demonstrated in previous studies by Whitfield et al. (2003), Gardner et al. (2006) as well as the comprehensive study by Milano et al. (2008) in which SSc samples were differentiated into four distinct groups based in gene expression patterns. Specifically for patients with dcSSc,

gene expression patterns differentiated them into two distinct groups labelled as “diffuse-proliferative” and “inflammatory”. The detection of these distinct patient groups in the present study is consistent with the literature, although our understanding of this differentiation remains simplistic for the time being. These gene expression patterns could point to differences in the disease aetiology, such as having ILD or myositis or may even correspond to distinct clinical outcomes, such as inflammation, for the patients. The latter is supported by evidence from a study that analysed changes in skin scores and disease outcome (Shand et al., 2007). According to the study by Milano et al. (2008), two models were proposed to account for these gene expression subsets. Firstly, there are multiple distinct groups of SSc patients, each exhibiting distinct gene expression profiles. These gene expression signatures are established early in disease and remain stable during disease progression. The second model proposes that the different gene expression subsets represent different stages of the disease. Both of these models have been tested and there is evidence for and against both models as described in various recent studies (Pendergrass et al., 2012, Johnson et al., 2015, Mahoney et al., 2015). It is clear however that more work needs to be done to elucidate which model, or combination of models is correct.

The two patient groups 1, (Patients 2, 4, 6 and 8) and 2 (Patient 3, 5, 7 and 9) display opposite gene expression patterns for the subset of those genes in the orange and purple gene clusters. The affected skin of patients in group 1 shows upregulation of genes in the purple cluster while the unaffected samples show a “normal gene expression profile” for genes in this cluster. The affected skin of patients in group 2 show upregulation of genes in the orange gene cluster while the unaffected samples displays a “normal gene expression profile”. The expression of the genes observed in the affected skin could differentiate these

diffuse SSc patients into two sub-groups based on either a more fibrotic disease or a disease with an inflammatory response. This is an interesting observation and one that is similar to what was previously seen in the literature.

2.4.5. Limitations

The major limitation of this study is use of whole skin biopsies that contain several different cell types including epithelial cells, fibroblasts, keratinocytes and melanocytes. We cannot be certain that the relative ratios of these cell types are constant across biopsies. The gene expression values that are assessed are an average of the gene expression across all the cells in the skin biopsy, as the source of the mRNA is unclear. The inflammatory infiltrate that varies amongst patients could also be influencing the gene expression results.

Another limitation of the study is that the control samples were not all from the same region of the body, as were the SSc skin samples. Four control samples were breast skin tissue and four were hand skin tissue samples. This did not appear to impact significantly on the analysis of the data, as the PCA plots (Figures 2.5 and 2.6) show that the control samples all cluster very tightly according to overall gene expression within the Wnt pathway, according to the qPCR array data. However, on closer inspection of the heatplot constructed following gene expression normalised to two housekeeping genes, there are some interesting trends showing that the following genes, *MYC, WIF1, EP300, VANGL1, CCND1, TCF7L1* and *WNT5B,* showed marked differences between the breast (C3, C5 and C8) and forearm (C1, C2, C6 and C7) skin biopsy samples from the controls.

The sample quality was of a high standard as evaluated by the RIN numbers generated by the Bioanalyser. The RNA samples, however, were extracted 24 months prior to the validation experiments, with the initial qPCR array experiment being conducted 18 months prior to the validation experiments. It is known that RNA is relatively unstable, even if stored in ideal conditions as was done in this study. With repeated freeze-thaw cycles of the samples, together with shipping from Barcelona, it is possible that the RNA quality and integrity was not optimal for the validation experiments and may have deteriorated (i.e. partially degraded) compared to when the original qPCR experiments were conducted in April 2014, perhaps accounting for some of the differences observed in the validation study.

2.4.6. Strengths of the study

The biggest strength of this study is the homogeneous sample group of patients that was studied. All patients were early disease; diffuse cutaneous SSc patients of the same ethnicity, black South African. Gene expression patterns observed in the patients from this study, stratifying them into two groups, are more likely to underlie disease than be confounded by heterogeneity arising from different stages of disease, different subtypes of disease and different ethnicities of the patients. In the Milano et al. (2008) study, different disease phenotypes were highlighted, however, the ethnicities of the patients were not mentioned, and could be a potential confounder.

In my study, whole skin punch biopsies were used, with RNA extracted from the sample as a whole. Other studies have used cultured fibroblasts in order to gain a better and clearer understanding of what gene expression changes are occurring in the specific cell type. The

utility of explanted cultured fibroblasts in studies of SSc may be limited due to gene expression changes during several passages and the prospect of finding meaningful results is greater when using patient skin biopsy specimens. In a study comparing gene expression in both biopsies and explanted (cultured) fibroblasts it appeared that phenotypic characteristics of SSc fibroblasts were eroded when they were cultured in a context that was, independent of the dermal milieu, as their differential gene expression when compared to that of control fibroblasts was altered and showed more variance relative to the biopsy samples (Gardner et al., 2006).

2.4.7. Future studies

To get a better understanding of the molecular pathogenesis of SSc and how this could lead to effective therapeutic interventions, we need to understand the origins and progression of the disease more fully.

Of the 84 genes on the Wnt pathway qPCR array, more than 30 were identified as significantly differentially expressed in the SSc patient skin samples. For this study, only 6 of those were chosen for validation using a secondary method. Future studies should include validation of all these genes.

Since gene expression changes do not always translate directly into changes in protein production, another validation approach that could be used in future studies is immunohistochemistry. This technique uses antibodies, which are specific to antigens on proteins to detect the presence, localisation (cellular and sub-cellular) and the amount of

the protein in the cells observed in a biopsy cross-section.

Epigenetic studies could be done to understand the potential mechanism of altered gene expression. The approach would be to identify genes that are validated and select them for methylation studies. This would be done to assess if there is hyper- or hypomethylation of these genes' promoters that may in part be responsible for the gene expression patterns observed. As SSc has varied and mostly unknown disease aetiology, epigenetic changes may be able to offer a mechanistic explanation and add to gaps in knowledge with respect to both aetiology and pathogenesis. The complex nature of SSc and the role of the environment in being able to trigger SSc-like symptoms, points to epigenetic mechanisms of disease. Future studies should perhaps not only focus on methylation but also on histone modifications and gene-gene interactions through techniques such as CHiP-seq or ATAC-seq. The role of small RNAs or microRNAs is discussed in Chapter 3.

Future studies could also include a more detailed account of patient phenotypic data. Having more clinical information on endophenotypes would assist with the identification of more robust correlations between gene expression patterns and clinical phenotype. The sample size should also be increased to increase the statistical power of detecting true correlations between gene expression and clinical data.

Chapter 3

Expression of Wnt pathway gene targeting microRNAs in SSc patients

3.1. Introduction

Autoimmune diseases are caused by a combination of genetic predisposition and environmental exposures that are likely to modulate gene expression through epigenetic mechanisms. Such as external environmental factors include diet, exposure to chemicals and stress induced responses. Epigenetic modifications, as mentioned in Chapter 1, are non-genetic factors that are defined as stable and heritable alterations that affect chromatin conformation (Bird, 2002). These alterations cause changes in gene expression and cellular function that do not involve changes to the DNA sequence. miRNAs together with DNA methylation and histone modifications are recognized as the major players in genes expression regulation through epigenetic modification.

3.1.1. Epigenetics in autoimmune diseases

In recent years, a growing body of evidence demonstrates that epigenetic regulation plays a pivotal role in the development of a number of human diseases, including autoimmune disorders (Lu, 2013). If epigenetic homeostasis of the immune response is not maintained due to external factors such as environmental stimuli, it will lead to aberrant gene expression. This in turn contributes to immune dysfunction and occasionally, the

development of autoimmunity in genetically susceptible individuals (Strickland and Richardson, 2008, Gervin et al., 2012).

DNA methylation plays a critical role in maintaining T-cell function. An inability to maintain these DNA methylation signatures in mature T cells can result in T cell autoreactivity, leading to autoimmunity. Failure to maintain the correct patterns of DNA methylation could be caused by certain drugs, or due to failed activation of genes encoding DNA methyltransferases during mitosis. This can result in development of systemic autoimmune disorders, such as systemic lupus erythematosus (SLE), rheumatoid arthritis (RA) and systemic sclerosis (SSc) (Richardson, 2003).

In SLE, a systemic multi-organ autoimmune disease, several studies have found that global hypomethylation of certain disease associated genes results in these genes being overexpressed. This may particularly affect the structure of T-cell chromatin resulting in cellular hyperactivity (Gorelik and Richardson, 2009). Data suggests that T-cells from patients with active SLE demonstrate decreased deoxymethylcytosine content and decreased DNMT1 transcripts (Sawalha et al., 2008). RA is characterized by destruction of the joints by invasive synovial fibroblasts, and epigenetic studies focusing on these cells have found global DNA hypomethylation. This is thought to lead to the overexpression of inflammatory cytokines in the synovial fluid (Karouzakis et al., 2009). The IL-6 is a pro-inflammatory cytokine that participates in B-cell response, and studies have shown that the CpG island of the IL-6 gene promoter in monocytes is hypomethylated in RA patients. This epigenetic state will cause IL-6 to be overexpressed and associated with local hyperactivation of the inflammatory circuit (Nile et al., 2008).

Histone modifications have been studied in both humans and in animal models of SLE. Nucleosomes are the primary antigen in SLE and are released in SLE as a result of the insufficient removal of apoptotic debris. Histone modifications including histone 3 lysine 4 trimethylation (H3K4me3) and histone 2B lysine 12 acetylation (H2BK12ac) cause an increase in the rate of apoptosis. These apoptotic nucleosomes cause the activation of antigen-presenting cells and autoantibody production, leading to an inflammatory response (van Bavel et al., 2010). Synovial tissues in patients with RA are characterised by modulating between HAT and HDAC activity (Grabiec and Reedquist, 2010). Treatment with an HDAC inhibitor (FK228) is able to inhibit joint swelling and synovial inflammation in murine models of the disease (Nishida et al., 2004).

MicroRNAs (miRNAs) are post-transcriptional regulators of 18-23 nucleotides in length (Bartel, 2004), are involved in many physiological and pathological processes, including an important role in immune responses and the development of autoimmunity, see Figure 3.1 (Cobb et al., 2006, Rodriguez et al., 2007, Pauley et al., 2009). Several studies have suggested that altered expression and function of miRNAs could be involved in the pathogenesis of RA (Stranczyk et al., 2008) and SLE (Dai et al., 2007). miR-146a is a negative regulator of Toll-like receptor (TLR) signaling and its expression is decreased in SLE patients (Tang et al., 2009). There is also evidence for the reduced expression of miR125a in SLE, which results in the upregulation and elevation of the inflammatory cytokine RANTES (regulated upon activation, normal T-cell expressed, and secreted) (Zhao et al., 2010). miRNAs are critical for disease pathogenesis in RA, for example, miR-155 is overexpressed in synovial fibroblasts and miR-146 is upregulated by proinflammatory cytokines (Li et al., 2010). The possible target for miR-155 is thought to be *MMP3* in RA.



Figure 3.1. Potential consequences of abnormal miRNA regulation in immune responses and functions (Pauley et al., 2009)

3.1.2. DNA methylation and histone modifications in SSc

Cultured SSc fibroblasts manifest cellular abnormalities through several generations and maintain a profibrotic phenotype, suggesting the presence of specific epigenetic signatures. One study demonstrated increased expression of epigenetic maintenance mediators at a global level in SSc fibroblasts, as well as increased expression of *DNMT1* (Wang et al., 2006). Friend leukemia integration 1 transcription factor (Fli-1) is encoded by the *FLI1* gene and acts as a transcription factor and is a negative regulator of collagen production in fibroblasts. Fli-1 expression is reduced in SSc leading to elevated collagen synthesis and thus accumulation of extracellular matrix components in SSc fibrotic skin (Wang et al., 2006).

Global histone 4 hyperacetlyation and global histone 3 lysine 9 (H3K9) hypomethylation is associated with down-regulation of both HDAC2 and HDAC7 in B cells from SSc patients. These changes in the chromatin are thought to lead to dysregulation of expression of immune regulated genes (Wang et al., 2006). Furthermore, inhibition of H3K27me3 stimulates the release of collagen in SSc fibroblasts in a bleomycin-induced experimental mouse model (Kramer et al., 2013).

In a recent genome-wide DNA methylation analysis of dermal fibroblasts from SSc patients identified common and disease sub-type specific methylation differences. The study revealed 2710 differentially methylated CpG sites in dcSSc patients and 1021 such sites in lcSSc patients. The majority of these sites were found to be hypomethylated compared to controls. The common differentially methylated sites between dcSSc and lcSSc represented 18 hypomethylated and 6 hypermethylated genes. A pathway analysis of these genes revealed an enrichment of genes that function in the extracellular matrix (Altorok et al., 2015). The novelty of studies such as this is that they demonstrate epigenetic differences between the different sub-types of SSc and in doing so, identify novel candidate disease genes.

3.1.3. MicroRNA

MicroRNAs are small RNA molecules that regulate mRNA translation by binding to complementary mRNA sequences to either degrade the mRNA or prevent translation (Bartel, 2004). MicroRNAs have also been implcated in activating protein production (Selbach et al., 2008) and have been observed to stimulate polyribosome loading of mRNAs, thus stimulation enhancing their translation (Orom et al., 2008). The ability of these miRNAs

to regulate the translation of mRNAs of specific genes plays an important role in cell differentiation, development and proliferation (Filipowicz et al., 2008). To date approximately 2000 annotated miRNAs have been described in humans (Friedlander et al., 2014). Some miRNAs are able to regulate specific targets, while others assume the role of master regulators with the ability to regulate the expression levels of hundreds of genes (Bentwich et al., 2005, Friedman et al., 2009). It is common to categorise microRNAs together with DNA methylation and histone acetylation as an epigenetic mechanism but microRNA should mostly be considered a post-transcriptional mechanism rather than an epigenetic mechanism.

3.1.4. MicroRNA modulation of the Wnt pathway

Many human diseases result from disruption of developmental signaling pathways where miRNAs play a key role in promoting or inhibiting protein translation which influences disease progression. Thus a thorough understanding of miRNA function, interaction and crosstalk with various signaling pathways is critical in understanding normal regulation of development and maintenance of tissue homeostasis. Numerous miRNA regulate the Wnt pathway in terms of development and also in the context of disease (Song et al., 2015).

For example, miR-200a downregulates β-catenin-mediated transcription through two mechanisms. Firstly by targeting E-cadherin repressors subsequently increasing the total E-cadherin available to bind to β-catenin thus inducing the formation of cell-cell adhesion complexes (Su et al., 2012). Secondly by regulating the expression of β-catenin and the activation of Wnt/β-catenin signaling by targeting the 3'UTR of β-catenin mRNA. Another miRNA that is able to regulate the Wnt pathway though β-catenin is miR-215. This miRNA is

able to directly regulate Catenin-β Interacting Protein (CTNNBIP1). This suppresses Wnt/β-catenin signaling thus leading to activation of α-SMA and fibronectin expression in TGF-β1 treated mouse mesangial cells (MMCs) (White et al., 2011). miR-215 has been shown to suppress CTNNBIP1, which promotes the TGF-β1 induced pathogenesis of diabetic nephropathy (Song et al., 2015). In patients with Duchene muscular dystrophy miR-199a-5p is elevated in the dystrophic muscle. This miRNA suppresses FZ4, JAG1, and Wnt2 that leads to inhibition of Wnt signaling factors that regulate myogenesis (Alexander et al., 2013).

Dysregulation of the Wnt/β-catenin signaling pathway is also observed in hepatocellular carcinoma (HCC). miR-214 directly and indirectly targets β-catenin by downregulating c-Myc, Cyclin D1, TCF-1 and LEF1 (Sun et al., 2013). miR-122 and miR-148b directly inhibit Wnt1, resulting in reduced β-catenin and c-Myc and prevent HCC cell growth (Zhang et al., 2015). Upregulation of miR-139 suppressed β-catenin signaling and inhibits cell proliferation and invasion, suggesting it as a potential therapeutic for treating HCC patients (Gu et al., 2014).

3.1.5. microRNAs in fibrosis

Approximately 40 miRNAs have been linked to fibrosis in various organs and disease settings (Table 3.2). As the miRNA profile of a given cell or tissue type is quite specific, many miRNAs with either pro- or anti-fibrotic properties are dysregulated in specific organs and fibrotic diseases (Vettori et al., 2012). A few of these miRNAs are differentially expressed in more than one fibrotic disease, with most of directly inducing or protecting from fibrosis by targeting TGFβ, the Wnt canonical and non-canonical pathways, connective tissue growth factor (CTGF) or extracellular matrix proteins (Kodama et al., 2011, van Almen et al., 2011). miRNAs are also able to regulate the development of fibrosis by affecting epithelial-to-

mesenchymal transition (Pottier et al., 2009) or by inducing or resisting apoptosis in myofibroblasts (Mann et al., 2010). The miR-29 family has been implicated in cardiac fibrosis following a report showing down-regulation of miR-29 family during myocardial infarction in mouse and human hearts (van Rooij et al., 2008). Multiple target genes of miR-29 have been identified including collagen and fibrillin. It has also been suggested that TGF-β-mediated down-regulation of miR-29 enhances fibrosis.

A study by Pottier et al. (2009) demonstrated that miR-155 expression was increased following treatment with TNFα and was reduced by TGFβ, when elucidating the role of miRNAs in lung fibrosis. Functional studies have indicated that increased miR-155 down-regulates keratinocyte growth factor expression and increases fibroblast migration through the induction of caspase-3 (Pottier et al., 2009).

Fibrosis is one of the key features of chronic hepatic diseases and a number of reports have demonstrated a role of miRNAs during hepatic stellate cell (HSC) activation. Measuring the changes in miRNA expression during HSC activation in rat studies have identified several up-regulated miRNAs, including miR-29c, miR-325-5p as well as a few that are down-regulated, including miR-341, miR-15b and miR-16 (Guo et al., 2009a). Over-expression of both miR-16 and miR-15b inhibits HSC proliferation and is able to induce apoptosis through the down-regulation of BCL2 (Guo et al., 2009b). Taken together, these findings propose miRNAs play a significant role in the progression of liver fibrosis via HSC activation.

Diabetic nephropathy, a common complication of diabetes, is often a model used to study renal fibrosis. As with other fibrotic conditions, the renal fibrosis observed in diabetic nephropathy has been linked to differential expression of several miRNAs. miR-192 has been shown as being upregulated in the glomeruli of type 1 and type 2 diabetic mice, as well

as cultured mesangial cells treated by TGFβ. In these TGFβ treated cells, increased miR-192 expression induced the expression of several collagens (Kato et al., 2007). Another up-regulated miRNA is miR-377 and it is thought to regulate the accumulation of fibronectin, frequently seen in diabetic nephropathy (Wang et al., 2008).

Table 3.1 miRNAs that have been associated with the development of fibrosis

Micro-RNA	Effect	Organ	Role in fibrosis	Reference
miR-142-3p	Pro-fibrotic	Kidney	Decreased interstitial fibrosis in allograft transplant	(Scian et al., 2011)
miR-155	Pro-fibrotic	Liver, Lung	Decreased mesenchymal-epithelial cross talk	(Pottier et al., 2009)
miR-192	Pro-fibrotic	Kidney	Increased collagen synthesis	(Kato et al., 2007)
miR-199a/b	Pro-fibrotic	Heart, Liver	Increased extracellular matrix synthesis	(da Costa Martins et al., 2010)
miR-208	Pro-fibrotic	Heart	Increased fibrosis by depression of negative regulators of stress response genes	(van Rooij et al., 2007)
miR-21	Pro-fibrotic	Lung, Heart, Kidney	Increased TGFβ signaling	(Liu et al., 2010)
miR-215	Pro-fibrotic	Kidney	Increased EMT	(Wang et al., 2010)
miR-23a/miR-27a cluster	Pro-fibrotic	Lung	Increased EMT	(Cho et al., 2011)
miR-32	Pro-fibrotic	Kidney	Decreased interstitial fibrosis in allograft transplant	(Scian et al., 2011)

miR-338	Pro-fibrotic	Lung	Increased fibroblast proliferation	(Zhang et al., 2010)
miR-337/miR-382 cluster	Pro-fibrotic	Kidney	Increased fibronectin synthesis	(Wang et al., 2008)
miR-107	Anti-fibrotic	Kidney	Decreased interstitial fibrosis in allograft transplant	(Scian et al., 2011)
miR-133	Anti-fibrotic	Heart	Decreased TGFβ and CTGF signaling	(Duisters et al., 2009)
miR-141	Anti-fibrotic	Kidney	Decreased TGFβ	(Wang et al., 2011)
miR-15b, miR-16	Anti-fibrotic	Liver. Lung	Increased apoptosis	(Guo et al., 2009b)
miR-150	Anti-fibrotic	Liver	Decreased activation and proliferation in HSC	(Venugopal et al., 2010)
miR-200a/b	Anti-fibrotic	Liver, Kidney	Decreased TGFβ signaling	(Pogribny et al., 2010)
miR-204	Anti-fibrotic	Kidney	Decreased interstitial fibrosis in allograft transplant	(Scian et al., 2011)
miR-29a/b/c	Anti-fibrotic	SSc skin, Heart, Lung, Kidney, Liver	Directly decreases ECM synthesis	(Maurer et al., 2010)
miR-30c	Anti-fibrotic	Heart, Lung	Decreased CTGF signaling	(Pandit et al., 2010)
miR-335	Anti-fibrotic	Liver	Decreased HSC activation	(Chen et al., 2011)

3.1.6. The role of microRNAs in SSc

miRNAs have been identified in skin fibroblasts and sera of patients with SSc (Zhu et al., 2012). The differential expression of these miRNAs may be a contributor to fibrosis either by acting in a profibrotic or antifibrotic manner (Maurer et al., 2010).

Several studies have shown that miR-29b levels were decreased in skin tissues and fibroblasts from SSc patients (Maurer et al., 2010, Kawashita et al., 2011, Zhu et al., 2012), and downregulation of miR-29b correlates with the upregulation of collagen type 1 (COL1A1) (Zhu et al., 2012). These studies suggest that a decrease in the expression of miR-29 expression is involved in fibrosis in SSc, as it encourages the upregulation of COL1A1 and thus the deposition of collagen in these tissues. Therefore these studies also suggest that miR-29b is able to suppress the development of fibrosis if it is upregulated.

Similarly, the aberrant expression of miR-21 and miR-145 have also been shown to be involved in the pathogenesis of SSc. miR-21 was upregulated while miR-145 was downregulated in SSc skin samples and fibroblasts with both miRNAs able to regulate genes such as COL1A1, SMAD3 and SMAD7 (Zhu et al., 2013b). As with miRNA-29b, the upregulation of COL1A1 is involved in the development of fibrosis through the increased deposition of collagen (Abraham et al., 2007). Studies have shown that after stimulation with TGFβ, miR-21 expression was increased which in turn decreased SMAD7 expression. Similarly, TGFβ increases miR-145 expression thereby reducing SMAD3 expression. These results indicate that both miR-21 and miR-145 may exert pro- or antifibrotic effects in SSc (Zhu et al., 2012).

miR-196a has also been associated with the development of fibrosis in SSc. Using q-PCR, a study reported that overexpression of miR-196a reduces the expression of type I collagen in SSc fibroblasts. The inhibition of miR-196a results in the overexpression of type I collagen in normal fibroblasts. Therefore it could be possible that miR-196a may lead to novel treatments using miRNAs (Honda et al., 2012).

A few more miRNAs identified as playing a role in fibrosis in SSc include miR-129-5p, miR-92a and miR-150. A recent study observed that miR-129-5p was under expressed in SSc fibroblasts. This miRNA can be upregulated by IL-17A expression, thereby reducing the expression of COL1A1 and CTGF (Nakashima et al., 2012). Upregulated miR-92a is able to downregulate the expression of MMP-1, a collagenase known to degrade collagen. Thus the increased expression of miR-92a leads to the increased deposition of collagen in SSc tissue (Sing et al., 2012). A study has also demonstrated that miR-150 expression is decreased in fibroblasts and sera of patients with SSc. Reduced expression of this miRNA increased COL1A1 expression via the induction of integrin b3 (Honda et al., 2013). miR-203 is able to repress several metalloproteinases and inhibit IL-6 (Stanczyk et al., 2008). A study using array analysis of microRNAs related to SSc identified 24 miRNAs that were differentially expressed in SSc patients compared with controls. Certain target genes that were regulated by a subset of six of the miRNAs could be correlated with SSc disease pathogenesis (Li et al., 2012).

A recent study of the miRNA profile in SSc skin done in a Caucasian population identified 26 miRNAs that were differentially expressed in SSc skin compared to controls. Eighteen of the

miRNAs differentially expressed in these patients clustered to the largest known miRNA cluster (miR-379/miR656) and three clustered on the X-chromosome (Salazar et al., 2014).

The role of miRNA regulation and dysregulation in autoimmune diseases still needs to be elucidated. The miRNAs mentioned above have been confirmed to have profibrotic or antifibrotic effects in SSc via different signaling pathways. Thus highlighting that miRNAs are emerging as a potential target for new therapies in the treatment and prevention of autoimmunity. Inhibiting the function of the profibrotic miRNAs or harnessing the effects of the antifibrotic miRNAs, could provide novel therapeutic options for the future.

The miRNAs that have thus far been discovered as playing a role in the development and pathogenesis of SSc may be population specific, with most work done in Caucasians. There are published data on miRNAs in SSc in African Americans (Salazar et al., 2014) and nothing at all in Africans. The aim of this study was to examine the differential expression of microRNAs that could potentially target Wnt pathway genes by small RNA profiling using sRNA-sequencing

3.2. Materials and Methodology

3.2.1. Subjects

Patient and control total RNA samples were from skin samples as described in Chapter 2. A flowchart summarizing the methodology used in this study can be seen in Figure 3.2.

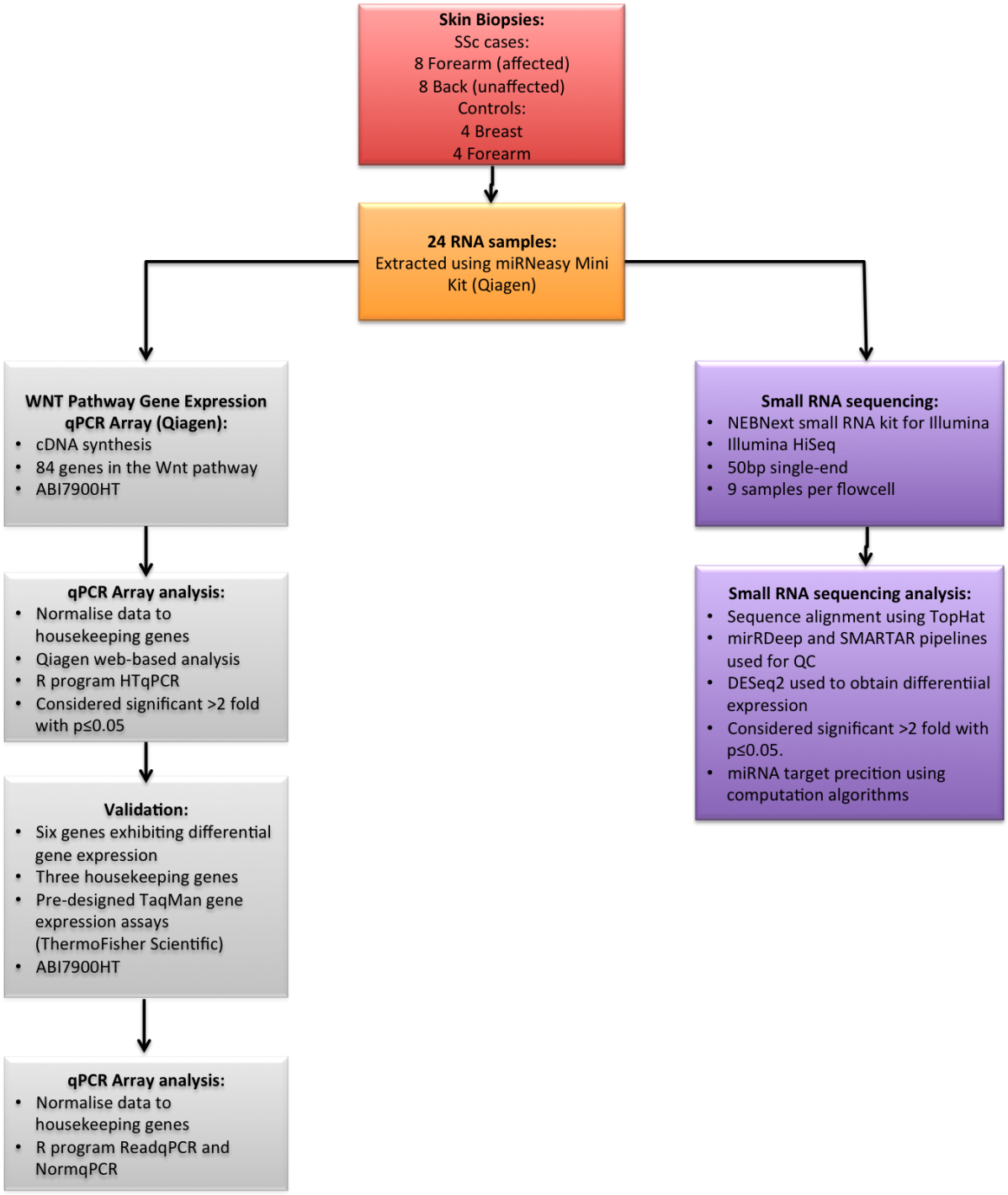


Figure 3.2. Flowchart summary of methodology to investigate miRNAs in skin samples of black South African SSc patients compared to controls.

3.2.2. sRNA-sequencing library preparation

sRNA sequencing libraries were prepared using a small RNA library preparation kit (New England Biosciences). The protocol was optimised for an input of 200ng of total RNA. The protocol in Appendix P details specific changes that were made for small RNA inputs. Fragments were prepared for 50bp single-end sequencing on the HiSeq machine.

3.2.3. Data analysis

3.2.3.1. sRNA-sequencing data analysis

Next generation sequencing data generated from the sRNA-sequencing experiment was first aligned to a reference transcriptome. The alignment software used was TopHat and Cufflinks (Trapnell et al., 2012), with downstream analyses being carried out in an in-house analysis pipeline called mirDeep and SMARTAR (small RNA transcriptome analyzer) (Friedlander et al., 2008). The count data produced was then imported into the R/Bioconductor package called DESeq2 (Love et al., 2014). Differential expression was considered significant if the adjusted p-value was <0.05 (Benjamini–Hochberg rule).

3.2.3.2. Quality Control

sRNA reads with homo-polymer and low PHRED scores were removed and ligation adaptors clipped using SeqBuster. The processed reads were then mapped to the human genome sequence, build hg19. Annotation and assembly pipelines using Genocide v8 were supplemented by various annotations. A detailed description of the QC process used is described elsewhere (Lappalainen et al., 2013). The SMARTAR software generated a QC config file. Quality scores were then assigned, the sequencing reads were trimmed to 36 nucleotide lengths, and PHRED quality scores were calculated for every nucleotide position

in every data set (min, mean, max). Contamination was assessed. As part of the QC, the pipeline identifies miRNAs that are specific to certain clades. Virtually all clade specific miRNAs identified are primate (Appendix Q). miRNA lengths are assessed next, the lengths of the processed sequences (after clipping of 3' adapters) are presented in table format and graphical format. The relative height of the peak at 22 nucleotides in length gives an idea of the content of argonaute-associated small RNAs.

3.2.3.3. Target prediction

To determine the target genes of the miRNAs of interest various computational algorithms are used. These algorithms use defined parameters to predict the probability of a functional miRNA binding site within a target mRNA. Three such target prediction algorithms are miRanda, TargetScan and PicTar. Each of these algorithms determine all the putative mRNA targets of a given mRNA. For increased confidence in the target prediction, it is recommended that at least two of the predictor algorithms must predict the same target binding site (Kuhn et al., 2008). For this study both TargetScan and miRanda were used to identify the Wnt pathway gene targets of the significantly differentially expressed miRNAs.

3.3. Results

The clinical characteristics of the patients were shown in Chapter 2.

3.3.1. Significant differentially expressed miRNA

In total, analysis of the count data using DESeq2 identified 48 miRNAs being significantly differentially expressed in SSc affected skin, and 24 significantly differentially expressed in unaffected SSc skin compared to controls. Only two miRNAs were significantly different when comparing affected SSc skin to unaffacted SSc skin. This list of significantly differentially expressed miRNAs were then filtered for those that specifically target genes in the Wnt pathway.

Princial component analysis of the global differentially expressed miRNAs revealed no distinct separation between the affected and the unaffected SSc skin. There was a horizontal separation of the patient and control samples (Figure 3.3).

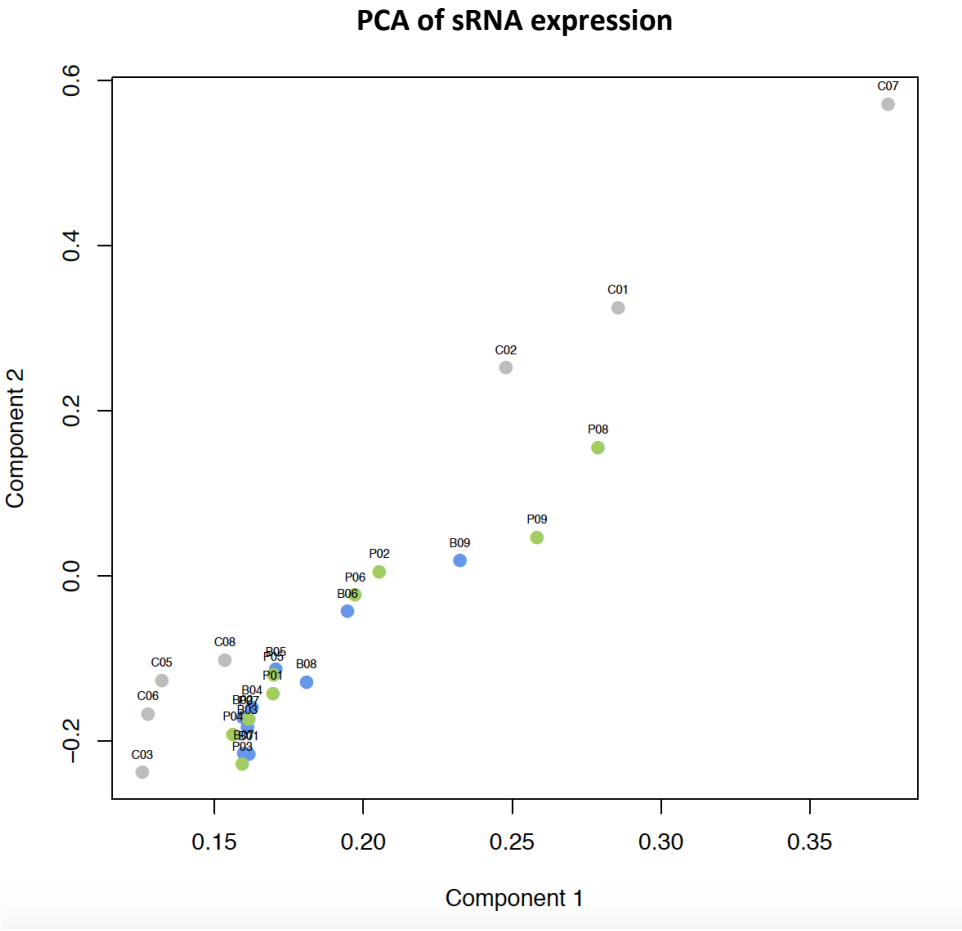


Figure 3.3. Principal component analysis of the sRNA-sequencing results in SSc patients and controls

3.3.2. Wnt pathway predicted targets

Using the two online algorithms, TargetScan and miRanda, 29 of the 84 Wnt pathway genes on the array were identified as targets for the significantly differentially expressed miRNAs. The number of miRNAs which were found to target these 29 genes is shown in Figure 3.4. In the figure it is clear that more miRNAs are found to be differentially expressed in the affected skin samples. For a proportion of the genes, more microRNAs are predicted to target the affected skin rather than the unaffected skin. This is true for *AXIN2, FBXW11, FRZB, FZD7, FZD8, MMP7, NKD1, PRICKLE1, TCF7L1, WIF1, WNT5B* and *CCND2* as is shown in Figure 3.5.

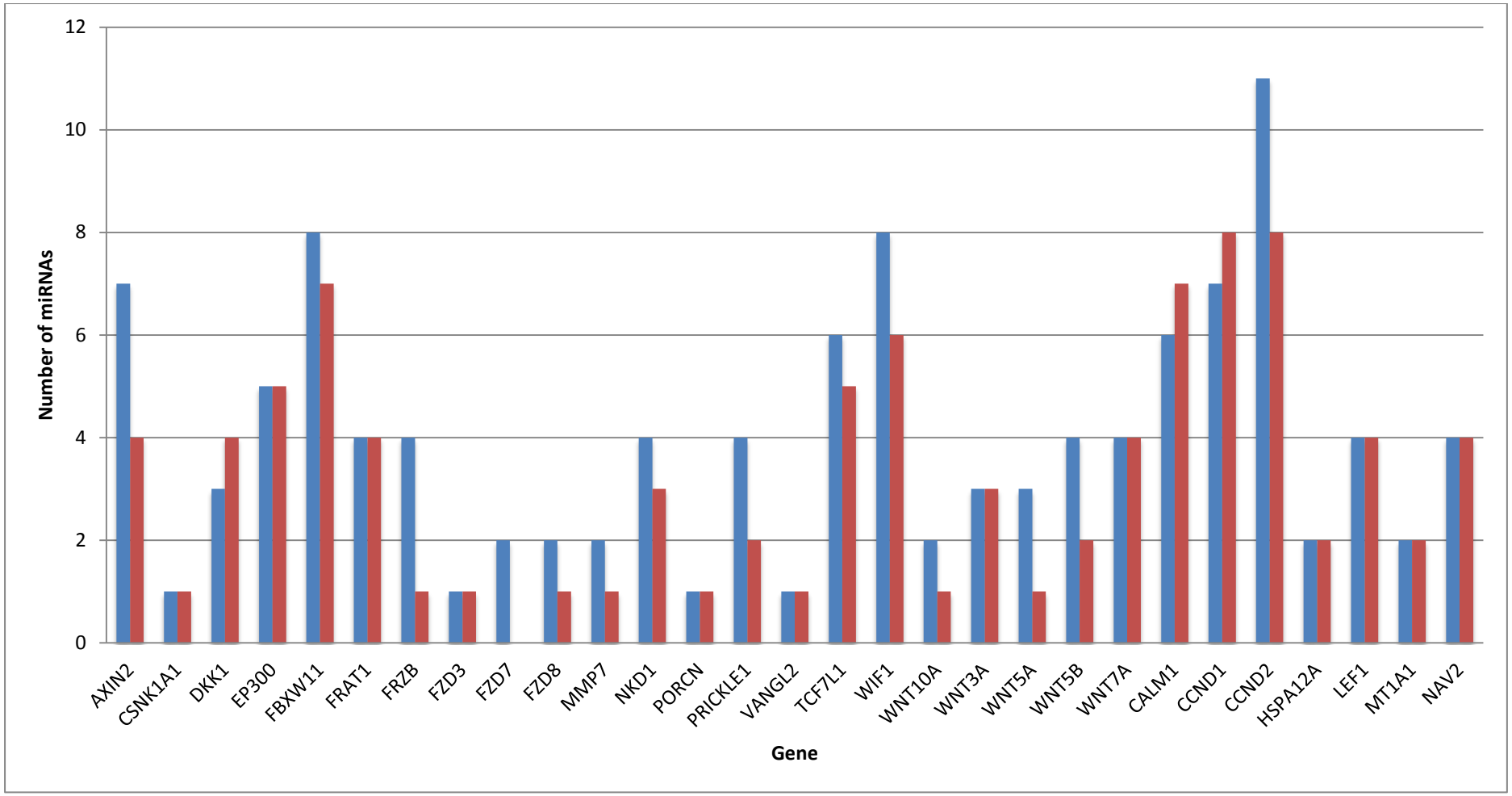


Figure 3.4. Graph representing the number of significantly differentially expressed miRNAs found to target the 29 Wnt pathway genes in affected (blue) and unaffected (red) skin of SSc patients

3.3.3. miRNA expression in SSc skin

Thirty-one significantly differentially expressed miRNAs were predicted to target specific Wnt pathway genes. These miRNAs are presented in Table 3.2, corresponding to the genes they are predicted to target.

3.3.4. miRNA expression in affected SSc skin

miRNA expression in the affected skin revealed that 10 of the 31 miRNAs shown in Table 3.2, are differentially expressed exclusively in the affected SSc skin. Figure 3.5 illustrates the miRNAs targeting Wnt pathway genes in affected skin samples (blue). From the data it would appear that miRNA-194-5p, which is downregulated in affected skin (-1.98 fold change, p=*0.029*), is predicted to target 6 Wnt pathway genes, including *FRZB*, *WIF1*, *MMP7*, *PRICKLE1*, *EP300* and *CCND2*. MiR-326 which is predicted to target 5 genes; *WNT5A*, *LEF1*, *NKD1*, *TCF7L1* and *WIF1*, is also downregulated in affected skin with a fold change of -2.14, p=*0.025*.

3.3.5. miRNA expression in unaffected SSc

Figure 3.5 illustrates the differential expression of miRNAs in unaffected SSc skin (red). Two of these miRNAs were observed only in the unaffected skin. MiR-335-5p, is upregulated in these skin samples by a fold change of 2.3, p=*0.01,* and is predicted to target 2 Wnt pathway genes; *CALM1* and *DKK1*, while miR-106a targets *NAV2* and *LEF1* and is down-regulated by a fold change of -2.58, p=*0.01*.

Table 3.2. Significantly differentially expressed miRNAs in affected and unaffected SSc skin compared to controls that are predicted to target Wnt pathway genes. Some miRNAs target multiple Wnt gene targets.

	miRNA-sequencing data					
	Affected skin			Unaffected skin		
Gene	miRNA	Fold Change	Adj p-value	miRNA	Fold Change	Adj p-value
AXIN1	miR-144-5p	-3.82	*0.0005*	miR-144-5p	-3.66	*0.0005*
	miR-15b-5p	-2.68	*0.001*	miR-15b-5p	-2.63	*0.0009*
	miR-15b-3p	-1.96	*0.029*			
	miR-18b-5p	-4.44	*0.029*			
	miR-16-5p	-1.92	*0.037*	miR-16-5p	-1.97	*0.03*
	miR-18a-5p	-2.16	*0.041*	miR-18a-5p	-2.72	*0.005*
	miR-130b-5p	1.91	*0.05*			
CSNK1A1	miR-543	2.47	*0.0061*	miR-543	2.04	*0.03*
DKK1	miR-335-3p	3.93	*0.00001*	miR-335-3p	4.48	*0.0000001*
				miR-335-5p	2.30	*0.01*
	miR-363	-1.92	*0.038*	miR-363	-2.18	*0.01*
	miR-543	2.47	*0.006*	miR-543	2.04	*0.03*
EP300	miR-194-5p	-1.98	*0.029*			
	miR-20b-5p	-2.46	*0.036*	miR-20b-5p	-2.70	*0.01*
	miR-363-3p	-1.91	*0.037*	miR-363-3p	-2.18	*0.01*
	miR-93-5p	-1.92	*0.037*	miR-93-5p	-2.08	*0.01*
				miR-106a	-2.58	*0.03*
	miR-543	2.47	*0.006*	miR-543	2.04	*0.03*
FBXW11	miR-144-5p	-3.82	*0.0005*	miR-144-5p	-3.66	*0.0005*
	miR-543	2.47	*0.006*	miR-543	2.04	*0.03*
	miR-106b-5p	-2.25	*0.009*	miR-106b-5p	-2.23	*0.009*
	miR-485-3p	2.11	*0.01*			
	miR-20b-5p	-2.46	*0.03*	miR-20b-5p	-2.70	*0.01*
	miR-93-5p	-1.92	*0.03*	miR-93-5p	-2.08	*0.01*
	miR-130b-5p	1.91	*0.05*			
	miR-204-5p	3.14	*0.0001*	miR-204-5p	2.49	*0.005*
				miR-106a-5p	-2.58	*0.03*
FRAT1	miR-144-5p	-1.98	*0.0005*	miR-144-5p	-3.66	*0.0005*
	miR-15b-5p	-2.02	*0.001*	miR-15b-5p	-2.63	*0.0009*
	miR15b-3p	-1.96	*0.02*	miR15b-3p	-2.11	*0.01*
	miR-16-5p	-1.92	*0.03*	miR-16-5p	-19.7	*0.03*
FRZB	miR-194-5p	-1.98	*0.02*			
	miR-30b-5p	-2.02	*0.02*			
	miR-363-3p	-1.91	*0.03*	miR-363-3p	-2.18	*0.01*
	miR-130b-5p	1.91	*0.05*			
FZD3	miR-543	2.47	*0.006*	miR-543	2.04	*0.03*
FZD7	miR-504	2.38	*0.003*			
	miR-379-3p	-2.48	*0.009*			
FZD8	miR-362-3p	-3.51	*0.003*	miR-362-3p	-2.52	*0.04*
	miR-18b-5p	-4.44	*0.02*			
MMP7	miR-194-5p	-1.98	*0.02*			
	miR-543	2.47	*0.006*	miR-543	2.04	*0.03*
NKD1	miR-15b-5p	-2.68	*0.001*	miR-15b-5p	-2.63	*0.0009*
	miR-15b-3p	-1.96	*0.02*	miR-15b-3p	-2.11	*0.01*
	miR-326	-2.14	*0.02*			
	miR-16-5p	-1.92	*0.03*	miR-16-5p	-1.97	*0.03*
PORCN	miR-324-5p	-2.12	*0.02*	miR-324-5p	-2.00	*0.04*

PRICKLE1	miR-144-5p	-3.83	*0.0005*	miR-144-5p	-3.66	*0.0005*
	miR-194-5p	-1.98	*0.02*			
	miR-30b-5p	-2.02	*0.02*			
	miR-16-5p	-1.92	*0.03*	miR-16-5p	-1.97	*0.03*
VANGL2	miR-362-3p	-3.51	*0.003*	miR-362-3p	-2.52	*0.04*
TCF7L1	miR-204-5p	3.15	*0.0001*	miR-204-5p	2.49	*0.005*
	miR-362-3p	-3.51	*0.003*	miR-362-3p	-2.52	*0.04*
	miR-326	-2.14	*0.02*			
	miR-93-5p	-1.92	*0.03*	miR-93-5p	-2.08	*0.01*
	miR-130b-5p	1.91	*0.05*			
	miR-20b-5p	-2.47	*0.03*	miR-20b-5p	-2.70	*0.01*
				miR-106a-5p	-2.58	*0.03*
WIF1	miR-144-5p	-3.82	*0.0004*	miR-144-5p	-3.66	*0.0005*
	miR15b-5p	-2.68	*0.001*	miR15b-5p	-2.63	*0.0009*
	miR-326	-2.14	*0.02*			
	miR15b-3p	-1.96	*0.02*	miR15b-3p	-2.11	*0.01*
	miR-194-5p	-1.98	*0.02*			
	miR-16-5p	-1.92	*0.03*	miR-16-5p	-1.97	*0.03*
	miR-543	2.47	*0.006*	miR-543	2.04	*0.03*
	miR-362-3p	-3.51	*0.003*	miR-362-3p	-2.52	*0.04*
WNT10A	miR-130b	1.91	*0.05*			
	miR-485-5p	2.11	*0.01*	miR-485-5p	2.32	*0.03*
WNT3A	miR-15b-5p	-2.68	*0.001*	miR-15b-5p	-2.63	*0.0009*
	miR-335-3p	3.93	*0.00001*	miR-335-3p	4.48	*0.0000001*
	miR-15b-3p	-1.96	*0.02*	miR-15b-3p	-2.11	*0.01*
	miR-543	2.47	*0.006*	miR-543	2.04	*0.03*
WNT5A	miR-363	-1.92	*0.03*	miR-363	-2.18	*0.01*
	miR-326	-2.14	*0.02*			
	miR-194	-1.98	*0.02*			
WNT5B	miR-144-5p	-3.82	*0.0005*	miR-144-5p	-3.66	*0.0005*
	miR-504	2.38	*0.003*			
	miR-543	2.47	*0.006*	miR-543	2.04	*0.03*
	miR-185	-2.13	*0.01*			
WNT7A	miR-15b-5p	-2,68	*0.001*	miR-15b-5p	-2.63	*0.009*
	miR-15b-3p	-1.96	*0.02*	miR-15b-3p	-2.11	*0.01*
	miR-15a-5p	-2.05	*0.02*	miR-15a-5p	-2.28	*0.007*
	miR-16	-1.93	*0.03*	miR-16	-1.98	*0.03*
CALM1	miR-335-3p	3.93	*0.00001*	miR-335-3p	4.48	*0.0000001*
	miR-15b-5p	-2.68	*0.001*	miR-15b-5p	-2.63	*0.0009*
	miR-362-3p	-3.51	*0.003*	miR-362-3p	-2.52	*0.04*
	miR-15b-3p	-1.96	*0.02*	miR-15b-3p	-2.11	*0.01*
	miR-16-5p	-1.92	*0.03*	miR-16-5p	-1.97	*0.03*
	miR-15a-5p	-2.05	*0.02*	miR-15a-5p	-2.28	*0.007*
				miR-335-5p	2.30	*0.01*
CCND1	miR-15b-5p	-2.68	*0.001*	miR-15b-5p	-2.63	*0.0009*
	miR-106b-5p	-2.25	*0.009*	miR-106b-5p	-2.23	*0.009*
	miR-15b-3p	-1.96	*0.02*	miR-15b-3p	-2.11	*0.01*
	miR-20b-5p	-2.46	*0.03*	miR-20b-5p	-2.70	*0.01*
	miR-93-5p	-1.92	*0.03*	miR-93-5p	-2.08	*0.01*
	miR-15a-5p	-2.05	*0.02*	miR-15a-5p	-2.28	*0.007*
				miR-106a-5p	-2.58	*0.03*
	miR-16	-1.93	*0.03*	miR-16	-1.98	*0.03*
CCND2	miR-15b-5p	-2.68	*0.001*	miR-15b-5p	-2.63	*0.0009*
	miR-15b-3p	-1.96	*0.02*	miR-15b-3p	2.49	*0.005*
	miR-194-5p	-1.98	*0.02*	miR-194-5p	-2.58	*0.03*
	miR-18b-5p	-4.44	*0.02*			

	miR-16-5p	-1.92	*0.03*	miR-16-5p	-1.97	*0.03*
	miR-93-5p	-1.92	*0.03*	miR-93-5p	-2.08	*0.01*
	miR-18a-5p	-2.16	*0.04*	miR-18a-5p	-2.72	*0.005*
	miR-204-5p	3.14	*0.0001*			
	miR-15a-5p	-2.05	*0.02*	miR-15a-5p	-2.28	*0.007*
	miR-20b-5p	-2.46	*0.03*	miR-20b-5p	-2.70	*0.01*
	miR-194	-1.98	*0.03*			
HSPA12A	miR-375	2.39	*0.006*	miR-375	2.00	*0.01*
	miR-543	2.47	*0.006*	miR-543	2.04	*0.03*
LEF1	miR-543	2.47	*0.006*	miR-543	2.04	*0.03*
	miR-326	-2.14	*0.02*			
	miR-93-5p	-1.92	*0.03*	miR-93-5p	-2.08	*0.01*
	miR-20b-5p	-2.46	*0.03*	miR-20b-5p	-2.70	*0.01*
				miR-106a-5p	-2.58	*0.03*
MT1A1	miR-144-5p	-3.82	*0.0005*	miR-144-5p	-3.66	*0.0005*
	miR-93-5p	-1.92	*0.03*	miR-93-5p	-2.08	*0.01*
NAV2	miR-106b-5p	-2.25	*0.009*	miR-106b-5p	-2.23	*0.009*
	miR-485-3p	2.11	*0.01*			
	miR-20b-5p	-2.46	*0.03*	miR-20b-5p	-2.70	*0.01*
	miR-93-5p	-1.92	*0.03*	miR-93-5p	-2.08	*0.01*
				miR-106a-5p	-2.58	*0.03*

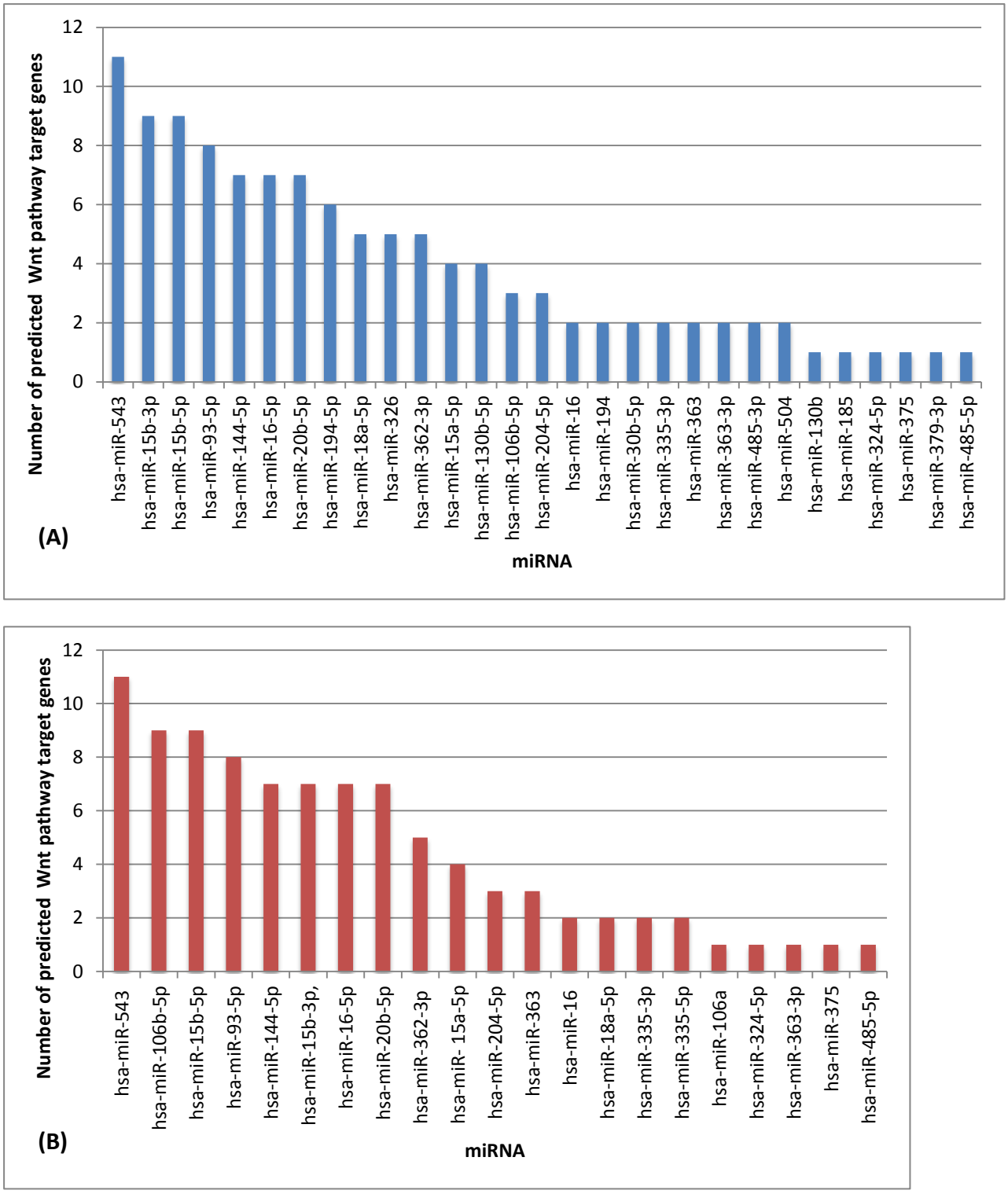


Figure 3.5. Graph representing the number of Wnt pathway genes that specific miRNAs are predicted to target. *(A) Twenty nine of the significantly differentially expressed miRNAs in affected skin (blue), ten of these exclusive to affected skin. (B) Twenty miRNAs are differentially expressed in unaffected skin (red), two of which are exclusive to unaffected skin.*

3.4. Discussion

In this study of skin samples from black South Africans with dcSSc, 48 differentially expressed miRNAs were observed when comparing affected SSc skin to controls. In unaffected SSc skin, 24 were significantly differentially expressed compared to controls. Of these, 31 were predicted to target specific Wnt pathway genes according to TargetScan and miRanda.

It is unknown how morphogen gradients are established and how they function in pattern development in tissues in a dose-dependent manner (Rogers and Schier, 2011). However, it is known that duration and concentration of morphogens determines cell fate in target cells in a spacio-temporal manner. This fine-tuned mechanism in biology is most likely controlled through various miRNAs (Martinez and Gregory, 2010). An example of this fine-tuned regulation would be that of nodal signaling by Wnt/β-catenin-inhibited miR-15 during dorso-ventral segmentation in *Xenopus.*

3.4.1. miRNAs in autoimmunity, inflammation and fibrosis

The discussion that follows will focus on differentially expressed miRNAs that have been identified as having a role in autoimmunity, inflammation or fibrosis (Table 3.2). Two miRNAs miR-335 and miR-204 are of particular interest due to their respective roles in tissue homeostasis and epithelial to mesenchymal transition (Yang et al., 2014a, Wang et al., 2013c).

miR-335 has been extensively studied in cancer. Increased expression of miR-335 correlated with a high frequency of recurrence and poor outcome in individuals with gastric cancer (Yan et al., 2012). miR-335 is able to silence the MEST gene in hepatocellular carcinoma (Dohi et

al., 2013). During normal development, miR-335 orchestrates cell proliferation, migration and differentiation in human mesenchymal cells. A study that aimed to further elucidate the role of miR-335 in normal development, found that the miRNA is able to target key endoderm transcription factors downstream of both TGFβ and Wnt/β-catenin signaling (Dohi et al., 2013).

There is a central role for miR-335 in the gene regulatory network that controls the tissue-repair activities of human mesenchymal stem cells (hMSCs). Expression of this miRNA is upregulated in undifferentiated multipotent hMSCs and is controlled by major signaling pathways such as the Wnt pathway. In a recent study by Yang et al. (2014a) the role of the canonical Wnt pathway, particularly WNT3A, as a positive regulator of miR-335 expression in hMSCs was confirmed. WNT3A functions to inhibit osteogenic differentiation in MSCs. The results of this study increase the understanding of the molecular mechanisms controlling hMSC activity and also strongly suggest that miR-335 plays an important role in tissue homeostasis.

Functional studies of miR-204 have revealed that this miRNA plays a role in both normal development as a negative regulator of RUNX2, thereby promoting adipogenesis of mesenchymal progenitor cells and bone marrow stromal cells (Huang et al., 2010). It also mediates migration and invasion of endometrial cancer through the regulation of FOXC1 (Chung et al., 2012). Several targets of miR-204 have been validated in other cell types that have roles in TGFβ signaling (Pollari et al., 2012). In our study, miR-204 is predicted to target both CCND2 and TCF7L1.

3.4.2. miRNAs differentially expressed in only affected skin from SSc patients

This study found that 10 miRNAs were differentially expressed only in the affected SSc skin samples when compared to controls. One of these miRNAs, miR-194-5p was predicted to target 6 Wnt pathway genes, *CCND2, EP300, FRZB, MMP7, PRICKLE1* and *WIF1*. miR-R194 is also predicted to target *WNT5A* and *CCND2.* Both of these miRNAs were observed to be under-expressed in affected skin compared to controls by almost 2-fold. In peritoneal fibrosis, a common complication in patients treated with long-term peritoneal dialysis, miR-194 was found to be under expressed in a rat model of peritoneal dialysis (Lin et al., 2015). The authors suggested that miR-194 might be associated with pathogenesis of peritoneal fibrosis.

miR-326 was found to be down-regulated by 2-fold when comparing affected skin from SSc patients to controls in the present study, with a p-value=0.026, and was predicted to target five of the Wnt pathway genes including; *WNT5A, LEF1, NKD1, TCF7L1* and *WIF1.* This miRNA has been found to display both increased and decreased expression in a variety of diseases and/or physiological processes. The anti-apoptotic Bcl-2 family regulator Bcl-xL has recently been identified as a target of this miR-326. A functional study demonstrated that miR-326 binds to the 3'-untranslated region of Bcl-xL, sufficient to inhibit Bcl-xL expression, thereby inducing apoptosis in platelets (Yu et al., 2015). This miRNA was also found to be upregulated in multiple sclerosis (MS), which is an inflammatory and neurodegenerative disease. This and other miRNAs may also be potentially used as diagnostic biomarkers in MS (Kucukali et al., 2015). Another study showed that increased miRNA-326 expression is involved in inflammation and/or autoimmunity using IL-10 (-/-) mice. These particular mice are used as an animal model of Th1-mediated inflammatory bowel disease. In these mice,

the development of colonic inflammation was accompanied by upregulation of several miRNAs, including miR-326 (Schaefer et al., 2011). A study analyzing the expression levels of miR-326 in peripheral blood lymphocytes from type 1 diabetic (T1D) patients concluded that miR-326 is expressed at higher levels in T1D subjects, particularly those with ongoing islet autoimmunity. This is similar to the results seen for another autoimmune disease, Multiple Sclerosis (Sebastiani et al., 2011). Converse to the above studies, and complementary to our results is a study that investigated the role of miR-326 in idiopathic pulmonary fibrosis (IPF), a fatal disorder resulting from the progressive remodeling of lungs. TGFβ is known as the master regulator of fibrosis and plays an essential role in lung fibrosis in this disease. One particular study identified miRNAs involved in TGFβ1 regulation, and specifically showed that miR-326 regulates TGFβ1 expression. The study also showed that miR-326 levels are inversely correlated to TGFβ1 protein levels. An increase in TGFβ1 expression during the progression of bleomycin-induced lung fibrosis in mice was associated with decreased miR-326 (Das et al., 2014). Human IPF lung specimens showed markedly diminished miR-326 expression compared with nonfibrotic specimens. The results of this study suggest that miR-326 plays a key role in regulating TGFβ1 expression (Das et al., 2014). In our study the downregulation of miR-326 suggests that there is an increase in levels of TGFβ1 in these patients and this could promote the fibrotic phenotype of the skin.

An increase in the expression levels of miR-130b was detected in this study when comparing affected SSc skin to controls (1.91 fold change, p=0.05). This miRNA has previously been found to be upregulated in SSc skin, as well as being increased in other inflammatory and fibrotic capacities. Increased miR-130b expression has been observed in cholestasis and

inflammation (Rieger et al., 2015), as well as being a predictive silencer of matrix metalloproteinase-2 (MMP2). In a study of prostate cancer the data revealed that miR-130b exerts a suppressive effect in prostate cancer metastasis through down-regulation of MMP2 (Chen et al., 2014). Specifically in a study on SSc patients, miR-130b was found to regulate peroxisome proliferator-activated receptor γ (PPARγ), thus increased expression of miR-130b decreased the levels of PPARγ in the dermis of the SSc skin biopsy samples and fibroblasts. Similar results were observed in the bleomycin-induced skin fibrosis model. This study demonstrated that miR-130b plays an important profibrotic role in SSc fibrosis by enhancing TGFβ signaling (Luo et al., 2015). Decreased expression of miRNA-130b was associated with increased TGFβR1, as well as the profibrotic gene collagen type IV. Together, these results demonstrate a novel miRNA- and host gene-mediated amplifying cascade initiated by TGFβ1, followed by up-regulation of profibrotic factors such as TGFβR1 and collagens associated with the progression of diabetic nephropathy (Castro et al., 2014, Lv et al., 2015). Our results complement previous studies in SSc where miR-130b was observed to have increased expression. These studies suggested that the miRNA could have an effect on both fibrosis and inflammation. Some studies are contradictory to our findings, in that a decreased expression of miR-130b leads to an increase in TGFβ1 levels, known to promote the development of fibrosis. It is clear that the exact mechanism of this miRNA is not yet known and further experimentation needs to be done to fully understand how this miRNA functions.

In our study, miR-30b was significantly downregulated in SSc affected skin compared to control skin (*p=0.02*). This finding supports a study done in 2013 where nineteen of 95

miRNAs tested in the sera of SSc patients were downregulated. This study also found that the levels of miR-30b were inversely correlated with the extent and severity of skin involvement, as measured by the MRSS. Moreover, the expression of miR-30b was downregulated in bleomycin-treated skin and in affected skin in SSc patients (Tanaka et al., 2013). The most strongly and significantly down-regulated miRNA our study was miR-30b (*p=0.00006*). miR-30b was decreased in interstitial fibrosis and tubular atrophy (IFTA) in kidney allografts (Ben-Dov et al., 2012). These studies, together with the results obtained in our own study, suggest that down-regulated miR-30b has a role generally in the pathogenesis of fibrosis and specifically fibrosis in SSc. An increase in the expression of miR-30b has, however, also been associated with increased inflammatory response (Chang et al., 2012), mainly through regulating phagocytosis and the production of inflammatory cytokines (Naqvi et al., 2015).

miR-185 was found to be decreased by 2.13-fold (p=0.01) in our study, it was predicted to target only one Wnt pathway gene, *WNT5A*. This miRNA has not been described in SSc or any other autoimmune disease, though it has been observed in one study to play a role in fibrosis in idiopathic pulmonary fibrosis (IPF). Five miRNAs, including miR-185, were found to be significantly increased in rapid progressing IPF lung biopsies compared to slow progressing lung biopsies. These data suggests that increased miR-185 could play a role in the development of fibrosis (Oak et al., 2011), and is supported by our study.

The final miRNA, which was exclusively differentially expressed in the affected SSc skin, is miR-379. This miRNA was decreased in the SSc skin biopsies by 2.48-fold (*p=0.009*). There is

not much data with regards to this particular miRNA, however, the increased expression of this miRNA has been associated with sex differences in the expression of lupus-associated miRNAs (Dai et al., 2010) and in a mouse model for lupus (Dai et al., 2013).

3.4.3. miRNAs differentially expressed in only unaffected skin from SSc patients

The miRNA exclusively differentially expressed in unaffected skin is miR-106a, which in our study was found to be under-expressed by 2.58-fold (*p=0.03*). It was also predicted to target only one Wnt pathway gene, *EP300*. Recent studies have indicated that an increase in the expression level of miR-106a is associated with increased proinflammatory cytokine release (Sharma et al., 2012) as well as macrophage activation (Zhu et al., 2013a). In a study by (Zhang et al., 2011), miR-335-5p was found to regulate the activation of the Wnt pathway through the inhibition of the Wnt pathway antagonist, *DKK1*. In our study, miR-335-5p is predicted to target DKK1 and is significantly upregulated by 4-fold in the unaffected skin samples of the SSc patients compared to controls.

3.4.4. Summary

To summarise the findings from the microRNA study, it is clear that there are a number of dysregulated miRNAs that target the Wnt pathway, therefore affecting the expression of the Wnt pathway genes they are targeting. miR-335 and miR204 are both important regulators of normal tissue development and their dysregulation would have a profound effect on tissue homeostasis. Other miRNAs dysregulated in this study have been linked to fibrotic diseases or with other autoimmune diseases, confirming their role in the development of fibrosis in SSc. Table 3.3 summarizes the role of several miRNAs that are significantly

differentially expressed in our study and that have been shown through various other studies to have a function in the development of autoimmunity, inflammation and fibrosis.

This study identified 48 differentially expressed miRNAs in SSc skin, a higher number than more what was identified by the study by (Salazar et al., 2014) identified 26 miRNAs dysregulated in SSc, most of these were clustered on the X chromosome. The authors also noted the importance of miRNA in biomarker development. A recent study in cancer recently noted that population specific genetic variation can affect the prevalence and baseline expression of miRNAs in diverse populations. The authors suggested that due to the differential expression of miRNA and specific genes observed among various populations, these differences may be contributing, at least in part, to the population differences observed in cancers (Rawlings-Goss et al., 2014). This population specific expression of miRNAs was also noted as an important consideration when assessing the utility of miRNA biomarkers for the clinic. These population differences are mostly likely present in SSc as well, although the studies to date are small and limited, and as this is the first study of a South African population with SSc this data will enhance the current understanding of microRNAs not only in pathogenesis but also in population differences observed in the disease.

Table 3.3. Most significantly differentially expressed miRNAs in SSc affected skin compared to controls, observed in this study that have specific functions in autoimmunity, inflammation and fibrosis amongst other functions

microRNA	Function	Reference
miR-335	• Overexpression represses endoderm differentiation by blocking Sox17	(Yang et al., 2014a)
	• Important role for the miRMA in tissue homeostasis (incl. Wnt pathway)	(Tome et al., 2011)
	• miR-335-5p activates Wnt signaling and promotes osteogenic differentiation by down-regulating DKK1	(Zhang et al., 2011)
miR-204-5p	• Regulates epithelial to mesenchymal transition • Targets have profound role in TGFβ signalling	(Wang et al., 2013c)
miR-451a	• mTORC1 has been established in rodent models of fibrosis → miR451a induces unrestrained mTORC1 activity	(Dey et al., 2012a, Dey et al., 2012b)
	• Hypertrophic cardiomyopathy is characterised by interstitial fibrosis, miR451a is downregulated in patients with this condition	(Song et al., 2014)
miR-15b-5p	• Upregulated in cardiac ischemia and heart failure and may induce apoptosis	(Small et al., 2010)
	• Downregulated in multiple sclerosis	(Ma et al., 2014)
	• Regulated by IL3 in Acute Myeloid Leukaemia	(Favreau and Sathyanarayana, 2012)
miR-15a-5p	• Downregulated in multiple sclerosis	(Ma et al., 2014)

	• Inflammatory miRNA	(Butovsky et al., 2014)
	• Participates in the Wnt signalling and mTOR pathways	(Leung et al., 2014a, Leung et al., 2014b)
miR-375	• Decreased in inflammatory bowel disease and Autoimmune Type 1 diabetes	(Manolis, 2012)
	• Upregulated in SSc	(Honda et al., 2012)
	• miR-375 also inhibited the Wnt/β-catenin pathway	(Wang et al., 2013b)
miR-543	• Regulates genes involved in inflammatory gene networks in idiopathic pulmonary fibrosis (IPF)	(Vaporidi et al., 2012)
miR-324-5p	• Liver fibrosis	(Murakami et al., 2012)
	• Upregulated in fibrotic liver tissue in rats	Li et al., (2010) FEBS
miR-18b-5p	• Important marker of cell proliferation and cell adhesion	(Murakami et al., 2013)
miR-20b-5p	• Downregulated in multiple sclerosis	(Ma et al., 2014)

Figure 3.6 is a schematic representation of the canonical and non-canonical Wnt pathways with the genes observed as differentially expressed in this study from Chapter 2. Overlayed onto this are the differentially expressed miRNAs that are predicted to target the genes they are in close proximity to in the diagram. In essence, this diagram attempts to summarise the findings of both Chapter 2 and Chapter 3 and conclude that the differential miRNA and gene expression observed in our study play a role in the development and pathogenesis of SSc in these patients.

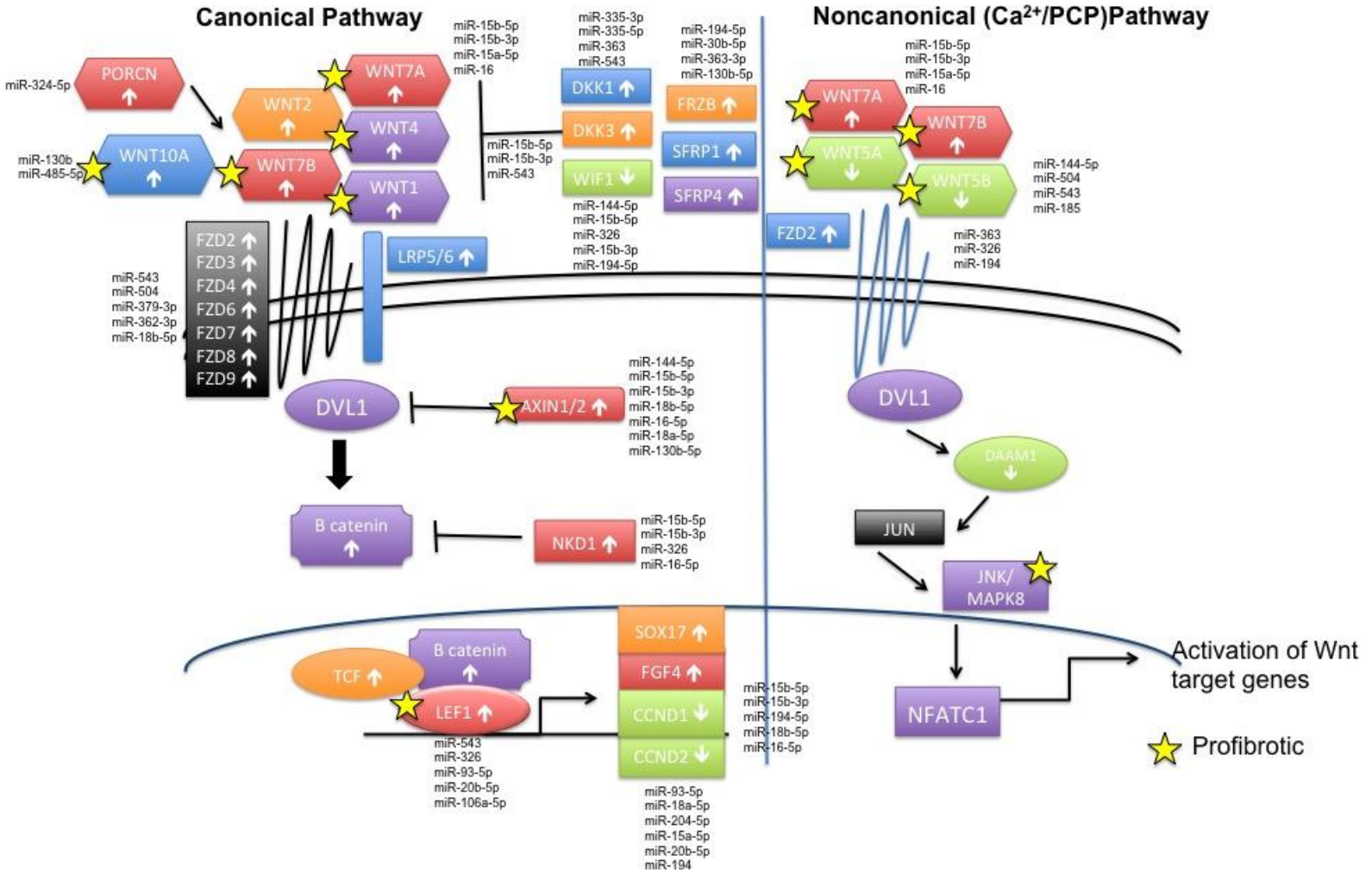


Figure 3.6. Schematic representation of the canonical and non-canonical Wnt pathways with the genes observed as differentially expressed in this study from Chapter 2. The miRNAs in the diagram are significantly differentially expressed in this study and are predicted to target the genes they are in close proximity to in the diagram. The magnitude of differential expression is shown in Table 3.2

3.4.5. Limitations

A limitation of this study is that the miRNA expression data as observed from sRNA-seq has not been validated using a secondary methodology. This could be done using pre-designed miRNA expression assays. Endogenous control miRNA will have to be included in the experiment in order to correctly normalize the miRNA expression values. In similar studies, SNORD 44 and SNORD 48 were used as reference miRNAs (Llorens et al., 2013). As with mRNA expression experiments, the use of endogenous controls in miRNA expression experiments are of vital importance, as variation in the amount of starting material, sample collection, RNA preparation and quality and reverse transcription efficiency can contribute to quantification errors.

Another limitation of the study is the use of the target prediction algorithms, such as TargetScan and miRanda, for predicting the mRNA targets of the miRNAs. Experimental evidence suggests that perfect seed-region paring of the miRNA with the target mRNA is not necessarily a reliable predictor for miRNA interactions and could possibly explain why some of the sites predicted *in-silico* are non-functional (Kuhn et al., 2008). Thus the importance of experimental validation of miRNA-target interactions cannot be overemphasised. Alternatively, experimental prediction of target mRNAs could be used. This will be discussed in further detail in the section below on future studies.

The small sample size of our study limits the power of detection. The findings would need to be validated in a larger group of patients with more detailed phenotypic data to enable the detection of specific miRNA differential expression with selected clinical manifestations in both affected and unaffected kin samples from SSc patients.

3.4.6. Future studies

Several high-throughput methods for identifying miRNA targets have been developed, usually involving overexpression/inhibition of the miRNA or the biochemical isolation of target mRNAs that are bound to miRNAs (Orom and Lund, 2010). A few of these techniques include: 1) Expression Profiling Following miRNA Overexpression/Inhibition, 2) Polysome Profiling Following miRNA Overexpression/Inhibition and 3) Pull-Down Assays with Members of miRISC (Martinez-Sanchez and Murphy, 2013). After in-silico prediction of miRNA target sites, the functional importance of a predicted miRNA/mRNA interaction should be experimentally validated. Generally, a large number of putative miRNA binding sites would have been predicted, thus a rapid and reproducible assay is needed to quickly eliminate any interaction sites that are not functional. The rationale for using a reporter system assay is that the binding of a given miRNA to its specific mRNA target site will repress reporter protein production thereby reducing activity/expression that can be measured and compared to a control (Martin et al., 2006).

Further functional validation, to prove that a specific mRNA is a real target of a given miRNA, would be to experimentally evaluate the change in protein expression of the protein encoded by the mRNA. A typical experimental approach to achieve this would be Western blot analysis, ELISA or immunohistochemistry (Zhao et al., 2007).

The sRNA-seq data are not only able to yield expression data for the miRNAs, but can also be analysed to identify single nucleotide polymorphisms that may be present in the miRNA. Thus far, six such mutations have been identified in the sRNA-seq data obtained from this project. These are all seed region mutations, which is significant as the seed region of

miRNAs is a 7-8 nucleotide long sequence on the 5' end of the miRNAs that is crucial for effective mRNA targeting. The miRNA isoforms found in our study with such seed region mutations are miR-30d-5p, miR-27b-3p, miR-23b-3p, miR-23a-3p, miR-30d-3p and miR-30a-5p. These SNPs can be validated using Sanger sequencing of the miRNA-encoding gene. Most research done on the role of miRNAs in disease pathogenesis focus on mutations in the target mRNA sequences that affect miRNA binding. If there is a single nucleotide polymorphism (SNP) in the seed region of a miRNA then it will no longer be able to bind to its target mRNA resulting in a variety of disease associated pathologies (Zhu et al., 2013a).

An important application of the data from this project would be the identification of specific microRNAs as biomarkers for disease. Fibrosis in SSc is the most prominent clinical feature with the extent and severity of the fibrosis closely correlated to disease prognosis and mortality. There is, however, an unmet medical need for informative biomarkers that could be used in SSc to accurately reflect the fibrotic process in this disease. The reason that miRNAs make such attractive biomarkers is because their expression patterns are reflective of the underlying pathological processes of various disease states. They can also be measured in a variety of sample types such as blood, tissue and other biologic fluids. The elevated expression of profibrotic miRNAs and/or the reduced expression of antifibrotic miRNAs are likely to be important factors in the development of fibrosis in SSc (Zhu et al., 2013b). An in depth analysis of the microRNA data together with comprehensive clinical data could elucidate biomarkers that would be useful for different aspect so disease, such as disease activity, severity, tissue damage, extent of fibrosis. Ideally the development of a predictive biomarker would be of extreme clinical utility and beneficial to clinicians.

The objective would be to identify several miRNAs that are significantly up and down regulated from the sRNA-seq data and then validate these as a large panel of SSc patients with detailed phenotypic data using a secondary methodology. This validation should be done in a replication cohort of patients and ideally blood samples should be used instead of skin biopsies. If indeed, these miRNAs do validate and they are detectable in the blood samples of the patients, this would be a significant result making SSc disease identification, diagnosis and prognosis much easier for clinicians.

Chapter 4

Conclusion

This is the first study to assess the role of the Wnt signaling pathway in black South African patients with early, diffuse cutaneous SSc, using a combination of quantitative PCR and s-RNA sequencing. The study demonstrated that the Wnt signaling pathway is dysregulated, which is consistent with its involvement in the development of fibrosis in several fibrotic diseases, including SSc, in other populations, involving both the canonical and non-canonical Wnt signaling pathways. The evidence comes from differential gene expression analysis of 84 Wnt pathway genes using the qPCR array, which revealed that there were five distinct clusters of genes exhibiting different patterns of gene expression between or within SSc patients and controls. In affected and unaffected SSc skin, although only 14 of these were significantly different compared to controls (Adj. $p<0.05$). Sixteen genes were downregulated in affected and unaffected skin compared to controls, though only six of these reached a level of significance (Adj. $p<0.05$). In Patient Group 1, 37 genes were significantly dysregulated in SSc skin compared to controls (Adj. $p<0.05$) , while in Patient Group 2, 30 genes were dysregulated in SSc skin compared to controls (Adj. $p<0.05$).

The largest number of genes in the group that showed differential gene expression between cases and controls (with the cases including all or the majority of the patients, both affected and unaffected) were upregulated in SSc patients. These genes included a myriad of Wnt ligands, Frizzled receptors and antagonists of the Wnt pathways. Two of the Wnt ligands,

WNT7A and *WNT7B*, are responsible for activating the canonical Wnt pathway as well as exhibiting potent profibrotic effects. Not only were effectors of the pathway observed as being upregulated, but also repressors of the pathway such as *AXIN1*, *AXIN2 and DKK1.* Although these molecules are antagonists of the Wnt pathway, they act only once the Wnt pathway has already been activated. Together, these data indicate that the Wnt pathway is constitutively activated in these SSc patients and leading to opposing signals in an attempt to maintain tissue homeostasis.

Genes that are downregulated in SSc patients, in both affected and unaffected skin, compared to controls, include *WNT5A* and *WNT5B,* both of which have been found to play a role in fibrotic and inflammatory diseases, such as renal fibrosis and inflammatory bowel disease, and could therefore play an important role in the pathogenesis of dcSSc.

SSc is recognized as being a heterogeneous disease, manifesting with a collection of symptoms that can vary in their severity and presence across patients. This molecular investigation of gene expression in the skin of affected and unaffected patients has stratified the patients into two patient groups 1 (Patients 2, 4, 6 and 8) and 2 (Patient 3, 5, 7 and 9). The majority of differentially expressed genes are either significantly upregulated (n=20) or downregulated (n=6) in all patient samples irrespective of whether the samples originate from the affected or the unaffected skin. A minority of genes contributes to the differences, which are responsible for delineating the two patients groups. The affected skin of patient group 1 shows 14 significantly upregulated genes, while the unaffected skin samples show no differential expression for these genes compared to controls. The affected skin of patient group 2 shows upregulation of 7 genes (none of which overlap with those genes upregulated

in Patient Group 1), while the unaffected skin display no difference compared to controls. Since patients with a more inflammatory gene expression pattern in their affected skin fall mostly into Patient Group 1, it is possible that this signature could differentiate diffuse SSc patients into two sub-groups. One with a more profibrotic disease manifestation in their affected skin and the other with an inflammatory clinical response. Similar observations have been made in other studies (Milano et al., 2008, Pendergrass et al., 2012).

A number of miRNAs that target genes in the Wnt pathway show differential expression between dcSSc patients and controls, potentially affecting the post-transcriptional regulation of Wnt pathway genes. For example, miR-335 and miR204 are both important regulators of normal tissue development and their dysregulation would have profound effects on tissue homeostasis. Other miRNAs dysregulated in this study have been linked to fibrotic diseases or with other autoimmune diseases, such as miR-324 and miR-326 that play a role in the development of fibrosis. MicroRNAs previously linked specifically to the development of SSc such as miR-30b and miR-379 (Tanaka et al., 2013, Chang et al., 2012), were also dysregulated in our study. These data support the role of these microRNAs in the development of fibrosis in SSc.

The role that differentially expressed microRNAs play in the dysregulation of the Wnt pathways should be further elucidated and therefore is an important aspect of research that should be continued. There are very few therapies available for the treatment of fibrosis in SSc or other diseases. MicroRNAs could be a novel form of therapy. MicroRNAs are measureable in a variety of bodily fluids including serum and plasma. The relative stability of microRNAs will enable the miRNAs to serve as informative biomarkers, with the ability to

monitor disease progression and response to treatment. The development of miRNA therapy for the management of skin fibrosis can be classified into therapies that increase the expression of antifibrotic miRNAs or reduce the expression of profibrotic miRNAs. Therapy that is either miRNA-directed or has the ability to modulate miRNA will potentially make a significant contribution to managing the development and progression of fibrosis in SSc and other diseases.

In summary, this study of a homogenous sample of early disease, black African dcSSc patients reveals that the Wnt signaling pathway is significantly dysregulated. A small group of differentially expressed genes delineates the patients into two distinct groups. It is possible that they define patients exhibiting a more fibrotic phenotype and distinguishing them from others who exhibit a more inflammatory phenotype. In addition, the sRNA-sequencing study revealed that a number of miRNAs were differentially expressed between these SSc patients and controls indicating that the pathogenesis, progression and clinical features of the disease are likely caused by epigenetic changes that affect gene expression and may be related to environmental changes, in the context of a disease susceptible genotype. This is consistent with the multifactorial nature of scleroderma.

References

Abraham, D. & Distler, O. 2007. How does endothelial cell injury start? The role of endothelin in systemic sclerosis. *Arthritis Res Ther,* 9 Suppl 2**,** S2.

Abraham, D. J., Eckes, B., Rajkumar, V. & Krieg, T. 2007. New developments in fibroblast and myofibroblast biology: implications for fibrosis and scleroderma. *Curr Rheumatol Rep,* 9**,** 136-43.

Abraham, D. J., Krieg, T., Distler, J. & Distler, O. 2009. Overview of pathogenesis of systemic sclerosis. *Rheumatology (Oxford),* 48 Suppl 3**,** iii3-7.

Adams Waldorf, K. M. & Nelson, J. L. 2008. Autoimmune disease during pregnancy and the microchimerism legacy of pregnancy. *Immunol Invest,* 37**,** 631-44.

Adelowo, O. O. & Oguntona, S. 2009. Scleroderma (systemic sclerosis) among Nigerians. *Clin Rheumatol,* 28**,** 1121-5.

Akhmetshina, A., Palumbo, K., Dees, C., et al. 2012. Activation of canonical Wnt signalling is required for TGF-beta-mediated fibrosis. *Nat Commun,* 3**,** 735.

Akhmetshina, A., Venalis, P., Dees, C., Busch, N., Zwerina, J., Schett, G., Distler, O. & Distler, J. H. 2009. Treatment with imatinib prevents fibrosis in different preclinical models of systemic sclerosis and induces regression of established fibrosis. *Arthritis Rheum,* 60**,** 219-24.

Alexander, M. S., Kawahara, G., Motohashi, N., et al. 2013. MicroRNA-199a is induced in dystrophic muscle and affects WNT signaling, cell proliferation, and myogenic differentiation. *Cell Death Differ,* 20**,** 1194-208.

Alonso-Ruiz, A., Zea-Mendoza, A. C., Salazar-Vallinas, J. M., Rocamora-Ripoll, A. & Beltran-Gutierrez, J. 1986. Toxic oil syndrome: a syndrome with features overlapping those of various forms of scleroderma. *Semin Arthritis Rheum,* 15**,** 200-12.

Altorok, N., Tsou, P. S., Coit, P., Khanna, D. & Sawalha, A. H. 2015. Genome-wide DNA methylation analysis in dermal fibroblasts from patients with diffuse and limited systemic sclerosis reveals common and subset-specific DNA methylation aberrancies. *Ann Rheum Dis,* 74**,** 1612-20.

Arao, T., Ueshima, K., Matsumoto, K., et al. 2013. FGF3/FGF4 amplification and multiple lung metastases in responders to sorafenib in hepatocellular carcinoma. *Hepatology,* 57**,** 1407-15.

Armando Laborde, H. & Young, P. 2012. [History of systemic sclerosis]. *Gac Med Mex,* 148**,** 201-8.

Arnett, F. C., Cho, M., Chatterjee, S., Aguilar, M. B., Reveille, J. D. & Mayes, M. D. 2001. Familial occurrence frequencies and relative risks for systemic sclerosis (scleroderma) in three United States cohorts. *Arthritis Rheum,* 44**,** 1359-62.

Arnett, F. C., Howard, R. F., Tan, F., et al. 1996. Increased prevalence of systemic sclerosis in a Native American tribe in Oklahoma. Association with an Amerindian HLA haplotype. *Arthritis Rheum,* 39**,** 1362-70.

Aumiller, V., Balsara, N., Wilhelm, J., Gunther, A. & Konigshoff, M. 2013. WNT/beta-catenin signaling induces IL-1beta expression by alveolar epithelial cells in pulmonary fibrosis. *Am J Respir Cell Mol Biol,* 49**,** 96-104.

Ball, M. P., Li, J. B., Gao, Y., Lee, J. H., Leproust, E. M., Park, I. H., Xie, B., Daley, G. Q. & Church, G. M. 2009. Targeted and genome-scale strategies reveal gene-body methylation signatures in human cells. *Nat Biotechnol,* 27**,** 361-8.

Bartel, D. P. 2004. MicroRNAs: genomics, biogenesis, mechanism, and function. *Cell,* 116**,** 281-97.

Bayle, J., Fitch, J., Jacobsen, K., Kumar, R., Lafyatis, R. & Lemaire, R. 2008. Increased expression of Wnt2 and SFRP4 in Tsk mouse skin: role of Wnt signaling in altered dermal fibrillin deposition and systemic sclerosis. *J Invest Dermatol,* 128**,** 871-81.

Ben-Dov, I. Z., Muthukumar, T., Morozov, P., Mueller, F. B., Tuschl, T. & Suthanthiran, M. 2012. MicroRNA sequence profiles of human kidney allografts with or without tubulointerstitial fibrosis. *Transplantation,* 94**,** 1086-94.

Benedek, T. G. & Rodnan, G. P. 1982a. A brief history of the rheumatic diseases. *Bull Rheum Dis,* 32**,** 59-68.

Benedek, T. G. & Rodnan, G. P. 1982b. The early history and nomenclature of scleroderma and of its differentiation from sclerema neonatorum and scleroedema. *Semin Arthritis Rheum,* 12**,** 52-67.

Bentwich, I., Avniel, A., Karov, Y., et al. 2005. Identification of hundreds of conserved and nonconserved human microRNAs. *Nat Genet,* 37**,** 766-70.

Bentzinger, C. F., Wang, Y. X., Von Maltzahn, J., Soleimani, V. D., Yin, H. & Rudnicki, M. A. 2013. Fibronectin regulates Wnt7a signaling and satellite cell expansion. *Cell Stem Cell,* 12**,** 75-87.

Besliu, A. N., Banica, L. M., Lonescu, R., et al. 2009. Role of cellular immunity in systemic sclerosis pathogenesis: update on CD4+T cells population studies. *Roum Arch Microbiol Immunol,* 68**,** 5-13.

Beyer, C., Dees, C. & Distler, J. H. 2012a. Morphogen pathways as molecular targets for the treatment of fibrosis in systemic sclerosis. *Arch Dermatol Res*.

Beyer, C. & Distler, J. H. 2013. Morphogen pathways in systemic sclerosis. *Curr Rheumatol Rep,* 15**,** 299.

Beyer, C., Distler, O. & Distler, J. H. 2012b. Innovative antifibrotic therapies in systemic sclerosis. *Curr Opin Rheumatol,* 24**,** 274-80.

Beyer, C., Schramm, A., Akhmetshina, A., et al. 2012c. beta-catenin is a central mediator of pro-fibrotic Wnt signaling in systemic sclerosis. *Ann Rheum Dis,* 71**,** 761-7.

Bhattacharyya, S., Chen, S. J., Wu, M., et al. 2008. Smad-independent transforming growth factor-beta regulation of early growth response-1 and sustained expression in fibrosis: implications for scleroderma. *Am J Pathol,* 173**,** 1085-99.

Bhattacharyya, S., Wei, J. & Varga, J. 2012. Understanding fibrosis in systemic sclerosis: shifting paradigms, emerging opportunities. *Nat Rev Rheumatol,* 8**,** 42-54.

Bhattacharyya, S., Wu, M., Fang, F., Tourtellotte, W., Feghali-Bostwick, C. & Varga, J. 2011. Early growth response transcription factors: key mediators of fibrosis and novel targets for anti-fibrotic therapy. *Matrix Biol,* 30**,** 235-42.

Bielefeld, K. A., Amini-Nik, S., Whetstone, H., Poon, R., Youn, A., Wang, J. & Alman, B. A. 2011. Fibronectin and beta-catenin act in a regulatory loop in dermal fibroblasts to modulate cutaneous healing. *J Biol Chem,* 286**,** 27687-97.

Bielesz, B., Sirin, Y., Si, H., et al. 2010. Epithelial Notch signaling regulates interstitial fibrosis development in the kidneys of mice and humans. *J Clin Invest,* 120**,** 4040-54.

Bird, A. 2002. DNA methylation patterns and epigenetic memory. *Genes Dev,* 16**,** 6-21.

Bird, A. 2007. Perceptions of epigenetics. *Nature,* 447**,** 396-8.

Blobe, G. C., Schiemann, W. P. & Lodish, H. F. 2000. Role of transforming growth factor beta in human disease. *N Engl J Med,* 342**,** 1350-8.

Blumenthal, A., Ehlers, S., Lauber, J., Buer, J., Lange, C., Goldmann, T., Heine, H., Brandt, E. & Reiling, N. 2006. The Wingless homolog WNT5A and its receptor Frizzled-5 regulate inflammatory responses of human mononuclear cells induced by microbial stimulation. *Blood,* 108**,** 965-73.

Bogatkevich, G. S., Ludwicka-Bradley, A., Highland, K. B., Hant, F., Nietert, P. J., Singleton, C. B., Feghali-Bostwick, C. A. & Silver, R. M. 2007. Impairment of the antifibrotic effect of hepatocyte growth factor in lung fibroblasts from African Americans: possible role in systemic sclerosis. *Arthritis Rheum,* 56**,** 2432-42.

Bohan, A. & Peter, J. B. 1975a. Polymyositis and dermatomyositis (first of two parts). *N Engl J Med,* 292**,** 344-7.

Bohan, A. & Peter, J. B. 1975b. Polymyositis and dermatomyositis (second of two parts). *N Engl J Med,* 292**,** 403-7.

Bossini-Castillo, L., Martin, J. E., Broen, J., et al. 2012. A GWAS follow-up study reveals the association of the IL12RB2 gene with systemic sclerosis in Caucasian populations. *Hum Mol Genet,* 21**,** 926-33.

Bossini-Castillo, L., Martin, J. E., Broen, J., et al. 2013. Confirmation of TNIP1 but not RHOB and PSORS1C1 as systemic sclerosis risk factors in a large independent replication study. *Ann Rheum Dis,* 72**,** 602-7.

Bossini-Castillo, L., Simeon, C. P., Beretta, L., et al. 2011. Confirmation of association of the macrophage migration inhibitory factor gene with systemic sclerosis in a large European population. *Rheumatology (Oxford),* 50**,** 1976-81.

Boulter, L., Guest, R. V., Kendall, T. J., et al. 2015. WNT signaling drives cholangiocarcinoma growth and can be pharmacologically inhibited. *J Clin Invest,* 125**,** 1269-85.

Bowley, E., O'gorman, D. B. & Gan, B. S. 2007. Beta-catenin signaling in fibroproliferative disease. *J Surg Res,* 138**,** 141-50.

Briggs, S. D., Xiao, T., Sun, Z. W., Caldwell, J. A., Shabanowitz, J., Hunt, D. F., Allis, C. D. & Strahl, B. D. 2002. Gene silencing: trans-histone regulatory pathway in chromatin. *Nature,* 418**,** 498.

Briscoe, J. 2009. Making a grade: Sonic Hedgehog signalling and the control of neural cell fate. *EMBO J,* 28**,** 457-65.

Broen, J. C., Bossini-Castillo, L., Van Bon, L., et al. 2012a. A rare polymorphism in the gene for Toll-like receptor 2 is associated with systemic sclerosis phenotype and increases the production of inflammatory mediators. *Arthritis Rheum,* 64**,** 264-71.

Broen, J. C., Coenen, M. J. & Radstake, T. R. 2012b. Genetics of systemic sclerosis: an update. *Curr Rheumatol Rep,* 14**,** 11-21.

Butovsky, O., Jedrychowski, M. P., Moore, C. S., et al. 2014. Identification of a unique TGF-beta-dependent molecular and functional signature in microglia. *Nat Neurosci,* 17**,** 131-43.

Castro, N. E., Kato, M., Park, J. T. & Natarajan, R. 2014. Transforming growth factor beta1 (TGF-beta1) enhances expression of profibrotic genes through a novel signaling cascade and microRNAs in renal mesangial cells. *J Biol Chem,* 289**,** 29001-13.

Chang, C. C., Zhang, Q. Y., Liu, Z., Clynes, R. A., Suciu-Foca, N. & Vlad, G. 2012. Downregulation of inflammatory microRNAs by Ig-like transcript 3 is essential for the differentiation of human CD8(+) T suppressor cells. *J Immunol,* 188**,** 3042-52.

Chen, C., Wu, C. Q., Zhang, Z. Q., Yao, D. K. & Zhu, L. 2011. Loss of expression of miR-335 is implicated in hepatic stellate cell migration and activation. *Exp Cell Res,* 317**,** 1714-25.

Chen, K., See, A. & Shumack, S. 2003. Epidemiology and pathogenesis of scleroderma. *Australas J Dermatol,* 44**,** 1-7; quiz 8-9.

Chen, Q., Zhao, X., Zhang, H., et al. 2014. MiR-130b suppresses prostate cancer metastasis through down-regulation of MMP2. *Mol Carcinog*.

Chen, Y., Shi-Wen, X., Van Beek, J., et al. 2005. Matrix contraction by dermal fibroblasts requires transforming growth factor-beta/activin-linked kinase 5, heparan sulfate-containing proteoglycans, and MEK/ERK: insights into pathological scarring in chronic fibrotic disease. *Am J Pathol,* 167**,** 1699-711.

Cho, J. H., Gelinas, R., Wang, K., et al. 2011. Systems biology of interstitial lung diseases: integration of mRNA and microRNA expression changes. *BMC Med Genomics,* 4**,** 8.

Choi, S. S., Omenetti, A., Syn, W. K. & Diehl, A. M. 2011. The role of Hedgehog signaling in fibrogenic liver repair. *Int J Biochem Cell Biol,* 43**,** 238-44.

Christner, P. J. & Jimenez, S. A. 2004. Animal models of systemic sclerosis: insights into systemic sclerosis pathogenesis and potential therapeutic approaches. *Curr Opin Rheumatol,* 16**,** 746-52.

Chung, T. K., Lau, T. S., Cheung, T. H., et al. 2012. Dysregulation of microRNA-204 mediates migration and invasion of endometrial cancer by regulating FOXC1. *Int J Cancer,* 130**,** 1036-45.

Clements, P. J. 2000. Systemic sclerosis (scleroderma) and related disorders: clinical aspects. *Baillieres Best Pract Res Clin Rheumatol,* 14**,** 1-16.

Clevers, H. 2006. Wnt/beta-catenin signaling in development and disease. *Cell,* 127**,** 469-80.

Cobb, B. S., Hertweck, A., Smith, J., et al. 2006. A role for Dicer in immune regulation. *J Exp Med,* 203**,** 2519-27.

Cockrill, T., Del Junco, D. J., Arnett, F. C., Assassi, S., Tan, F. K., Mcnearney, T., Fischbach, M., Perry, M. & Mayes, M. D. 2010. Separate influences of birth order and gravidity/parity on the development of systemic sclerosis. *Arthritis Care Res (Hoboken),* 62**,** 418-24.

Corbett, L., Mann, J. & Mann, D. A. 2015. Non-Canonical Wnt Predominates in Activated Rat Hepatic Stellate Cells, Influencing HSC Survival and Paracrine Stimulation of Kupffer Cells. *PLoS One,* 10**,** e0142794.

Cowie, R. L. 1987. Silica-dust-exposed mine workers with scleroderma (systemic sclerosis). *Chest,* 92**,** 260-2.

Cowie, R. L. & Dansey, R. D. 1990. Features of systemic sclerosis (scleroderma) in South African goldminers. *S Afr Med J,* 77**,** 400-2.

Da Costa Martins, P. A., Salic, K., Gladka, M. M., et al. 2010. MicroRNA-199b targets the nuclear kinase Dyrk1a in an auto-amplification loop promoting calcineurin/NFAT signalling. *Nat Cell Biol,* 12**,** 1220-7.

Dai, R., Mcreynolds, S., Leroith, T., Heid, B., Liang, Z. & Ahmed, S. A. 2013. Sex differences in the expression of lupus-associated miRNAs in splenocytes from lupus-prone NZB/WF1 mice. *Biol Sex Differ,* 4**,** 19.

Dai, R., Zhang, Y., Khan, D., Heid, B., Caudell, D., Crasta, O. & Ahmed, S. A. 2010. Identification of a common lupus disease-associated microRNA expression pattern in three different murine models of lupus. *PLoS One,* 5**,** e14302.

Das, S., Kumar, M., Negi, V., Pattnaik, B., Prakash, Y. S., Agrawal, A. & Ghosh, B. 2014. MicroRNA-326 regulates profibrotic functions of transforming growth factor-beta in pulmonary fibrosis. *Am J Respir Cell Mol Biol,* 50**,** 882-92.

De Langhe, E., Aznar-Lopez, C., De Vooght, V., Vanoirbeek, J. A., Luyten, F. P. & Lories, R. J. 2014. Secreted frizzled related proteins inhibit fibrosis in vitro but appear redundant in vivo. *Fibrogenesis Tissue Repair,* 7**,** 14.

De Langhe, E. & Lories, R. 2015. Fibrogenesis, novel lessons from animal models. *Semin Immunopathol,* 37**,** 565-74.

De Ruijter, A. J., Van Gennip, A. H., Caron, H. N., Kemp, S. & Van Kuilenburg, A. B. 2003. Histone deacetylases (HDACs): characterization of the classical HDAC family. *Biochem J,* 370**,** 737-49.

Dees, C. & Distler, J. H. 2013. Canonical Wnt signalling as a key regulator of fibrogenesis - implications for targeted therapies? *Exp Dermatol,* 22**,** 710-3.

Dees, C., Tomcik, M., Zerr, P., et al. 2011a. Notch signalling regulates fibroblast activation and collagen release in systemic sclerosis. *Ann Rheum Dis,* 70**,** 1304-10.

Dees, C., Zerr, P., Tomcik, M., et al. 2011b. Inhibition of Notch signaling prevents experimental fibrosis and induces regression of established fibrosis. *Arthritis Rheum,* 63**,** 1396-404.

Denton, C. P., Black, C. M. & Abraham, D. J. 2006. Mechanisms and consequences of fibrosis in systemic sclerosis. *Nat Clin Pract Rheumatol,* 2**,** 134-44.

Denton, C. P. & Ong, V. H. 2013. Targeted therapies for systemic sclerosis. *Nat Rev Rheumatol,* 9**,** 451-64.

Derk, C. T. & Jimenez, S. A. 2003. Systemic sclerosis: current views of its pathogenesis. *Autoimmun Rev,* 2**,** 181-91.

Dey, N., Das, F., Ghosh-Choudhury, N., Mandal, C. C., Parekh, D. J., Block, K., Kasinath, B. S., Abboud, H. E. & Choudhury, G. G. 2012a. microRNA-21 governs TORC1 activation in renal cancer cell proliferation and invasion. *PLoS One,* 7**,** e37366.

Dey, N., Ghosh-Choudhury, N., Kasinath, B. S. & Choudhury, G. G. 2012b. TGFbeta-stimulated microRNA-21 utilizes PTEN to orchestrate AKT/mTORC1 signaling for mesangial cell hypertrophy and matrix expansion. *PLoS One,* 7**,** e42316.

Diehl, J. A., Cheng, M., Roussel, M. F. & Sherr, C. J. 1998. Glycogen synthase kinase-3beta regulates cyclin D1 proteolysis and subcellular localization. *Genes Dev,* 12**,** 3499-511.

Dieude, P., Dawidowicz, K., Guedj, M., et al. 2010. Phenotype-haplotype correlation of IRF5 in systemic sclerosis: role of 2 haplotypes in disease severity. *J Rheumatol,* 37**,** 987-92.

Dieude, P., Wipff, J., Guedj, M., et al. 2009. BANK1 is a genetic risk factor for diffuse cutaneous systemic sclerosis and has additive effects with IRF5 and STAT4. *Arthritis Rheum,* 60**,** 3447-54.

Dijksterhuis, J. P., Baljinnyam, B., Stanger, K., Sercan, H. O., Ji, Y., Andres, O., Rubin, J. S., Hannoush, R. N. & Schulte, G. 2015. Systematic Mapping of WNT-FZD Protein Interactions Reveals Functional Selectivity by Distinct WNT-FZD Pairs. *J Biol Chem,* 290**,** 6789-98.

Ding, H., Zhou, D., Hao, S., Zhou, L., He, W., Nie, J., Hou, F. F. & Liu, Y. 2012. Sonic hedgehog signaling mediates epithelial-mesenchymal communication and promotes renal fibrosis. *J Am Soc Nephrol,* 23**,** 801-13.

Diot, E., Lesire, V., Guilmot, J. L., et al. 2002. Systemic sclerosis and occupational risk factors: a case-control study. *Occup Environ Med,* 59**,** 545-9.

Distler, J. H. & Distler, O. 2009. Imatinib as a novel therapeutic approach for fibrotic disorders. *Rheumatology (Oxford),* 48**,** 2-4.

Dohi, O., Yasui, K., Gen, Y., et al. 2013. Epigenetic silencing of miR-335 and its host gene MEST in hepatocellular carcinoma. *Int J Oncol,* 42**,** 411-8.

Dolmans, G. H., Werker, P. M., Hennies, H. C., et al. 2011. Wnt signaling and Dupuytren's disease. *N Engl J Med,* 365**,** 307-17.

Dong, C., Zhu, S., Wang, T., et al. 2002. Deficient Smad7 expression: a putative molecular defect in scleroderma. *Proc Natl Acad Sci U S A,* 99**,** 3908-13.

Duisters, R. F., Tijsen, A. J., Schroen, B., et al. 2009. miR-133 and miR-30 regulate connective tissue growth factor: implications for a role of microRNAs in myocardial matrix remodeling. *Circ Res,* 104**,** 170-8, 6p following 178.

Ehrlich, M., Gama-Sosa, M. A., Huang, L. H., Midgett, R. M., Kuo, K. C., Mccune, R. A. & Gehrke, C. 1982. Amount and distribution of 5-methylcytosine in human DNA from different types of tissues of cells. *Nucleic Acids Res,* 10**,** 2709-21.

Erasmus, L. D. 1957. Scleroderma in goldminers on the Witwatersrand with particular reference to pulmonary manifestations. *S Afr J Lab Clin Med,* 3**,** 209-31.

Evron, E., Umbricht, C. B., Korz, D., et al. 2001. Loss of cyclin D2 expression in the majority of breast cancers is associated with promoter hypermethylation. *Cancer Res,* 61**,** 2782-7.

Fan, S. & Zhang, X. 2009. CpG island methylation pattern in different human tissues and its correlation with gene expression. *Biochem Biophys Res Commun,* 383**,** 421-5.

Fanning, G. C., Welsh, K. I., Bunn, C., Du Bois, R. & Black, C. M. 1998. HLA associations in three mutually exclusive autoantibody subgroups in UK systemic sclerosis patients. *Br J Rheumatol,* 37**,** 201-7.

Favreau, A. J. & Sathyanarayana, P. 2012. miR-590-5p, miR-219-5p, miR-15b and miR-628-5p are commonly regulated by IL-3, GM-CSF and G-CSF in acute myeloid leukemia. *Leuk Res,* 36**,** 334-41.

Feghali-Bostwick, C., Medsger, T. A., Jr. & Wright, T. M. 2003. Analysis of systemic sclerosis in twins reveals low concordance for disease and high concordance for the presence of antinuclear antibodies. *Arthritis Rheum,* 48**,** 1956-63.

Filipowicz, W., Bhattacharyya, S. N. & Sonenberg, N. 2008. Mechanisms of post-transcriptional regulation by microRNAs: are the answers in sight? *Nat Rev Genet,* 9**,** 102-14.

Fonseca, C., Renzoni, E., Sestini, P., et al. 2006. Endothelin axis polymorphisms in patients with scleroderma. *Arthritis Rheum,* 54**,** 3034-42.

Frech, T., Khanna, D., Markewitz, B., Mineau, G., Pimentel, R. & Sawitzke, A. 2010. Heritability of vasculopathy, autoimmune disease, and fibrosis in systemic sclerosis: a population-based study. *Arthritis Rheum,* 62**,** 2109-16.

Friedlander, M. R., Chen, W., Adamidi, C., Maaskola, J., Einspanier, R., Knespel, S. & Rajewsky, N. 2008. Discovering microRNAs from deep sequencing data using miRDeep. *Nat Biotechnol,* 26**,** 407-15.

Friedlander, M. R., Lizano, E., Houben, A. J., et al. 2014. Evidence for the biogenesis of more than 1,000 novel human microRNAs. *Genome Biol,* 15**,** R57.

Friedman, R. C., Farh, K. K., Burge, C. B. & Bartel, D. P. 2009. Most mammalian mRNAs are conserved targets of microRNAs. *Genome Res,* 19**,** 92-105.

Fries, J. F., Hochberg, M. C., Medsger, T. A., Jr., Hunder, G. G. & Bombardier, C. 1994. Criteria for rheumatic disease. Different types and different functions. The American College of Rheumatology Diagnostic and Therapeutic Criteria Committee. *Arthritis Rheum,* 37**,** 454-62.

Frost, J., Ramsay, M., Mia, R., Moosa, L., Musenge, E. & Tikly, M. 2012. Differential gene expression of MMP-1, TIMP-1 and HGF in clinically involved and uninvolved skin in South Africans with SSc. *Rheumatology (Oxford)*.

Furst, D. 2011. Epidemiology of Systemic Sclerosis in a Large United States Managed Care Population. *Arthritis & Rheumatism,* 63**,** 1.

Furst, D. E., Clements, P. J., Steen, V. D., Medsger, T. A., Jr., Masi, A. T., D'angelo, W. A., Lachenbruch, P. A., Grau, R. G. & Seibold, J. R. 1998. The modified Rodnan skin score is an accurate reflection of skin biopsy thickness in systemic sclerosis. *J Rheumatol,* 25**,** 84-8.

Fuschiotti, P., Medsger, T. A., Jr. & Morel, P. A. 2009. Effector CD8+ T cells in systemic sclerosis patients produce abnormally high levels of interleukin-13 associated with increased skin fibrosis. *Arthritis Rheum,* 60**,** 1119-28.

Gaine, S. P. & Rubin, L. J. 1998. Primary pulmonary hypertension. *Lancet,* 352**,** 719-25.

Gaj, S., Eijssen, L., Mensink, R. P. & Evelo, C. T. 2008. Validating nutrient-related gene expression changes from microarrays using RT(2) PCR-arrays. *Genes Nutr,* 3**,** 153-7.

Gallet, A. 2011. Hedgehog morphogen: from secretion to reception. *Trends Cell Biol,* 21**,** 238-46.

Gardner, H., Shearstone, J. R., Bandaru, R., et al. 2006. Gene profiling of scleroderma skin reveals robust signatures of disease that are imperfectly reflected in the transcript profiles of explanted fibroblasts. *Arthritis Rheum,* 54**,** 1961-73.

Gasse, P., Mary, C., Guenon, I., et al. 2007. IL-1R1/MyD88 signaling and the inflammasome are essential in pulmonary inflammation and fibrosis in mice. *J Clin Invest,* 117**,** 3786-99.

Gelber, A. C., Manno, R. L., Shah, A. A., Woods, A., Le, E. N., Boin, F., Hummers, L. K. & Wigley, F. M. 2013. Race and association with disease manifestations and mortality in scleroderma: a 20-year experience at the Johns Hopkins Scleroderma Center and review of the literature. *Medicine (Baltimore),* 92**,** 191-205.

Gervin, K., Vigeland, M. D., Mattingsdal, M., et al. 2012. DNA methylation and gene expression changes in monozygotic twins discordant for psoriasis: identification of epigenetically dysregulated genes. *PLoS Genet,* 8**,** e1002454.

Gilbane, A. J., Denton, C. P. & Holmes, A. M. 2013. Scleroderma pathogenesis: a pivotal role for fibroblasts as effector cells. *Arthritis Res Ther,* 15**,** 215.

Gorelik, G. & Richardson, B. 2009. Aberrant T cell ERK pathway signaling and chromatin structure in lupus. *Autoimmun Rev,* 8**,** 196-8.

Gorlova, O., Martin, J. E., Rueda, B., et al. 2011. Identification of novel genetic markers associated with clinical phenotypes of systemic sclerosis through a genome-wide association strategy. *PLoS Genet,* 7**,** e1002178.

Grabiec, A. M. & Reedquist, K. A. 2010. Histone deacetylases in RA: epigenetics and epiphenomena. *Arthritis Res Ther,* 12**,** 142.

Green, M. C., Sweet, H. O. & Bunker, L. E. 1976. Tight-skin, a new mutation of the mouse causing excessive growth of connective tissue and skeleton. *Am J Pathol,* 82**,** 493-512.

Greenwood, B. M. 1968. Autoimmune disease and parasitic infections in Nigerians. *Lancet,* 2**,** 380-2.

Grumet, F. C., Coukell, A., Bodmer, J. G., Bodmer, W. F. & Mcdevitt, H. O. 1971. Histocompatibility (HL-A) antigens associated with systemic lupus erythematosus. A possible genetic predisposition to disease. *N Engl J Med,* 285**,** 193-6.

Gu, W., Li, X. & Wang, J. 2014. miR-139 regulates the proliferation and invasion of hepatocellular carcinoma through the WNT/TCF-4 pathway. *Oncol Rep,* 31**,** 397-404.

Guo, C. J., Pan, Q., Cheng, T., Jiang, B., Chen, G. Y. & Li, D. G. 2009a. Changes in microRNAs associated with hepatic stellate cell activation status identify signaling pathways. *FEBS J,* 276**,** 5163-76.

Guo, C. J., Pan, Q., Li, D. G., Sun, H. & Liu, B. W. 2009b. miR-15b and miR-16 are implicated in activation of the rat hepatic stellate cell: An essential role for apoptosis. *J Hepatol,* 50**,** 766-78.

He, T. C., Sparks, A. B., Rago, C., Hermeking, H., Zawel, L., Da Costa, L. T., Morin, P. J., Vogelstein, B. & Kinzler, K. W. 1998. Identification of c-MYC as a target of the APC pathway. *Science,* 281**,** 1509-12.

He, W. & Dai, C. 2015. Key Fibrogenic Signaling. *Curr Pathobiol Rep,* 3**,** 183-192.

He, W., Dai, C., Li, Y., Zeng, G., Monga, S. P. & Liu, Y. 2009. Wnt/beta-catenin signaling promotes renal interstitial fibrosis. *J Am Soc Nephrol,* 20**,** 765-76.

He, X., Semenov, M., Tamai, K. & Zeng, X. 2004. LDL receptor-related proteins 5 and 6 in Wnt/beta-catenin signaling: arrows point the way. *Development,* 131**,** 1663-77.

Hill, R. H., Jr., Schurz, H. H., Posada De La Paz, M., et al. 1995. Possible etiologic agents for toxic oil syndrome: fatty acid esters of 3-(N-phenylamino)-1,2-propanediol. *Arch Environ Contam Toxicol,* 28**,** 259-64.

Hinchcliff, M. & Varga, J. 2008. Systemic sclerosis/scleroderma: a treatable multisystem disease. *Am Fam Physician,* 78**,** 961-8.

Hinz, B., Phan, S. H., Thannickal, V. J., Galli, A., Bochaton-Piallat, M. L. & Gabbiani, G. 2007. The myofibroblast: one function, multiple origins. *Am J Pathol,* 170**,** 1807-16.

Honda, N., Jinnin, M., Kajihara, I., et al. 2012. TGF-beta-mediated downregulation of microRNA-196a contributes to the constitutive upregulated type I collagen expression in scleroderma dermal fibroblasts. *J Immunol,* 188**,** 3323-31.

Honda, N., Jinnin, M., Kira-Etoh, T., et al. 2013. miR-150 down-regulation contributes to the constitutive type I collagen overexpression in scleroderma dermal fibroblasts via the induction of integrin beta3. *Am J Pathol,* 182**,** 206-16.

Hopwood, B., Tsykin, A., Findlay, D. M. & Fazzalari, N. L. 2007. Microarray gene expression profiling of osteoarthritic bone suggests altered bone remodelling, WNT and transforming growth factor-beta/bone morphogenic protein signalling. *Arthritis Res Ther,* 9**,** R100.

Horn, A., Palumbo, K., Cordazzo, C., et al. 2012. Hedgehog signaling controls fibroblast activation and tissue fibrosis in systemic sclerosis. *Arthritis Rheum*.

Hrdlickova, R., Nehyba, J., Bargmann, W. & Bose, H. R., Jr. 2014. Multiple tumor suppressor microRNAs regulate telomerase and TCF7, an important transcriptional regulator of the Wnt pathway. *PLoS ONE,* 9**,** e86990.

Hsu, E., Shi, H., Jordan, R. M., Lyons-Weiler, J., Pilewski, J. M. & Feghali-Bostwick, C. A. 2011. Lung tissues in patients with systemic sclerosis have gene expression patterns unique to pulmonary fibrosis and pulmonary hypertension. *Arthritis Rheum,* 63**,** 783-94.

Huang, H. C. & Klein, P. S. 2004. The Frizzled family: receptors for multiple signal transduction pathways. *Genome Biol,* 5**,** 234.

Huang, J., Zhao, L., Xing, L. & Chen, D. 2010. MicroRNA-204 regulates Runx2 protein expression and mesenchymal progenitor cell differentiation. *Stem Cells,* 28**,** 357-64.

Huang, W., Chang, H. Y., Fei, T., Wu, H. & Chen, Y. G. 2007. GSK3 beta mediates suppression of cyclin D2 expression by tumor suppressor PTEN. *Oncogene,* 26**,** 2471-82.

Hughes, K. R., Sablitzky, F. & Mahida, Y. R. 2011. Expression profiling of Wnt family of genes in normal and inflammatory bowel disease primary human intestinal myofibroblasts and normal human colonic crypt epithelial cells. *Inflamm Bowel Dis,* 17**,** 213-20.

Huguet, E. L., Smith, K., Bicknell, R. & Harris, A. L. 1995. Regulation of Wnt5a mRNA expression in human mammary epithelial cells by cell shape, confluence, and hepatocyte growth factor. *J Biol Chem,* 270**,** 12851-6.

Ihn, H. 2008. Autocrine TGF-beta signaling in the pathogenesis of systemic sclerosis. *J Dermatol Sci,* 49**,** 103-13.

Illingworth, R. S. & Bird, A. P. 2009. CpG islands--'a rough guide'. *FEBS Lett,* 583**,** 1713-20.

Ishida, W., Mori, Y., Lakos, G., et al. 2006. Intracellular TGF-beta receptor blockade abrogates Smad-dependent fibroblast activation in vitro and in vivo. *J Invest Dermatol,* 126**,** 1733-44.

Jenkins, D. 2009. Hedgehog signalling: emerging evidence for non-canonical pathways. *Cell Signal,* 21**,** 1023-34.

Jho, E. H., Zhang, T., Domon, C., Joo, C. K., Freund, J. N. & Costantini, F. 2002. Wnt/beta-catenin/Tcf signaling induces the transcription of Axin2, a negative regulator of the signaling pathway. *Mol Cell Biol,* 22**,** 1172-83.

Jimenez, S. A. & Christner, P. 1994. Animal models of systemic sclerosis. *Clin Dermatol,* 12**,** 425-36.

Johnson, M. E., Mahoney, J. M., Taroni, J., Sargent, J. L., Marmarelis, E., Wu, M. R., Varga, J., Hinchcliff, M. E. & Whitfield, M. L. 2015. Experimentally-derived fibroblast gene signatures identify molecular pathways associated with distinct subsets of systemic sclerosis patients in three independent cohorts. *PLoS One,* 10**,** e0114017.

Jones, S. E. & Jomary, C. 2002. Secreted Frizzled-related proteins: searching for relationships and patterns. *Bioessays,* 24**,** 811-20.

Julka, P. K., Chacko, R. T., Nag, S., et al. 2008. A phase II study of sequential neoadjuvant gemcitabine plus doxorubicin followed by gemcitabine plus cisplatin in patients with operable breast cancer: prediction of response using molecular profiling. *Br J Cancer,* 98**,** 1327-35.

Jungel, A., Distler, J. H., Gay, S. & Distler, O. 2011. Epigenetic modifications: novel therapeutic strategies for systemic sclerosis? *Expert Rev Clin Immunol,* 7**,** 475-80.

Kallenberg, C. G., Jansen, H. M., Elema, J. D. & The, T. H. 1984. Steroid-responsive interstitial pulmonary disease in systemic sclerosis. Monitoring by bronchoalveolar lavage. *Chest,* 86**,** 489-92.

Karouzakis, E., Gay, R. E., Michel, B. A., Gay, S. & Neidhart, M. 2009. DNA hypomethylation in rheumatoid arthritis synovial fibroblasts. *Arthritis Rheum,* 60**,** 3613-22.

Kasifoglu, T., Yasar Bilge, S., Yildiz, F., et al. 2016. Risk factors for malignancy in systemic sclerosis patients. *Clin Rheumatol,* 35**,** 1529-33.

Kato, M., Zhang, J., Wang, M., Lanting, L., Yuan, H., Rossi, J. J. & Natarajan, R. 2007. MicroRNA-192 in diabetic kidney glomeruli and its function in TGF-beta-induced collagen expression via inhibition of E-box repressors. *Proc Natl Acad Sci U S A,* 104**,** 3432-7.

Kavian, N., Servettaz, A., Mongaret, C., et al. 2010. Targeting ADAM-17/notch signaling abrogates the development of systemic sclerosis in a murine model. *Arthritis Rheum,* 62**,** 3477-87.

Kawano, Y. & Kypta, R. 2003. Secreted antagonists of the Wnt signalling pathway. *J Cell Sci,* 116**,** 2627-34.

Kawashita, Y., Jinnin, M., Makino, T., et al. 2011. Circulating miR-29a levels in patients with scleroderma spectrum disorder. *J Dermatol Sci,* 61**,** 67-9.

Kielty, C. M., Raghunath, M., Siracusa, L. D., Sherratt, M. J., Peters, R., Shuttleworth, C. A. & Jimenez, S. A. 1998. The Tight skin mouse: demonstration of mutant fibrillin-1 production and assembly into abnormal microfibrils. *J Cell Biol,* 140**,** 1159-66.

Kikuchi, A., Yamamoto, H., Sato, A. & Matsumoto, S. 2012. Wnt5a: its signalling, functions and implication in diseases. *Acta Physiol (Oxf),* 204**,** 17-33.

Kissin, E. Y., Merkel, P. A. & Lafyatis, R. 2006. Myofibroblasts and hyalinized collagen as markers of skin disease in systemic sclerosis. *Arthritis Rheum,* 54**,** 3655-60.

Kodama, T., Takehara, T., Hikita, H., et al. 2011. Increases in p53 expression induce CTGF synthesis by mouse and human hepatocytes and result in liver fibrosis in mice. *J Clin Invest,* 121**,** 3343-56.

Kohn, A. D. & Moon, R. T. 2005. Wnt and calcium signaling: beta-catenin-independent pathways. *Cell Calcium,* 38**,** 439-46.

Komiya, Y. & Habas, R. 2008. Wnt signal transduction pathways. *Organogenesis,* 4**,** 68-75.

Konigshoff, M., Balsara, N., Pfaff, E. M., Kramer, M., Chrobak, I., Seeger, W. & Eickelberg, O. 2008. Functional Wnt signaling is increased in idiopathic pulmonary fibrosis. *PLoS One,* 3**,** e2142.

Kramer, M., Dees, C., Huang, J., et al. 2013. Inhibition of H3K27 histone trimethylation activates fibroblasts and induces fibrosis. *Ann Rheum Dis,* 72**,** 614-20.

Kratochwil, K., Galceran, J., Tontsch, S., Roth, W. & Grosschedl, R. 2002. FGF4, a direct target of LEF1 and Wnt signaling, can rescue the arrest of tooth organogenesis in Lef1(-/-) mice. *Genes Dev,* 16**,** 3173-85.

Krupnik, V. E., Sharp, J. D., Jiang, C., et al. 1999. Functional and structural diversity of the human Dickkopf gene family. *Gene,* 238**,** 301-13.

Kucukali, C. I., Kurtuncu, M., Coban, A., Cebi, M. & Tuzun, E. 2015. Epigenetics of multiple sclerosis: an updated review. *Neuromolecular Med,* 17**,** 83-96.

Kuhn, D. E., Martin, M. M., Feldman, D. S., Terry, A. V., Jr., Nuovo, G. J. & Elton, T. S. 2008. Experimental validation of miRNA targets. *Methods,* 44**,** 47-54.

Kuwana, M. 2006. Potential benefit of statins for vascular disease in systemic sclerosis. *Curr Opin Rheumatol,* 18**,** 594-600.

Lam, A. P. & Gottardi, C. J. 2011. beta-catenin signaling: a novel mediator of fibrosis and potential therapeutic target. *Curr Opin Rheumatol,* 23**,** 562-7.

Lam, A. P., Herazo-Maya, J. D., Sennello, J. A., et al. 2014. Wnt coreceptor Lrp5 is a driver of idiopathic pulmonary fibrosis. *Am J Respir Crit Care Med,* 190**,** 185-95.

Lappalainen, T., Sammeth, M., Friedlander, M. R., et al. 2013. Transcriptome and genome sequencing uncovers functional variation in humans. *Nature,* 501**,** 506-11.

Leask, A. 2006. Scar wars: is TGFbeta the phantom menace in scleroderma? *Arthritis Res Ther,* 8**,** 213.

Lemaire, R., Farina, G., Bayle, J., Dimarzio, M., Pendergrass, S. A., Milano, A., Perbal, B., Whitfield, M. L. & Lafyatis, R. 2010. Antagonistic effect of the matricellular signaling protein CCN3 on TGF-beta- and Wnt-mediated fibrillinogenesis in systemic sclerosis and Marfan syndrome. *J Invest Dermatol,* 130**,** 1514-23.

Leroy, E. C., Black, C., Fleischmajer, R., Jablonska, S., Krieg, T., Medsger, T. A., Jr., Rowell, N. & Wollheim, F. 1988. Scleroderma (systemic sclerosis): classification, subsets and pathogenesis. *J Rheumatol,* 15**,** 202-5.

Leung, C. M., Chen, T. W., Li, S. C., et al. 2014a. MicroRNA expression profiles in human breast cancer cells after multifraction and single-dose radiation treatment. *Oncol Rep,* 31**,** 2147-56.

Leung, C. M., Li, S. C., Chen, T. W., et al. 2014b. Comprehensive microRNA profiling of prostate cancer cells after ionizing radiation treatment. *Oncol Rep,* 31**,** 1067-78.

Li, H., Yang, R., Fan, X., Gu, T., Zhao, Z., Chang, D. & Wang, W. 2012. MicroRNA array analysis of microRNAs related to systemic scleroderma. *Rheumatol Int,* 32**,** 307-13.

Li, J., Wan, Y., Guo, Q., et al. 2010. Altered microRNA expression profile with miR-146a upregulation in CD4+ T cells from patients with rheumatoid arthritis. *Arthritis Res Ther,* 12**,** R81.

Liang, P., Song, F., Ghosh, S., et al. 2011. Genome-wide survey reveals dynamic widespread tissue-specific changes in DNA methylation during development. *BMC Genomics,* 12**,** 231.

Lin, F., Wu, X., Zhang, H., You, X., Zhang, Z., Shao, R. & Huang, C. 2015. A microrna screen to identify regulators of peritoneal fibrosis in a rat model of peritoneal dialysis. *BMC Nephrol,* 16**,** 48.

Lisanti, M. P., Tsirigos, A., Pavlides, S., et al. 2014. JNK1 stress signaling is hyper-activated in high breast density and the tumor stroma: connecting fibrosis, inflammation, and stemness for cancer prevention. *Cell Cycle,* 13**,** 580-99.

Liu, G., Friggeri, A., Yang, Y., Milosevic, J., Ding, Q., Thannickal, V. J., Kaminski, N. & Abraham, E. 2010. miR-21 mediates fibrogenic activation of pulmonary fibroblasts and lung fibrosis. *J Exp Med,* 207**,** 1589-97.

Liu, Y., El-Serag, H. B., Jiao, L., et al. 2013. WNT signaling pathway gene polymorphisms and risk of hepatic fibrosis and inflammation in HCV-infected patients. *PLoS One,* 8**,** e84407.

Livak, K. J. & Schmittgen, T. D. 2001. Analysis of relative gene expression data using real-time quantitative PCR and the 2(-Delta Delta C(T)) Method. *Methods,* 25**,** 402-8.

Llorens, F., Banez-Coronel, M., Pantano, L., Del Rio, J. A., Ferrer, I., Estivill, X. & Marti, E. 2013. A highly expressed miR-101 isomiR is a functional silencing small RNA. *BMC Genomics,* 14**,** 104.

Logan, C. Y. & Nusse, R. 2004. The Wnt signaling pathway in development and disease. *Annu Rev Cell Dev Biol,* 20**,** 781-810.

Lonzetti, L. S., Joyal, F., Raynauld, J. P., Roussin, A., Goulet, J. R., Rich, E., Choquette, D., Raymond, Y. & Senecal, J. L. 2001. Updating the American College of Rheumatology preliminary classification criteria for systemic sclerosis: addition of severe nailfold capillaroscopy abnormalities markedly increases the sensitivity for limited scleroderma. *Arthritis Rheum,* 44**,** 735-6.

Love, M. I., Huber, W. & Anders, S. 2014. Moderated estimation of fold change and dispersion for RNA-seq data with DESeq2 *bioRxiv*.

Low, E. A. 2013. Disease Characteristics of the Singapore Systemic Sclerosis Cohort. *Proceedings of Singapore Healthcare,* 22**,** 7.

Lu, Q. 2013. The critical importance of epigenetics in autoimmunity. *J Autoimmun,* 41**,** 1-5.

Ludwicka, A., Ohba, T., Trojanowska, M., Yamakage, A., Strange, C., Smith, E. A., Leroy, E. C., Sutherland, S. & Silver, R. M. 1995. Elevated levels of platelet derived growth factor and transforming growth factor-beta 1 in bronchoalveolar lavage fluid from patients with scleroderma. *J Rheumatol,* 22**,** 1876-83.

Luo, H., Zhu, H., Zhou, B., Xiao, X. & Zuo, X. 2015. MicroRNA-130b regulates scleroderma fibrosis by targeting peroxisome proliferator-activated receptor gamma. *Mod Rheumatol***,** 1-8.

Luo, Y., Wang, Y., Wang, Q., Xiao, R. & Lu, Q. 2013. Systemic sclerosis: genetics and epigenetics. *J Autoimmun,* 41**,** 161-7.

Lutalo, S. K. 1985. Chronic inflammatory rheumatic diseases in black Zimbabweans. *Ann Rheum Dis,* 44**,** 121-5.

Lv, C., Zhou, Y. H., Wu, C., Shao, Y., Lu, C. L. & Wang, Q. Y. 2015. The changes in miR-130b levels in human serum and the correlation with the severity of diabetic nephropathy. *Diabetes Metab Res Rev*.

Ma, X., Zhou, J., Zhong, Y., Jiang, L., Mu, P., Li, Y., Singh, N., Nagarkatti, M. & Nagarkatti, P. 2014. Expression, regulation and function of microRNAs in multiple sclerosis. *Int J Med Sci,* 11**,** 810-8.

Macdonald, B. T., Tamai, K. & He, X. 2009. Wnt/beta-catenin signaling: components, mechanisms, and diseases. *Dev Cell,* 17**,** 9-26.

Maeda, M., Nishimura, Y., Kumagai, N., et al. 2010. Dysregulation of the immune system caused by silica and asbestos. *J Immunotoxicol,* 7**,** 268-78.

Mahoney, J. M., Taroni, J., Martyanov, V., Wood, T. A., Greene, C. S., Pioli, P. A., Hinchcliff, M. E. & Whitfield, M. L. 2015. Systems level analysis of systemic sclerosis shows a network of immune and profibrotic pathways connected with genetic polymorphisms. *PLoS Comput Biol,* 11**,** e1004005.

Manetti, M., Allanore, Y., Saad, M., et al. 2012. Evidence for caveolin-1 as a new susceptibility gene regulating tissue fibrosis in systemic sclerosis. *Ann Rheum Dis,* 71**,** 1034-41.

Mann, J., Chu, D. C., Maxwell, A., Oakley, F., Zhu, N. L., Tsukamoto, H. & Mann, D. A. 2010. MeCP2 controls an epigenetic pathway that promotes myofibroblast transdifferentiation and fibrosis. *Gastroenterology,* 138**,** 705-14, 714 e1-4.

Manolis, A. S. a. M., T.A 2012. Micro RNAs: a Revolutionary Discovery in Biology. *Hospital Chronicles,* 7**,** 4.

Marie, I. & Gehanno, J. F. 2015. Environmental risk factors of systemic sclerosis. *Semin Immunopathol,* 37**,** 463-73.

Marie, I., Gehanno, J. F., Bubenheim, M., et al. 2014. Prospective study to evaluate the association between systemic sclerosis and occupational exposure and review of the literature. *Autoimmun Rev,* 13**,** 151-6.

Marie, I., Menard, J. F., Duval-Modeste, A. B., et al. 2015. Association of occupational exposure with features of systemic sclerosis. *J Am Acad Dermatol,* 72**,** 456-64.

Martin, M. M., Lee, E. J., Buckenberger, J. A., Schmittgen, T. D. & Elton, T. S. 2006. MicroRNA-155 regulates human angiotensin II type 1 receptor expression in fibroblasts. *J Biol Chem,* 281**,** 18277-84.

Martinez, N. J. & Gregory, R. I. 2010. MicroRNA gene regulatory pathways in the establishment and maintenance of ESC identity. *Cell Stem Cell,* 7**,** 31-5.

Martinez-Sanchez, A. & Murphy, C. L. 2013. MicroRNA Target Identification-Experimental Approaches. *Biology (Basel),* 2**,** 189-205.

Masi, A. T., Subcommittee for Scleroderma Criteria of the American Rheumatism Association, D. & Therapeutic Criteria, C. 1980. Preliminary criteria for the classification of systemic sclerosis (scleroderma). *Arthritis & Rheumatism,* 23**,** 581-590.

Matsuno, Y., Coelho, A. L., Jarai, G., Westwick, J. & Hogaboam, C. M. 2012. Notch signaling mediates TGF-beta1-induced epithelial-mesenchymal transition through the induction of Snai1. *Int J Biochem Cell Biol,* 44**,** 776-89.

Maul, G. G., Jimenez, S. A., Riggs, E. & Ziemnicka-Kotula, D. 1989. Determination of an epitope of the diffuse systemic sclerosis marker antigen DNA topoisomerase I: sequence similarity with retroviral p30gag protein suggests a possible cause for autoimmunity in systemic sclerosis. *Proc Natl Acad Sci U S A,* 86**,** 8492-6.

Maurer, B., Stanczyk, J., Jungel, A., et al. 2010. MicroRNA-29, a key regulator of collagen expression in systemic sclerosis. *Arthritis Rheum,* 62**,** 1733-43.

Mayes, M. D., Bossini-Castillo, L., Gorlova, O., et al. 2014. Immunochip analysis identifies multiple susceptibility loci for systemic sclerosis. *Am J Hum Genet,* 94**,** 47-61.

Mcmahon, A. P. & Moon, R. T. 1989. Ectopic expression of the proto-oncogene int-1 in Xenopus embryos leads to duplication of the embryonic axis. *Cell,* 58**,** 1075-84.

Mcnearney, T. A., Reveille, J. D., Fischbach, M., et al. 2007. Pulmonary involvement in systemic sclerosis: associations with genetic, serologic, sociodemographic, and behavioral factors. *Arthritis Rheum,* 57**,** 318-26.

Messadi, D. V., Doung, H. S., Zhang, Q., Kelly, A. P., Tuan, T. L., Reichenberger, E. & Le, A. D. 2004. Activation of NFkappaB signal pathways in keloid fibroblasts. *Arch Dermatol Res,* 296**,** 125-33.

Milano, A., Pendergrass, S. A., Sargent, J. L., George, L. K., Mccalmont, T. H., Connolly, M. K. & Whitfield, M. L. 2008. Molecular subsets in the gene expression signatures of scleroderma skin. *PLoS ONE,* 3**,** e2696.

Miller, F. W., Alfredsson, L., Costenbader, K. H., Kamen, D. L., Nelson, L. M., Norris, J. M. & De Roos, A. J. 2012. Epidemiology of environmental exposures and human autoimmune diseases: findings from a National Institute of Environmental Health Sciences Expert Panel Workshop. *J Autoimmun,* 39**,** 259-71.

Moinzadeh, P., Fonseca, C., Hellmich, M., Shah, A. A., Chighizola, C., Denton, C. P. & Ong, V. H. 2014. Association of anti-RNA polymerase III autoantibodies and cancer in scleroderma. *Arthritis Res Ther,* 16**,** R53.

Mori, Y., Chen, S. J. & Varga, J. 2003. Expression and regulation of intracellular SMAD signaling in scleroderma skin fibroblasts. *Arthritis Rheum,* 48**,** 1964-78.

Morin, F., Kavian, N. & Batteux, F. 2015. Animal models of systemic sclerosis. *Curr Pharm Des,* 21**,** 2365-79.

Murahovschi, V., Pivovarova, O., Ilkavets, I., et al. 2015. WISP1 is a novel adipokine linked to inflammation in obesity. *Diabetes,* 64**,** 856-66.

Murakami, M., Nguyen, L. T., Zhuang, Z. W., Moodie, K. L., Carmeliet, P., Stan, R. V. & Simons, M. 2008. The FGF system has a key role in regulating vascular integrity. *J Clin Invest,* 118**,** 3355-66.

Murakami, Y., Tamori, A., Itami, S., et al. 2013. The expression level of miR-18b in hepatocellular carcinoma is associated with the grade of malignancy and prognosis. *BMC Cancer,* 13**,** 99.

Murakami, Y., Toyoda, H., Tanahashi, T., Tanaka, J., Kumada, T., Yoshioka, Y., Kosaka, N., Ochiya, T. & Taguchi, Y. H. 2012. Comprehensive miRNA expression analysis in peripheral blood can diagnose liver disease. *PLoS One,* 7**,** e48366.

Murea, M., Park, J. K., Sharma, S., et al. 2010. Expression of Notch pathway proteins correlates with albuminuria, glomerulosclerosis, and renal function. *Kidney Int,* 78**,** 514-22.

Nakashima, T., Jinnin, M., Yamane, K., et al. 2012. Impaired IL-17 signaling pathway contributes to the increased collagen expression in scleroderma fibroblasts. *J Immunol,* 188**,** 3573-83.
Naqvi, A. R., Fordham, J. B. & Nares, S. 2015. miR-24, miR-30b, and miR-142-3p regulate phagocytosis in myeloid inflammatory cells. *J Immunol,* 194**,** 1916-27.
Niehrs, C. 2006. Function and biological roles of the Dickkopf family of Wnt modulators. *Oncogene,* 25**,** 7469-81.
Niehrs, C. 2012. The complex world of WNT receptor signalling. *Nat Rev Mol Cell Biol,* 13**,** 767-79.
Nietert, P. J., Mitchell, H. C., Bolster, M. B., Shaftman, S. R., Tilley, B. C. & Silver, R. M. 2006. Racial variation in clinical and immunological manifestations of systemic sclerosis. *J Rheumatol,* 33**,** 263-8.
Niida, A., Hiroko, T., Kasai, M., Furukawa, Y., Nakamura, Y., Suzuki, Y., Sugano, S. & Akiyama, T. 2004. DKK1, a negative regulator of Wnt signaling, is a target of the beta-catenin/TCF pathway. *Oncogene,* 23**,** 8520-6.
Nile, C. J., Read, R. C., Akil, M., Duff, G. W. & Wilson, A. G. 2008. Methylation status of a single CpG site in the IL6 promoter is related to IL6 messenger RNA levels and rheumatoid arthritis. *Arthritis Rheum,* 58**,** 2686-93.
Niranjan, T., Bielesz, B., Gruenwald, A., Ponda, M. P., Kopp, J. B., Thomas, D. B. & Susztak, K. 2008. The Notch pathway in podocytes plays a role in the development of glomerular disease. *Nat Med,* 14**,** 290-8.
Nishida, K., Komiyama, T., Miyazawa, S., et al. 2004. Histone deacetylase inhibitor suppression of autoantibody-mediated arthritis in mice via regulation of p16INK4a and p21(WAF1/Cip1) expression. *Arthritis Rheum,* 50**,** 3365-76.
Nusse, R. 2012. Wnt signaling. *Cold Spring Harb Perspect Biol,* 4.
Nusse, R. & Varmus, H. E. 1982. Many tumors induced by the mouse mammary tumor virus contain a provirus integrated in the same region of the host genome. *Cell,* 31**,** 99-109.
Oak, S. R., Murray, L., Herath, A., et al. 2011. A micro RNA processing defect in rapidly progressing idiopathic pulmonary fibrosis. *PLoS One,* 6**,** e21253.
Okamoto, M., Udagawa, N., Uehara, S., et al. 2014. Noncanonical Wnt5a enhances Wnt/beta-catenin signaling during osteoblastogenesis. *Sci Rep,* 4**,** 4493.
Olesen, A. B., Svaerke, C., Farkas, D. K. & Sorensen, H. T. 2010. Systemic sclerosis and the risk of cancer: a nationwide population-based cohort study. *Br J Dermatol,* 163**,** 800-6.
Onishi, A., Sugiyama, D., Kumagai, S. & Morinobu, A. 2013. Cancer incidence in systemic sclerosis: meta-analysis of population-based cohort studies. *Arthritis Rheum,* 65**,** 1913-21.
Orom, U. A. & Lund, A. H. 2010. Experimental identification of microRNA targets. *Gene,* 451**,** 1-5.
Orom, U. A., Nielsen, F. C. & Lund, A. H. 2008. MicroRNA-10a binds the 5'UTR of ribosomal protein mRNAs and enhances their translation. *Mol Cell,* 30**,** 460-71.
Palarasah, Y., Nielsen, C., Sprogoe, U., et al. 2011. Novel assays to assess the functional capacity of the classical, the alternative and the lectin pathways of the complement system. *Clin Exp Immunol,* 164**,** 388-95.
Pandit, K. V., Corcoran, D., Yousef, H., et al. 2010. Inhibition and role of let-7d in idiopathic pulmonary fibrosis. *Am J Respir Crit Care Med,* 182**,** 220-9.
Pannu, J., Gardner, H., Shearstone, J. R., Smith, E. & Trojanowska, M. 2006. Increased levels of transforming growth factor beta receptor type I and up-regulation of matrix gene program: A model of scleroderma. *Arthritis Rheum,* 54**,** 3011-21.
Parish, A., Schwaederle, M., Daniels, G., et al. 2015. Fibroblast growth factor family aberrations in cancers: clinical and molecular characteristics. *Cell Cycle,* 14**,** 2121-8.
Pauley, K. M., Cha, S. & Chan, E. K. 2009. MicroRNA in autoimmunity and autoimmune diseases. *J Autoimmun,* 32**,** 189-94.
Pendergrass, S. A., Lemaire, R., Francis, I. P., Mahoney, J. M., Lafyatis, R. & Whitfield, M. L. 2012. Intrinsic gene expression subsets of diffuse cutaneous systemic sclerosis are stable in serial skin biopsies. *J Invest Dermatol,* 132**,** 1363-73.

Penders, J., Stobberingh, E. E., Van Den Brandt, P. A. & Thijs, C. 2007. The role of the intestinal microbiota in the development of atopic disorders. *Allergy,* 62**,** 1223-36.

Perkins, J. R., Dawes, J. M., Mcmahon, S. B., Bennett, D. L., Orengo, C. & Kohl, M. 2012. ReadqPCR and NormqPCR: R packages for the reading, quality checking and normalisation of RT-qPCR quantification cycle (Cq) data. *BMC Genomics,* 13**,** 296.

Perou, C. M., Sorlie, T., Eisen, M. B., et al. 2000. Molecular portraits of human breast tumours. *Nature,* 406**,** 747-52.

Pfaff, E. M., Becker, S., Gunther, A. & Konigshoff, M. 2011. Dickkopf proteins influence lung epithelial cell proliferation in idiopathic pulmonary fibrosis. *Eur Respir J,* 37**,** 79-87.

Pogribny, I. P., Starlard-Davenport, A., Tryndyak, V. P., Han, T., Ross, S. A., Rusyn, I. & Beland, F. A. 2010. Difference in expression of hepatic microRNAs miR-29c, miR-34a, miR-155, and miR-200b is associated with strain-specific susceptibility to dietary nonalcoholic steatohepatitis in mice. *Lab Invest,* 90**,** 1437-46.

Pollari, S., Leivonen, S. K., Perala, M., Fey, V., Kakonen, S. M. & Kallioniemi, O. 2012. Identification of microRNAs inhibiting TGF-beta-induced IL-11 production in bone metastatic breast cancer cells. *PLoS One,* 7**,** e37361.

Portela, A. & Esteller, M. 2010. Epigenetic modifications and human disease. *Nat Biotechnol,* 28**,** 1057-68.

Pottier, N., Maurin, T., Chevalier, B., et al. 2009. Identification of keratinocyte growth factor as a target of microRNA-155 in lung fibroblasts: implication in epithelial-mesenchymal interactions. *PLoS One,* 4**,** e6718.

Rawlings-Goss, R. A., Campbell, M. C. & Tishkoff, S. A. 2014. Global population-specific variation in miRNA associated with cancer risk and clinical biomarkers. *BMC Med Genomics,* 7**,** 53.

Reinl, W. 1957. [Scleroderma caused by trichloroethylene effects]. *Zentralbl Arbeitsmed,* 7**,** 58-60.

Richardson, B. 2003. DNA methylation and autoimmune disease. *Clin Immunol,* 109**,** 72-9.

Rieger, J. K., Reutter, S., Hofmann, U., Schwab, M. & Zanger, U. M. 2015. Inflammation-Associated MicroRNA-130b Down-Regulates Cytochrome P450 Activities and Directly Targets CYP2C9. *Drug Metab Dispos,* 43**,** 884-8.

Rijsewijk, F., Schuermann, M., Wagenaar, E., Parren, P., Weigel, D. & Nusse, R. 1987. The Drosophila homolog of the mouse mammary oncogene int-1 is identical to the segment polarity gene wingless. *Cell,* 50**,** 649-57.

Roberts-Thomson, P. J. & Walker, J. G. 2006. Scleroderma: it has been a long hard journey. *Intern Med J,* 36**,** 519-23.

Rodriguez, A., Vigorito, E., Clare, S., et al. 2007. Requirement of bic/microRNA-155 for normal immune function. *Science,* 316**,** 608-11.

Rogers, K. W. & Schier, A. F. 2011. Morphogen gradients: from generation to interpretation. *Annu Rev Cell Dev Biol,* 27**,** 377-407.

Ropiquet, F., Giri, D., Kwabi-Addo, B., Mansukhani, A. & Ittmann, M. 2000. Increased expression of fibroblast growth factor 6 in human prostatic intraepithelial neoplasia and prostate cancer. *Cancer Res,* 60**,** 4245-50.

Ross, D. T., Scherf, U., Eisen, M. B., et al. 2000. Systematic variation in gene expression patterns in human cancer cell lines. *Nat Genet,* 24**,** 227-35.

Ross, R. 1999. Atherosclerosis--an inflammatory disease. *N Engl J Med,* 340**,** 115-26.

Russell, S. B., Russell, J. D., Trupin, K. M., Gayden, A. E., Opalenik, S. R., Nanney, L. B., Broquist, A. H., Raju, L. & Williams, S. M. 2010. Epigenetically altered wound healing in keloid fibroblasts. *J Invest Dermatol,* 130**,** 2489-96.

Saito, F., Tasaka, S., Inoue, K., et al. 2008. Role of interleukin-6 in bleomycin-induced lung inflammatory changes in mice. *Am J Respir Cell Mol Biol,* 38**,** 566-71.

Saitoh, T. & Katoh, M. 2001. Molecular cloning and characterization of human WNT5B on chromosome 12p13.3 region. *Int J Oncol,* 19**,** 347-51.

Salazar, G. A., Assassi, S., Wu, M., Hagan, J. & Mayes, M. D. 2014. A3.34 The global microrna profile of skin in systemic sclerosis. *Annals of the Rheumatic Diseases,* 73**,** A55-A56.

Sargent, J. L., Li, Z., Aliprantis, A. O., et al. 2016. Interspecies comparative genomics identifies optimal mouse models of systemic sclerosis. *Arthritis Rheumatol*.

Sato, H., Lagan, A. L., Alexopoulou, C., et al. 2004. The TNF-863A allele strongly associates with anticentromere antibody positivity in scleroderma. *Arthritis Rheum,* 50**,** 558-64.

Sato, M. 2006. Upregulation of the Wnt/beta-catenin pathway induced by transforming growth factor-beta in hypertrophic scars and keloids. *Acta Derm Venereol,* 86**,** 300-7.

Sato, S., Shimizu, M., Hosokawa, T., Saito, T., Okabe, M., Niioka, T. & Kurasaki, M. 2000. Distribution of zinc-binding metallothionein in cirrhotic liver of rats administered zinc. *Pharmacol Toxicol,* 87**,** 292-6.

Satoh, T., Ishikawa, O., Ihn, H., et al. 2009. Clinical usefulness of anti-RNA polymerase III antibody measurement by enzyme-linked immunosorbent assay. *Rheumatology (Oxford),* 48**,** 1570-4.

Sawalha, A. H., Jeffries, M., Webb, R., et al. 2008. Defective T-cell ERK signaling induces interferon-regulated gene expression and overexpression of methylation-sensitive genes similar to lupus patients. *Genes Immun,* 9**,** 368-78.

Schaefer, J. S., Montufar-Solis, D., Vigneswaran, N. & Klein, J. R. 2011. Selective upregulation of microRNA expression in peripheral blood leukocytes in IL-10-/- mice precedes expression in the colon. *J Immunol,* 187**,** 5834-41.

Scian, M. J., Maluf, D. G., David, K. G., et al. 2011. MicroRNA profiles in allograft tissues and paired urines associate with chronic allograft dysfunction with IF/TA. *Am J Transplant,* 11**,** 2110-22.

Sebastiani, G., Grieco, F. A., Spagnuolo, I., Galleri, L., Cataldo, D. & Dotta, F. 2011. Increased expression of microRNA miR-326 in type 1 diabetic patients with ongoing islet autoimmunity. *Diabetes Metab Res Rev,* 27**,** 862-6.

Selbach, M., Schwanhausser, B., Thierfelder, N., Fang, Z., Khanin, R. & Rajewsky, N. 2008. Widespread changes in protein synthesis induced by microRNAs. *Nature,* 455**,** 58-63.

Selmi, C., Feghali-Bostwick, C. A., Lleo, A., et al. 2012. X chromosome gene methylation in peripheral lymphocytes from monozygotic twins discordant for scleroderma. *Clin Exp Immunol,* 169**,** 253-62.

Selmi, C., Invernizzi, P. & Gershwin, M. E. 2006. The X chromosome and systemic sclerosis. *Curr Opin Rheumatol,* 18**,** 601-5.

Shams, S., Mohsin, S., Nasir, G. A., Khan, M. & Khan, S. N. 2015. Mesenchymal Stem Cells Pretreated with HGF and FGF4 Can Reduce Liver Fibrosis in Mice. *Stem Cells Int,* 2015**,** 747245.

Shand, L., Lunt, M., Nihtyanova, S., Hoseini, M., Silman, A., Black, C. M. & Denton, C. P. 2007. Relationship between change in skin score and disease outcome in diffuse cutaneous systemic sclerosis: application of a latent linear trajectory model. *Arthritis Rheum,* 56**,** 2422-31.

Sharif, R., Mayes, M. D., Tan, F. K., et al. 2012. IRF5 polymorphism predicts prognosis in patients with systemic sclerosis. *Ann Rheum Dis,* 71**,** 1197-202.

Sharma, A., Kumar, M., Ahmad, T., Mabalirajan, U., Aich, J., Agrawal, A. & Ghosh, B. 2012. Antagonism of mmu-mir-106a attenuates asthma features in allergic murine model. *J Appl Physiol (1985),* 113**,** 459-64.

Sharma, S., Sirin, Y. & Susztak, K. 2011. The story of Notch and chronic kidney disease. *Curr Opin Nephrol Hypertens,* 20**,** 56-61.

Sharma, S., Tantisira, K., Carey, V., et al. 2010. A role for Wnt signaling genes in the pathogenesis of impaired lung function in asthma. *Am J Respir Crit Care Med,* 181**,** 328-36.

Shi-Wen, X., Thompson, K., Khan, K., Liu, S., Murphy-Marshman, H., Baron, M., Denton, C. P., Leask, A. & Abraham, D. J. 2012. Focal adhesion kinase and reactive oxygen species contribute to the persistent fibrotic phenotype of lesional scleroderma fibroblasts. *Rheumatology (Oxford),* 51**,** 2146-54.

Siau, K., Laversuch, C. J., Creamer, P. & O'rourke, K. P. 2011. Malignancy in scleroderma patients from south west England: a population-based cohort study. *Rheumatol Int,* 31**,** 641-5.

Silman, A. J. & Newman, J. 1996. Epidemiology of systemic sclerosis. *Curr Opin Rheumatol,* 8**,** 585-9.

Silver, N., Best, S., Jiang, J. & Thein, S. L. 2006. Selection of housekeeping genes for gene expression studies in human reticulocytes using real-time PCR. *BMC Mol Biol,* 7**,** 33.

Silver, R. M. 2002. E. Carwile LeRoy, MD, 1933–2002. *Arthritis & Rheumatism,* 46.

Silver, R. M., Heyes, M. P., Maize, J. C., Quearry, B., Vionnet-Fuasset, M. & Sternberg, E. M. 1990. Scleroderma, fasciitis, and eosinophilia associated with the ingestion of tryptophan. *N Engl J Med,* 322**,** 874-81.

Sing, T., Jinnin, M., Yamane, K., et al. 2012. microRNA-92a expression in the sera and dermal fibroblasts increases in patients with scleroderma. *Rheumatology (Oxford),* 51**,** 1550-6.

Siracusa, L. D., Mcgrath, R., Ma, Q., Moskow, J. J., Manne, J., Christner, P. J., Buchberg, A. M. & Jimenez, S. A. 1996. A tandem duplication within the fibrillin 1 gene is associated with the mouse tight skin mutation. *Genome Res,* 6**,** 300-13.

Sirin, Y. & Susztak, K. 2012. Notch in the kidney: development and disease. *J Pathol,* 226**,** 394-403.

Sluis-Cremer, G. K., Hessel, P. A., Nizdo, E. H., Churchill, A. R. & Zeiss, E. A. 1985. Silica, silicosis, and progressive systemic sclerosis. *Br J Ind Med,* 42**,** 838-43.

Slusarski, D. C., Yang-Snyder, J., Busa, W. B. & Moon, R. T. 1997. Modulation of embryonic intracellular Ca2+ signaling by Wnt-5A. *Dev Biol,* 182**,** 114-20.

Small, E. M., Frost, R. J. & Olson, E. N. 2010. MicroRNAs add a new dimension to cardiovascular disease. *Circulation,* 121**,** 1022-32.

Smith, G. P. & Chan, E. S. 2010. Molecular pathogenesis of skin fibrosis: insight from animal models. *Curr Rheumatol Rep,* 12**,** 26-33.

Somorin, A. O. & Mordi, V. I. 1980. Connective tissue disease in Nigeria with emphasis on scleroderma. *Cent Afr J Med,* 26**,** 59-63.

Song, J. L., Nigam, P., Tektas, S. S. & Selva, E. 2015. microRNA regulation of Wnt signaling pathways in development and disease. *Cell Signal,* 27**,** 1380-91.

Song, L., Su, M., Wang, S., et al. 2014. MiR-451 is decreased in hypertrophic cardiomyopathy and regulates autophagy by targeting TSC1. *J Cell Mol Med,* 18**,** 2266-74.

Sorlie, T., Perou, C. M., Tibshirani, R., et al. 2001. Gene expression patterns of breast carcinomas distinguish tumor subclasses with clinical implications. *Proc Natl Acad Sci U S A,* 98**,** 10869-74.

Stanczyk, J., Pedrioli, D. M., Brentano, F., Sanchez-Pernaute, O., Kolling, C., Gay, R. E., Detmar, M., Gay, S. & Kyburz, D. 2008. Altered expression of MicroRNA in synovial fibroblasts and synovial tissue in rheumatoid arthritis. *Arthritis Rheum,* 58**,** 1001-9.

Steen, V., Domsic, R. T., Lucas, M., Fertig, N. & Medsger, T. A., Jr. 2012. A clinical and serologic comparison of African American and Caucasian patients with systemic sclerosis. *Arthritis Rheum,* 64**,** 2986-94.

Steen, V. D. 1998. Clinical manifestations of systemic sclerosis. *Semin Cutan Med Surg,* 17**,** 48-54.

Stewart, G. A., Hoyne, G. F., Ahmad, S. A., Jarman, E., Wallace, W. A., Harrison, D. J., Haslett, C., Lamb, J. R. & Howie, S. E. 2003. Expression of the developmental Sonic hedgehog (Shh) signalling pathway is up-regulated in chronic lung fibrosis and the Shh receptor patched 1 is present in circulating T lymphocytes. *J Pathol,* 199**,** 488-95.

Strickland, F. M. & Richardson, B. C. 2008. Epigenetics in human autoimmunity. Epigenetics in autoimmunity - DNA methylation in systemic lupus erythematosus and beyond. *Autoimmunity,* 41**,** 278-86.

Su, J., Zhang, A., Shi, Z., Ma, F., Pu, P., Wang, T., Zhang, J., Kang, C. & Zhang, Q. 2012. MicroRNA-200a suppresses the Wnt/beta-catenin signaling pathway by interacting with beta-catenin. *Int J Oncol,* 40**,** 1162-70.

Sugimura, R. & Li, L. 2010. Noncanonical Wnt signaling in vertebrate development, stem cells, and diseases. *Birth Defects Res C Embryo Today,* 90**,** 243-56.

Sun, X., He, Y., Huang, C., Ma, T. T. & Li, J. 2013. Distinctive microRNA signature associated of neoplasms with the Wnt/beta-catenin signaling pathway. *Cell Signal,* 25**,** 2805-11.

Szekanecz, E., Szamosi, S., Horvath, A., Nemeth, A., Juhasz, B., Szanto, J., Szucs, G. & Szekanecz, Z. 2012. Malignancies associated with systemic sclerosis. *Autoimmun Rev,* 11**,** 852-5.

Tager, R. E. & Tikly, M. 1999. Clinical and laboratory manifestations of systemic sclerosis (scleroderma) in Black South Africans. *Rheumatology (Oxford),* 38**,** 397-400.

Tan, F. K., Hildebrand, B. A., Lester, M. S., et al. 2005. Classification analysis of the transcriptosome of nonlesional cultured dermal fibroblasts from systemic sclerosis patients with early disease. *Arthritis Rheum,* 52**,** 865-76.

Tan, F. K., Wang, N., Kuwana, M., Chakraborty, R., Bona, C. A., Milewicz, D. M. & Arnett, F. C. 2001. Association of fibrillin 1 single-nucleotide polymorphism haplotypes with systemic sclerosis in Choctaw and Japanese populations. *Arthritis Rheum,* 44**,** 893-901.

Tanaka, S., Suto, A., Ikeda, K., et al. 2013. Alteration of circulating miRNAs in SSc: miR-30b regulates the expression of PDGF receptor beta. *Rheumatology (Oxford),* 52**,** 1963-72.

Tang, Y., Luo, X., Cui, H., et al. 2009. MicroRNA-146A contributes to abnormal activation of the type I interferon pathway in human lupus by targeting the key signaling proteins. *Arthritis Rheum,* 60**,** 1065-75.

Tao, Q., Yokota, C., Puck, H., et al. 2005. Maternal wnt11 activates the canonical wnt signaling pathway required for axis formation in Xenopus embryos. *Cell,* 120**,** 857-71.

Tejpar, S., Li, C., Yu, C., Poon, R., Denys, H., Sciot, R., Van Cutsem, E., Cassiman, J. J. & Alman, B. A. 2001. Tcf-3 expression and beta-catenin mediated transcriptional activation in aggressive fibromatosis (desmoid tumour). *Br J Cancer,* 85**,** 98-101.

Thysen, S., Luyten, F. P. & Lories, R. J. 2015. Loss of Frzb and Sfrp1 differentially affects joint homeostasis in instability-induced osteoarthritis. *Osteoarthritis Cartilage,* 23**,** 275-9.

Tikly, M., Rands, A., Mchugh, N., Wordsworth, P. & Welsh, K. 2004. Human leukocyte antigen class II associations with systemic sclerosis in South Africans. *Tissue Antigens,* 63**,** 487-90.

Toh, P. P., Li, J. J., Yip, G. W., Lo, S. L., Guo, C. H., Phan, T. T. & Bay, B. H. 2010. Modulation of metallothionein isoforms is associated with collagen deposition in proliferating keloid fibroblasts in vitro. *Exp Dermatol,* 19**,** 987-93.

Tomasek, J. J., Gabbiani, G., Hinz, B., Chaponnier, C. & Brown, R. A. 2002. Myofibroblasts and mechano-regulation of connective tissue remodelling. *Nat Rev Mol Cell Biol,* 3**,** 349-63.

Tome, M., Lopez-Romero, P., Albo, C., Sepulveda, J. C., Fernandez-Gutierrez, B., Dopazo, A., Bernad, A. & Gonzalez, M. A. 2011. miR-335 orchestrates cell proliferation, migration and differentiation in human mesenchymal stem cells. *Cell Death Differ,* 18**,** 985-95.

Trapnell, C., Roberts, A., Goff, L., et al. 2012. Differential gene and transcript expression analysis of RNA-seq experiments with TopHat and Cufflinks. *Nat Protoc,* 7**,** 562-78.

Valentini, G., Della Rossa, A., Bombardieri, S., et al. 2001. European multicentre study to define disease activity criteria for systemic sclerosis. II. Identification of disease activity variables and development of preliminary activity indexes. *Ann Rheum Dis,* 60**,** 592-8.

Van Almen, G. C., Verhesen, W., Van Leeuwen, R. E., et al. 2011. MicroRNA-18 and microRNA-19 regulate CTGF and TSP-1 expression in age-related heart failure. *Aging Cell,* 10**,** 769-79.

Van Bavel, C. C., Dieker, J. W., Tamboer, W. P., Van Der Vlag, J. & Berden, J. H. 2010. Lupus-derived monoclonal autoantibodies against apoptotic chromatin recognize acetylated conformational epitopes. *Mol Immunol,* 48**,** 248-56.

Van Den Hoogen, F., Khanna, D., Fransen, J., et al. 2013. 2013 classification criteria for systemic sclerosis: an American college of rheumatology/European league against rheumatism collaborative initiative. *Ann Rheum Dis,* 72**,** 1747-55.

Van Rooij, E., Sutherland, L. B., Qi, X., Richardson, J. A., Hill, J. & Olson, E. N. 2007. Control of stress-dependent cardiac growth and gene expression by a microRNA. *Science,* 316**,** 575-9.

Van Rooij, E., Sutherland, L. B., Thatcher, J. E., Dimaio, J. M., Naseem, R. H., Marshall, W. S., Hill, J. A. & Olson, E. N. 2008. Dysregulation of microRNAs after myocardial infarction reveals a role of miR-29 in cardiac fibrosis. *Proc Natl Acad Sci U S A,* 105**,** 13027-32.

Vaporidi, K., Vergadi, E., Kaniaris, E., Hatziapostolou, M., Lagoudaki, E., Georgopoulos, D., Zapol, W. M., Bloch, K. D. & Iliopoulos, D. 2012. Pulmonary microRNA profiling in a mouse model of ventilator-induced lung injury. *Am J Physiol Lung Cell Mol Physiol,* 303**,** L199-207.

Varga, J. 2002. Scleroderma and Smads: dysfunctional Smad family dynamics culminating in fibrosis. *Arthritis Rheum,* 46**,** 1703-13.

Varga, J. & Abraham, D. 2007. Systemic sclerosis: a prototypic multisystem fibrotic disorder. *J Clin Invest,* 117**,** 557-67.

Varga, J. & Pasche, B. 2009. Transforming growth factor beta as a therapeutic target in systemic sclerosis. *Nat Rev Rheumatol,* 5**,** 200-6.

Venugopal, S. K., Jiang, J., Kim, T. H., Li, Y., Wang, S. S., Torok, N. J., Wu, J. & Zern, M. A. 2010. Liver fibrosis causes downregulation of miRNA-150 and miRNA-194 in hepatic stellate cells, and their overexpression causes decreased stellate cell activation. *Am J Physiol Gastrointest Liver Physiol,* 298**,** G101-6.

Vettori, S., Gay, S. & Distler, O. 2012. Role of MicroRNAs in Fibrosis. *Open Rheumatol J,* 6**,** 130-9.

Volkmann, E. R., Chang, Y. L., Barroso, N., et al. 2016. Association of Systemic Sclerosis With a Unique Colonic Microbial Consortium. *Arthritis Rheumatol,* 68**,** 1483-92.

Wang, B., Herman-Edelstein, M., Koh, P., et al. 2010. E-cadherin expression is regulated by miR-192/215 by a mechanism that is independent of the profibrotic effects of transforming growth factor-beta. *Diabetes,* 59**,** 1794-802.

Wang, B., Koh, P., Winbanks, C., et al. 2011. miR-200a Prevents renal fibrogenesis through repression of TGF-beta2 expression. *Diabetes,* 60**,** 280-7.

Wang, L., Zhou, Z., Saari, J. T. & Kang, Y. J. 2005. Alcohol-induced myocardial fibrosis in metallothionein-null mice: prevention by zinc supplementation. *Am J Pathol,* 167**,** 337-44.

Wang, Q., Wang, Y., Minto, A. W., Wang, J., Shi, Q., Li, X. & Quigg, R. J. 2008. MicroRNA-377 is up-regulated and can lead to increased fibronectin production in diabetic nephropathy. *FASEB J,* 22**,** 4126-35.

Wang, S. H., Xu, F., Dang, H. X. & Yang, L. 2013a. Genetic variations in the Wnt signaling pathway affect lung function in asthma patients. *Genet Mol Res,* 12**,** 1829-33.

Wang, Y., Fan, P. S. & Kahaleh, B. 2006. Association between enhanced type I collagen expression and epigenetic repression of the FLI1 gene in scleroderma fibroblasts. *Arthritis Rheum,* 54**,** 2271-9.

Wang, Y., Huang, C., Reddy Chintagari, N., Bhaskaran, M., Weng, T., Guo, Y., Xiao, X. & Liu, L. 2013b. miR-375 regulates rat alveolar epithelial cell trans-differentiation by inhibiting Wnt/beta-catenin pathway. *Nucleic Acids Res,* 41**,** 3833-44.

Wang, Y., Li, W., Zang, X., Chen, N., Liu, T., Tsonis, P. A. & Huang, Y. 2013c. MicroRNA-204-5p regulates epithelial-to-mesenchymal transition during human posterior capsule opacification by targeting SMAD4. *Invest Ophthalmol Vis Sci,* 54**,** 323-32.

Wang, Z., Lin, L., Thomas, D. G., Nadal, E., Chang, A. C., Beer, D. G. & Lin, J. 2015. The role of Dickkopf-3 overexpression in esophageal adenocarcinoma. *J Thorac Cardiovasc Surg,* 150**,** 377-385 e2.

Wei, J., Bhattacharyya, S., Tourtellotte, W. G. & Varga, J. 2011a. Fibrosis in systemic sclerosis: emerging concepts and implications for targeted therapy. *Autoimmun Rev,* 10**,** 267-75.

Wei, J., Fang, F., Lam, A. P., et al. 2012. Wnt/beta-catenin signaling is hyperactivated in systemic sclerosis and induces Smad-dependent fibrotic responses in mesenchymal cells. *Arthritis Rheum*.

Wei, J., Melichian, D., Komura, K., Hinchcliff, M., Lam, A. P., Lafyatis, R., Gottardi, C. J., Macdougald, O. A. & Varga, J. 2011b. Canonical Wnt signaling induces skin fibrosis and subcutaneous lipoatrophy: a novel mouse model for scleroderma? *Arthritis Rheum,* 63**,** 1707-17.

Wesche, J., Haglund, K. & Haugsten, E. M. 2011. Fibroblast growth factors and their receptors in cancer. *Biochem J,* 437**,** 199-213.

White, N. M., Khella, H. W., Grigull, J., et al. 2011. miRNA profiling in metastatic renal cell carcinoma reveals a tumour-suppressor effect for miR-215. *Br J Cancer,* 105**,** 1741-9.

Whitfield, M. L., Finlay, D. R., Murray, J. I., et al. 2003. Systemic and cell type-specific gene expression patterns in scleroderma skin. *Proc Natl Acad Sci U S A,* 100**,** 12319-24.

Wooten, M. 2008. Systemic sclerosis and malignancy: a review of the literature. *South Med J,* 101**,** 59-62.

Wu, S., Rhee, K. J., Albesiano, E., et al. 2009. A human colonic commensal promotes colon tumorigenesis via activation of T helper type 17 T cell responses. *Nat Med,* 15**,** 1016-22.

Yamamoto, H., Ochiya, T., Takahama, Y., Ishii, Y., Osumi, N., Sakamoto, H. & Terada, M. 2000. Detection of spatial localization of Hst-1/Fgf-4 gene expression in brain and testis from adult mice. *Oncogene,* 19**,** 3805-10.

Yamamoto, T., Takagawa, S., Katayama, I., Yamazaki, K., Hamazaki, Y., Shinkai, H. & Nishioka, K. 1999. Animal model of sclerotic skin. I: Local injections of bleomycin induce sclerotic skin mimicking scleroderma. *J Invest Dermatol,* 112**,** 456-62.

Yamane, K., Ihn, H., Kubo, M. & Tamaki, K. 2002. Increased transcriptional activities of transforming growth factor beta receptors in scleroderma fibroblasts. *Arthritis Rheum,* 46**,** 2421-8.

Yan, Z., Xiong, Y., Xu, W., Gao, J., Cheng, Y., Wang, Z., Chen, F. & Zheng, G. 2012. Identification of hsa-miR-335 as a prognostic signature in gastric cancer. *PLoS One,* 7**,** e40037.

Yang, D., Lutter, D., Burtscher, I., Uetzmann, L., Theis, F. J. & Lickert, H. 2014a. miR-335 promotes mesendodermal lineage segregation and shapes a transcription factor gradient in the endoderm. *Development,* 141**,** 514-25.

Yang, L., Perez, A. A., Fujie, S., et al. 2014b. Wnt modulates MCL1 to control cell survival in triple negative breast cancer. *BMC Cancer,* 14**,** 124.

Yasuda, K., Torigoe, T., Mariya, T., et al. 2014. Fibroblasts induce expression of FGF4 in ovarian cancer stem-like cells/cancer-initiating cells and upregulate their tumor initiation capacity. *Lab Invest,* 94**,** 1355-69.

Yazawa, N., Kikuchi, K., Ihn, H., Fujimoto, M., Kubo, M., Tamaki, T. & Tamaki, K. 2000. Serum levels of tissue inhibitor of metalloproteinases 2 in patients with systemic sclerosis. *J Am Acad Dermatol,* 42**,** 70-5.

Yi, L., Wang, J. C., Guo, X. J., et al. 2013. STAT4 is a genetic risk factor for systemic sclerosis in a Chinese population. *Int J Immunopathol Pharmacol,* 26**,** 473-8.

You, J., Nguyen, A. V., Albers, C. G., Lin, F. & Holcombe, R. F. 2008. Wnt pathway-related gene expression in inflammatory bowel disease. *Dig Dis Sci,* 53**,** 1013-9.

Youn, J., Hwang, S. H., Ryoo, Z. Y., Lynes, M. A., Paik, D. J., Chung, H. S. & Kim, H. Y. 2002. Metallothionein suppresses collagen-induced arthritis via induction of TGF-beta and down-regulation of proinflammatory mediators. *Clin Exp Immunol,* 129**,** 232-9.

Young-Min, S. A., Beeton, C., Laughton, R., Plumpton, T., Bartram, S., Murphy, G., Black, C. & Cawston, T. E. 2001. Serum TIMP-1, TIMP-2, and MMP-1 in patients with systemic sclerosis, primary Raynaud's phenomenon, and in normal controls. *Ann Rheum Dis,* 60**,** 846-51.

Yu, S., Huang, H., Deng, G., et al. 2015. miR-326 Targets Antiapoptotic Bcl-xL and Mediates Apoptosis in Human Platelets. *PLoS One,* 10**,** e0122784.

Yue, W., Sun, Q., Dacic, S., Landreneau, R. J., Siegfried, J. M., Yu, J. & Zhang, L. 2008. Downregulation of Dkk3 activates beta-catenin/TCF-4 signaling in lung cancer. *Carcinogenesis,* 29**,** 84-92.

Zhang, H., Liu, X., Chen, S., et al. 2010. Tectorigenin inhibits the in vitro proliferation and enhances miR-338* expression of pulmonary fibroblasts in rats with idiopathic pulmonary fibrosis. *J Ethnopharmacol,* 131**,** 165-73.

Zhang, J., Tu, Q., Bonewald, L. F., He, X., Stein, G., Lian, J. & Chen, J. 2011. Effects of miR-335-5p in modulating osteogenic differentiation by specifically downregulating Wnt antagonist DKK1. *J Bone Miner Res,* 26**,** 1953-63.

Zhang, J. G., Shi, Y., Hong, D. F., Song, M., Huang, D., Wang, C. Y. & Zhao, G. 2015. MiR-148b suppresses cell proliferation and invasion in hepatocellular carcinoma by targeting WNT1/beta-catenin pathway. *Sci Rep,* 5**,** 8087.

Zhang, X., Ibrahimi, O. A., Olsen, S. K., Umemori, H., Mohammadi, M. & Ornitz, D. M. 2006. Receptor specificity of the fibroblast growth factor family. The complete mammalian FGF family. *J Biol Chem,* 281**,** 15694-700.

Zhao, W., Sun, Z., Wang, S., Li, Z. & Zheng, L. 2015. Wnt1 Participates in Inflammation Induced by Lipopolysaccharide Through Upregulating Scavenger Receptor A and NF-kB. *Inflammation,* 38**,** 1700-6.

Zhao, X., Tang, Y., Qu, B., et al. 2010. MicroRNA-125a contributes to elevated inflammatory chemokine RANTES levels via targeting KLF13 in systemic lupus erythematosus. *Arthritis Rheum,* 62**,** 3425-35.

Zhao, Y., Ransom, J. F., Li, A., et al. 2007. Dysregulation of cardiogenesis, cardiac conduction, and cell cycle in mice lacking miRNA-1-2. *Cell,* 129**,** 303-17.

Zhou, X., Tan, F. K., Xiong, M., Arnett, F. C. & Feghali-Bostwick, C. A. 2005. Monozygotic twins clinically discordant for scleroderma show concordance for fibroblast gene expression profiles. *Arthritis Rheum,* 52**,** 3305-14.

Zhou, X., Tan, F. K., Xiong, M., Milewicz, D. M., Feghali, C. A., Fritzler, M. J., Reveille, J. D. & Arnett, F. C. 2001. Systemic sclerosis (scleroderma): specific autoantigen genes are selectively overexpressed in scleroderma fibroblasts. *J Immunol,* 167**,** 7126-33.

Zhu, D., Pan, C., Li, L., et al. 2013a. MicroRNA-17/20a/106a modulate macrophage inflammatory responses through targeting signal-regulatory protein alpha. *J Allergy Clin Immunol,* 132**,** 426-36 e8.

Zhu, H., Li, Y., Qu, S., et al. 2012. MicroRNA expression abnormalities in limited cutaneous scleroderma and diffuse cutaneous scleroderma. *J Clin Immunol,* 32**,** 514-22.

Zhu, H., Luo, H. & Zuo, X. 2013b. MicroRNAs: their involvement in fibrosis pathogenesis and use as diagnostic biomarkers in scleroderma. *Exp Mol Med,* 45**,** e41.

Zimmermann, A. F. & Pizzichini, M. M. 2013. Update on etiopathogenesis of systemic sclerosis. *Rev Bras Reumatol,* 53**,** 516-24.

Appendices

Appendix A – Ethics Certificate

UNIVERSITY OF THE WITWATERSRAND, JOHANNESBURG
Division of the Deputy Registrar (Research)

HUMAN RESEARCH ETHICS COMMITTEE (MEDICAL)
R14/49 Ms Jacqueline M Frost

CLEARANCE CERTIFICATE	**M120512**
PROJECT	The Role of the Canonical Pathway in Inducing Skin Fibrosis in Black South African Patients with Systemic Sclerosis
INVESTIGATORS	Ms Jacqueline M Frost.
DEPARTMENT	Internal Medicine and Human Genetics
DATE CONSIDERED	25/05/2012
DECISION OF THE COMMITTEE*	Approved unconditionally

Unless otherwise specified this ethical clearance is valid for 5 years and may be renewed upon application.

DATE 07/08/2012 **CHAIRPERSON** .....
(Professor PE Cleaton-Jones)

*Guidelines for written 'informed consent' attached where applicable
cc: Supervisor : Prof Mohammed Tikly

DECLARATION OF INVESTIGATOR(S)
To be completed in duplicate and **ONE COPY** returned to the Secretary at Room 10004, 10th Floor, Senate House, University.
I/We fully understand the conditions under which I am/we are authorized to carry out the abovementioned research and I/we guarantee to ensure compliance with these conditions. Should any departure to be contemplated from the research procedure as approved I/we undertake to resubmit the protocol to the Committee. **I agree to a completion of a yearly progress report.**

Appendix A2 – Amendment to ethics certificate

University
of the Witwatersrand,
Johannesburg

Human Research Ethics Committee (Medical)
(formerly Committee for Research on Human Subjects (Medical)
Secretariat: Research Office, Room SH10005, 10th floor, Senate House • Telephone: +27 11 717-1234 • Fax: +27 11 339-5708
Private Bag 3, Wits 2050, South Africa

25 September 2013

Ms Jacqueline Frost
School of Pathology
Division of Human Genetics
University of Witwatersrand
PO Box 1038
Johannesburg
2000
Sent by email: frost.jacqueline@gmail.com

Re: **Protocol M120512 The Role of the Canonical Pathway inn Inducing Skin Fibrosis in Black South African Patients with Systemic Sclerosis**
Principal Investigator (PI): Ms Jacqueline M Frost
Protocol Amendment

This letter serves to confirm that the Chairman of Human Research Ethics Committee (Medical) has approved the amendment on the above mentioned protocol as detailed on your letter dated 16 August 2013

- Request to add additional study site: Centre for Genome Regulation (CRG) in Barcelona, Spain
- Anonymised Samples for the abovementioned study will be shipped on dry ice to CRG in the form of tissue biopsies and extracted DNA
- The PI will be the only person working with the samples while in Spain
- PI will have a Material Transfer Agreement with the CRG and export permit for the samples will be sourced from the Department of Health

Thank you for keeping us informed and updated.

Yours Sincerely,

Zanelello.....

Ms Zanele Ndlovu
Administrative Officer
Human Research Ethics Committee (Medical)

Appendix B – Patient and Control Information and Consent forms

GENETIC STUDY OF FIBROSIS IN SYSTEMIC SCLEROSIS

(Control skin biopsy)

Information Sheet

Dear Sir/Madam

My name is Jacqueline Frost, a research assistant and PhD student at the National Health Laboratory Service, and I would like to invite you to participate in a genetics study aimed at finding out what causes fibrosis (skin hardening) in Systemic sclerosis. If you decide to participate in the study please note that a questionnaire needs to be completed, please allow 5 minutes for the questionnaire/interview to be completed.

Participation is entirely voluntary and you will not be disadvantaged in any way if you choose not to participate.

Systemic sclerosis is a complex, multi-system disease which is known to involve the immune system, blood vessels and the skin. The symptom which is most commonly identified in the disease is the gradual thickening and tightening (fibrosis) of the skin. Often ulcers are found, particularly on the fingertips, which are slow to heal due to poor circulation.

The aim of this study is to understand the genetic basis of the fibrosis of the skin. The knowledge gained could help to improve treatment for this symptom of the disease, although this will not be immediately available and could take several decades.

As in any research study I need control samples. These samples will come from individuals who do not have systemic sclerosis or keloids. To do these studies we need to take one (1) skin sample. The skin sample from non patient participants will need to be taken while the

individual is undergoing skin graft surgery. A plastic surgeon at Helen Joseph Hospital will be responsible for the removal of the small sample of skin during the course of a prearranged surgical operation. Since this will be done under a general anaesthetic there will be no additional pain or discomfort. All samples will be coded and any information obtained from this study will be kept confidential and used only for research purposes. Results of the study will be made available in the biomedical literature.

The test will not involve any costs to the participant and participation is completely voluntary. You will not be disadvantaged in any way if you decide not to participate.

Should you require any further information, please do not hesitate to contact:

Professor Mohammed Tikly
Division of Rheumatology, Chris Hani Baragwanath Hospital
University of the Witwatersrand

Or

Professor Peter Cleaton-Jones
Chairman of the Human Research Ethics Committee
University of the Witwatersrand

GENETIC STUDY OF FIBROSIS IN SYSTEMIC SCLEROSIS

(Patient skin biopsy and blood)

Information Sheet

Dear Sir/Madam

My name is Jacqueline Frost, a research assistant and PhD student at the National Health Laboratory Service, and I would like to invite you to participate in a genetics study aimed at finding out what causes fibrosis (skin hardening) in Systemic sclerosis. If you decide to participate in the study please note that a questionnaire needs to be completed, please allow 5 minutes for the questionnaire/interview to be completed.

Participation is entirely voluntary and you will not be disadvantaged in any way if you choose not to participate.

Systemic sclerosis is a complex, multi-system disease which is known to involve the immune system, blood vessels and the skin. The symptom which is most commonly identified in the disease is the gradual thickening and tightening (fibrosis) of the skin. Often ulcers are found, particularly on the fingertips, which are slow to heal due to poor circulation. The aim of this study is to understand the genetic basis of the fibrosis of the skin, and also if there are changes in the expression of genes after a period of treatment. The knowledge gained could help to improve treatment for this symptom of the disease, although this will not be immediately available and could take several decades.

This procedure might cause some discomfort and pain. It involves the removal of a small piece of skin (4mm in diameter) by punch biopsy. After the procedure a steri-strip will be placed over the biopsy region to prevent any infections and to help the wound heal better. No stitches will be needed. The procedure will be carried out by a qualified dermatologist. I also need to take a blood sample from individuals with Systemic sclerosis. A nurse or doctor

will take the blood samples. There will be little pain and discomfort. We will take the equivalent of two or three tablespoons (10-30ml) of blood from each individual. There is a small risk of infection after blood has been taken, but precautions will be made to make sure that the risk of infection is minimised

All samples will be coded and any information obtained from this study will be kept confidential and used only for research purposes. Results will not be made available to you personally as they will need to be interpreted in the context of the group and their clinical value may not be apparent for several years.

The test will not involve any costs to the participant and participation is completely voluntary. You will not be disadvantaged in any way if you decide not to participate. If you wish to withdraw from the study, you are able to do so at any time. Participation in the study does not advantage you in any way, you will receive treatment as normal.

Should you require any further information, please do not hesitate to contact:

Professor Mohammed Tikly, Division of Rheumatology

Chris Hani Baragwanath Hospital and the University of the Witwatersrand

Or

Professor Peter Cleaton-Jones

Chairman of the Human Research Ethics Committee

University of the Witwatersrand

GENETIC STUDY OF FIBROSIS IN SYSTEMIC SCLEROSIS

Consent to Participate in Research Study

You have been asked to participate in a research study which will look at the genetics of systemic sclerosis.

You have been informed about the study by
_____

Have you been informed about the procedures involved in the study? **YES / NO**

Have you been informed that your participation in the study is entirely voluntary and you will not be penalised in any way it you wish not to participate? **YES / NO**

Are you consenting to giving skin biopsies? **YES / NO**

Do you understand that results of the study will not be made available to you? **YES / NO**

You may contact Professor Mohammed Tikly at (011) 933-**** any time if you have any questions about the research.

You may contact the Research Ethics Committee at (011) 717-*** if you have any questions about your rights as a research participant.

The research study, including all information, has been described to me. I understand what my involvement in the study means and I voluntarily agree to participate.

Full name of participant (optional):_____

_____ _____

Signature of Participant Date

_____ _____

Signature of witness Date

Appendix C - miRNeasy mini Kit (Qiagen)

1. Set centrifuge to **4°C**
2. Place on bench at room temperature for **5 minutes**
3. Add **140µl** chloroform – shake vigorously for 15 seconds
4. Place on bench at room temperature for **3 minutes**
5. Centrifuge for **15 minutes** at 12 000g (4°C)
6. Set centrifuge to **25°C**
7. Contents of tube separates into 3 layers – transfer the **upper** clear layer containing the RNA to a new tube
8. Add **1.5x 100% EtOH** – mix by pipetting up and down
9. Pipette **700µl** sample into RNeasy mini spin column
10. Centrifuge at 8000g for **15 seconds** – DISCARD FLOW THROUGH (Repeat x2)
11. Add **700µl RWT** buffer to column
12. Centrifuge at 10 000g for **15 seconds** - DISCARD FLOW THROUGH
13. Add **500µl RPE** buffer to column
14. Centrifuge at 10 000g for **15 seconds** - DISCARD FLOW THROUGH
15. Add **500µl RPE** buffer to column
16. Centrifuge at 10 000g for **2 minutes**
17. Place column in new tube and spin at full speed for **1 minute**
18. Place column in 1.5ml eppendorf and pipette **50µl** RNAse free water onto membrane
19. Centrifuge for **1 minute** at 10 000g to elute RNA

Appendix D – RNA Quality and Quantity

Patients	Weight (mg)	Concentation	Volume	RIN*
P1	20	63.39	45	6.8
1B	24	59.09	45	6.2
P2	26	75.03	45	8
2B	14	38.29	45	8.1
P3	20	40.4	45	7.9
3B	23	46.61	45	7.4
P4	20	38.94	45	8.2
4B	20	29.84	45	7.7
P5	27	57.2	45	8.4
5B	21	46.9	45	7.5
P6	15	49.67	45	8.4
6B	16	60.71	45	8.8
P7	10	37.58	45	8.5
7B	22	71.64	45	7.9
P8	13	70.64	45	9.2
8B	13	41.99	45	8.7
P9	18	88.41	45	8.9
9B	34	86.44	45	7.3
Controls	**Weight (mg)**	**Concentation**	**Volume**	**RIN***
1	10	57.17	45	7.5
2	14	41.1	45	7.7
3	37	68.82	45	8.8
4	35	189.6	45	6.3
5	30	389.24	45	6.7
6	10	185.46	45	7.8
7	28	316.09	45	8.4
8	26	419.06	45	7.3

*RNA Integrity Number

Appendix E – List of genes on the Wnt pathway qPCR array

Wnt signaling pathways:

Canonical: APC, AXIN1, AXIN2, CSNK1A1, CTBP1, CTNNB1, CTNNB1P1, DKK1, DKK3, DVL1, DVL2, EP300, FRAT1, FZD1, FZD2, FZD3, FZD4, FZD5, FZD6, FZD7, FZD8, FZD9, GSK3B, LEF1, LRP5, LRP6, NKD1. PORCN, RUVBL1, SFRP1, SFRP4, SKP2, SOX17, TCF7, TCF7L1, WIF1, WNT1, WNT10A, WNT2, WNT2B, WNT3, WNT3A, WNT4, WNT6, WNT7A, WNT7B, WNT8A

Planar cell polarity (PCP): DAAM1, DVL1, DVL2, MAPK8, NKD1, PRICKLE1, RHOA, VANGL2, WNT9A

Wnt/Ca^{2+}: FZD2, NFATC1, WNT1, WNT10A, WNT11, WNT2, WNT2B, WNT3, WNT3A, WNT4, WNT5A, WNT5B, WNT6, WNT7A, WNT7B, WNT8, WNT9A

Wnt signaling negative regulation: APC, AXIN1, AXIN2, BTRC, CCND1, CTBP1, CTNNB1P1, DKK1, DKK3, FBXW11, FRZB, KREMEN1, LRP6, NLK, NKD1, SFRP1, SFRP4, SOX17, WIF1

Wnt signaling target genes: AXIN2, BTRC, CCND1, CCND2, DAB2, FOSL1, JUN, MMP7, MYC, PITX2, PPARD, WISP1

Development Processes:

Cell fate: CTNNB1, DKK1, WNT1, WNT3, WNT3A

Tissue polarity: AXIN2, FZD2, FZD3, FZD5, FZD6, VANGL2

Cell growth and proliferation: APC, CCND1, CCND2, CTBP1, CTNNB1, CTNNB1P1, DAB2, EP300, FGF4, FOSL1, FZD3, JUN, LRP5, MMP7, MYC, PPARD, WISP1, WNT3A

Cell migration: APC, DKK1, LRP5, LRP6, RHOA, WNT1

Cell cycle: APC, BTRC, CCND1, CCND2, CTNNB1, EP300, FOSL1, JUN, MYC, RHOA, RUVBL1, TCF7L1

Cellular homeostasis: APC, FZD2, JUN, MYC

Pathway signature genes: BOD1, CALM1, CCND1, CCND2, CHSY1, CXADR, CYP4V2, HSPA12A, LEF1, MT1A1, MTFP1, MTSS1, MYC, NAV2, PRMT6, SKP2

Appendix F - RT^2 Profiler PCR Array Protocol

cDNA Synthesis
The RT2 PreAMP cDNA Synthesis Kit and RT2 PreAMP Pathway Primer Mix maximizes positive calls at low amounts of total RNA
Recommend starting material of 10-50ng total RNA from fresh/frozen samples

1. Prepare the genomic DNA elimination mix for each RNA sample in a sterile PCR tube. Pipette up and down, centrifuge briefly

Component	Amount for one sample of RNA (fresh/frozen)
RNA	10-50ng
Buffer GE	2µl
RNAse free water	variable
Total volume	**10µl**

2. Incubate at 42°C for 5 min, place immediately on ice for 1 min
3. Prepare the reverse-transcription mix

Component	Volume for 1 reaction
5X Buffer BC3	4µl
Control P2	1µl
cDNA synthesis enzyme mix	1µl
RNAse inhibitor	1µl
RNAse free water	3µl
Total volume	**10µl**

4. Add 10µl reverse-transcription mix to each tube containing 10µl genomic DNA elimination mix. Pipette up and down, centrifuge briefly
5. Incubate at 42°C for exactly 30 min. Then immediately stop the reaction by incubating at 95°C for 5 min
6. Place the reactions on ice and proceed with the *preamplification* protocol

If you wish to store the reactions overnight prior to real-time PCR, transfer to a -20°C freezer. Longer storage times are not recommended

Preamplification of cDNA Target Templates

- Each RT2 PreAMP Pathway Primer Mix is specific for a particular pathway RT2 Profiler PCR Array
- Check to verify the correct pathway-specific RT2 PreAMP Pathway Primer Mix is used for the RT2 Profiler PCR Array
- Verify that the lot numbers are compatible

1. Thaw the RT2 PreAMP PCR Mastermix and RT2 PreAMP Pathway Primer Mix at room temperature. If precipitates are visible, warm the reagents at 42°C for 1 min, vortex briefly
2. Prepare the preamplification mix

Component	Amount for 1 sample
RT2 PreAMP PCR Mastermix	12.5µl
RT2 PreAMP PCR Primer Mix	7.5µl
Total volume	**20µl**

3. Pipet 5µl cDNA synthesis reaction (from step 6 above) into a 0.2 ml PCR tube. Add 20 µl preamplification mix
4. Pipetting up and down, spin briefly
5. Place the tubes in the real-time cycler and start the program as below

Cycles	Duration	Temperature	Comments
1	10 minutes	95°C	HotStart Taq activated
12	15 seconds 2 minutes	95°C 60°C	
Hold		4°C	

6. When finished, take the tubes and place on ice
7. Add 2µl Side Reaction Reducer to each preamplified reaction. Pipette up and down, spin briefly
8. Incubate at 37°C for 15 min followed by heat inactivation at 95°C for 5 min
9. Immediately add 84µl nuclease-free water. Mix well.
10. Place on ice prior to real-time PCR, or store overnight at –20°C

Real-Time PCR Using RT2 Profiler PCR Arrays

1. Briefly centrifuge the RT2 SYBR Green Mastermix
2. Prepare the PCR components mix in a 5 ml tube or a loading reservoir depending on the RT2 Profiler PCR Array format

Array format	384-well (E, G/4x96)
2X RT2 SYBR Green Mastermix	550µl
Preamplification reaction (Step 10 above)	102µl
RNAse free water	448µl
Total volume	**1100µl**

Continue from the corresponding step 3 onwards of the "*Real-Time PCR for RT2 Profiler PCR Arrays*" Protocol in the RT2 Profiler PCR Array Handbook
Save the remaining 9 µl cDNA synthesis reaction at –20°C, as it may be needed to perform quality control analysis

Dispense the PCR components mix into the RT2 Profiler PCR Array depending on the RT2 Profiler PCR Array format. Note: Change pipet tips following each pipetting step to avoid cross- contamination between the wells.

Formats E or G 384 (4 x 96) option

- Each 384-well plate contains 4 replicates of 96 assays that can be used for analysis of 4 samples, with reactions for each sample separated from one another by only one well
- The spacing between the tips of standard multichannel pipettes allows rows or columns to be skipped when adding each sample. Be sure to load each sample into the correct set of wells
- Carefully remove the RT2 Profiler PCR Array from its sealed bag
- If the PCR components mix is in a tube, transfer to a loading reservoir
- Add PCR components mix to each well of the RT2 Profiler PCR Array using an 8-channel pipette and the 384EZLoad Covers (provided)
- Place Cover 1 (white) on the plate. Add 10µl PCR components mix for sample 1 to the open wells (odd number wells of rows A, C, E, G, I, K, M, and O). Remove and discard Cover 1
- Place Cover 2 (yellow) on the plate. Add 10µl PCR components mix for sample 2 to the open wells (even number wells of rows A, C, E, G, I, K, M, and O). Remove and discard Cover 2
- Place Cover 3 (black) on the plate. Add 10µl PCR components mix for sample 3 to the open wells (odd number wells of rows B, D, F, H, J, L, N, and P). Remove and discard Cover 3
- Place Cover 4 (red) on the plate. Add 10µl PCR components mix for sample 4 to the open wells (even number wells of rows B, D, F, H, J, L, N, and P). Remove and discard Cover 4

3. Carefully, tightly seal the RT2 Profiler PCR Array with Optical Adhesive Film (Formats C, E, F, and G)
4. Centrifuge for 1 min at 1000 g at 15–25°C
5. Place the RT2 Profiler PCR Array on ice while setting up the PCR cycling program
6. Program the real-time cycler. If prompted by your cycler software, select "Absolute Quantitation" to begin

Cycles	Duration	Temperature	Comments
1	10 minutes	95°C	HotStart Taq is activated
40	15 seconds	95°C	
	1 minute	60°C	Perform fluorescence data collection

7. Place the Array in the real-time cycler. If recommended by the cycler user manual, use a compression pad with PCR Arrays sealed with optical adhesive film (formats C, E, F, and G). Start the run
8. Calculate the threshold cycle (CT) for each well using the real-time cycler software, as described in the following steps
9. Define the baseline by choosing the automated baseline option if the cycler has the adaptive baseline function. If the cycler does not have the adaptive baseline function, set the baseline manually. To set the baseline manually, use the linear view of the amplification plots to determine the earliest visible amplification. Set the cycler to use the readings from cycle number 2 through 2 cycles before the earliest visible amplification, but no more than cycle 15. The earliest amplification will usually be visible between cycles 14 and 18
10. Manually define the threshold by using the log view of the amplification plots. Choose a threshold value above the background signal but within the lower one-third to lower one-half of the linear phase of the amplification plot.
11. Export the CT values for all wells to a blank Excel® spreadsheet for use with the SABiosciences PCR Array Data Analysis Template Excel or Web-based software
12. Recommended: Perform dissociation (melting) curve analysis to verify PCR specificity. Run a melting curve program and generate a first derivative dissociation curve for each well using the real-time cycler software. A single peak should appear in each reaction at temperatures greater than 80°C

Appendix G – TaqMan Gene Expression Assays

Prepare the cDNA sample (High Capacity RNA to cDNA kit)

- 250ng of Total RNA
- Allow the kit components to thaw on ice

Component	+RT reaction (µl)	-RT reaction (µl)
2x RT Buffer	10	10
2x Enzyme mix	1	-
RNA sample	Up to 9	Up to 9
Nuclease-free water	Up to 20	Up to 20
Total per reaction	20	20

1. Aliquot reaction mix into plate or tubes
2. Seal plate or tubes
3. Briefly centrifuge and keep on ice
4. Incubate at:
    - 37°C for 60 minutes
    - 95°C for 5 minutes
    - 4°C hold

Recommended cDNA:

- 25ng of cDNA per 20ul amplification reaction
- The same amount of cDNA in each reaction
- Quantify cDNA (Nanodrop)
- Store cDNA at -20°C

Prepare the reaction mix and load plate

1. Thaw reagents on ice (20X gene expression assay, cDNA samples)
2. Mix reagents by gentle vortex and centrifuge
3. Calculate number of reactions (3 replicates of each reaction)
    - A TaqMan assay for each cDNA sample
    - Endogenous controls
    - No template controls

Prepare PCR reaction mix

1. For each sample (to be run in triplicate), pipette the following into 1.5ml tube

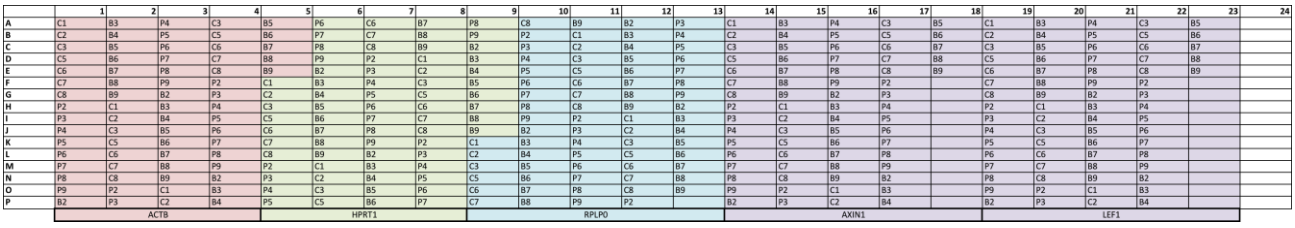
	Volume per 20µl reaction (µl)	
PCR reaction Mix component	**Single reaction**	**40x**
20X TaqMan Gene Expression Assay	1.0	40
2X TaqMan GenEx Master Mix	10.0	400
cDNA template (1-100ng)	1.0	-
RNAse-free water	8.0	320

2. Cap the tube and invert it several times to mix
3. Centrifuge briefly

Load the plate

1. Transfer 20ul of each PCR reaction into each well of the 384-well reaction plate
2. Seal the plate with an appropriate cover
3. Centrifuge plate briefly
4. Load plate into instrument

Plate layout



Run the real-time PCR reaction

1. Create a plate document/experiment for the run using the following parameter values:

				Thermal cycling conditions		
System	Run	Reaction plate	Plate document/experiment parameters	Stage	Temp (C)	Time (mm:ss)
Applied Biosystems 7900HT	Standard	384-well standard	Rxn volume: 20µl Ramp rate: standard	Hold* Hold Cycle (40x)	50 95 95 60	2:00 10:00 0:15 1:00
	Fast	384-well standard	Rxn volume: 20µl Ramp rate: fast	Hold* Hold Cycle (40x)	50 95 95 60	2:00 0:20 0:01 0:20

2. Run the plate.

Analyze the results

1. View amplification plots for the entire plate
2. Set baseline and threshold values
3. Compare Ct values to analyse data
4.

Appendix H – Clinical data

Sample	Sex	Age	Onset of Disease	Disease duration (months)	Diffuse	Skin score (0-51)	Affected skin score	Disease Activity Score	ESR (>30)	CRP	Lung disease	Renal disease	Myositis	ANA	Low C4	DLCO	Anti-Scl 70
P2	F	54	2009	36	1	34	3	2.5	0	5	1	0	1	1	1	62%	1
P3	F	48	2010	36	0	4	1	3	1	8.8	0	0	0	1	1	64%	0
P4	F	52	2007	60	1	9	2	3	1	12.5	0	0	1	1	1	109%	0
P5	F	49	2010	36	1	16	2	4	1	25	1	0	0	1	1	45%	0
P6	F	55	2010	36	1	32	3	6.5	1	13	1	0	1	1	1	50%	1
P7	F	58	2011	24	1	5	1	4.5	0	7	0	0	0	1	1	83%	0
P8	F	46	2012	12	1	25	2	4	1	21	1	0	0	1	1	40%	1
P9	M	64	2012	12	1	22	1	7.5	1	8	0	0	0	1	1	65%	0

Appendix I– Dates samples were extracted and processed for qPCR

Samples	Date extracted	qPCR plate	Run date
C1	13/11/2013	1	10/04/2014
C2	13/11/2013	1	10/04/2014
C3	13/11/2013	1	10/04/2014
C5	13/11/2013	1	10/04/2014
C6	15/11/2013	2	11/04/2014
C7	15/11/2013	2	11/04/2014
C8	15/11/2013	2	11/04/2014
P1	2/12/2013	2	11/04/2014
P2	2/12/2013	3	11/04/2014
P3	2/12/2013	3	11/04/2014
P4	2/12/2013	3	11/04/2014
P5	2/12/2013	3	11/04/2014
P6	2/12/2013	4	13/04/2014
P7	4/12/2013	4	13/04/2014
P8	4/12/2013	4	13/04/2014
P9	4/12/2013	4	13/04/2014
1B	4/12/2013	5	13/04/2014
2B	4/12/2013	5	13/04/2014
3B	4/12/2013	5	13/04/2014
4B	5/12/2013	5	13/04/2014
5B	5/12/2013	6	14/04/2014
6B	5/12/2013	6	14/04/2014
7B	5/12/2013	6	14/04/2014
8B	5/12/2013	6	14/04/2014
9B	5/12/2013	7	14/04/2014

Appendix J – Summary Table of gene cluster colours and Patient groups

Colour of gene expression cluster	**Differential expression**
Red	Genes upregulated in both affected and unaffected SSc skin compared to controls
Blue	Genes upregulated in both affected and unaffected SSc skin compared to controls, but pattern is noisy and heterogeneous. Mostly likely due to the high expression observed in sample 8B, which could be due to a normalization artifact.
Green	Genes downregulated in both affected and unaffected SSc skin compared to controls
Orange and Purple	According to the gene expression patterns observed in these clusters, the patients are delineated into two distinct patient groups, explained below.
Patient Groups delineated by PCA	**Samples and pattern of expression**
Patient Group 1	Contains samples 2, 4, 6 and 8. The affected skin of this group shows upregulation in the purple gene cluster while the unaffected skin shows a “normal-like” expression pattern comparable to the control samples.
Patient Group 2	Contains samples 3, 5, 7 and 9. The affected skin of this group shows upregulation in the orange gene cluster while the unaffected skin shows a “normal-like” expression pattern comparable to the control samples.
Gene expression patterns observed in orange and purple expression cluster	**Groups and pattern of expression**
Gene expression cluster A	The genes in cluster A are upregulated in the affected skin of Patient Group 2 and downregulated in the affected skin of Patient Group 1, for the genes in the orange expression cluster. The opposite is observed for the genes in the purple expression cluster
Gene expression cluster B	The genes in cluster B are upregulated in the affected skin of Patient Group 1 and downregulated in the affected skin of Patient Group 2, for the genes in the purple expression cluster. The opposite is observed for the genes in the orange expression cluster

Appendix K – Data normalised expression to *ACTB*

Twenty one genes were significantly differentially expressed in both the affected skin and the unaffected skin samples. 13 were over-expressed compared to the controls (Table J.1), while eight were under-expressed compared to controls (Table J.2). Again, the differential expression within the patient, thus between affected and unaffected skin, is not significant.

Table J.1. Genes significantly up regulated in SSc cases (affected and unaffected skin)

	Wnt signalling pathway qPCR Array					
Gene	**Affected skin v Controls Fold change**	**Adj p-value**	**Unaffected skin v Controls Fold change**	**Adj p-value**	**Affected skin v Unaffected skin Fold change**	**Adj p-value**
PITX2	7.96	*0.00001*	9.36	*0.00001*	-1.40	0.59
WNT1	6.26	*0.00001*	7.82	*0.00001*	-1.50	0.60
WNT3A	6.02	*0.00012*	6.09	*0.00008*	-0.08	0.96
FZD8	4.56	*0.00001*	5.57	*0.00001*	-1.01	0.69
LEF1	4.07	*0.00005*	4.25	*0.00002*	-0.18	0.94
FRZB	4.02	*0.00599*	4.27	*0.00329*	-0.25	0.95
FZD2	3.81	*0.00006*	4.86	*0.00001*	-1.05	0.59
NAV2	3.03	*0.00204*	4.03	*0.00010*	-1.00	0.65
FZD4	2.63	*0.00612*	2.70	*0.00937*	0.33	0.96
PRICKLE1	2.57	*0.00012*	2.27	*0.00038*	-0.29	0.85
NKD1	2.46	*0.00017*	3.31	*0.00001*	-0.67	0.65
DKK1	1.89	*0.00064*	2.71	*0.00001*	-0.82	0.56
FZD7	1.86	*0.00249*	2.44	*0.00015*	-0.58	0.65
PORCN	1.54	*0.00012*	2.05	*0.00001*	-0.51	0.59
SFRP1	1.44	*0.05513*	1.74	*0.01842*	-0.30	0.85
HSPA12A	1.38	*0.01768*	2.29	*0.00022*	-0.91	0.60

MT1A1	1.67	*0.04666*	1.66	0.09945	-1.15	0.59
AXIN1	2.35	*0.00003*	3.26	*0.00001*	-0.91	0.59
AXIN2	2.11	*0.00324*	2.83	*0.00017*	-0.71	0.65
FZD9	4.24	0.05967	6.22	*0.00001*	-1.28	0.59
WNT7A	5.53	*0.00023*	6.85	*0.00002*	-1.32	0.65
DKK1	1.88	*0.00064*	2.70	*0.00001*	-0.81	0.59
FZD3	3.52	*0.00003*	4.38	*0.00000*	-0.86	0.59
WNT6	3.00	*0.03352*	4.88	*0.00086*	-1.88	0.59
WNT7B	4.86	*0.00003*	6.40	*0.00000*	-1.55	0.59
WNT8A	14.01	*0.00000*	15.44	*0.00000*	-1.43	0.76
WNT10A	4.24	*0.00009*	5.55	*0.00000*	-1.32	0.59
DKK3	1.23	0.08293	1.78	*0.05036*	-0.53	0.75

There are two Wnt signaling molecules upregulated in both affected and unaffected skin, *WNT1* and *WNT3A.* Four frizzled receptors are up regulated in SSc skin compared to controls and three antagonists of the Wnt pathway are also upregulated in the SSc skin; *FRZB*, *SFRP1* and *DKK1*. These antagonists are usually upregulated in response to continued Wnt pathway signaling.

Table J.2. Genes significantly down regulated in SSc cases (involved and uninvolved skin)

	Wnt signalling pathway qPCR Array					
Gene	**Affected skin v Controls Fold change**	**Adj p-value**	**Unaffected skin v Controls Fold change**	**Adj p-value**	**Affected skin v Unaffected skin log2 Fold change**	**Adj p-value**
WNT5B	-12.19	*0.00026*	-13.27	*0.00010*	1.08	0.91
CSNK1A1	-2.51	*0.00063*	-1.87	*0.00719*	-0.65	0.65
WIF1	-3.04	*0.01582*	-2.76	*0.02346*	-0.28	0.94
CALM1	-3.05	*0.00019*	-2.99	*0.00021*	-0.06	0.96

WNT5A	-3.07	*0.00006*	-2.45	*0.00050*	-0.62	0.65
MMP7	-4.27	*0.00964*	-3.88	*0.01597*	-0.39	0.95
RHOA	-5.22	0.05782	-7.32	*0.00807*	-0.85	0.72
CCND2	-6.13	*0.00001*	-6.08	*0.00001*	-0.05	0.96
FRAT1	-1.68	*0.00788*	-1.39	0.09713	-0.28	0.85
JUN	-1.14	*0.02409*	-0.71	0.15065	-0.43	0.71
FBXW11	-1.01	0.99456	-2.87	*0.00007*	0.13	0.94
MYC	-3.05	0.21817	-5.22	*0.03803*	-1.89	0.72
RUVBL1	-2.94	0.20072	-4.59	*0.04631*	-1.64	0.77

Eight genes were down-regulated in the SSc skin compared to controls. The two Wnt signaling molecules, *WNT5A* and *WNT5B* are both initiators of the non-canonical Wnt pathway. *WIF1* is also down-regulated. This is a potent inhibitor of the Wnt signaling pathway. As there was no significant differential expression between the affected and unaffected skin samples, Tables J.3 and J.4 represent the analyses done when the patient samples were combined.

Table J.3. Genes significantly up-regulated in SSc skin compared to controls

	Wnt signalling pathway qPCR Array	
Gene	**SSc Skin v Controls log2 Fold change**	**p-value**
WNT8A	14.56	*0.00016*
FGF4	18.60	*0.00014*
PITX2	9.12	*0.00016*
WNT1	7.31	*0.01596*
WNT7A	6.67	*0.00016*
WNT3A	6.11	*0.04027*

WNT7B	5.97	*0.00008*
WNT9A	5.55	*0.00050*
FZD8	5.19	*0.00015*
WNT10A	4.99	*0.00245*
FZD2	4.57	*0.00004*
LEF1	4.35	*0.00004*
FZD3	4.05	*0.00014*
NKD1	3.01	*0.00008*
AXIN1	2.92	*0.00016*
AXIN2	2.56	*0.00014*
MT1A1	2.51	*0.02251*
PRICKLE1	2.46	*0.01596*
FZD9	2.37	*0.00016*
DKK1	2.29	*0.00085*
FZD7	2.20	*0.00020*
SOX17	2.00	*0.03802*
PORCN	1.80	*0.00016*
HSPA12A	1.79	*0.00525*
SFRP1	1.45	*0.02251*
TCF7	1.22	*0.02640*
PRMT6	1.17	*0.00329*

Table J.4. Genes significantly down-regulated in SSc skin compared to controls

	Wnt signalling pathway qPCR Array	
Gene	**SSc skin v Controls log2 Fold change**	**p-value**
WNT5B	-11.31	*0.00010*
CCDN2	-6.54	*0.00014*
RHOA	-5.57	*0.00016*
TCF7L1	-5.15	*0.00014*
MMP7	-4.57	*0.00069*
CCND1	-3.50	*0.00007*
CALM1	-3.29	*0.00000*
MYC	-3.11	*0.00015*
WIF1	-3.10	*0.01777*
VANGL2	-3.10	*0.00156*
FBXW11	-3.02	*0.00000*
RUVBL1	-2.95	*0.00002*
WNT5A	-2.93	*0.00000*
CSNK1A1	-2.37	*0.00001*
CXADR	-2.37	*0.00111*
CTBP1	-2.32	*0.04471*
EP300	-2.18	*0.00032*
CTNNB1	-2.18	*0.00668*
GSK3B	-1.87	*0.01168*
DAAM1	-1.66	*0.00207*
FRAT1	-1.65	*0.00137*
MAPK8	-1.36	*0.00558*
WISP1	-1.35	*0.00852*

Appendix L – Data normalised expression to *ACTB, HPRT1* and *RPLP0*

Thirty seven genes were significantly upregulated in both the affected skin and the unaffected skin samples (Table K.1), while ten were under-expressed compared to controls (Table K.2). Again, the differential expression within the patient, thus between affected and affected skin, is not significant.

Table K.1. Genes significantly up regulated in SSc cases (affected and unaffected skin)

	Wnt signalling pathway qPCR Array					
Gene	**Affected skin v Controls Fold change**	**Adj p-value**	**Unaffected skin v Controls Fold change**	**Adj p-value**	**Affected skin v Unaffected skin Fold change**	**Adj p-value**
FGF4	23.24	*0.023*	23.47	*0.008*	-0.08	0.96
WNT8A	19.46	*0.02*	19.17	*0.03*	-0.18	0.94
PITX2	13.78	*0.001*	13.96	*0.001*	-0.25	0.95
WNT1	11.82	*0.037*	12.31	*0.046*	-0.29	0.85
WNT3A	11.37	*0.041*	10.37	*0.047*	-0.30	0.85
WNT7A	11.33	*0.002*	11.49	*0.002*	-0.51	0.59
WNT7B	10.48	*0.019*	10.96	*0.012*	-0.53	0.75
FZD9	10.36	*0.029*	10.82	*0.016*	-0.58	0.65
WNT9A	10.27	*0.022*	10.34	*0.031*	-0.67	0.65
FZD8	9.69	*0.003*	10.20	*0.009*	-0.71	0.65
WNT10A	9.47	*0.035*	10.02	*0.038*	-0.81	0.59
LEF1	9.34	*0.017*	8.87	*0.023*	-0.82	0.56
FZD2	9.25	*0.028*	9.40	*0.036*	-0.86	0.59
FZD3	8.73	*0.018*	8.87	*0.026*	-0.91	0.60
NAV2	8.21	*0.047*	8.31	*0.024*	-0.91	0.59
WNT6	8.04	*0.031*	9.73	*0.05*	-1.00	0.65

LRP5	7.90	*0.05*	7.19	*0.033*	-1.01	0.69
NKD1	7.59	*0.012*	7.95	*0.007*	-1.05	0.59
PRICKLE1	7.57	*0.046*	6.86	*0.029*	-1.15	0.59
AXIN1	7.49	*0.004*	7.86	*0.003*	-1.28	0.59
AXIN2	7.16	*0.013*	7.46	*0.011*	-1.32	0.65
MT1A	6.99	*0.045*	7.54	*0.034*	-1.32	0.59
DKK1	6.90	*0.005*	7.18	*0.02*	-1.40	0.59
FZD7	6.72	*0.011*	7.18	*0.006*	-1.43	0.76
PORCN	6.45	*0.006*	6.67	*0.004*	-1.50	0.60
HSPA12A	6.20	*0.025*	6.88	*0.014*	-1.55	0.59
SFRP1	6.17	*0.007*	6.24	*0.028*	-1.88	0.59
PRMT6	5.83	*0.008*	6.02	*0.01*	0.33	0.96
TCF7	5.68	*0.032*	6.28	*0.032*	-0.58	0.65
FZD6	5.43	*0.009*	5.82	*0.005*	-1.00	0.65
WNT2B	5.37	*0.015*	5.78	*0.042*	-0.91	0.60
NLK	5.28	*0.024*	5.43	*0.013*	-0.91	0.59
CYP4V2	4.56	*0.016*	4.71	*0.018*	-0.86	0.59
MTSS1	4.37	*0.026*	4.51	*0.037*	-0.82	0.56
LRP6	4.37	*0.034*	5.15	*0.027*	-0.81	0.59
PPARD	3.94	*0.04*	4.59	*0.021*	-0.71	0.65
CHSY1	3.79	*0.043*	3.78	*0.039*	-0.67	0.65
JUN	3.75	*0.01*	3.76	*0.025*	-0.29	0.85
WNT3	3.57	*0.048*	4.73	*0.044*	-0.30	0.85
KREMEN1	3.48	*0.039*	4.14	*0.019*	-0.51	0.59
MAPK8	3.44	*0.038*	3.33	*0.045*	-0.82	0.56
DAAM1	3.11	*0.042*	3.07	*0.043*	-0.81	0.59
FRAT1	3.01	*0.014*	3.18	*0.035*	-0.71	0.65
GSK3B	3.00	*0.044*	2.75	*0.048*	-0.67	0.65

EP300	2.47	*0.027*	2.66	*0.015*	-0.18	0.94
CSNK1A1	2.07	*0.03*	2.69	*0.022*	-0.25	0.95
WNT5A	1.43	*0.049*	2.21	*0.041*	-0.53	0.75
CALM1	1.39	*0.036*	1.52	*0.049*	-0.58	0.65

Amongst the 48 upregulated genes are ten Wnt signaling molecules including, *WNT7B* and *WNT3A.* Six frizzled receptors are up regulated in SSc skin compared to controls, and three antagonists of the Wnt pathway are also upregulated in the SSc skin; *AXIN1*, *AXIN2* and *DKK1*.

Table K.2. Genes significantly down regulated in SSc cases (involved and uninvolved skin)

	Wnt signalling pathway qPCR Array					
Gene	**Affected skin v Controls Fold change**	**Adj p-value**	**Unaffected skin v Controls Fold change**	**Adj p-value**	**Affected skin v Unaffected skin log2 Fold change**	**Adj p-value**
CCND2	-1.96	*0.033*	-1.63	*0.04*	-0.91	0.59
WNT5B	-6.38	*0.021*	-6.75	*0.017*	-0.53	0.75

As there was no significant differential expression between the affected and unaffceted skin samples, Tables K.3 and K.4 represent the analyses done when the patient samples were combined.

Table K.3. Genes significantly up-regulated in SSc skin compared to controls

	Wnt signalling pathway qPCR Array	
Gene	**SSc Skin v Controls log2 Fold change**	**p-value**

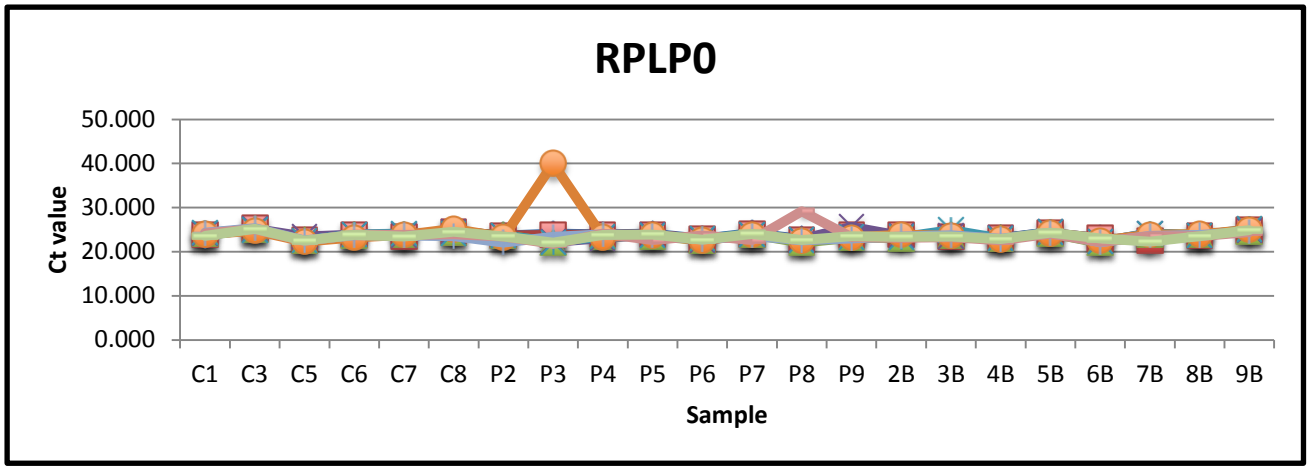
FGF4	23.35	*0.001*
WNT8A	19.31	*0.026*
PITX2	13.87	*0.002*
WNT1	12.06	*0.047*
WNT7A	11.41	*0.003*
WNT7B	10.72	*0.004*
FZD9	10.59	*0.021*
WNT9A	10.30	*0.029*
FZD8	9.95	*0.005*
WNT10A	9.75	*0.040*
FZD2	9.33	*0.035*
LEF1	9.10	*0.022*
FZD3	8.80	*0.025*
NAV2	8.26	*0.048*
NKD1	7.77	*0.007*
AXIN1	7.67	*0.008*
AXIN2	7.31	*0.009*
MT1A	7.27	*0.042*
DKK1	7.04	*0.010*
FZD7	6.95	*0.011*
PORCN	6.56	*0.012*
HSPA12A	6.54	*0.023*
SFRP1	6.21	*0.024*
TCF7	5.98	*0.039*
PRMT6	5.92	*0.013*
FZD6	5.62	*0.014*
WNT2B	5.58	*0.041*
NLK	5.36	*0.015*

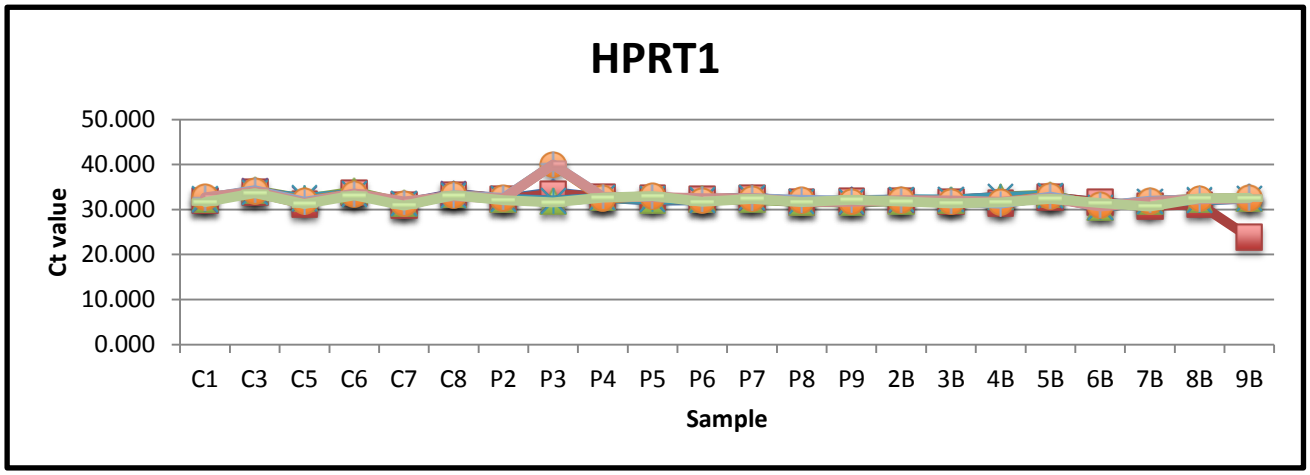
NFATC1	5.10	*0.038*
MTFP1	4.80	*0.030*
LRP6	4.76	*0.037*
CYP4V2	4.64	*0.016*
MTSS1	4.44	*0.036*
PPARD	4.26	*0.033*
KREMEN1	3.81	*0.032*
CHSY1	3.78	*0.046*
JUN	3.75	*0.017*
WISP1	3.40	*0.049*
MAPK8	3.39	*0.043*
FRAT1	3.09	*0.034*
DAAM1	3.09	*0.045*
EP300	2.57	*0.018*
CSNK1A1	2.38	*0.027*
WNT5A	1.82	*0.050*

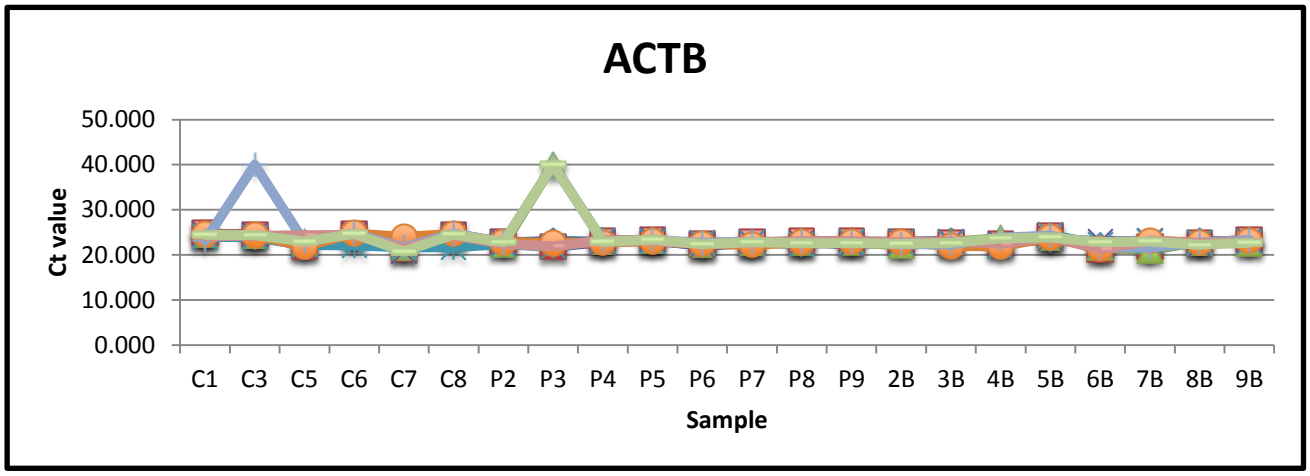
Table K.4. Genes significantly down-regulated in SSc skin compared to controls

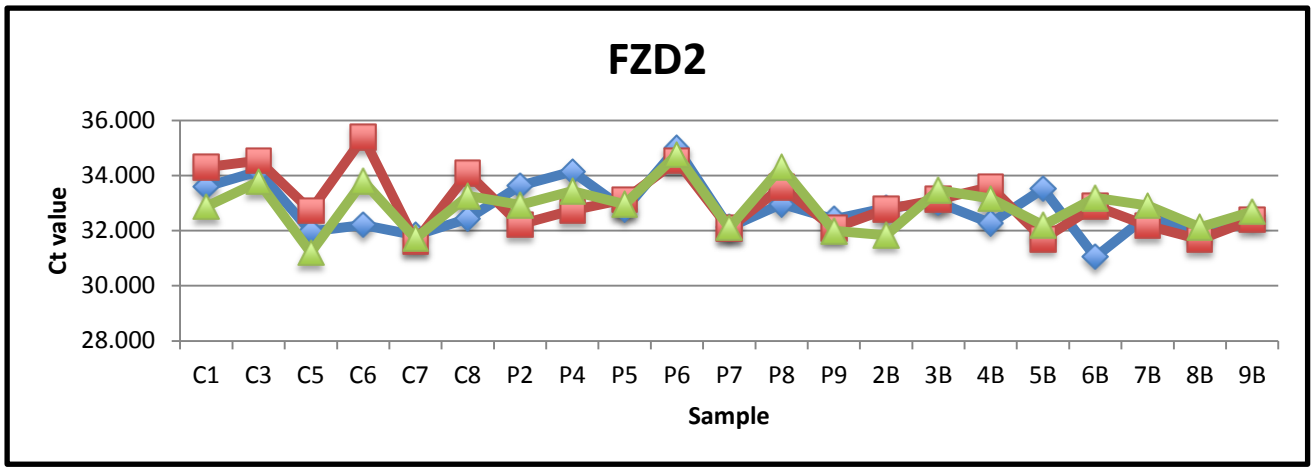
	Wnt signalling pathway qPCR Array	
Gene	**SSc skin v Controls log2 Fold change**	**p-value**
CCND2	-1,79	*0,028*
WNT5B	-6.57	*0.020*

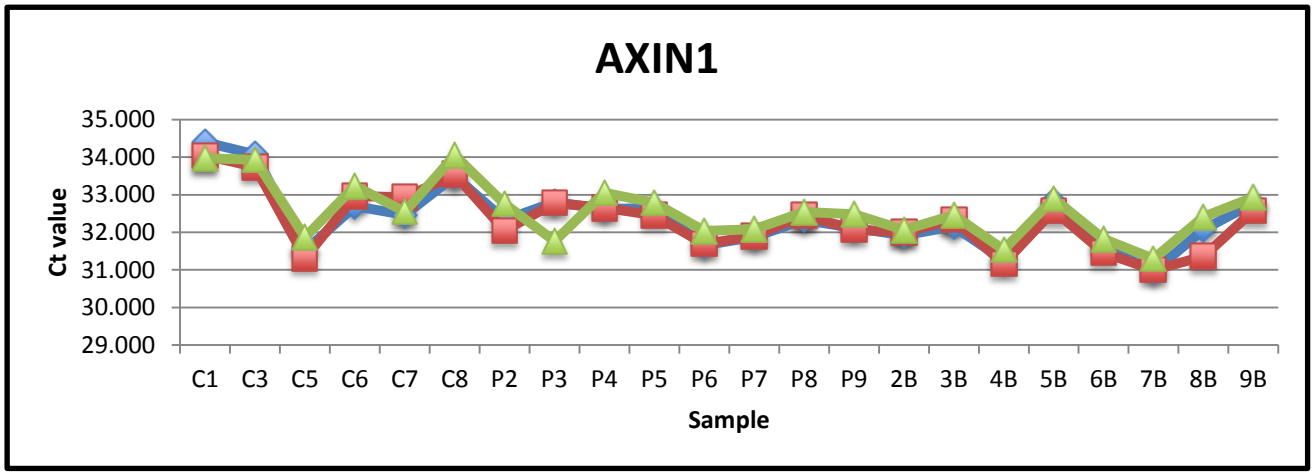
Appendix M – Graphs of Ct values across samples (validation experiments)

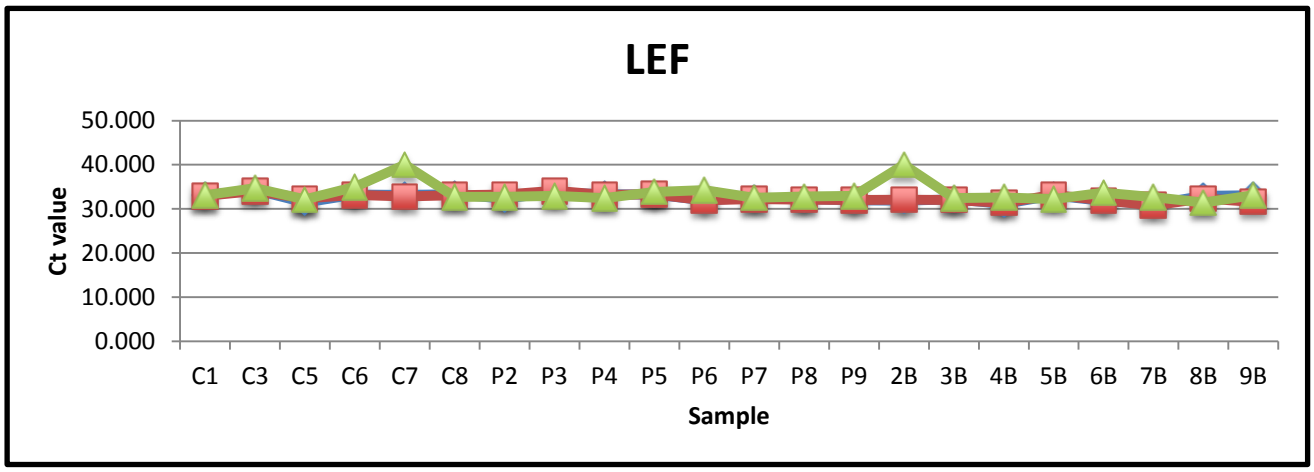


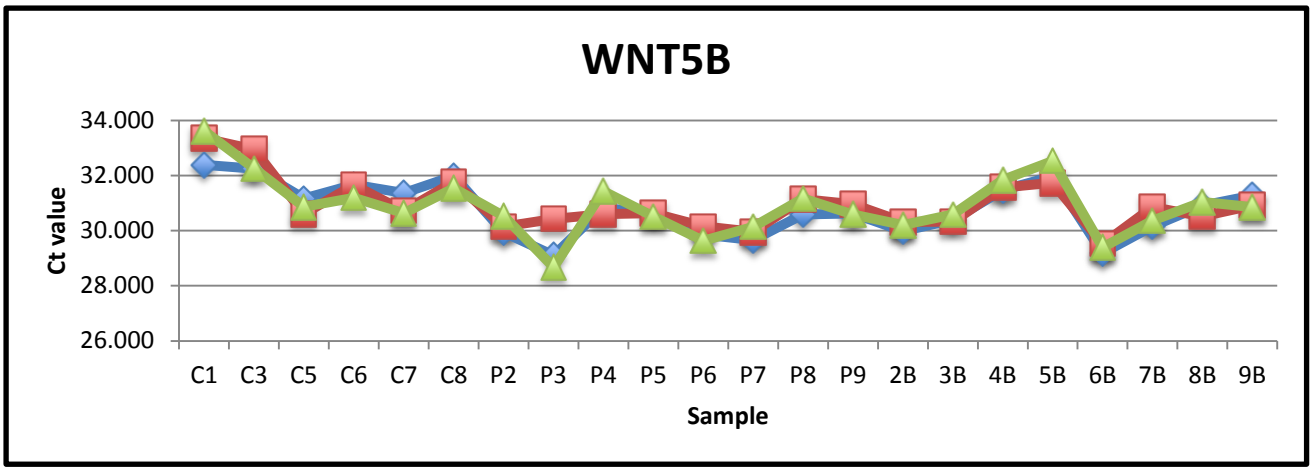


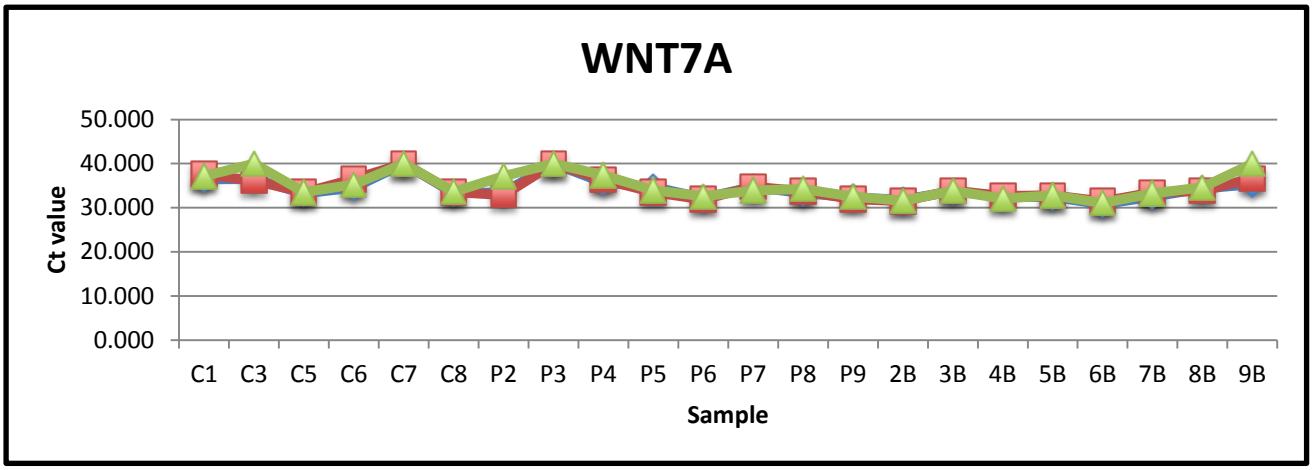



FZD2
36.000
34.000
32.000
30.000
28.000
Ct value
C1 C3 C5 C6 C7 C8 P2 P4 P5 P6 P7 P8 P9 2B 3B 4B 5B 6B 7B 8B 9B
Sample

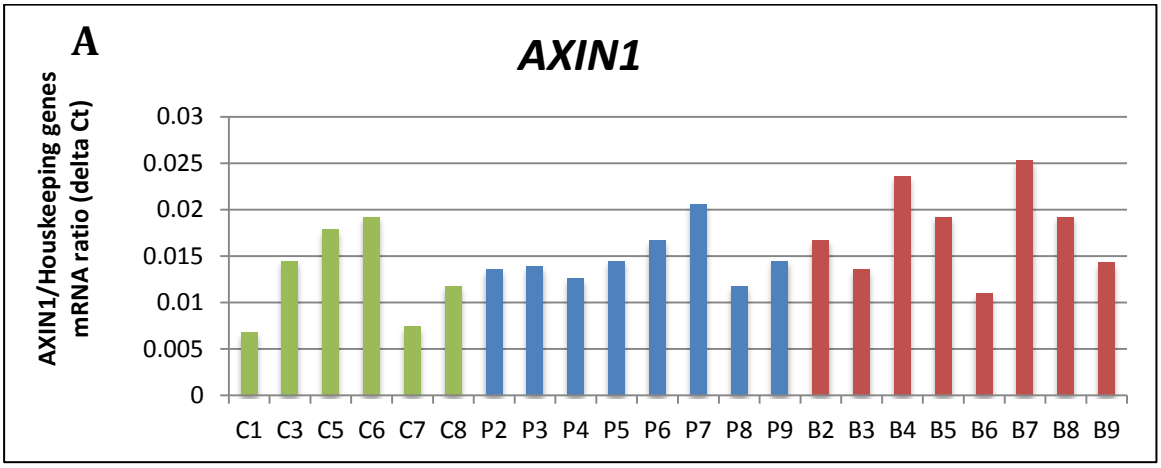

AXIN1
35.000
34.000
33.000
32.000
31.000
30.000
29.000
Ct value
C1 C3 C5 C6 C7 C8 P2 P3 P4 P5 P6 P7 P8 P9 2B 3B 4B 5B 6B 7B 8B 9B
Sample

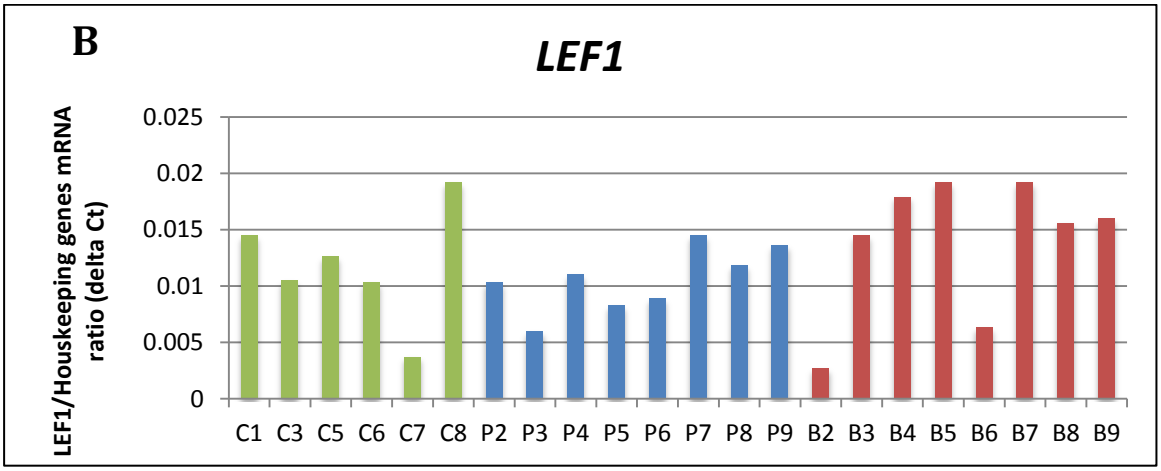

LEF
50.000
40.000
30.000
20.000
10.000
0.000
Ct value
C1 C3 C5 C6 C7 C8 P2 P3 P4 P5 P6 P7 P8 P9 2B 3B 4B 5B 6B 7B 8B 9B
Sample

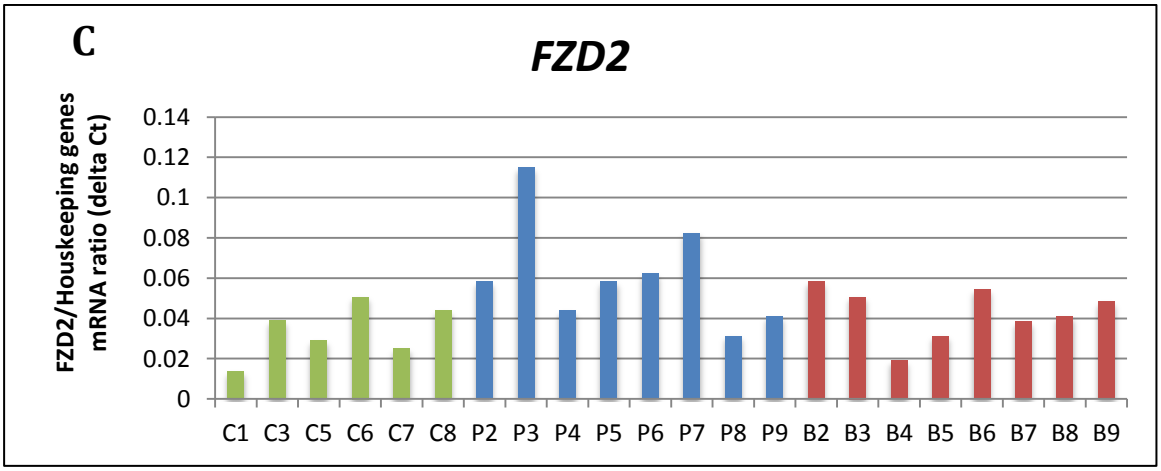

WNT5B
34.000
32.000
30.000
28.000
26.000
Ct value
C1 C3 C5 C6 C7 C8 P2 P3 P4 P5 P6 P7 P8 P9 2B 3B 4B 5B 6B 7B 8B 9B
Sample


WNT7A
50.000
40.000
30.000
20.000
10.000
0.000
Ct value
C1 C3 C5 C6 C7 C8 P2 P3 P4 P5 P6 P7 P8 P9 2B 3B 4B 5B 6B 7B 8B 9B
Sample

Appendix N – Gene expression ratios (GOI vs Houskeeping genes: ΔCt)







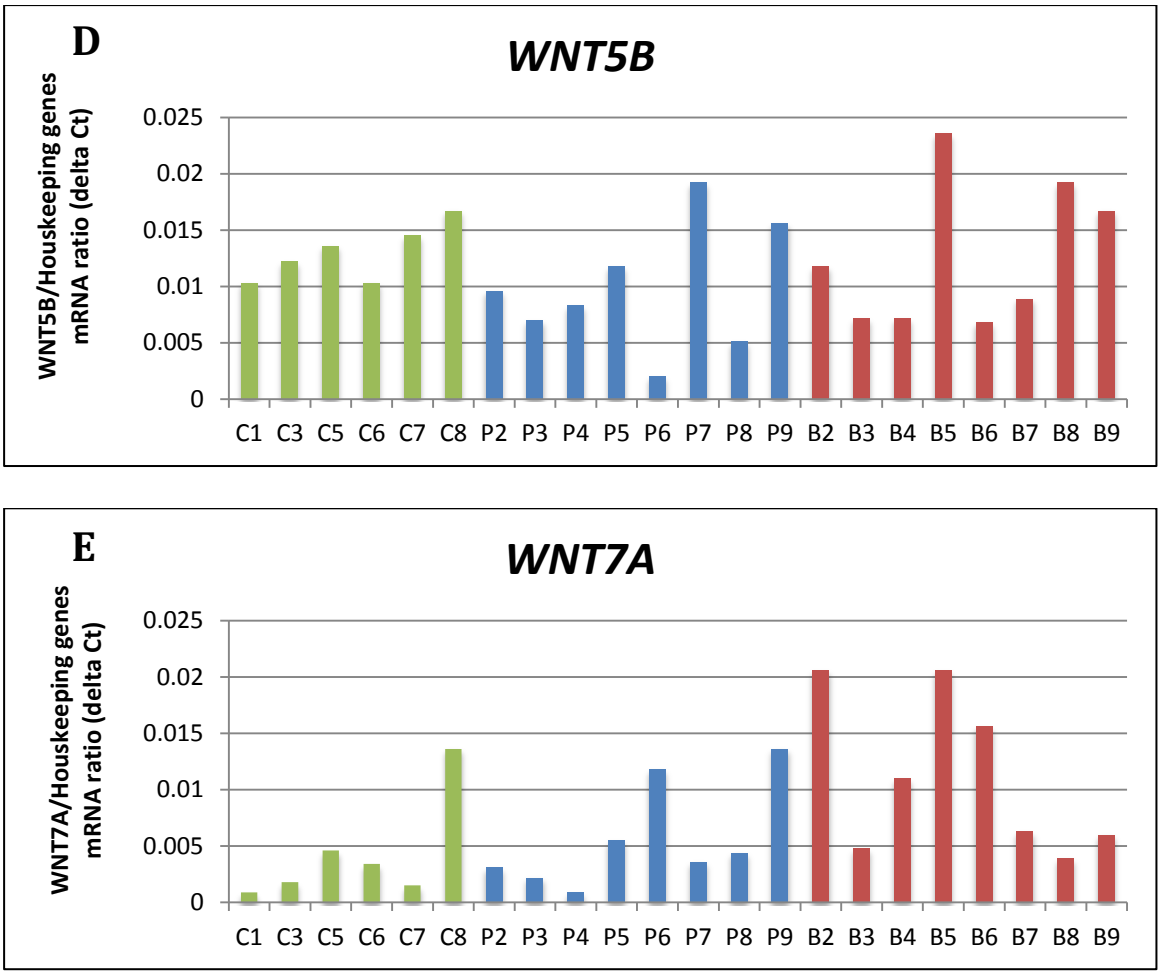
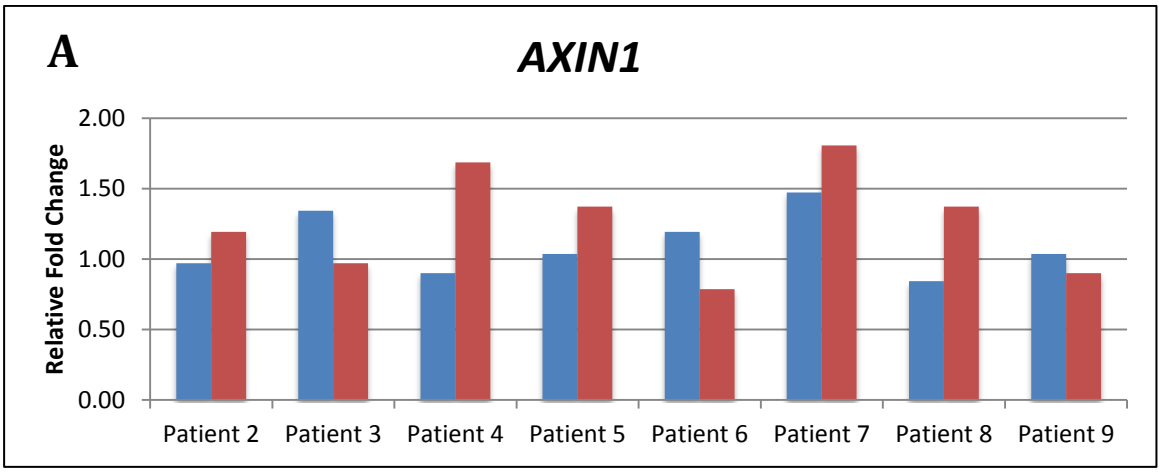
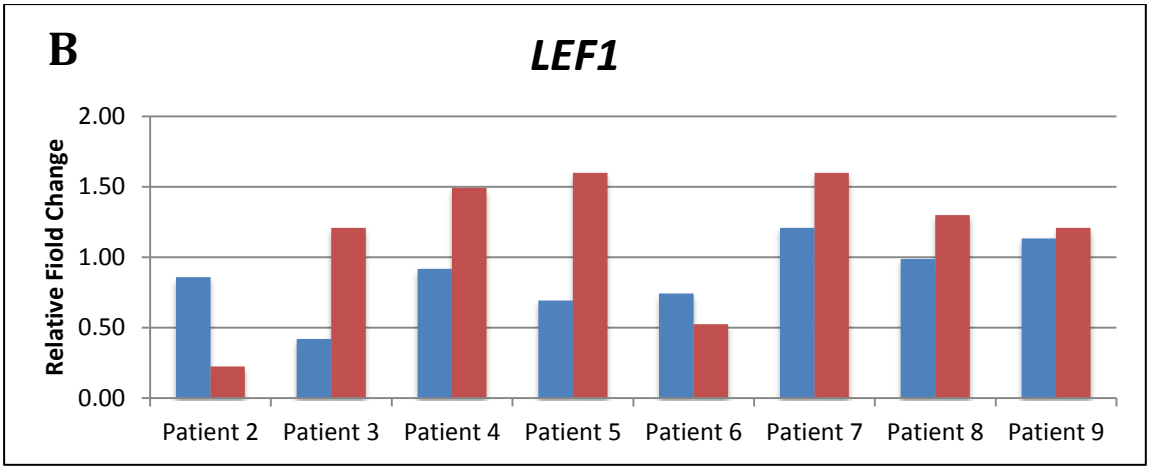
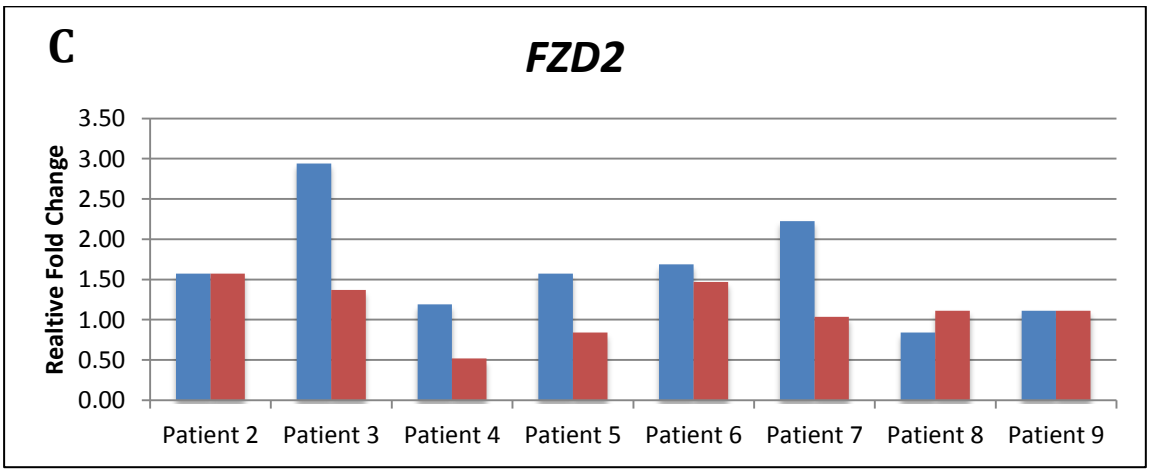


Figure M.1. The ΔCt gene expression ratio values for five of the six chosen genes for validation experiments; A) AXIN1, B) LEF1, C)FZD2, D)WNT5B and E) WNT7A. The control samples are green, the affected SSc skin samples are blue and the unaffected SSc skin samples are red. These ratios are calculated from the Ct values obtained from the TaqMan validation experiment, normalised to three housekeeping genes; ACTB, HPRT1 and RPLP0.

Appendix O – Fold change gene expression for affected and unaffected skin in each SSc patient







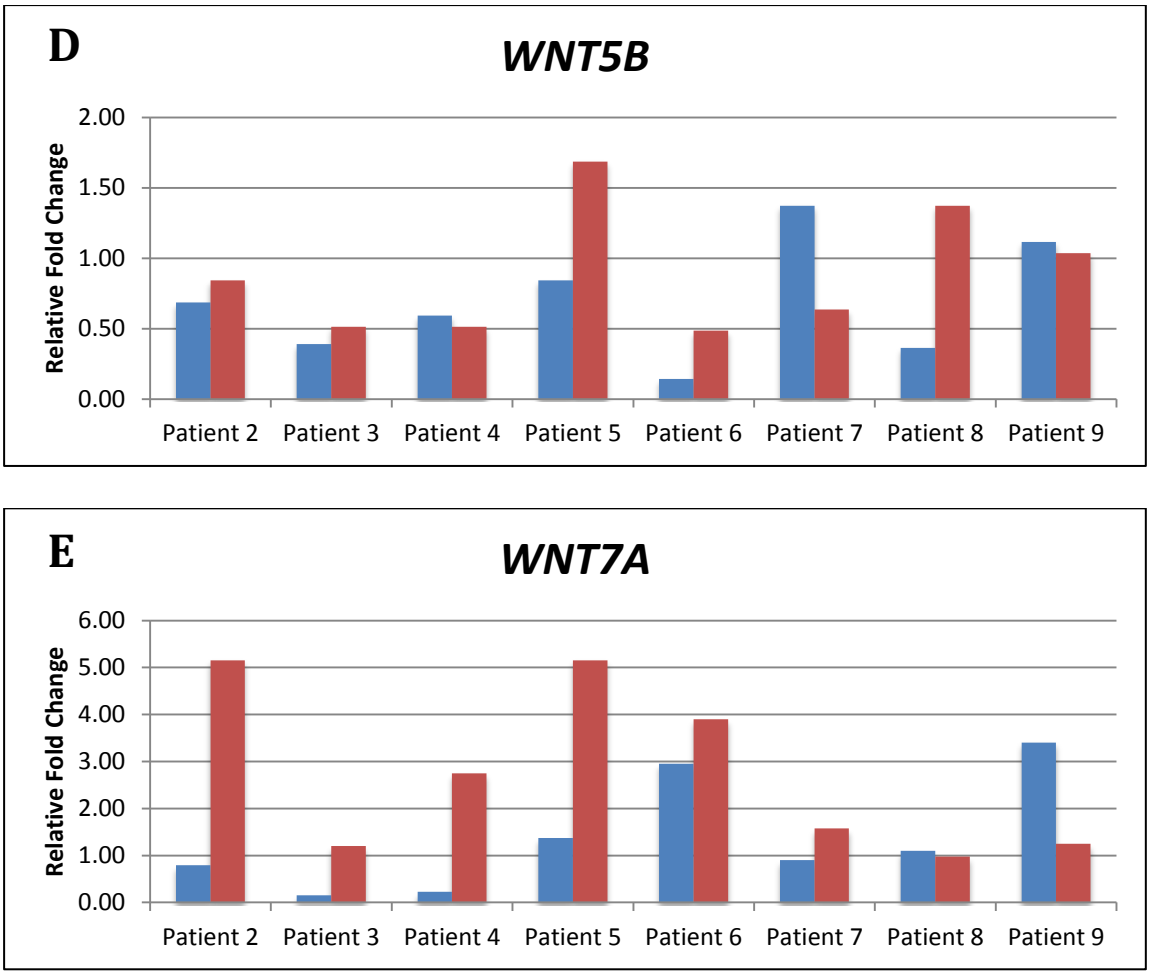


Figure N.1. The differential expression of affected (blue) and unaffected (red) skin from each patient for A) AXIN1, B) LEF1, C) FZD2, D) WNT5B and E) WNT7A. The relative expression values are displayed as a fold change for each gene.

Appendix P - NEBNext small RNA Library Prep for Illumina

Ligate 3' Adapter

Note: For total RNA inputs of 100ng dilute the 3' Adapter 1:2 in nuclease free water 1µl Adapter + 1 µl water

1. Mix the following in a PCR tube:

3' Adapter	1µl
Input RNA	6µl
Total	**7µl**

2. Incubate in a preheated thermal cycler for 2 minutes at 70°C. Transfer tube to ice
3. Add the following components:

3' Ligation Reaction Buffer (2x)	10µl
3' Ligation Enzyme Mix	3µl
Total	**20µl**

4. Incubate for 1 hour at 25°C in a thermal cycler

Hybridise the Reverse Transcription Primer

Note: For total RNA inputs of 100ng dilute the SR RT Primer 1:2 in nuclease free water 1µl ST primer + 1µl water

5. Add the following components to the ligation mixture from (4):

Nuclease free water	4.5µl
SR RT Primer	1µl
Total	**25.5µl**

6. Heat samples for:
   75°C for 5 minutes
   37°C for 15 minutes
   25°C for 15 minutes

Ligate the 5' SR Adapter

7. Resuspend the 5'SR Adapter in 120µl nuclease free water

Note: For total RNA inputs of 100ng dilute the 5' SR Adapter 1:2 in nuclease free water 1.1µl Adapter + 1.1µl water

8. Aliquot 1.1N 5' SR Adapter into a separate 200µl PCR tube
9. Incubate Adapter at 70°C for 2 minutes in thermal cycler, transfer immediately to ice

Store remaining 5' SR Adapter at -80°C

10. Add the following to the mixture for (6):

5' SR Adapter (denatured)	1µl
5' Ligation Reaction Buffer (10x)	1µl

5’ Ligation Enzyme Mix	2.5µl
Total	**30µl**

11. Incubate for 1 hour at 25°C in a thermal cycler

Perform Reverse Transcription

12. Mix the following components in a tube:

Adapter ligated RNA from (11)	30µl
First Strand Synthesis Reaction Buffer	8µl
Murine RNAse Inhibitor	1µl
ProtoScript II Reverse Transcriptase	1µl
Total	**40µl**

13. Incubate for 1 hour at 50°C
14. Proceed immediately to PCR amplification

Safe stopping point → If not planning to proceed immediately, heat inactivate the RT reaction to 70°C for 15 minutes. Samples can then be stored at -15°C – 25°C ·

Perform PCR Amplification

15. Add following components to mix from (14):

LongAmp Taq 2x Master Mix	50µl
SR Primer	2.5µl
Index (X) Primer	2.5µl
Nuclease free water	5µl
Total	**100µl**

16. PCR Cycling conditions:

94°C for 30 seconds
94°C for 15 seconds
62°C for 30 seconds
70°C for 15 seconds } 15 cycles (suggested for small input RNA)
70°C for 5 minutes
4°C for hold

QC Check and Size Selection using 6% Polyacrylaminde gel

1. Purify the PCR amplified cDNA (100µl) using a QiaQuick PCR Purification Kit
    a. Add 500µl Buffer PB to 100µl PCR product
    b. Add sample to spin column, centrifuge at 13 000rpm for 1 minute. DISCARD FLOW THROUGH
    c. Add 750µl Buffer PE to column, centrifuge at 13 000rpm for 1 minute. DISCARD FLOW THROUGH
    d. Centrifuge column for an additional minute at 13 000rpm
    e. With lid open, centrifuge column at 13 000rpm for 5 minutes
    f. Place column in 1.5ml collection tube
2. Elute amplified DNA in 25µl nuclease free water
3. Mix the purified PCR product (25µl) with 5µl gel loading dye

4. Load 5µl Molecular Weight marker in one well
5. Load two wells (15µl each) or one well (30ml) of the cDNA and loading dye
6. Run the gel for 1 hour at 120V
7. Stain gel using SyberSafe, SybrGold etc. for 3 minutes
8. View under the transilluminator
9. The 140-150bp bands correspond to the adapter ligated microRNA
10. Cut out the fragments and place gel slices in a 1.5ml tube, crush the slices and then soak in 250ul DNA Gel Elution Buffer (1x) → centrifuge at 13 000rpm for 2 minutes
11. Rotate and room temperature for at least 2 hours
12. Transfer eluate and gel debris to a filtration column (cut off tip of 1000µl pipette tip)
13. Centrifuge the filter for 2 minutes at > 13 200rpm
14. Recover eluate, add 1µl linear acrylaminde, 25ul 3M sodium acetate (pH 5.5) and 750µl 100% ethanol
15. Vortex well
16. Precipitate at -80C for at least 30 minutes (-20°C overnight)
17. Centrifuge for 30 minutes at > 14 000rpm (4°C)
18. Remove supernatant without disturbing pellet
19. Wash pellet with 80% ethanol and vortex vigorously
20. Centrifuge for 30 minutes at > 14 000rpm (4°C)
21. Air dry pellet for 10 minutes at room temperature
22. Resuspend pellet in 12µl TE buffer
23. Validate sample on a DNA1000 Bioanalyzer chip (size, purity, concentration)

Appendix Q – miRNA QC graphs

